Investigating the potential for environmental perception and adaptation in the amoebaflagellate *Naegleria gruberi*

Connor Sykes U1363969

A thesis submitted to the University of Huddersfield in partial fulfilment of the requirements for the degree of Master of Science by Research.

Division of Biological Sciences & Nutrition, School of Applied Sciences, University of Huddersfield

January 2019

Acknowledgements

First and foremost, I would like to express my deepest gratitude to my research supervisors, Professor Michael Ginger and Dr. Jane Harmer, who have supported me throughout the entirety of the MSc year and kept their cool when I was losing mine. Without their continuing guidance and dedicated involvement, this year of work and subsequent manuscript would have never come to fruition.

In addition, I would like to thank all of those who worked within the MLG lab, especially Asma, Kim and Kayleigh, for their help and comradery, especially on the days when nothing went to plan!

Finally, I would like to profoundly thank my wonderful family, particularly my mother and father, I don't know how you have managed to put up with me for so long, but it's finally done! Mum, you're an absolute star and you have the patience of a saint. I want you to know you are amazing, and that I love you to the moon and back! Dad, I don't think I could count the number of times you have ferried me to or from somewhere with utmost urgency, I can't thank you enough for all of the support over the past year. Elliott, you have always been my best friend, through thick and thin, and you always manage to make everything better in times of dire stress. I couldn't have done it without you broski.

And finally, to Sophie, my gorgeous girl who has stood by me the entire way, offering late-night proofreading and all of the encouragement I could ever ask for and more. I love you truly and deeply, and can't wait for us to begin our next chapter once this MSc is done.

This thesis stands as a testament to each of you,

Thank you.

Abstract

The construction and function of flagella in eukaryotes is often vital to feeding, survival and reproduction. The last 15 years has seen a realisation that some eukaryotes, which contain the majority of eukaryotic biodiversity, possess flagella that play a function as sensory antennae. There are ongoing attempts to elucidate these sensory mechanisms, which allow cells to perceive and respond to external stimuli. This is also important in a medical context, as many cells throughout the human body build cilia as a motile or sensory apparatus, which if defective, can result in genetic syndromes known as ciliopathies. Ciliopathies have been shown to predispose individuals to chronic health conditions, including cancer, obesity and diabetes.

The predatory amoeba *Naegleria gruberi* is capable of a transformation, in which the cell differentiates into a motile flagellate cell. This occurs via assembly of two flagella and a microtubule-based cytoskeleton *de novo*, in response to environmental cues such as nutriment deficit. With the advent of whole genome sequencing, the genome of *N. gruberi* has been decoded, revealing an intriguingly large repertoire of metabolic pathway and sensory signaling proteins. RNA microarray studies have revealed that a large number of these proteins are developmentally regulated throughout the differentiation process, which suggests that the flagellate form of *Naegleria* is likely well equipped for perception of environmental conditions. This stands to reason, as the primary role of the temporary flagellate form is to find a new habitable environment before the cell expires, in order to resume amoebic growth and proliferation.

Throughout the MSc a bioinformatic analysis of various serpentine receptor proteins was carried out, utilizing previously published microarray data, to categorise these proteins by expression levels and expression patterns during the differentiation process. I also studied the effects of different environmental triggers upon differentiation and encystment of *N. gruberi*, with the intent to elucidate how vastly different environmental conditions would influence the ameboflagellate differentiation sensory response. Finally, the purification of recombinant proteins of interest was carried out, with the aim to later localise these proteins via immunolocalization and biochemical fractionation, to assess the sensory capability of the flagellum of *N. gruberi* both during and after differentiation.

Contents

Abbreviations and Terms

µg = Micrograms

µl = Microlitres

AK3 = Adenylate kinase (XP_002679669.1)

APS = Ammonium persulphate

Arl6 = G-protein ADP ribosylation factor like GTPase 6

AS = Amoeba saline

ATP = Adenosine triphosphate

Azide = Sodium azide

BBS = Bardet–Biedl syndrome

BLAST = Basic Local Alignment Search Tool

blastp = protein-protein BLAST

BLUF = blue-light using FAD

C8 = Adenylate/Guanylate cyclase (XP_002675238.1)

$CaCl_2$ = Calcium chloride

cAMP = Cyclic adenosine monophosphate

cGMP = 3', 5'-cyclic guanosine monophosphate

CNS = Central nervous system

CO_2 = Carbon dioxide

DMSO = Dimethyl sulfoxide

DNA = Deoxy-ribonucleic acid

DTT = Dithiothreitol

Ex (E1, E3, etc.) = Elution fraction number (1st elution fraction, 3rd elution fraction, etc.)

FBS = Foetal bovine serum

FT = Flow through fraction

FLA2 = Kinesin 2 homolog

g = Grams

G = Relative centrifugal force

GDP = Guanosine diphosphate

GEX1 = Gamete expressed 1

GPCR = G protein-coupled cell-surface receptor

GTP = Guanosine triphosphate

H_2O = deionised water

HAP2 = Hapless 2

IFT = Intraflagellar transport

IPTG = Isopropyl β-D-1-thiogalactopyranoside

JGI = Joint Genome Institute

JGIDB = Joint Genome Institute data base

KAN = Kanamycin

kb = Kilobases

kD = kilodaltons

KH_2PO_4 = Potassium phosphate monobasic

kV = Kilovolts

L = Litres

Ladder = 1 kb protein Ladder

LB = Lysogeny broth

M = Molar concentration

mg = Milligrams

$MgSO_4$ = Magnesium sulphate

min = Minute

mins = Minutes

ml = Millilitres

MSc = Master of science

MTOCS = Microtubule organising centres

Na_2HPO_4 = Sodium phosphate dibasic

NaCl = Sodium chloride

NCBI = National Centre for Biotechnology Information

NIT = Nitrate and nitrite sensing

nm = Nanometer

NO^-_2 = Nitrite

NO^-_3 = Nitrate

NTA = Nitrilotriacetic acid

O_2 = Oxygen

PAGE = Polyacrylamide gel electrophoresis

PAM = Primary amoebic meningoencephalitis

PAS = Per-Arnt-Sim

Pas1 = Predicted adenylate/guanylate cyclase with PAS domain (XP_002682199.1)

PBS = Phosphate buffered saline

PDB = Protein Data Bank

pH = Logarithmic unit of acidity

PMSF = Phenylmethylsulfonyl fluoride

pp-PFK = pyrophosphate-dependent phosphofructo-1-kinase (XP_002680445.1)

RNA = Ribonucleic acid

SAS-6 = Spindle assembly abnormal protein 6

SDS = Sodium dodecyl sulfate

SEM = Scanning electron microscopy.

SWISS-MODEL = Online protein modelling software

T0 = Initial time point

TCA cycle = Tricarboxylic acid cycle

TEMED = Tetramethylethylenediamine

TRIS/Tris = Tris(hydroxymethyl)aminomethane

Troph = Trophozoite

TWEEN = Polyoxyethylene sorbitan monolaurate

Tx (T1, T3.5, etc.) = x hour time point (1 hour time point, 3.5 hour time point, etc.)

UV = Ultra violet

V = Volts

v/v = Volume to volume concentration

w/v = Weight to volume concentration

Contents of figures

Contents of tables

Chapter 1: Introduction

1.1 - The life cycle and evolution of *Naegleria* species

1.1.1 - The evolution of *Naegleria*

Naegleria are a genus of free-living amphitrophic eukaryotic protists, which are widely accepted to have been first discovered by Franz Schardinger in 1899, when he drew images of both trophozoites and cysts (Schardinger, 1899; De Jonckheere, 2014). *Naegleria* are non-obligate, opportunistic parasites usually found in fresh warm water or soil (De Jonckheere, 2002; Pánek, Ptáčková & Čepička, 2014). Most available literature holds the consensus that terrestrial *Naegleria* species are halophobic, however the presence of halotolerant *Naegleria* in salt water has been recorded (Reyes-Batlle et al., 2017).

As a group, protists form the bulk of eukaryotic diversity (Slapeta, Moreira & Lopez-Garcia, 2005; Bardele, 1997; Adl et al., 2007; Ginger, Fritz-Laylin, Fulton, Cande & Dawson, 2010). The genus *Naegleria* falls under the Family Vahlkampfiidae, Order Schizopyrenida and the Class Heterolobosea as shown in figure 1. The Heterolobosea are closely related to the Euglenozoa, both of which include organisms with mitochondria containing discoid cristae for increased respiratory surface area (Pánek, Ptáčková & Čepička,

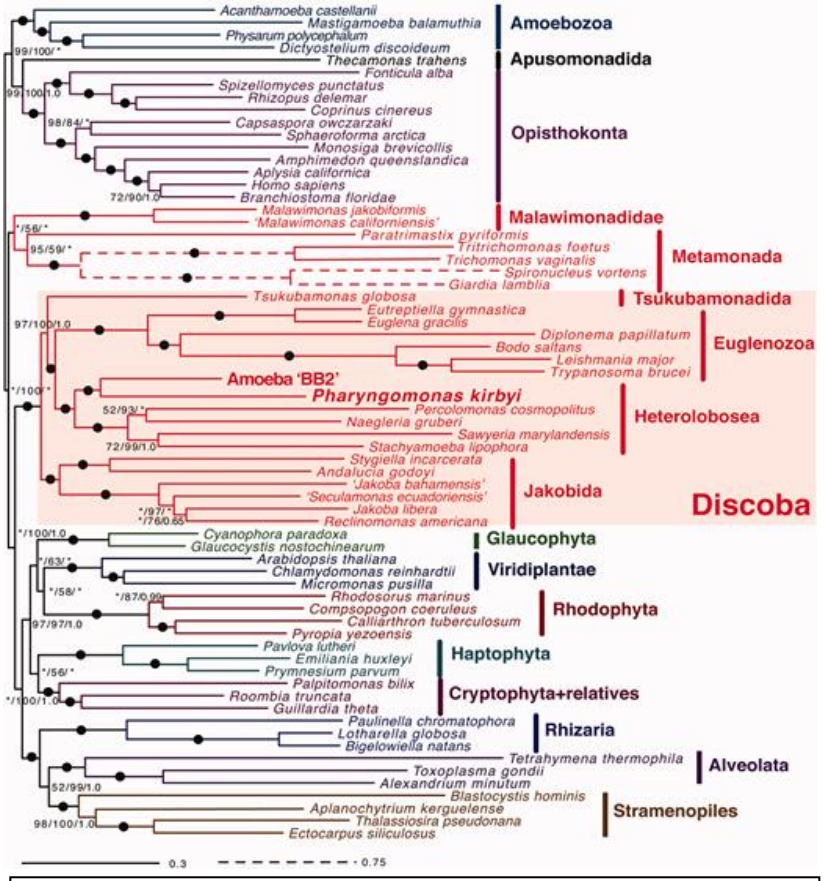

Figure 1: A protist phylogeny tree.

A phylogeny tree created by Yang et al. to give an overview of protist phylogeny. This includes the placement of *Naegleria* within the class Heterobolosea, alongside adjacent relatives Euglenozoa and Jakobida (Yang, Harding, Kamikawa, Simpson & Roger, 2017).

2014; Percival, 2014). Heterolobosea are also closely related to the Jakobids, which contain flagellates with two anterior flagella, used for movement and to facilitate food intake (Lara, Chatzinotas & Simpson, 2006; Simpson & Patterson, 2001). These organisms all fall under the supergroup Excavata, which tend to possess a ventral feeding groove (Simpson & Patterson, 1999) and either a single or an absent mitochondrion (Hampl et al., 2009). Some species in this supergroup such as *Naegleria,* which possesses multiple mitochondria (Fritz-Laylin et al., 2010) and does not contain a feeding groove (Hanousková, Táborský & Čepička, 2018), lack these key features and are instead associated due to genomic studies (Hampl et al., 2009).

1.1.2 - *Naegleria* characterisation and morphology

Over 40 different species of *Naegleria* have been documented (De Jonckheere, 2014; "Taxonomy Browser", 2018). While most *Naegleria* species are morphologically indistinguishable in their amoeboid forms (De Jonckheere, 2002), species can be identified based on minor differences between cyst morphology, temperature tolerance and pathogenicity (Marciano-Cabral, 1988). Species differentiation is also readily determined through the use of molecular methods including gene sequencing (Robinson, Christy, Hayes & Dobson, 1992), immunologic criteria and isoenzyme patterns (Pernin, 1984; De Jonckheere, 2002).

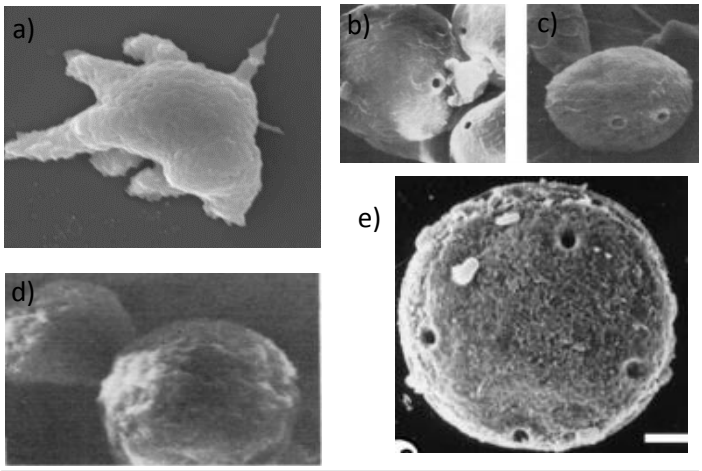

Figure 2: Previously published SEM images of *N. gruberi*.

A collection of SEM images of *Naegleria gruberi* that have been previously published by different labs. a) An *N. gruberi* cell in the trophic form obtained from Jamerson, da Rocha-Azevedo, Cabral & Marciano-Cabral, 2012. b), c) + d) Various encysted cells, some of which have distinguishable ostioles taken from Lastovica, 1974. e) An SEM image of an encysted cell with distinguishable ostioles (Dyková, Kyselová, Pecková, Oborník & Lukes, 2001).

Naegleria are most commonly observed as a 15-µm predatory trophic 'ameboid' form shown in figure 2a (Fritz-Laylin & Fulton, 2016). However, *Naegleria* species are also capable of encystment when under duress as shown in figure 2b-2e (Fulton, 1970, Lastovica, 1974). Once encysted, the trophozoites excyst via movement through preformed ostioles within the cyst wall, highlighted in figure 2e (Lastovica, 1974; Sanders, 2018).

Naegleria feed primarily in their trophic form, on a diet consisting mostly of bacteria, (Grace, Asbill & Virga, 2015; Fritz-Laylin & Fulton, 2016) and are capable of limited limacine movement throughout their environment through the creation and use of large singular pseudopodia as shown in figure 3 (Page, 1967; Vickerman, 1962; Preston & O'Dell, 1980). In order to feed, *Naegleria* digest cells via phagocytosis.

1.1.3 - Molecular, cellular, and ecological biology of *Naegleria*

Organisms within the genus *Naegleria* possess an actin cytoskeleton while in the trophozoite form, seen in figure 3, (Fritz-Laylin & Fulton, 2016). *Naegleria* also harbour a multitude of metabolic pathways, many of which are conceivably found in metabolically flexible mitochondria (Ginger et al. 2010).

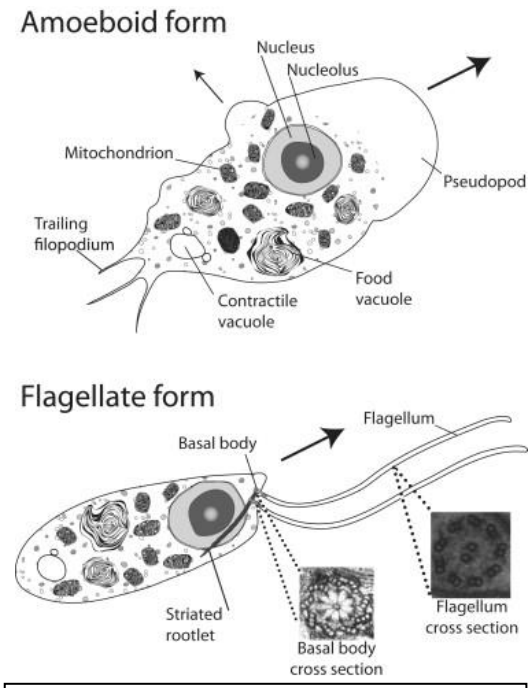

Figure 3: Cellular biology of *N. gruberi*.

An illustration of the cellular biology of both the ameboid and flagellate forms of *N. gruberi* obtained from Fritz-Laylin et al., 2010.

Naegleria species are able to adapt well to many different environments and trophozoites tend to be found in soil and bodies of freshwater (Grace, Asbill & Virga, 2015). Species of *Naegleria* have been isolated from many natural sources, such as freshwater lakes (Michel & De Jonckheere, 1983; Griffin, 1983), thermal springs (Brown, Cursons, Keys, Marks & Miles, 1983) and soil samples (Denet, Coupat-Goutaland, Nazaret, Pélandakis & Favre-Bonté, 2017; De Jonckheere, 2002). *Naegleria* has also been obtained from many man-made and maintained sources such as partially chlorinated swimming pools (Červa, 1971) and even domestic water supplies (Marciano-Cabral, MacLean, Mensah & LaPat-Polasko, 2003).

Most *Naegleria* species are understood to be primarily aerobic. Their development is stunted in environments containing low amounts of oxygen and amoebic growth is not observed in atmospheres of 90% Nitrogen with 10% Carbon Monoxide (Weik & John, 1977). However, some *Naegleria* species have been routinely extracted from anaerobic environments on more than one occasion, which suggests *Naegleria* may be able to survive as facultative anaerobes under certain conditions (Wellings, Amuso, Chang & Lewis, 1977; Wellings, Amuso, Farmelo & Moody, 1977). An example of such behaviour has been observed during the addition of high amounts of CO_2, which leads to excystation of cysted *Naegleria gruberi* cells (Blackler and Sommerville, 1988). It has also been noted that while

glucose is only actively metabolised in small amounts, it is essential for growth of different of *Naegleria* species (Nerad, Visvesvara & Daggett, 1983).

1.1.4 - *N. fowleri* and human infectious disease

The most recognised species of *Naegleria*, in both the public eye and the eyes of health officials, is *N. fowleri* (Grace, Asbill & Virga, 2015). *N. fowleri*, like all *Naegleria* species, is an amphitrophic amoeba that can survive in a free-living state in water or soil. However, unlike all other species of the *Naegleria* genus, it is a facultative pathogen capable of utilising and surviving within the central nervous system (CNS) of a human host (Grace, Asbill & Virga, 2015; De Jonckheere, 2011) and is the only species of *Naegleria* known that is pathogenic to humans (De Jonckheere, 2004).

Infection with *N. fowleri* gives rise to *Naegleria*sis, a disease first discovered in the late 1960s (Culbertson, Ensminger & Overton, 1968) (Butt, 1966). The disease is more commonly known as primary amoebic meningoencephalitis (PAM), a term first used by Cecil Butt (Butt, 1966). PAM is an affliction which is categorised by widespread destruction of brain tissues. *N. fowleri* is thought to infect human hosts by entering the body when warm water containing the organism makes contact with the nasal cavity. *N. fowleri* Trophozoites first adhere to the nasal mucosa and migrate through the cribriform plate, via pores through which the olfactory nerves are interwoven (Marciano-Cabral & Cabral, 2007; Dando et al., 2014; López-Elizalde et al., 2017; Jarolim, McCosh, Howard & John, 2000). The pathogenic cells then migrate to the olfactory bulb and begin lysis of erythrocytes and neurons, causing an acute inflammatory reaction (Grace, Asbill & Virga, 2015; Cervantes-Sandoval, Serrano-Luna, García-Latorre, Tsutsumi & Shibayama, 2008). The inflammation damages the blood-brain barrier allowing for invasion of *N. fowleri*, which then disseminates and digests brain tissues, giving rise to PAM (Marciano-Cabral & Cabral, 2007).

The overwhelming lethality of PAM is a major factor of interest in the disease, worldwide PAM proves fatal in more than 97% of cases (Cogo et al., 2004; Zysset-Burri et al., 2014; Linam et al., 2015). In the United States alone, between 1962 and 2016, 143 individuals were clinically diagnosed with PAM. Of those 143 individuals, only four survived ("General Information | *Naegleria Fowleri* | CDC", 2018).

1.1.5 - *Naegleria* amoeba-to-flagellate differentiation and life cycle

Naegleria is an ameboflagellate and as a species, it is most well-known for its remarkable ability to recognise certain environmental cues and convert from a trophic amoeboid form into a flagellate form as depicted in figure 4. The cell initiates this process due to detecting the presence of specific environmental conditions and stresses such as temperature changes, osmotic changes, or pH shifts (Fulton, 1970). The most common source of environmental stress leading to differentiation is nutritional deprivation of the cells (Willmer, 1956). *Naegleria* can undergo differentiation from trophic to flagellate form between 60 to 100 minutes after being transferred from a normal growth environment to a nutrient free aqueous environment as shown in figure 4 (Walsh, 2007; Fulton, 1970; Fulton, 1993). The flagellate forms of *Naegleria* are temporary forms that do not reproduce. They are capable of swimming for an hour or more before eventually reverting to the ameboid form which they do when they either find a food source or can no longer derive sufficient energy for continued locomotion (Fulton, 1970; Fulton, 1993). While *Naegleria* in its trophic form possesses a cellular actin cytoskeleton, during the ameboflagellate transformation, the actin cytoskeleton is completely degraded, and a tubulin cytoskeleton is constructed *de novo* inside the cell (Walsh, 1984; Misook & Joo Hun, 2001). The cell also constructs two fully functional flagella, complete with basal bodies and a cytoplasmic microtubule array (Fritz-Laylin & Cande, 2010).

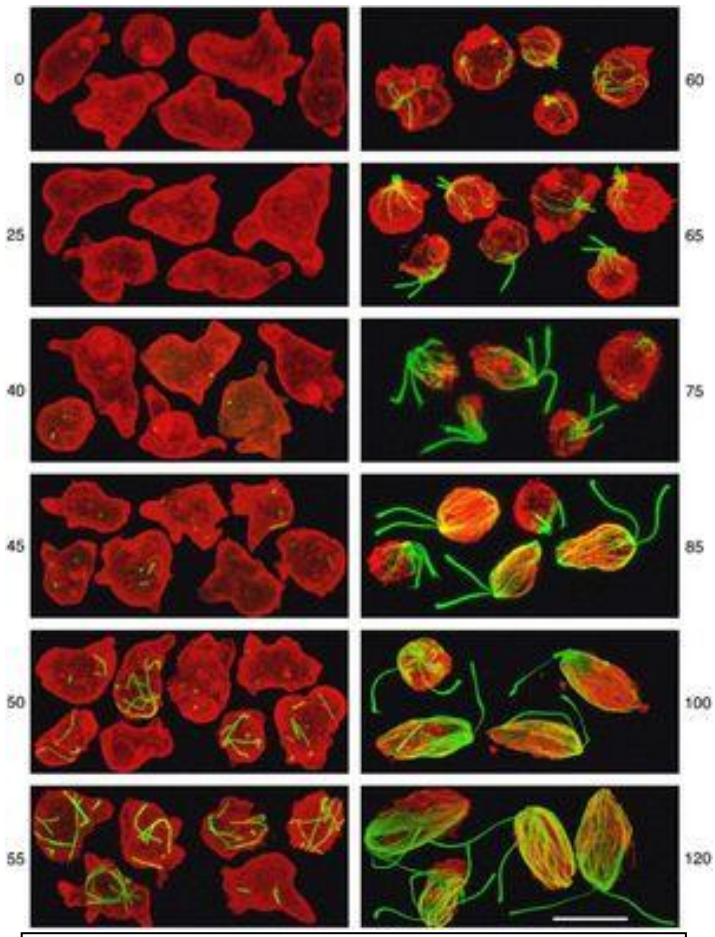

Figure 4: Fluorescence imaging of *N. gruberi* amoebaflagellate differentiation.

An electron micrograph showing the degradation of actin molecules (red) and the construction of the two flagella and the microtubule cytoskeleton (green) over the course of the ameboflagellate differentiation process, obtained from Walsh, 2007. The time in minutes is given next to each image.

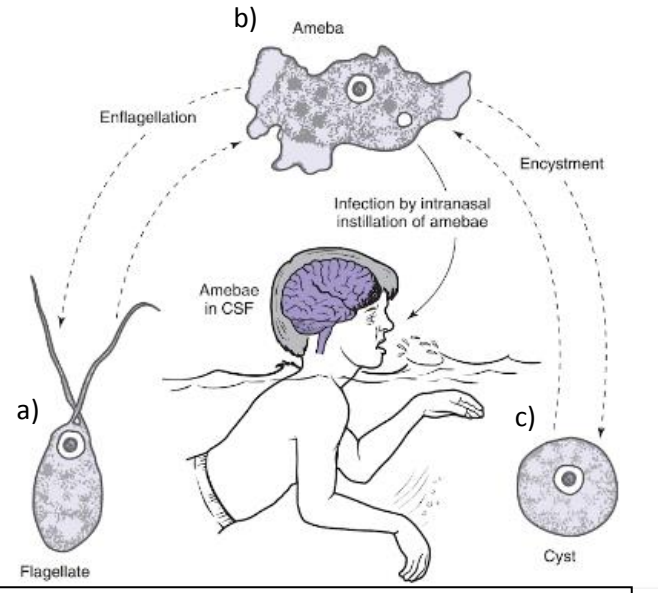

Figure 5: The potential life cycles of *Naegleria fowleri.*

An illustration depicting the three separate forms of N. fowleri; a) the flagellate form, b) the trophic amoeba form and c) the cyst form. Obtained from John, Petri, Markell & Voge, 2006.

Naegleria has 3 separate distinct life cycles as shown in figure 5 (John, Petri, Markell & Voge, 2006). The life cycle that each individual cell takes is entirely due to the environment it is located in. In a suitably habitable environment, *Naegleria* remain as amoebae in the trophic form and reproduce via asexual mitosis (De Jonckheere, 2014; Fulton, 1970; Fulton, 1993). During the amoeba stage of the life cycle, cells feed with a cell cycle time of ~1.6 hours dividing by binary fission (De Jonckheere, 2002). There is also some evidence supporting potential sexual reproductive capabilities of *Naegleria* in the form of the heterozygous tetraploid genomic nature of strain NEG-M (Fritz-Laylin et al., 2010). The genome encodes homologs of seemingly functional meiosis-specific genes (Fritz-Laylin et al., 2010) along with both hapless 2 (HAP2) and gamete expressed 1 (GEX1) gene homologs, utilised in cellular and nuclear fusion (Speijer D et al., 2015) though this has not yet been proven.

The second most commonly encountered life cycle stage of *Naegleria gruberi* is the cyst, which is found when *Naegleria* is placed under select environmental pressures. Cysts are spherical in shape and the cell is protectively contained within an endocyst made of two thick layers composed of a mucoid sheath (Chiovetti, 1976). Several adverse conditions are known to trigger the encystment of cells, including exposure to hazardous temperatures (Blackler and Sommerville, 1988). While in this form the cells are resistant to these environmental hardships. Thus, encystment is a defensive mechanism, built as a reaction to combat hostile environmental pressures and affords protection against desiccation (Chiovetti, 1976).

Finally, the flagellate life cycle of *Naegleria gruberi* is often the most short lived one. For amoeba to differentiate into the flagellates requires a lack of nutrition whilst being submerged in an aqueous environment (De Jonckheere, 2014). During this time the cells construct flagella which assist with locomotion and ultimately, the discovery of nutrients (Fulton, 1993; De Jonckheere, 2014). *N. gruberi* is able to build a complete microtubule cytoskeleton from scratch in a synchronous and highly regulated manner (Fritz-Laylin et al., 2010) and harbours novel putative genes associated specifically

with amoeboid motility (Fritz-Laylin, 2018). During the ameboflagellate differentiation, division by mitosis is impossible for most species of *Naegleria*. This infers that individual members of a population in this state must obtain a source of nutrition, in order to revert to an amoeba and continue to reproduce, otherwise the population will expire (De Jonckheere, 2014; Fritz-Laylin et al., 2010).

1.1.6 - *N. gruberi* as a model organism

Naegleria gruberi is used as a model organism when studying *Naegleria*. It is closely related to *N. fowleri*, which is at the heart of aforementioned health concerns, due to its fatal pathogenicity to humans. However, *N. gruberi* is non-pathogenic to humans, which results in an innocuous organism to work with and culture in a laboratory setting. *N. gruberi* subsists on easily cultured organisms such as the bact*eria Klebsiella pneumo*niae, shown in figure 6 (Fulton, 1993). *N. gruberi* also grows quickly in undefined media under easily replicable conditions and has a completely decoded whole genomic sequence, which allows for a much greater insight into the organism and its cellular components (Fritz-Laylin et al. , 2010).

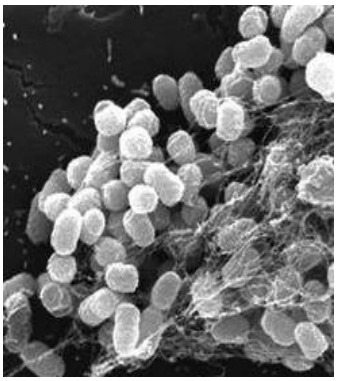

Figure 6: A previously published SEM image of *Klebsiella pneumoniae*.

An SEM image showing *Klebsiella pneumoniae*, the common nutrient source of xenic *N. gruberi*. Obtained from Alcántar-Curiel et al., 2013; Rajeshwari, Nagveni, Oli, Parashar & Chandrakanth, 2009.

As an ameboflagellate, *N. gruberi* makes for an excellent model in regard to basal body and flagellar assembly research, due to its ability to differentiate from crawling amoebae into swimming flagellates in a reproducible manner (Fritz-Laylin, Ginger, Walsh, Dawson & Fulton, 2011). This process has been investigated using microarray analysis to document the upregulation and downregulation of proteins over the course of the ameboflagellate transformation (Fritz-Laylin & Cande, 2010). The genomic analysis of the differentiation of *N. gruberi* reveals a multitude of vast transcriptional changes throughout this process which affect expression of genes involved in signaling, metabolism and stress responses, although the significance of many of these changes has yet to be given consideration (Fritz-Laylin & Cande, 2010).

1.2 - Environmental perception and intercellular signalling in eukaryotes

1.2.1 - G protein-coupled cell-surface receptors (GPCRs) and G proteins

When the genome of *N. gruberi* was sequenced, it was shown to contain a larger number of intracellular signaling proteins and metabolic pathways than would have originally been anticipated (Fritz-Laylin, Ginger, Walsh, Dawson & Fulton, 2011). Genome sequencing also revealed a multitude of sensory G protein coupled receptors (GPCRs) within *N. gruberi (*Fritz-Laylin et al., 2010).

G protein-coupled cell-surface receptors (GPCRs) are a family of seven-fold transmembrane receptor proteins with an extracellular N-terminus, that are found ubiquitously throughout eukaryotic cells (Dosil, Giot, Davis & Konopka, 1998; Preininger & Hamm, 2004). The GPCR family is one of the largest and most versatile families of signaling receptors (Mykytyn & Askwith, 2017). The tertiary structure forms a barrel shape, made of seven transmembrane α helices, which is typically found spanning the cell membrane (Dosil, Giot, Davis & Konopka, 1998; Dosil, Giot, Davis & Konopka, 1998; Preininger & Hamm, 2004). These cellular receptors variously respond to changes in the incident wavelengths of light, or bind a wide range of different ligands in both gaseous and solid form. These ligands include hormones (He, Zhu, Corbin, Plagge & Bastepe, 2015), neurotransmitters (Xie et al., 2015), chemokines (Robichaux et al., 2017), glycoproteins (Kim et al., 2013), odorants (de March, Kim, Antonczak, Goddard & Golebiowski, 2015), glucose (Karunanithi et al., 2014), lipids (Guéguinou et al., 2015; and photons (Gao et al., 2017).

GPCRs utilise sensory cues to regulate intracellular processes (Rosenbaum, Rasmussen & Kobilka, 2009), that are present throughout a wide range of eukaryotic organisms (Dosil, Giot, Davis & Konopka, 1998). G protein-coupled cell-surface receptors are observed in many different organisms including plants (Romero-Castillo, Roy Choudhury, León-Félix & Pandey, 2015; Trusov & Botella, 2016), mammals (Chatterjee et al., 2015; Arizmendi & Kulka, 2018) and unicellular eukaryotes (Shalaeva, Galperin & Mulkidjanian, 2015; Simon, Strathmann & Gautam, 1991). A prime example is the G protein-coupled receptor family 3 protein 8 (*GrlH)* gene product, which is an integral component of chemotaxis in social amoeba (also known as slime mould) *Dictyostelium discoideum* (Tang et al., 2018; Williams, Noegel & Eichinger, 2005; Xu & Jin, 2017). G protein coupled receptors are also known to be involved in developmental control, cellular growth and migration and other sensory processes such as density sensing and neurotransmission (Brazill, Lindsey, Bishop & Gomer, 1998; Bockaert & Pin, 1999; Pierce, Premont & Lefkowitz, 2002; Rosenbaum, Rasmussen & Kobilka, 2009).

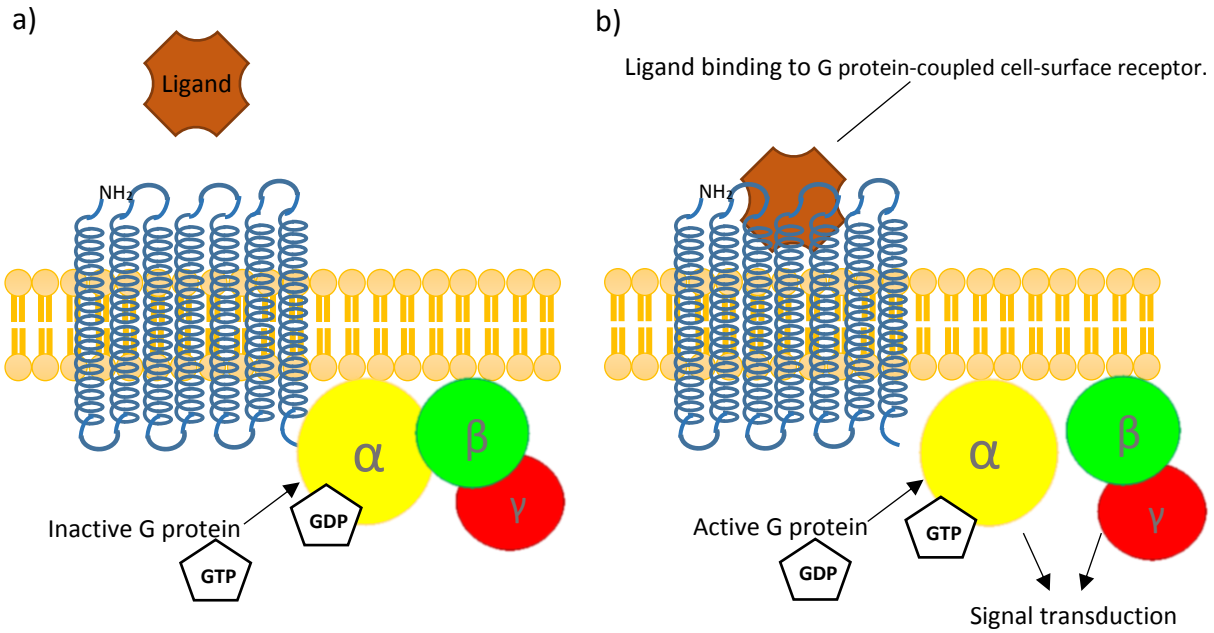

Figure 7: The mechanism of G protein-coupled cell-surface receptor activation.

An image depicting mechanism of G protein-coupled cell-surface receptor activation. The G protein-coupled cell-surface receptor (blue) is shown bound to the three G protein subunits α (yellow), β (green) and γ (red). a) The ligand (brown) has not yet bound to the GPCR, and the G protein is subsequently in the inactive GDP-bound state. b) The ligand has bound to the GPCR and the GTP has subsequently bound to the α subunit of the G protein. The resulting conformational change results in the release of the α subunit and the β and γ subunit heterodimer, both of which induce further intercellular signalling. Figure adapted from Flock et al., 2015 and Zhou et al., 2016.

1.2.2 - Signalling cyclases and kinases

Both guanylate cyclases and adenylate cyclases are members of the class III nucleotidyl cyclase group (Rauch, Leipelt, Russwurm & Steegborn, 2008). Adenylate cyclases are key regulatory enzymes found thus far in all eukaryotic cells (Hancock, 2010). Typically, in their classic form, when the α subunit of the active adenylate cyclase is released, its active site utilises a metallic ion, usually in the form of a magnesium ion, to catalyse the conversion of adenosine triphosphate (ATP) to 3', 5' cyclic adenosine monophosphate (cAMP) for further cell signalling (Neil, Lakey & Tomlinson, 1985; Herbst et al., 2013). The cAMP molecule acts as a prototypical, secondary messenger and is central to regulating hormone responses and signal transduction throughout the cell (Zhang, Liu, Ruoho & Hurley, 1997; Neil, Lakey & Tomlinson, 1985).

Guanylate cyclases are transmembrane enzymes that are also found in many eukaryotes (Rauch, Leipelt, Russwurm & Steegborn, 2008). In contrast to most adenylate cyclases, the guanylate cyclases contain both external and internal cellular domains, eliminating the need for GPCRs to receive external stimuli (Potter, 2011). In the active state, two guanylate cyclase proteins typically bind to form a homodimer (Potter, 2011). In this form, guanylate cyclase catalyzes the degradation of guanosine triphosphate (GTP) to 3', 5'-cyclic guanosine monophosphate (cGMP) and pyrophosphate. cGMP is an important secondary messenger that modulates processes including; platelet aggregation, neurotransmission, blood pressure and peristalsis (Potter, 2011).

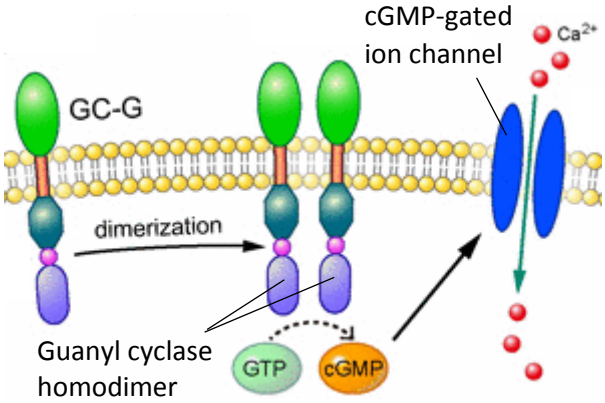

Figure 8: Guanylate cyclase activation.

An image illustrating the process of guanylate cyclase dimerization and cGMP synthesis, followed by subsequent activation of cGMP-gated ion channels. Retrieved from Chao, Chen, Lin, Breer, Fleischer & Yang, 2014.

Naegleria houses a much larger number of adenylate cyclases and guanylate cyclases than originally predicted (Fritz-Laylin et al., 2010). *N. gruberi* contains at least 108 cyclases, which is almost twice the number found in the human genome and is likely able to utilise both the cAMP-dependent signaling pathway and the two component signaling pathway due to the use of adenyl/guanyl cyclases and histidine kinases (Fritz-Laylin et al., 2010; Kabbara et al., 2018). Many of these cyclase proteins are thought to contain predicted Per-Arnt-Sim (PAS), nitrate and nitrite sensing (NIT) and blue-light using FAD (BLUF) functional domains to bind ligands or detect changing light intensity (Fritz-Laylin et al., 2010). The adenyl cyclase cohort in *Naegleria* is much larger than the number of adenyl cyclases found

in related organisms (Fritz-Laylin et al., 2010), which is of interest as the *Naegleria* cohort includes a diverse number of different sensory domains (Winger, Derbyshire, Lamers, Marletta & Kuriyan, 2008; Fritz-Laylin et al., 2010). PAS domains have several intercellular chemosensory capabilities (Garcia, Orillard, Johnson & Watts, 2017), and function in intracellular energy regulation (Söderbäck et al., 2002; Rebbapragada et al., 1997). NIT domains are primarily associated with the detection of changing nitrate ($NO^-_{3)}$ or nitrite (NO^-_2) concentrations (Shu, Ulrich & Zhulin, 2003). BLUF domains act as a sensory photoreceptor and are responsible for the detection of light intensity (Iseki et al., 2002; Masuda & Bauer, 2002).

The predicted signalling network of *Naegleria* also includes a large number of histidine kinases (Kabbara et al., 2018; Fritz-Laylin et al., 2010). Histidine kinases are a large family of transmembrane phosphotransferases that play a role in signal transduction across the cell membrane via autophosphorylation of conserved histidine residues (Koretke, Lupas, Warren, Rosenberg & Brown, 2000; Mechaly et al., 2017). Reversible phosphorylation of signaling proteins is one of the most widespread regulatory signal transduction mechanisms (Casino, Miguel-Romero & Marina, 2014). Histidine kinases are usually homodimers which consist of three separate domains. The extracellular domain binds to specific extracellular hormones (Wang, Cheng, Wu, Ren & Qian, 2017) or growth factors (Xu et al., 2016). The conserved hydrophobic transmembrane domain anchors the protein to the cell membrane (Kim et al., 2017). The intercellular domain induces intracellular signalling by utilising ATP to induce a conformational change in G proteins (Casino, Miguel-Romero & Marina, 2014; Willett & Crosson, 2016).

1.3 - Cilia and flagella as sensory antennae

1.3.1 - Structure of flagella and cilia

Microorganisms have been under scientific observation since the mid-1600s due to emergence of the optical lenses necessary for such work (Wollman, Nudd, Hedlund & Leake, 2015; Chung & Liu, 2017). One of the first scientists to both observe and document their findings in this manner was Robert Hooke, who coined the term 'Cell' in his Micrographia (Hooke, 1665; Chung & Liu, 2017). It was not until 1676-1677 that the first flagella were observed and documented as 'thin little feet, or little legs' by Antonie van Leeuwenhoek upon his observation of *Colpidium colpoda* (Lane, 2015). Leeuwenhoek was one of the first individuals to culture, see, and describe a large array of microbial life including *Vorticella*, *Giardia*, *Euglena* and *Selenomonas* (Lane, 2015; Antony van Leeuwenhoek, 2019; Discovery Of Bacteria - by Antony van Leeuwenhoek, 2019; Chung & Liu, 2017) and widely regarded as 'The Father of Microbiology' (Haimo & Rosenbaum, 1981; Lane, 2015; Wollman, Nudd, Hedlund & Leake, 2015). Flagella and cilia are complex cellular organelles which share the same fundamental structure, however they are typically divergent in size, quantity and function (Lodish et al., 2000). Typically, cells possessing flagella only contain a single or several long flagella, whereas ciliated cells tend to contain numerous smaller cilia (Lodish et al., 2000). Eukaryotic flagella form long, slender, hair-like, cylindrical cellular protrusions that emanate from the cell membrane as shown in figure 9 (Ainsworth, 2007; Szymanska & Johnson, 2012). The flagellum contains a complex highly conserved cytoskeletal structure known as the axoneme, which is responsible for cellular locomotion (Mitchell, 2004; Lodish et al., 2000; Ostrowski, Dutcher & Lo, 2011).

With regards to structure of cilia, there are two different types of cilia, primary cilia and non-primary cilia (Mitchell, 2004, Gluenz et al., 2010). Primary cilia have a structural variation of the axoneme as the central two microtubules are missing, creating a 9+0 axoneme as seen in figure 9. Dynein is usually absent from these cilia, which as a consequence tend to be incapable of undulation, instead the 9+0 axoneme is mainly found in cilia with sensory roles (Gluenz et al., 2010). By comparison non-primary cilia and flagella house the more classically observed 9+2 arrangement, shown in figures 9 and 10 (Mitchell, 2004).

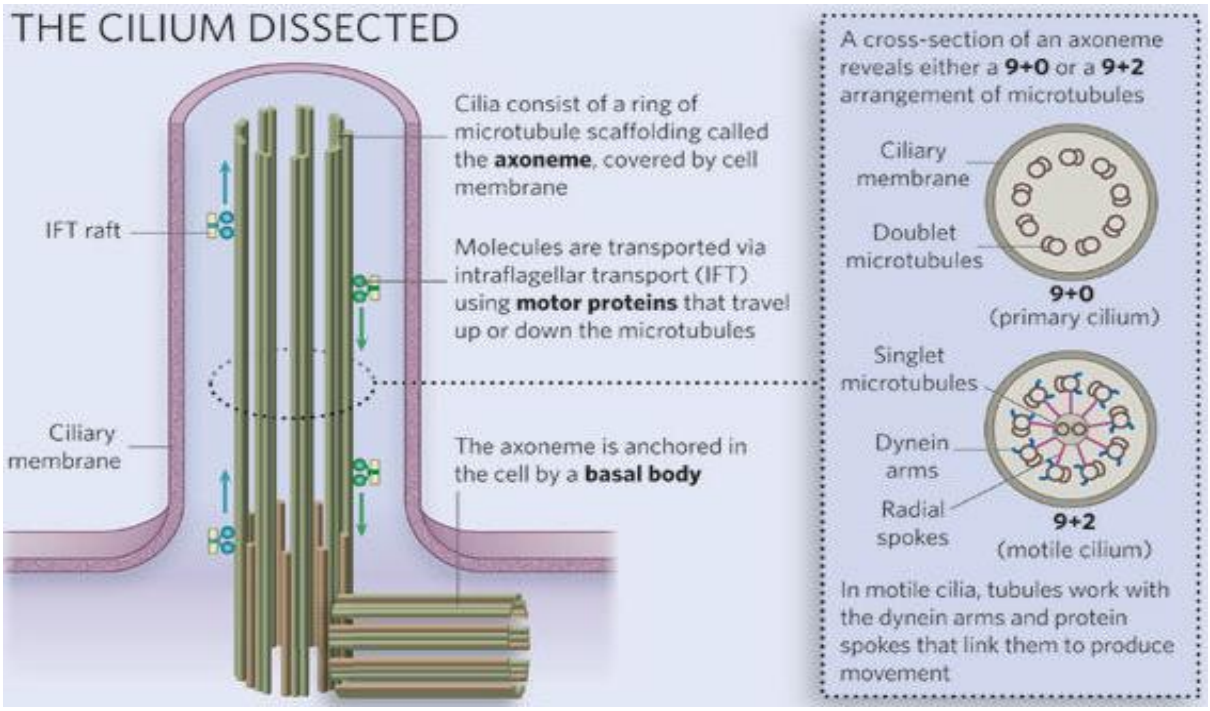

Figure 9: The Internal structure of the primary cilium.

A basic illustration of an isometric bisection of a typical primary 9+0 cilia, with a show of the intraflagellar transport system. Displayed inset is a cross-section of both a motile and non-motile cilial axoneme. Obtained from Ainsworth, 2007.

The bacterial flagellum is constructed of fewer than 30 different proteins (Morimoto & Minamino, 2014; Moran, McKean & Ginger, 2014). By comparison, the eukaryotic flagellum is a far more complex organelle, instead utilising hundreds of proteins for its construction and subsequent function (Diniz, Pacheco, Farias & De Oliveira, 2012; Moran, McKean & Ginger, 2014). As basal body construction is initiated, the protein spindle assembly abnormal protein 6 (SAS-6) readily forms homodimers which assemble into a ring-like structure, from which extends coiled-coil domains of the SAS-6 dimers (Breugel, Wilcken, McLaughlin,

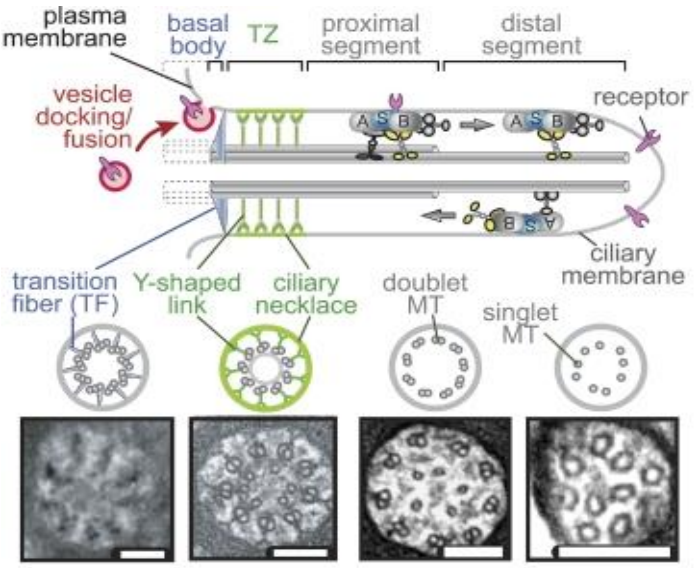

Figure 10: A cross section along the length of the cilium.

An illustration displaying the microtubule structure across the length of the cilia, including the basal body and transition zone. Intraflagellar transport proteins are shown along the cilia and inset images show electron microscopy images of cross sections within each area . Obtained from Williams et al., 2011.

Rutherford & Johnson, 2014). This results in the formation of the centriolar hub, a cartwheel shaped structure with ninefold symmetry which is established as the proximal end of the flagella. If SAS-6 is not present, the assembly of the centriolar hub fails (Nakazawa, Hiraki, Kamiya & Hirono, 2007; Moran, McKean & Ginger, 2014). Following basal body biogenesis and transition zone extension, intraflagellar transport (IFT) proteins are utilised along with kinesins in axoneme extension as shown in figure 10 (Deane, Cole, Seeley, Diener & Rosenbaum, 2001).

Bardet–Biedl syndrome (BBS) proteins form the BBSome, an eight-membered protein complex recruited to form a portion of the basal body by the G-protein ADP ribosylation factor like GTPase 6 (Arl6) (Jin & Nachury, 2009; Jin et al., 2010; Klink et al., 2017). The IFT pathway utilises IFT and BBSome protein assemblies, which exploit motor proteins to produce anterograde and retrograde movement of molecular cargo up and down the axonemal microtubules to the flagellar tip (Moran, McKean & Ginger, 2014; Prevo, Scholey & Peterman, 2017).

1.3.2 - Sensory functions

There are numerous functions besides movement that can be carried out by flagella, examples being active roles in eukaryotic reproduction (Wood, Huang, Diener & Rosenbaum, 2013), cellular feeding or chemical recognition (Moran, McKean & Ginger, 2014). Furthermore, a large subset of primary cilia, which have no use for locomotion, and some eukaryotic flagella fill a primary role as a cellular signaling organelle (Bloodgood, 2010; Mykytyn & Askwith, 2017; Nechipurenko, Doroquez & Sengupta, 2013). Cillia are found in a sensory capacity in the renal system (Pluznick & Caplan, 2014; Praetorius & Leipziger, 2013), the retina (Li, Anand, Rao & Khanna, 2015; Wheway, Parry & Johnson, 2013). stereocilia and within the ear (Gillespie & Müller, 2009; Jones & Chen, 2008; Tucker, et al., 2013) Furthermore, flagella have been documented to contain adenyl cyclase mediated cAMP signaling systems for social motility in *Trypanosoma brucei* (Lopez, Saada & Hill, 2014; Saada, DeMarco, Shimogawa & Hill, 2015). Cilia perform vastly different functions, and are thought to be expressed in almost every cell type throughout the human body at some point over the course of its life cycle (Ostrowski, Dutcher & Lo, 2011). As such there are a number of complications that can occur when cilia behave in an erroneous manner (Barker, Thomas & Dawe, 2013).

1.3.3 - Ciliopathies

Genetic abnormalities can give rise to defects in both primary and motile cilia, these defects underpin many genetic conditions termed ‘ciliopathies’ (Barker, Thomas & Dawe, 2013; Sloboda & Rosenbaum, 2007). Due to the ubiquitous nature of the ciliary axoneme and its wide-ranging application within eukaryotes, there are a wide variety of ciliopathies which stem from genetic defects of ciliary assembly

or function (Moran, McKean & Ginger, 2014; Wang & Dong, 2013; Ostrowski, Dutcher & Lo, 2011). The underlying pathology of these diseases is usually a consequence of altered sensory perception, or lack of a cellular signalling pathway (Sloboda & Rosenbaum, 2007; Moran, McKean & Ginger, 2014). Examples of ciliopathies include retinitis pigmentosa, Bardet-Biedl syndrome, Kartagener's syndrome, cone-rod degeneration and many others (Li, Anand, Rao & Khanna, 2015; Sloboda & Rosenbaum, 2007). Ciliopathies are also thought to have the potential to cause a predisposition to chronic disorders including cancer, obesity and diabetes (Sloboda & Rosenbaum, 2007; Moran, McKean & Ginger, 2014).

1.4 - The aims of this MSc Thesis

The ultimate aim of this thesis, and the studies within, was to progress towards elucidating the mechanisms behind flagella as sensory antennae, by further understanding the way in which *Naegleria* perceives its environment.

This originally began with the purification of several recombinant proteins of interest, which are thought to be potential sensory proteins. The goal here was to localise these proteins to confirm whether they will congregate within the flagella as expected. This work will need to be continued by another researcher in the future.

Due to the large signalling repertoire of *Naegleria gruberi*, the bioinformatic analysis of a pre-existing RNA microarray was carried out. The aim here was to highlight potential serpentine receptor signalling proteins that are upregulated during differentiation, as understanding how they are upregulated may be useful in understanding the sensory function of flagella in future.

During this time, the environmental differentiation and SEM experiments were also carried out. These experiments were designed to probe which sensory triggers were conducive to differentiation, in order to better understand the underlying sensory proteins involved.

Furthering the understanding of which sensory proteins are responsible for differentiation provides an insight into how this organism is able to utilise the flagellum as a sensory organelle. This is important, as the mechanisms behind sensory cilia can cause ciliopathies and other chronic diseases. This work also contributes to the greater understanding of *N. gruberi* and by extension the deadly pathogen *N. fowleri*.

Chapter 2: Materials and Methods

2.1 - General lab practice

For further information about the equipment and materials used, consult table 5 in the appendix.

2.1.1 - Preparing a kanamycin stock

A 1000x master stock of kanamycin was prepared by adding 1 g of kanamycin powder to 20 ml ddH2O in a 50 ml centrifuge tube. This was inverted gently until fully dissolved to achieve a concentration of 50 mg/ml. This stock was used at a ratio of 1:1000.

2.1.2 - Preparation of LB media

25 g of high salt lysogeny broth (LB) was suspended in 1000 ml of ddH_2O in a 1 L Schott bottle. This was then autoclaved at 126 °C and 1.4bar for 26 mins and left to cool. The broth was distributed as desired under sterile conditions.

2.1.3 - Preparation of LB agar plates

16 g of granulated Miller LB agar was weighed and added to 400 ml ddH_2O in a 500 ml Schott bottle, before being autoclaved at 126 °C and 1.4bar for 40 mins. After autoclaving the agar was removed and left to cool enough to be handled. 20mmx90mm Petri plates were placed on a bench by a Bunsen burner, using aseptic technique the LB agar was poured into the plates with a volume of 12 ml per plate.

2.1.4 - Preparation of amoeba saline agar plates

2.5 ml of AS stock 1 and 2.5 ml of AS stock 2 were added to 495 ml of ddH_2O in a 500 ml Schott bottle. 7.5 g of Agar No. 2 was added to the bottle before being autoclaved at 126 °C and 1.4bar for 40 mins. After autoclaving the agar was removed and left to cool enough to be handled. 20mmx90mm Petri plates were placed on a bench by a Bunsen burner, using aseptic technique the LB agar was poured into the plates with a volume of 12 ml per plate.

2.1.5 - Maintaining *Naegleria gruberi* Cultures

Klebsiella pneumoniae was used as the primary food source for *Naegleria*. LB Agar plates were prepared and seeded with *Klebsiella* using aseptic technique and a disposable sterile loop. The plates were then incubated overnight at 25 °C to allow the bacterial lawn to grow.

Amoeba saline plates were prepared, and the bacterial lawn was transferred to the amoeba saline plate using aseptic technique and a sterile spreader. A section of the previous *N. gruberi* plate was then excised and transferred to the freshly seeded amoeba saline plate with the amoeba containing side placed face down on the edge of the bacterial lawn.

2.1.6 - Picking colonies and preparing overnight cultures

Using aseptic technique, 4 ml of LB media was added to universal tubes along with 40 µl of 100x ampicillin stock solution. Ampicillin plates from previous transformations were removed from the incubator and the colonies were picked using aseptic technique with sterile pipette tips and placed into universal tubes containing 4 ml of LB media with added ampicillin. The universal tubes were then placed into a shaking orbital incubator set to incubate overnight at 37 °C spinning at 180 rpm.

2.1.7 - Initial protein induction

Glycerol stock solutions of *E. coli,* which expressed the proteins of interest, were kept at -80 °C. They were streaked onto an LB agar plate containing Kanamycin, using aseptic conditions, before being incubated at 37 °C overnight. 3 ml cultures of LB media with added kanamycin were prepared and individual colonies were picked from the plates and grown in in an orbital incubator overnight at 37 °C and 180 rpm. The plates were stored at 4 °C. 100 µl of each of the 3 ml cultures was taken and added to 3 ml of LB media without kanamycin under aseptic conditions. 30 µl of 10 mM Isopropyl β-D-1-thiogalactopyranoside (IPTG) was then added to each culture. 100 µl samples were taken at timepoint 0 (T0) when the clock began and before the IPTG was added, then at each subsequent hour for 3 hours (T1, T2 + T3) and kept at -20 °C.

2.1.8 - Preparing 1x sodium dodecyl sulfate (SDS) loading buffer

500 µl 2xSDS, 400 µl 1x Phosphate-buffered saline (PBS) and 100 µl Dithiothreitol (DTT) (1M) were added to an Eppendorf tube before being inverted several times and boiled on a heating block before use.

2.1.9 - Preparing 2xSDS loading buffer

800 µl of 2xSDS loading buffer and 200 µl DTT (1M) were added to an Eppendorf tube before being inverted several times and boiled on a heating block before use.

2.1.10 - Preparing samples for running on an SDS polyacrylamide gel electrophoresis (PAGE) gel

The 100 µl T0-T3 samples were spun in a bench top centrifuge at 8,000g for 2 mins. The supernatant was discarded, and the pellet was resuspended in 100 µl of boiling 1xSDS loading buffer. 15 µl of the sample was then added to the SDS PAGE gel wells while boiling.

2.1.11 - Preparing 5x SDS running buffer

15.1 g of tris(hydroxymethyl)aminomethane (TRIS) and 94 g of Glycine was dissolved in 900 ml ddH_2O using a magnetic stirrer. 25 ml of 20% SDS was added and the solution was made up to 1 L with ddH_2O in a measuring cylinder before being transferred to a 1 L Schott bottle for storage.

2.1.12 - Sodium Dodecyl Sulfate Polyacrylamide Gel Electrophoresis

In order to prepare 10 ml of the SDS PAGE stacking gel, the following reagents were added to a sterile 50 ml falcon tube;

ddH_2O	- 5,975 µl
30% acrylamide mix	- 5,000 µl
1.5 M Tris solution (pH8.8)	- 3,800 µl
20% SDS	- 75 µl

A 15% ammonium persulphate (APS) stock was then made by adding 0.15 g of ammonium persulphate to 1 ml of ddH_2O in an Eppendorf tube before inverting until fully dissolved.

The short and long plates from the Bio Rad SDS PAGE kit were assembled in a frame and checked for potential leaks using 1 ml of ddH_2O. The frame was then dried and 150 µl APS and 6 µl of tetramethylethylenediamine (TEMED) was added to the 50 ml falcon tube.

The solution was inverted twice to mix and quickly pipetted between the plates leaving enough room for the resolving gel. 1 ml of Isopropanol was also added to make the stacking gel level before it had set. Once the gel had set, the Isopropanol was removed from the top of the gel by washing with ddH_2O.

The resolving gel was made by mixing the following components in a 15 ml falcon tube;

ddH_2O	- 3,400 µl

30% acrylamide mix	- 830 µl
1.5M Tris solution (pH8.8)	- 630 µl
20% SDS	- 50 µl
Ammonium persulphate stock	- 50 µl
TEMED	- 6 µl

The mixture was inverted twice and quickly pipetted over the top of the gels until the short plate had been filled to the brim. Then the comb from the Bio Rad SDS PAGE kit was then placed between the two plates and the resolving gel was allowed to set. Once the resolving gel had set, the comb was removed, and the wells left behind were washed with ddH_2O to remove any pieces of gel in the wells.

The gels were fully submerged in 1xSDS running buffer in a Biorad PAGE unit and the samples were loaded into each well.

The negative and positive wires for the anode and cathode were plugged into the corresponding terminals on the Biorad Powerpac™ which was programmed to run at 200 V for 50 mins. The gels were removed and placed into a clean plastic container with 7 ml of instant blue dye, which was left on a shaker to stain for 20 mins. The gel was then placed in an Ultraviolet Benchtop Transilluminator with a white background panel to be imaged under white light.

2.1.13 - Small-scale protein induction

Glycerol stock solutions of *E. coli* which expressed the proteins of interest were kept at -80 °C. They were streaked onto an LB agar plate containing Kanamycin using aseptic conditions before being incubated at 37 °C overnight. 3 ml cultures of LB media with added kanamycin were prepared and individual colonies were picked from the plates and grown in in an orbital incubator overnight at 37 °C and 180 rpm. The plates were stored at 4 °C.

100 µl of each of the 3 ml cultures were taken and added to 3 ml of LB media without kanamycin under aseptic conditions. 30 µl of 10 mM IPTG was then added to each culture. Samples were taken before the IPTG was added (T0) and then at each subsequent hour for 3 hours (T1, T2 + T3). These samples were then prepared and run on an SDS PAGE gel to ensure that correct protein expression was observed.

2.1.14 - Large-scale protein induction

100 ml of LB media was prepared in a 200 ml Schott bottle and autoclaved. Once cool 20 ml was transferred to a large falcon tube and an appropriate antibiotic was added. This culture was then inoculated with a single colony from the glycerol stock plate and incubated overnight in an orbital

shaking incubator at 37 °C at 180 rpm. 2x600 ml LB solutions were also prepared in large baffled conical flasks and autoclaved.

The 20 ml cultures were then decanted into the 2x600 ml LB media flasks using aseptic technique and incubated in an orbital incubator at 37 °C at 180 rpm for 2hours after which point 100 µl of the culture was kept for future trouble shooting.

Protein production of both cultures was then Induced through addition of 1 mM IPTG using 1 µl IPTG per 1 ml of culture using a 1 M IPTG stock. The cultures were then incubated for a further 3 hours. After the incubation, the cultures were centrifuged at 8,000g for 25 minutes at 4 °C. The supernatant was then discarded and the pelleted cells were scraped into a new falcon tube using a sterile spatula and stored at -20 °C ready for Ni NTA purification.

2.1.15 - Preparation of lysis buffer for Nickel Nitrilotriacetic acid (Ni NTA) protein purification under denaturing conditions

286.5 g of guanidine hydrochloride, 14.6 g of sodium chloride and 0.68 g of imidazole were added to a 500 ml Schott bottle with 10 ml of 1 M Tris-HCl stock (pH 8.0), 0.1 ml Tritin-X, 50 ml glycerol and 300 ml ddH_20 and mixed until fully dissolved. ddH_20 was added until the volume was 500 ml and thoroughly filtered before use.

2.1.16 - Preparation of wash buffer for Ni NTA protein purification under denaturing conditions

240.2 g of urea, 14.6 g of sodium chloride and 0.68 g of imidazole were added to a 500 ml Schott bottle with 10 ml of 1 M Tris-HCl stock (pH 8.0), 0.1 ml Tritin-X, 50 ml glycerol and 300 ml ddH_20 and mixed until fully dissolved. ddH_20 was added until the volume was 500 ml and thoroughly filtered before use.

2.1.17 - Preparation of elution buffer for Ni NTA protein purification under denaturing conditions

240.2 g of urea, 14.6 g of sodium chloride and 17.02 g of imidazole were added to a 500 ml Schott bottle with 10 ml of 1 M Tris-HCl stock (pH 8.0), 0.1 ml Tritin-X, 50 ml glycerol and 300 ml ddH_20 and mixed until fully dissolved. ddH_20 was added until the volume was 500 ml and thoroughly filtered before use.

2.1.18 - Preparation of lysis buffer for Ni NTA protein purification under native conditions

8.76 g of sodium chloride and 0.34 g of imidazole were added to a 500 ml Schott bottle with 10 ml of 1 M Tris-HCl stock (pH 8.0), 0.1 ml Tritin-X, 50 ml glycerol and 300 ml ddH_20 and mixed until fully dissolved. ddH_20 was added until the volume was 500 ml and mixed thoroughly.

2.1.19 - Preparation of wash buffer for Ni NTA protein purification under native conditions

8.76 g of sodium chloride and 0.68 g of imidazole were added to a 500 ml Schott bottle with 10 ml of 1 M Tris-HCl stock (pH 8.0), 0.1 ml Tritin-X, 50 ml glycerol and 300 ml ddH_20 and mixed until fully dissolved. ddH_20 was added until the volume was 500 ml and mixed thoroughly.

2.1.20 - Preparation of elution buffer for Ni NTA protein purification under native conditions

8.76 g of sodium chloride and 17.02 g of imidazole were added to a 500 ml Schott bottle with 10 ml of 1 M Tris-HCl stock (pH 8.0), 0.1 ml Tritin-X, 50 ml glycerol and 300 ml ddH_20 and mixed until fully dissolved. ddH_20 was added until the volume was 500 ml and mixed thoroughly.

2.1.21 - Ni NTA purification

The cell pellet was resuspended in 20 ml denaturing/native lysis buffer (depending on the protein) and agitated on a shaker at room temperature for 30 minutes. 200 µl of 100 mM phenylmethylsulfonyl fluoride (PMSF) was added to the sample, which was then sonicated for 10 mins with 5 seconds on and 15 seconds off at an amplitude of 95%. The sample was centrifuged at 20,000 rpm for 30 mins at 4 °C and the supernatant was retained.

A small amount of glass wool was placed at the bottom of a 20 ml syringe and the His affinity suspension was inverted until homogeneous. The bottom of the syringe was capped and 1 ml of the affinity suspension was transferred into the syringe and allowed to settle by gravity. Any clear supernatant was then removed. 2.5 ml of lysis buffer was added and the top of the syringe was capped so that the slurry could be inverted to equilibrate the resin, which was left to settle by gravity again.

20 ml of supernatant was added to the syringe and incubated at room temperature on a shaker for 1 hour. The flow-through was collected in a falcon tube and labeled as the ‘flow-through’ fraction.

Using a new falcon tube to collect the run off, the column was washed with 5 ml Wash buffer. This was repeated 3 times. The bottom of the syringe was capped and 0.5 ml Elution buffer was added. The syringe was incubated for 15 mins at room temperature on a shaker and an Eppendorf tube was used to collect the elution fraction. This was repeated 4-5 times using 0.5 ml Elution buffer each time. All fractions were stored at -20 °C.

2.1.22 - Preparation of AS stock 1

A litre of the first amoeba saline stock was prepared by adding 24 g of NaCL, 0.8 g of $MgSO_4$ and 1.2g $CaCl_2$ to a 1 litre Schott bottle. The bottle was then filled to the 1 L mark with ddH_2O and mixed until the particulates had completely dissolved.

2.1.23 - Preparation of AS stock 2

A litre of the second amoeba saline stock was prepared by adding 28.4 g of Na_2HPO_4 and 27.2g KH_2PO_4 to a 1 litre Schott bottle. The bottle was then filled to the 1 L mark with ddH_2O and mixed until the particulates had completely dissolved.

2.1.24 - Preparation of AS solution for differentiation

In order to prepare AS solution for differentiation, 50 ml of AS solution was prepared by mixing 250 µl of AS stock 1 and 250 µl of AS stock 2 in a 50 ml falcon tube. Then using ddH_2O the amount was topped up to 50 ml. A larger amount can also be made by mixing 5 ml stock 1 and 5 ml stock 2 with 990 ml ddH2O and autoclaving.

2.2 - Differentiation

2.2.1 - Preparing *Naegleria gruberi* differentiation plates

Klebsiella pneumoniae was used as the primary food source for *Naegleria*. An LB Agar plate was prepared and seeded with *Klebsiella* using aseptic technique and a disposable sterile loop. The plate was then incubated overnight at 25 °C to allow the bacterial lawn to grow. An amoeba saline plate was prepared, and half of the bacterial lawn was transferred to the amoeba saline plate using aseptic technique and a sterile, disposable spreader. A section of the previous *N. gruberi* plate was then excised and transferred to the outermost seeded area of the amoeba saline plate lawn using aseptic technique.

2.2.2 - Observation and selection of cells

The plate was incubated overnight at 25 °C, until the advancing amoebae had spread to a point that it had left behind a visibly clear section of consumed bacterial lawn, which covered at least a third of the plate. The cells were observed under a microscope and areas were marked out where the cells had consumed all of the bacteria but had not yet undergone encystment. A 1 cm x 0.5 cm chunk of the plate was excised and transferred, using aseptic technique, into an Eppendorf tube for each condition to be tested.

2.2.3 - Differentiation procedure

The cells in each of the Eppendorf tubes were washed by pipetting 1 ml of AS solution kept at room temperature into the Eppendorf tubes. These samples were vortexed for several seconds to separate the food source from the *Naegleria* cells. This was considered to be 'Timepoint 0' (T0). The cells were immediately placed into a benchtop centrifuge and synchronously spun at 1,800 rpm for 2 mins.

It was important that the cells were left in the pelleted state for as little time as possible, so the supernatant was then immediately discarded by simply inverting the Eppendorf above a discard bucket and allowing the supernatant to pour out. With immediacy in mind, 1 ml of AS was then added to the Eppendorf tubes and the tubes were vortexed again to resuspend the *Naegleria* cells in a food deficient environment.

The cells were then pooled together in a small Petri dish and 1 ml of the cell suspension was mixed with 1 ml AS solution in the small Petri dishes. At this point toxins/nutrients were added to the Petri dishes or the dishes were placed in different environments depending on the experimental procedure.

2.2.4 - Differentiation cell counting

The smaller Petri dishes were placed under a microscope at x40 magnification. The cells were counted using three separate hand tally counters to count cells at the three different stages of differentiation. The cells were counted either as 'non-flagellates' which describes normal ameboid cells, 'spinners' which describes the transitory stage when the cells are capable of movement, but the flagella are not fully formed (which results in a spinning motion) or 'swimmers' which describes cells that have fully differentiated and move in a specific direction.

In order to count the cells, the microscope focus was zoomed out completely, the plate was moved into a position where a random section of the sample was observed and the focus was moved inwards with each cell being counted along the way. When all of the cells in the small 'cross-section' had been counted the results could be recorded if over 100 cells had been counted in total, otherwise a new cross-section was counted, and the total scores added. The time of each count was taken and the results were kept in order to build excel graphs of the differentiation patterns under different environmental stresses.

2.2.5 - Sodium azide experiments

1 µl and 10 µl of 0.1 M sodium azide solution were pipetted into the smaller Petri dishes containing 2 ml AS solution along with control dishes containing no sodium azide.

2.2.6 - Sodium Nitrate + Sodium Nitrite plates

1 M stock solutions of sodium nitrate and sodium nitrite were prepared by adding 85mg sodium nitrate and 69mg sodium nitrite to separate Eppendorf tubes containing 1 ml ddH_20. From these 1 M stock solutions 2 µl and 20 µl were pipetted into the 2 ml Petri dishes to create 1 µM and 10 µM conditions respectively.

2.2.7 - Foetal bovine serum (FBS) experiments

100 µl FBS was added to 900 µl of ddH_2O to create a tenfold dilution. 20 µl of the FBS dilution was added to plates containing 2 ml to create a 1% FBS v/v differentiation environment. 4 µl of the FBS dilution was added to different plates containing 2 ml to create a 0.2% FBS v/v differentiation environment.

2.2.8 - Glucose experiments

18 mg of glucose was added to 1 ml ddH_2O to create a 10% glucose stock solution. 20 µl of the solution was added to the small Petri dish to give a 1% glucose concentration.

2.2.9 - Anaerobic and microaerophilic CO_2 rich environments

To prepare low O_2 environments both Anerogen™ compact and Campygen™ compact sachets were used as detailed in table 5. The sachets were added to a sealed bag for 15 minutes during sample plate preparation. After this time, the plates containing the cells and experimental conditions were placed in the same bag and it was re-sealed to maintain the low O_2 environment. During cell counting, the bags remained sealed until motion in other samples was observed, the bags were then opened and cells in each environment were counted, which gave rise to some delayed data collection.

2.2.10 - TWEEN20 (polyoxyethylenesorbitan, monolaurate) experiments

100 µl TWEEN20was added to 900 µl of ddH_2O to create a tenfold dilution. 20µl of the TWEEN20 dilution was added to plates containing 2 ml to create a 1% TWEEN20 v/v differentiation environment. 4 µl of the TWEEN20 dilution was added to different plates containing 2 ml to create a 0.2% TWEEN20 v/v differentiation environment.

2.2.11 - Differentiation data processing

In order to process the differentiation data, an excel spreadsheet was created. A table was created to record the results of each experiment as seen in figure 11a.

The results were then recalculated to show the swimmer, spinner and non-flagellate *Naegleria* counted in each stage as a percentage of the population.
The percentage population data was plotted into scatter graphs to give a comparative visual indication of the changes in population over time. Non-flagellate data is shown as a dashed line with triangular data points, the spinner data is shown as a dotted line with circular data points and the swimmer data is shown as an unbroken line with square data points. The results for each condition are differentiated by colours located in the legend, as shown in figure 11c.

After this, a second set of scatter graphs were created that directly compared the effects of each experimental condition as shown in figure 11d.

a)

Data timepoint	Time (mins)	Conditions	Non-flagellate	Spinners	Swimmers
T1	0	0.2%FBS	100		
	0	1%FBS	100		
	0	0.2%FBS anerogen	100		
	0	1%FBS anerogen	100		
	0	0.2%FBS campygen	100		
	0	1%FBS campygen	100		
T2	30	0.2%FBS	49	52	11
	34	1%FBS	43	31	19
	38	0.2%FBS anerogen	23	20	59
	42	1%FBS anerogen	57	21	26
	46	0.2%FBS campygen	19	32	56
	50	1%FBS campygen	32	43	56

b)

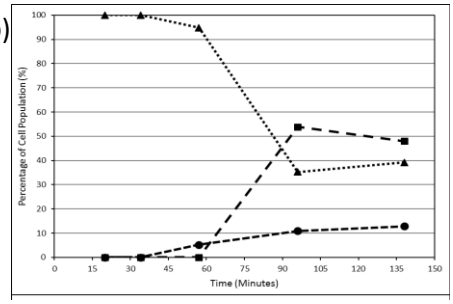

c)

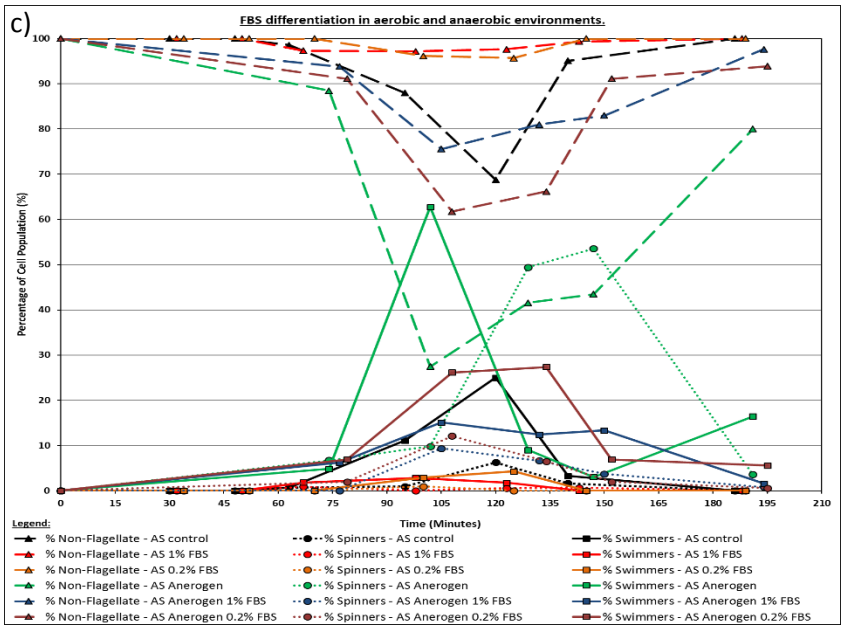

Figure 11: Differentiation data processing examples.

a) The excel sheet setup used for data collection of cell count over time. b) An example of the differentiation graphs generated from the datasets which can be found in the appendix. c) An example of the multiparametric graphs used to compare the results. d) An example of a comparative graph generated to provide a comparison between expression across all environmental conditions.

d)

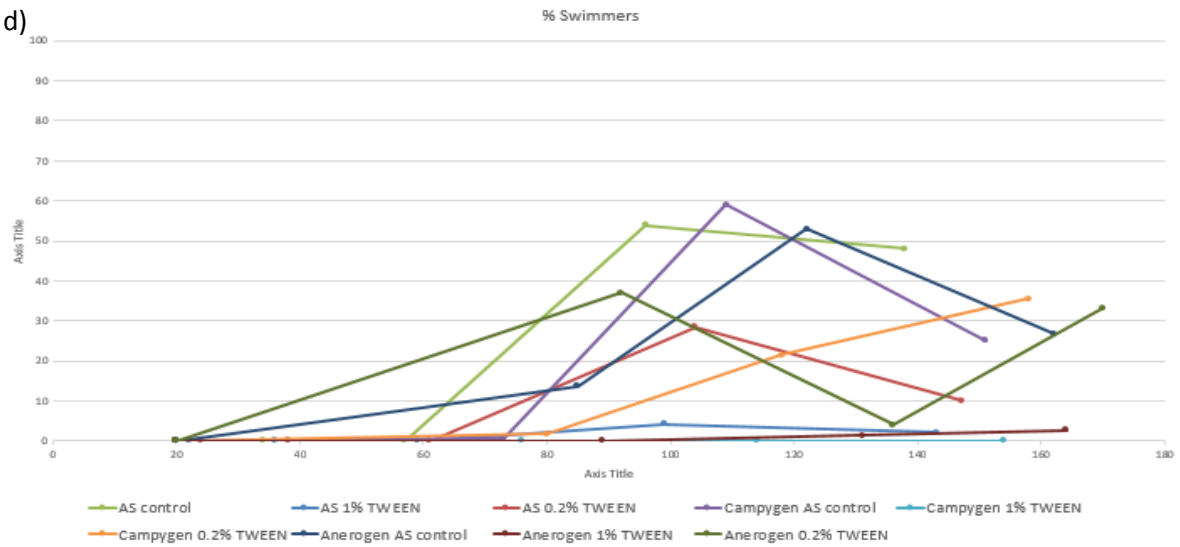

2.3 - Bioinformatic Microarray Analysis

2.3.1 - Obtaining the microarray data

A freely available microarray dataset compiled by L. Fritz-Laylin & W. Cande in the paper 'Ancestral centriole and flagella proteins identified by analysis of *Naegleria* differentiation' was used to carry out bioinformatic analysis of different proteins of interest (Fritz-Laylin & Cande, 2010). The dataset details deviations of mRNA within *Naegleria* undergoing differentiation and was analysed to produce a visual representation of expression of proteins of interest.

Both the microarray and accompanying paper were freely available on the National Center for Biotechnology Information (NCBI) website (Goujon, 2010) (NCBI Resource Coordinators, 2016).

To obtain the microarray dataset, the full paper was found, and the data was obtained by following the links 'GEO Datasets' and 'Expression analysis of *Naegleria gruberi* (strain NEG) during differentiation from the amoeba to the flagellate form'.

Under 'Series Matrix File(s)', the 'GSE21527_series_matrix.txt.gz' file was downloaded, and the 'GSE21527_series_matrix.txt' file was copied to a suitable folder. Under 'MINiML formatted family file(s)', the 'GSE21527_family.x ml (1).tgz' file was downloaded and the 'GPL10359-tbl-1.txt' file was copied to a suitable folder. Once complete, a new excel spreadsheet was created to store the data.

2.3.2 - Organising the microarray library

The data from the 'GPL10359-tbl-1.txt' file was copied and pasted into cell A4, the page was titled 'Microarray Raw Data'. The results of the microarray were then copied from the 'GSE21527_series_matrix.txt' file into cell E4. Cells E4 to T71 were deleted along with cell F33264 was also deleted.

Finally to align the two data sets perfectly, cells E4 to T33263 were selected and alphabetically sorted. The data columns were then given headings that better organised the data. In order to use the data, a visual representation of the protein expression during differentiation of *Naegleria gruberi* needed to be built. In order to do this, a new sheet was created and named 'Microarray Graph'.

The data from a specific protein was copied into this page and the surrounding cells were used to calculate the averages, largest and smallest values, and the potential error of the triplicate results from 0min to 80min.

2.3.3 - Plotting the microarray data

A 2D clustered column graph was used to represent the data. This graph was programmed to populate itself when the data set from a protein was pasted into the appropriate cells. This allowed for a fast throughput visualisation of each of the proteins of interest that were returned from later bioinformatic analysis. The data sheet eventually gave tables as shown in figure 12.

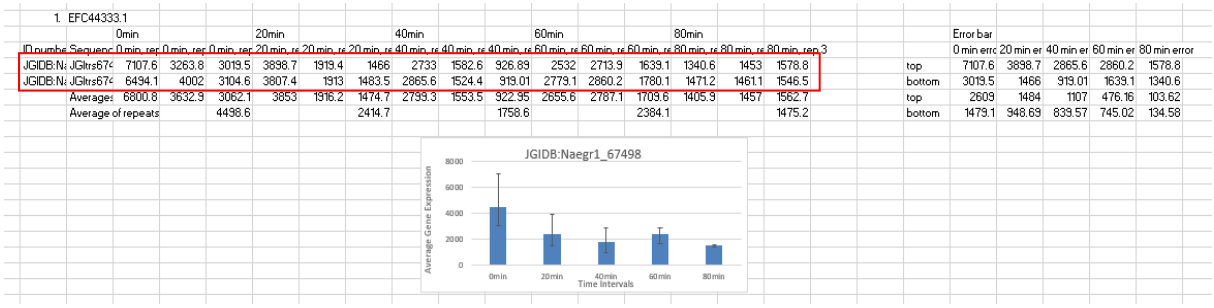

Figure 12: The "Automated Graph" data processing.

An image of the data entry and subsequent automation of graph production. The area encased in red denoted the data copied and pasted from the microarray. The averages and error bars are then calculated and a resulting graph of steady state mRNA synthesis during differentiation is produced.

2.4 - Analysis of proteins of interest

The phrase 'serpentine *Naegleria*' was searched on the NCBI website and three different protein results for *Naegleria gruberi* were returned. The protein sequence of each result was entered into a protein BLAST search, using *Naegleria gruberi* as the organism to be searched. Once this was done, the proteins related to each of the three initial results with an e-value better than e-04 were viewed in separate tabs and the Joint Genome Institute database (JGIDB) identifier of every protein sequence was collected. The sequences of each of the three serpentine proteins were also used in a blastp search against the Joint Genome Institute (JGI) *Naegleria* database. Each resulting protein had the JGIDB identifier collected.

The data sheet was used to find the corresponding microarray data for each of the proteins in the three Basic Local Alignment Search Tool (BLAST) searches. The data was found by searching the microarray data for the JGIDB identifier of each protein. A new excel sheet was created to house the results and labelled 'Stage Specific Data'. Both rows of the relevant data were copied and the data was pasted into the 'Stage Specific Data' sheet along with the graph generate from the data in the 'Microarray Graph' sheet.

2.4.1 - Using controls

The proteins SAS-6 and IFT88 from the paper '*Ancestral centriole and flagella proteins identified by analysis of Naegleria differentiation*' were found on the NCBI database and the JGIDB identifying numbers were copied and were used to locate the proteins in the data set as described above. The data of both SAS-6 and IFT88 was then copied into the 'Microarray Graph' sheet. Other protein controls were used, which would be highly stage specific, such as; Tubulin, Centrin, FLA2 (kinesin 2 homolog), Flagellar calmodulin and other proteins encoding proteins such as dynein. Each protein graph was compared to expected values and the created graphs and datasets of these proteins were stored as shown in figures 13 and 14.

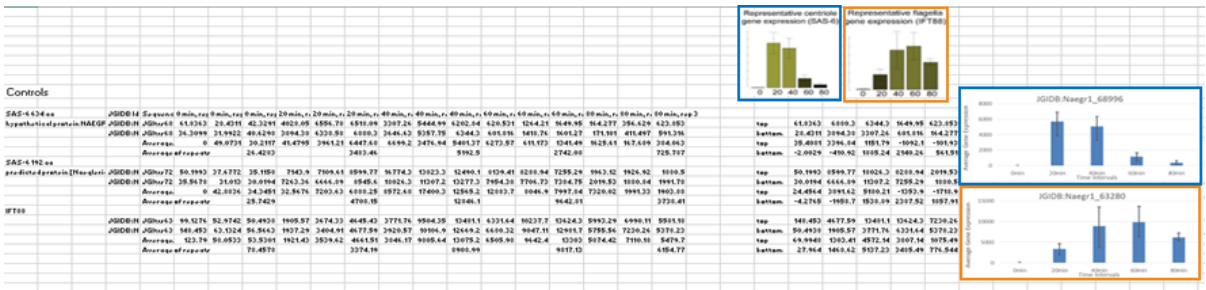

Figure 13: Using controls to validate the data calculation and graph production process.

An image of the previously generated expression graphs for SAS-6 (blue) and IFT88 (orange) obtained from the microarray paper, in comparison to the graphs for each protein produced from my analysis.

2.4.2 - Sorting results and further protein analysis

The graphs for each protein were sorted with regard to whether the proteins showed an amoeba specific, flagellate specific or constitutive expression pattern throughout the differentiation process by colour coding them red, yellow and blue respectively. The data was sorted into these 3 patterns and then further sorted in order of which proteins were the most expressed to least expressed.

2.4.3 - Finding similar proteins to the most expressed proteins of interest

The proteins that were most expressed were further analysed by copying the number at the end of the JGI identifier and using it to search for the protein on the JGIDB website. Using the protein ID a blastp was carried out on the NCBI website. The nearest proteins were found and compared in the same manner as above and were sorted into amoeba specific, flagellate specific or constitutive expression patterns.

2.5 - Morphology of cysts formed within different environments

2.5.1 - Preparing plates for cyst experiments

Naegleria gruberi cultures were prepared and maintained as described previously with the exception that the *Naegleria* cells were spread onto the amoeba saline (AS) plate to evenly coat it. The cells were then incubated and monitored to give them enough time to multiply and consume all *Klebsiella* food sources without encysting. The plates were then placed into different environments according to each experimental condition.

2.5.2 - Cultivating cysts in anaerobic and microaerophilic CO_2 rich environments

Experiments were carried out using anaerobic and microaerophilic CO_2 rich environments by placing plates into two separate 2.5 L Oxoid™ AneroJar™ containers. A 2.5 L Campygen™ or Anaerogen™ sachet was placed into each of the containers to generate the required conditions and the cells were then left to encyst.

2.5.3 - Cultivating cysts in nitrite and nitrate rich environments

1 mM Nitrate AS plates and 1 mM Nitrite AS plates were prepared and seeded with *Klebsiella*. *Naegleria* cells were then transferred across from a normal plate with a sterile spreader under aseptic conditions. The cells were then left to encyst.

2.5.4 - Preparation of *Naegleria* for scanning electron microscopy (SEM)

Once all of the plates had fully encysted, the cells were removed by washing the plate with 1 ml AS solution and dislodging the cells with a sterile spreader. The cells were then pipetted from each plate into a separate Eppendorf tube and spun at 500g for 2mins. The supernatant was pipetted away and discarded. This process was repeated three times with 1 ml of AS solution.

After the final wash, 100 µl of AS solution was added and the cells were vortexed to homogeneity before 3 µl of gluteraldehyde was added. The cells were then pipetted onto a clean glass slide cover and left to fix in the 3% gluteraldehyde solution for 60 mins.

The cells were then washed with increasing amounts of ethanol in order to completely dry the sample. First 150 µl of 25% ethanol in AS solution was pipetted onto the glass slide and left to permeate the cells for 5 mins. After this the excess liquid was carefully removed so as not to disturb the cells that had settled on the glass during the fixation process.

The cells were then washed with 25% ethanol, 50% ethanol, 75% ethanol, 95% ethanol and 100% ethanol in turn. Finally, the cells were washed twice more with 100% ethanol and left to dry.

2.5.5 - Scanning Electron Microscopy

The glass slides containing the cells were placed into an ion sputtering machine and the cells were coated with a 30 nm layer of gold alloy. The slides were then placed into the scanning electron microscope which operated at an accelerating voltage of 20 kV.

Chapter 3: Results

3.1 - Bioinformatic analysis of microarray data – Stage regulation of sensory proteins

As previously discussed, *Naegleria gruberi* contains an expansive intracellular signalling network, including a large presence of cyclase proteins thought to be utilised in environmental perception and signalling (Fritz-Laylin et al., 2010). Due to this, the G protein-coupled cell-surface receptors were targeted for bioinformatic analysis to visualise their upregulation patterns during differentiation (Fritz-Laylin et al., 2010; Ginger, Fritz-Laylin, Fulton, Cande & Dawson, 2010). The analysis was carried out utilizing previously obtained microarray data which was freely available on the NCBI website (Fritz-Laylin & Cande, 2010). The microarray detailed RNA expression values in *N. gruberi* at several timepoints over the course of amoeba flagellate differentiation (Fritz-Laylin & Cande, 2010; Ginger, Fritz-Laylin, Fulton, Cande & Dawson, 2010).

3.1.1 - Analysis of serpentine proteins

The bioinformatic analysis began with finding the G protein-coupled cell-surface receptors within the *Naegleria* species. The term 'serpentine *Naegleria*' was searched in the protein database of the NCBI website (Altschul, Gish, Miller, Myers & Lipman, 1990; NCBI Resource Coordinators, 2016). Of the five results that were returned, there were three different protein results for *Naegleria gruberi.* These proteins were identified by the accession numbers EFC44333.1, EFC40821.1 and EFC35362.1. In order to find related proteins in *N. gruberi*, the amino acid sequence of the three proteins was taken in FASTA format and used to perform a protein BLAST search using both the NCBI and JGI websites (NCBI Resource Coordinators, 2016; Grigoriev et al., 2011). The BLAST searches were restricted to the sequences of *Naegleria gruberi* and of the many results, only the proteins with an e-value of e-04 or greater were utilised, as shown in figures 30 to 32.

3.1.2 - Bioinformatic controls

Ahead of the bioinformatical analysis of the publicly available microarray for *N. gruberi* differentiation, it was important to check that I could replicate the analysis of control data in previously published material (Fritz-Laylin & Cande, 2010). Specifically, I replicated the analysis of figure 2 from the 2010 paper '*Ancestral centriole and flagella proteins identified by analysis of Naegleria differentiation*' As the first control graphs appeared successful, several other proteins connected to centriole/flagellar assembly were selected from the paper to be analysed. Each of the proteins chosen, had well documented expression patterns in other flagellates, and therefore also had an expected pattern of upregulation.

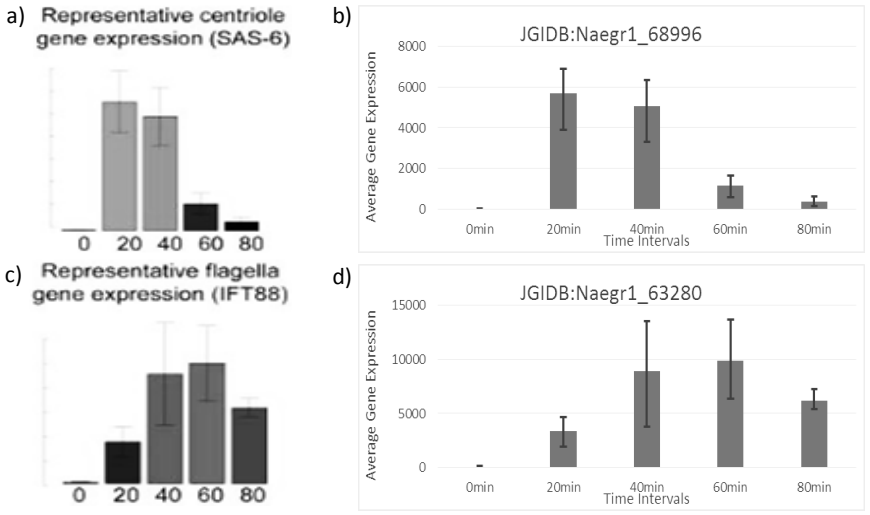

Figure 14: Microarray control graph comparison against my analysis of controls.

A comparison of the SAS-6 and IFT88 RNA expression graphs shown in the microarray paper, in comparison to those created as controls. a) SAS-6 graph from the microarray paper. b) SAS-6 control graph for comparison. c) IFT88 graph from the microarray paper. d) IFT88 control graph for comparison. Control graphs were obtained from Fritz-Laylin & Cande, 2010.

In order to check that the graphs were giving a correct representation, control proteins with a known pattern of expression were used to evaluate them. A graph of each of the control proteins was created and compared to the known expression patterns. The proteins used in this manner included; Tublins, SAS proteins, BBS proteins and IFT proteins. The tubulins are upregulated early as they are essential for nucleation of microtubule organising centre (MTOC) assembly, which is a precursor for formation of the basal body and microtubule cytoskeleton to take place (Misook & Joo Hun, 2001; Beisson & Wright, 2003; Walsh, 2007; Walsh, 1984). Once the microtubule organising centre is complete, the SAS proteins are then expressed and localised to the cartwheel structure, which is built from α-tubulin and β-tubulin microtubules (Nakazawa, Hiraki, Kamiya & Hirono, 2007; Winey & O'Toole, 2014; Lodish, 2016). IFT proteins are only upregulated during differentiation and flagellar formation (Cao, Park & Sun, 2010; Sloboda & Rosenbaum, 2007), and continues to be expressed by cells in the flagellate form. The BBS proteins form the BBSome, an eight-membered protein complex recruited to form a portion

of the basal body (Jin & Nachury, 2009; Jin et al., 2010; Klink et al., 2017). BBS proteins form complexes with IFT proteins (Lechtreck, 2015) and are responsible for protein trafficking along the length of the flagellum via selection of ciliary transmembrane proteins for IFT-mediated transport (Berbari, Lewis, Bishop, Askwith & Mykytyn, 2008; Jin et al., 2010; Klink et al., 2017).

A graph was created to show a comparative expression of the tubulin, IFT and BBS data analysed so far. The expected tubulin expression closely followed by IFT and BBS expression was recorded, as shown in figure 15, so the analysis continued and moved to other control proteins.

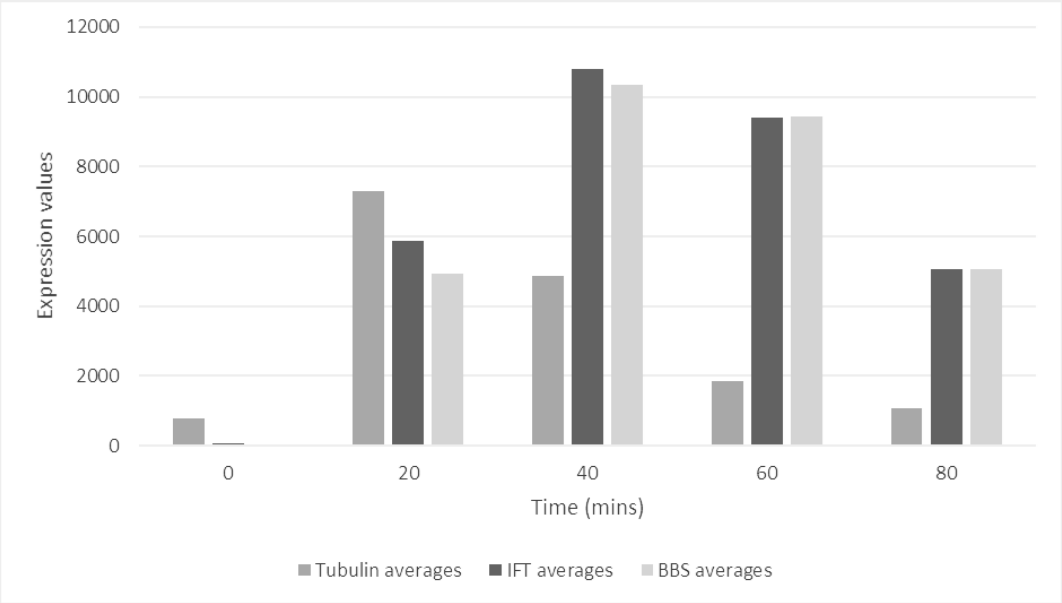

Figure 15: Comparative expression patterns of the flagellate structural control proteins.

A graph depicting the comparative expression of mRNA over time, for the control tubulins, IFT proteins and BBS proteins.

Finally, several other structural proteins in the supplementary table were also analysed (Fritz-Laylin & Cande, 2010). Most of these proteins are used entirely for flagellar construction and function and so are only expressed at different points in the amoebaflagellate and flagellate stages of differentiation as shown in table 1.

Gene product	Function	References
α-tubulin	Dimerize to form microtubules, which are then utilised in the construction of the cartwheel structure and elongation of flagella.	Winey & O'Toole, 2014; Nogales, Wolf & Downing, 1998
β-tubulin		
ODA9 (outer arm dynein intermediate chain)	Forms a structural component of the outer arm dynein.	Wilkerson, King, Koutoulis, Pazour & Witman, 1995
D1bLIC (dynein light intermediate chain)	Forms the light intermediate dynein chain which stabilizes the dynein dimer.	Hou, Pazour & Witman, 2004
ODA1 (p66 outer dynein arm docking complex protein)	Required for assembly of the outer dynein arm and the outer dynein arm-docking complex on the doublet microtubule.	Takada, Wilkerson, Wakabayashi, Kamiya & Witman, 2002
ODA12	Required for assembly of the outer dynein arm.	Pazour et al., 1999
RIB72	Components of the specialised ribbon compartment of flagellar microtubules.	Ikeda et al., 2002
RIB43A-domain containing protein		Norrander, deCathelineau, Brown, Porter & Linck, 2000
Radial head spoke protein 4 (RSP4)	Components of the radial spoke head.	Diener et al., 2011; Curry, Williams & Rosenbaum, 1992
Radial spoke-head-like		
PF16	Involved in central microtubule stability and flagellar motility.	Smith & Lefebvre, 1996
PF20/SPG16	Tryptophan-aspartic acid repeat protein required for central microtubule assembly and flagellar motility.	Smith & Lefebvre, 1997
PACRG	PACRG is associated with outer doublet microtubules and tubulin dimers as a structural molecule and regulates ciliary dyneins through microtubule sliding. It is also hypothesised to possess cilium-associated sensory/signaling functions.	Ikeda, 2008; Mizuno, Dymek & Smith, 2016; Loucks et al., 2016; Ikeda, Ikeda, Morikawa & Kamiya, 2007
Flagellar calmodulin (CAM1)	Calmodulin localises to the central microtubule and radial spoke stalks. It plays a role in motility and calcium control of flagellar bending.	Yang, Diener, Rosenbaum & Sale, 2001; Hisanaga & Pratt, 1984; Yang, Yang & Sale, 2004; Wargo, 2005
KLP1 (kinesin-9)	KLP1 is Klp1 a motor protein localised to the central pair of microtubules in the axoneme and is essential for flagellar motility.	Bernstein, Beech, Katz & Rosenbaum, 1994; Yokoyama, O'Toole, Ghosh & Mitchell, 2004

Table 1: Structural proteins used as controls.

A table displaying the different structural proteins with predictable mRNA expression that were used as controls. A summary of the known function of each protein is included alongside appropriate previous studies.

3.1.3 - Sorting results and further protein analysis

Earlier bioinformatic analysis of the microarray stated that the majority of predicted adenylate cyclase sensory proteins were upregulated during the flagellate stage (Kelly, 2013) as shown in table 2. In order to better identify potential signalling receptors in my analysis, all of the proteins returned from the BLAST searches were used to create graphs, these were then manually sorted into stage specificity by visually assessing the RNA expression pattern , seen in figures 30 to 32. They were sorted into groups of; amoeba specific, flagellate specific or constitutive expression patterns and then further ordered by RNA expression levels. If a protein did not have a clear expression pattern, it was not sorted into either of the three categories and was disregarded, this left a total of 47 clearly stage specific proteins, that were sorted as shown in table 3.

Domain	Total number	Transmembrane	Total stage specific
All	116	87	80
PAS	47	41	35
HAMP	6	6	5
NIT	4	4	4
BLUF	2	0	2

Table 2: Previous analysis of sensory adenylate cyclases.

A table showing a previously produced analysis of potential sensory adenylate cyclase expression during differentiation of *N. gruberi* adapted from Table 4.2 of Kelly, 2013.

Expression values	**Flagellate specific**	**Amoeba specific**	**Constitutive**
0 – 1,000	8	7	19
1,000 – 10,000	3	6	2
10,000 – 100,000	0	2	0
Totals	11	15	21

Table 3: Protein grouping according to stage expression abundance.

A table indicating how the 47 proteins, identified as having an expression pattern through my analysis, were sorted. The proteins were further grouped based on the intensity of mRNA expression.

3.1.4 - Searching for homologous protein expression in the most upregulated proteins

After having sorted the proteins by stage expression, an analysis of the most upregulated proteins was carried out to check if any closely related proteins followed the same patterns. To achieve this, the most upregulated proteins in the amoeba specific, flagellate specific and constitutive groups were searched on the NCBI website and the amino acid sequences were used in a protein BLAST. The resulting proteins returned from the BLAST search were then used to create expression graphs as shown in figures 45 to 51. These were compared against the serpentine receptor protein expression patterns.

3.2 - Environmental triggers for differentiation

My analysis of the microarray data indicated considerable complexity and stage specificity in the expression of candidate serpentine receptor proteins, responsible for activating signalling pathways in response to detection of environmental cues (Mykytyn & Askwith, 2017; Rosenbaum, Rasmussen & Kobilka, 2009). In an attempt to better understand the roles of these signalling proteins, I investigated the behaviour of *N. gruberi* with regards to its capacity to differentiate under specific environmental stresses and conditions. This analysis provides a framework under which the signalling transcriptome could be explored further. The genome sequence of *N. gruberi* has highlighted it as an unexpectedly metabolically flexible protist (Fritz-Laylin et al., 2010). Due to this, it was concluded that revisiting parameters for differentiation was a worthwhile exercise. The different experimental parameters investigated can be found in table 4.

3.2.1 - Initial optimization

The first set of differentiation experiments were done in order to find the optimal conditions to grow and differentiate *Naegleria* with the novel methodology inspired by earlier work (Fulton, 1970). The goal was to secure maximal numbers of flagellate cells from differentiation.

The first set of experiments carried out were to test the best way to transfer cells. The goal was to ensure that as few encysted cells were transferred to the AS solution as possible. In comparison with previously published methods, I scaled down the volumes used. Later experiments showed that excision and centrifugation of agar at 1,800 rpm for 2 mins gave the best differentiation.

The use of cold environments, Tris buffer and agitation from previous protocols (Fulton & Dingle, 1966; Fulton, 1970) was then tested. The lower temperatures, agitation and use of Tris buffer all appeared to inhibit the differentiation of cells.

After several optimisation tests, a final optimization experiment comparing buffers, temperatures and spin techniques showed that the protocol employed in the methods section was best for the environmental experiments as seen in figure 58 in the appendix.

	Condition numbers and associated figures																			
Conditions tested	1	2	3	4	5	6	7	8	9	10	11	12	13	14	15	16	17	18	19	20	21
Aerobic	X	X	X				X	X						X	X	X	X				
Microaerophilic, CO_2 rich											X	X	X					X	X		
Anaerobic				X	X	X			X	X										X	X
10 µM Sodium azide (NaN_3)		X			X																
1 µM Sodium azide (NaN_3)			X			X															
0.2% FBS							X		X			X									
1% FBS								X		X			X								
0.2% Glucose														X							
1% Glucose															X						
0.2% Tween20																X		X		X	
1% Tween20																	X		X		X

Table 4: The different environmental parameters investigated.

Table 4 indicates all of the different environmental parameters investigated within this MSc. The condition numbers show which of the environmental conditions were tested simultaneously

3.2.2 - Differentiation in the presence of mitochondrial respiratory chain inhibitor sodium azide (NaN_3)

Due to the multitude of potential mitochondrial metabolic pathways in *Naegleria* (Fritz-Laylin et al., 2010; Ginger et al. 2010) a set of experiments were carried out using the mitochondrial respiratory chain inhibitor sodium azide. Sodium azide arrests metabolism through inhibition of mitochondrial cytochrome oxidase (Lichstein & Soule, 1944; Berndt, Callaway & Gonzalez-Lima, 2001; Yoshikawa & Orii, 1972). The effect of concentrations of 1 mM and 0.1 mM sodium azide upon the differentiation of *Naegleria* was tested in both aerobic and anaerobic environments to observe how inhibition of oxidative phosphorylation in oxygen rich and oxygen depleted environments would affect differentiation.

The results in figure 16 suggested that high concentrations of sodium azide had an inhibitory effect upon differentiation, which appeared to be more prominent in the presence of an anaerobic atmosphere. However, the presence of an anaerobic atmosphere or the presence of 0.1 mM sodium azide alone improved differentiation into flagellates which may be due to low levels of the toxin culminating in a biphasic adaptive response effect (Kaiser, 2003; Calabrese et al., 2007; Mattson, 2015).

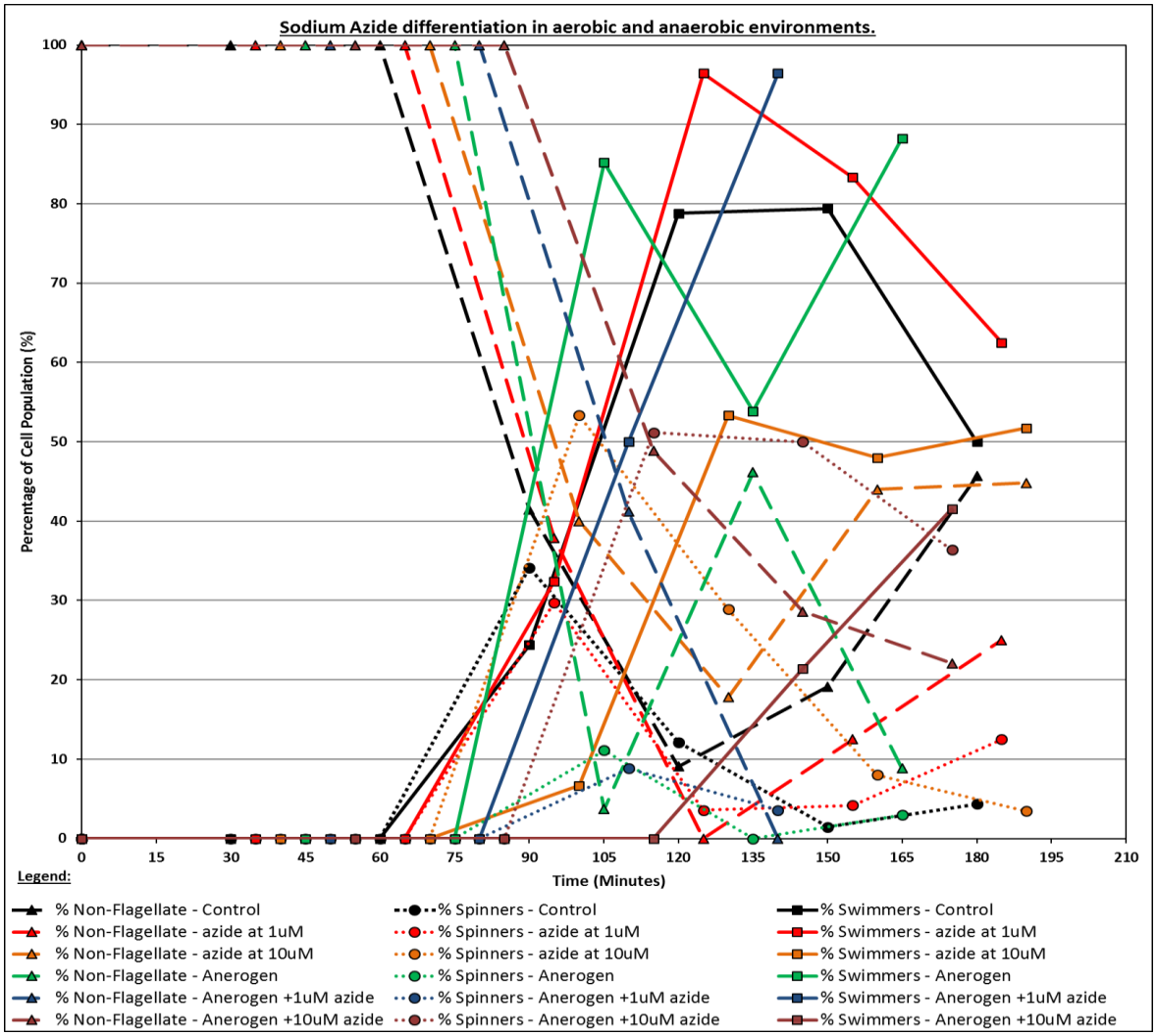

Figure 16: Sodium azide differentiation results.

A graph showing the differentiation patterns of N. gruberi when subjected to differing amounts of sodium azide, in both aerobic and anaerobic environments.

3.2.3 - Differentiation in the presence of foetal bovine serum (FBS)

The experiments concerning sodium azide gave evidence to show that oxidative phosphorylation may not be obligatory for differentiation so the next experiments tested the effects of different nutrient sources upon differentiation. The effect of foetal bovine serum (FBS), a partially defined nutrient-rich media containing proteins and lipids, was observed in both normal and glucose-rich aerobic and microaerophilic CO_2 rich environments.

The results in figures 17 and 18 showed further evidence that differentiation is increased as O_2 is depleted. The results also repeatedly showed evidence that addition of FBS reduced the number of flagellates observed, leading me to believe that FBS is detected as a nutrient source. Strangely the cells in glucose behaved like the control samples and did not seem to catabolise the glucose present as seen in red in figure 18. This agrees with findings in recent studies (Bexkens et al., 2018).

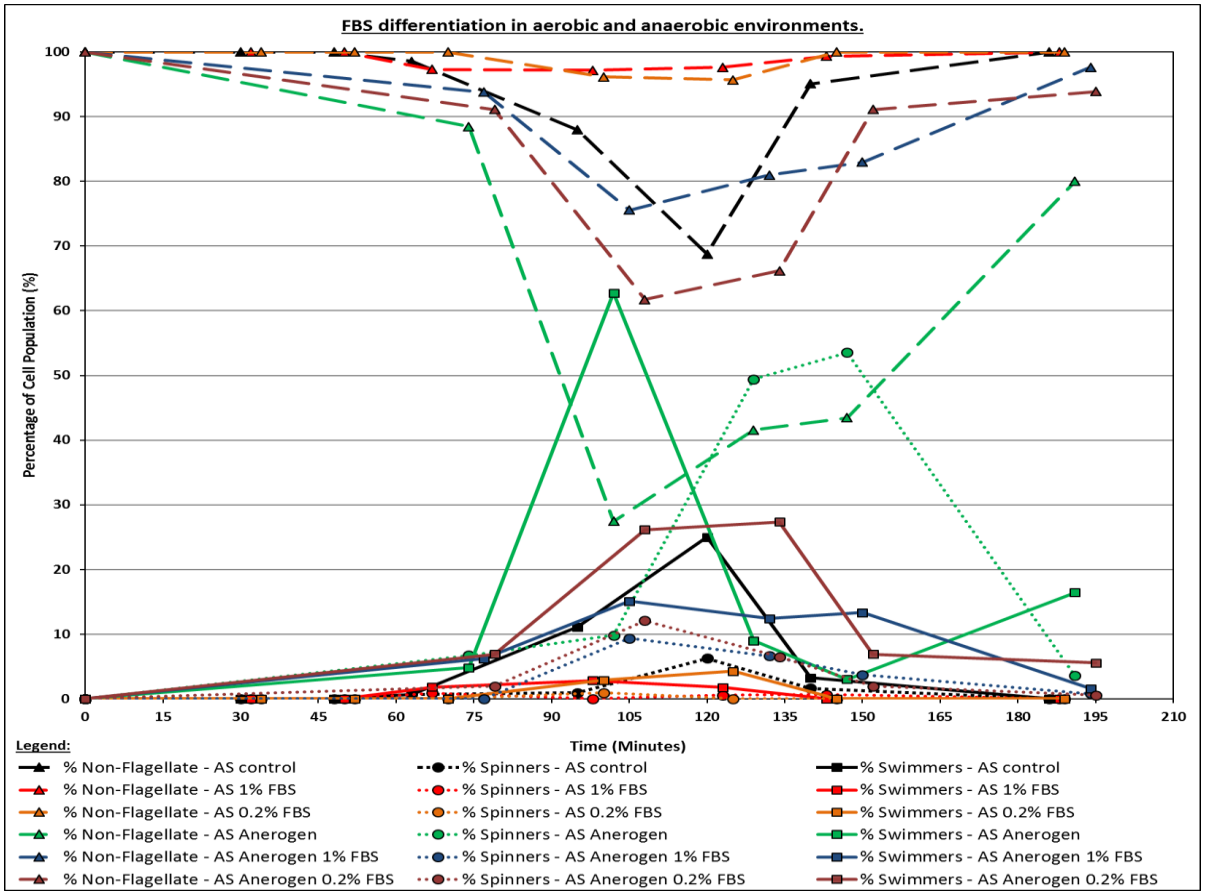

Figure 17: FBS differentiation results.

A graph showing the differentiation patterns of N. gruberi with differing amounts of FBS in both aerobic and anaerobic environments.

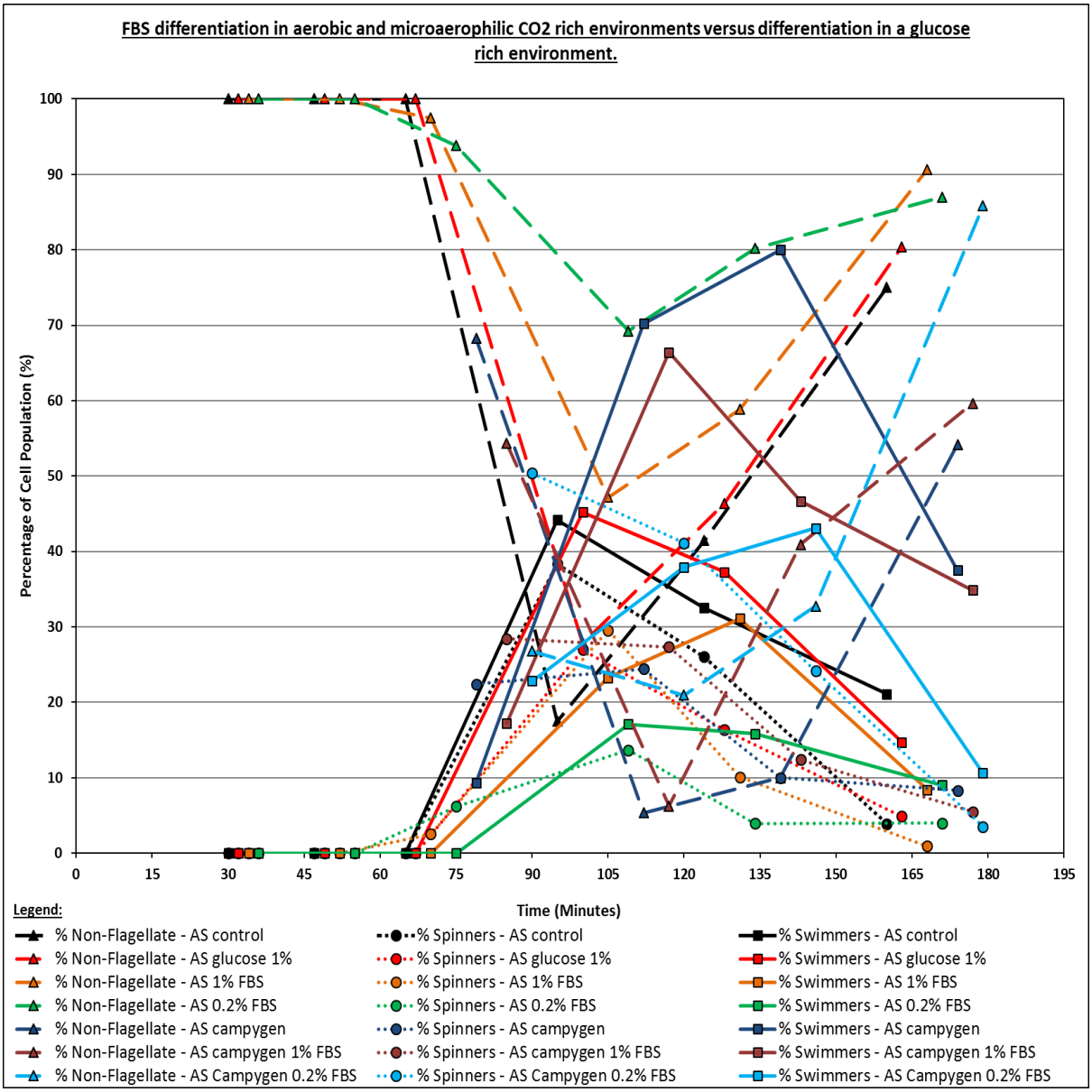

Figure 18: FBS vs glucose differentiation results.

A graph showing the differentiation patterns of N. gruberi with differing amounts of glucose and FBS in aerobic and microaerophilic CO_2 rich environments.

3.2.4 - Differentiation in the presence of Polyoxyethylene sorbitan monolaurate (TWEEN20)

TWEEN20 is a lipid molecule containing a twelve carbon-long fatty acid chain. Recent studies have shown that *Naegleria* may actively select for the oxidation of fatty acids as a substrate preference (Bexkens et al., 2018). With this in mind, I attempted to test this using a mixture of glucose rich and TWEEN20 rich environments in both microaerophilic CO_2 rich and aerobic environments.

The addition of TWEEN20 had the most pronounced inhibitory effect upon differentiation of all the environmental effects observed. The results in figure 19 suggested that TWEEN20 is utilised as a carbon source as it inhibits differentiation, this is particularly fascinating considering that the addition of readily available glucose was once again ignored by *N. gruberi* cells. The cells in the presence of TWEEN20 and a low oxygen environment differentiated and then reverted quickly once oxygen was introduced.

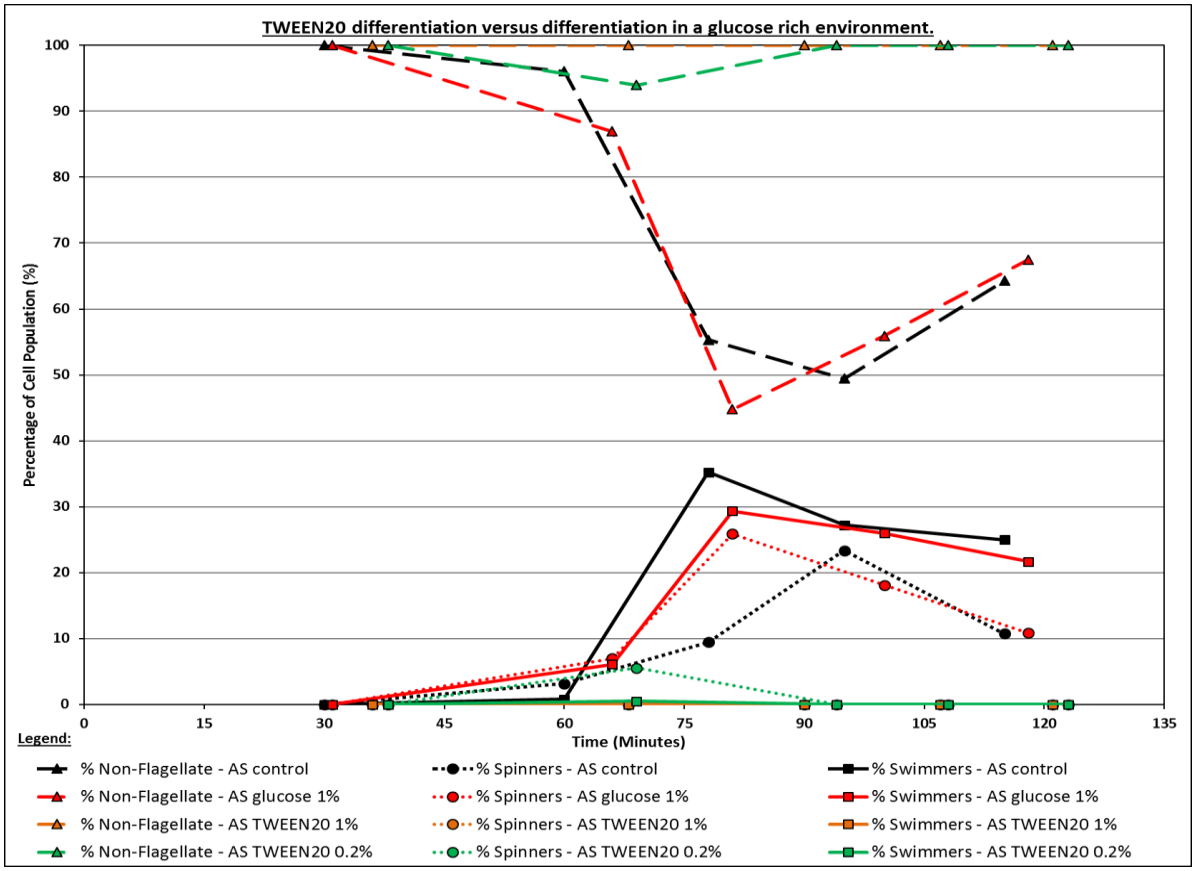

Figure 19: TWEEN20 vs glucose differentiation results.

A graph comparing the differentiation patterns of N. gruberi in a glucose rich environment against differentiation in a lipid rich environment.

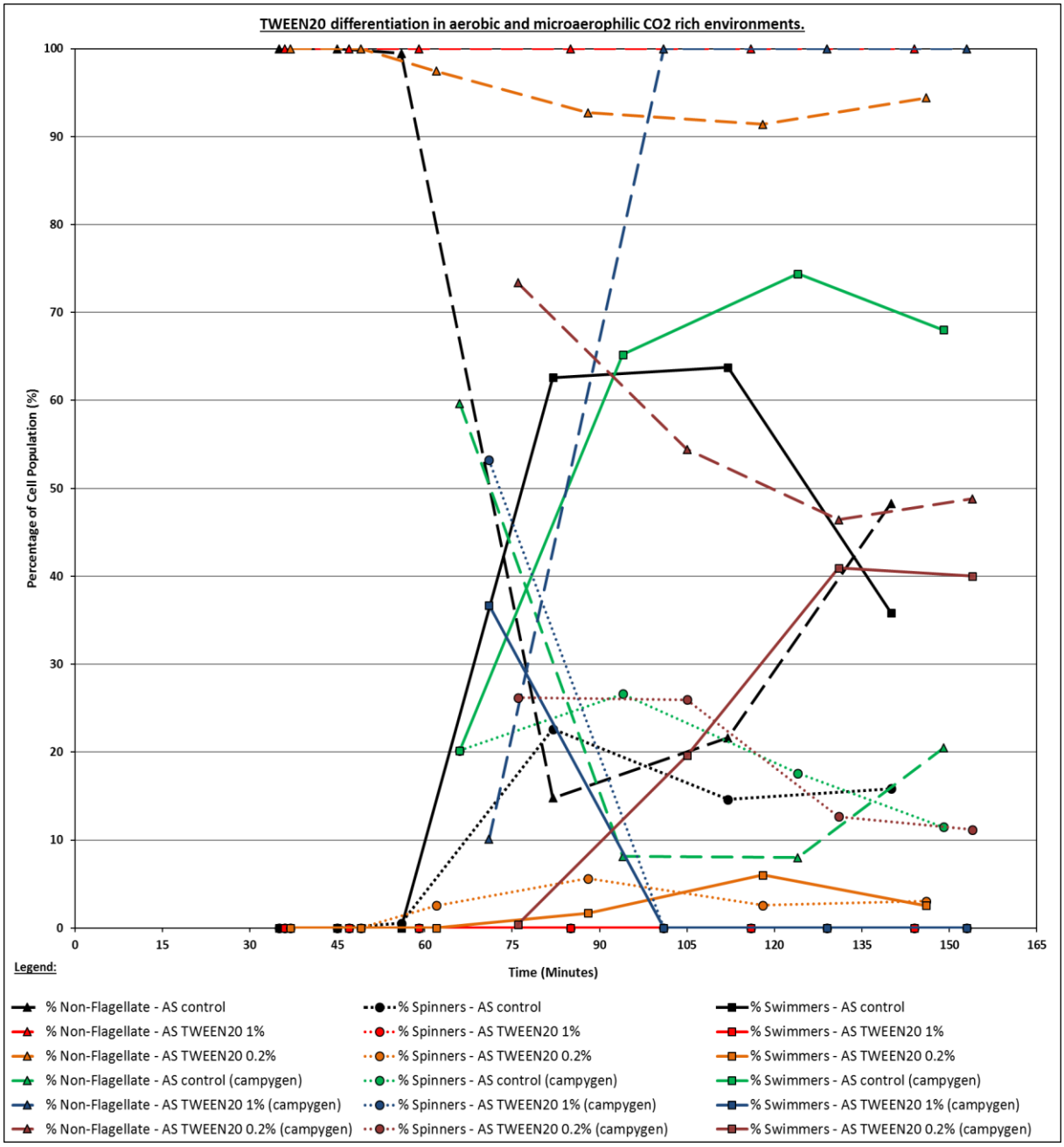

Figure 20: TWEEN20 differentiation results.

A graph showing the differentiation patterns of N. gruberi with differing amounts of TWEEN20 in aerobic and microaerophilic CO_2 rich environments.

3.3 - Scanning electron microscopy analysis of cysts formed under different environmental conditions

In order to continue the functional studies into environmental perception by *Naegleria* in the timeframe given, further experiments were carried out to assess the phenotypic effect of environmental conditions upon differentiation using scanning electron microscopy. The morphology of *Naegleria gruberi* has been studied previously in both the trophic form (Jamerson, da Rocha-Azevedo, Cabral & Marciano-Cabral, 2012), and encysted form (Lastovica, 1974; Dyková, Kyselová, Pecková, Oborník & Lukes, 2001) as seen in figure 2.

3.3.1 - Initial SEM analysis and troubleshooting

The initial SEM experiments were carried out by fixing the cells with 2.5% gluteraldehyde for 40 mins. The cells were taken through a graded ethanol wash. This was unsuccessful and after some troubleshooting I increased the concentration of glutaraldehyde to 3% glutaraldehyde and raised the incubation time to 60 min, as done in earlier published SEM work with *N. gruberi* (Lastovica, 1974). The resulting images were promising as several cysts retained a spherical morphology.

The cells were eventually fixed with 3% glutaraldehyde with an incubation time of 60min, as previously detailed in the methodology section and seen in figure 21. Cysts were then cultivated in nitrate rich, nitrite rich, anaerobic and microaerophilic CO_2 rich environments before being prepared for SEM imaging.

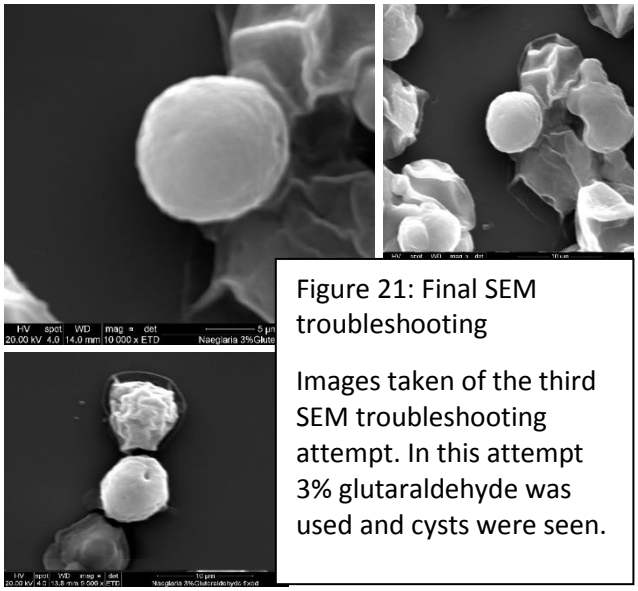

Figure 21: Final SEM troubleshooting

Images taken of the third SEM troubleshooting attempt. In this attempt 3% glutaraldehyde was used and cysts were seen.

3.3.2 - Control sample

The cysts that were imaged as part of the control group in figure 22 appeared similar to those in figures 2b), 2c) and 2e) (Lastovica, 1974; Dyková, Kyselová, Pecková, Oborník & Lukes, 2001). Many of the cysts had a spherical morphology with both open and blocked visible exit pores (Lastovica, 1974).

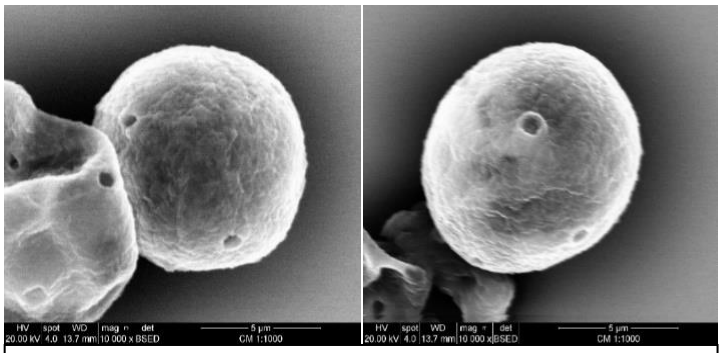

Figure 22: SEM control sample.

SEM images of the control cells, which were similar to the control images of previous studies (Lastovica, 1974; Dyková, Kyselová, Pecková, Oborník & Lukes, 2001) and had visible ostioles.

3.3.3 - Effects of Anaerobic and Microaerophilic CO_2 rich environments upon encystment

Many of the cysts imaged in both the anaerobic and microaerophilic CO_2 rich environments had a normal spherical morphology. The cysts that were observed in the microaerophilic CO_2 rich environment had a similar morphology to those of the control group in figure 22, whereas the cysts that were formed in the anaerobic environment had an irregular surface similar to those in figure 2d).

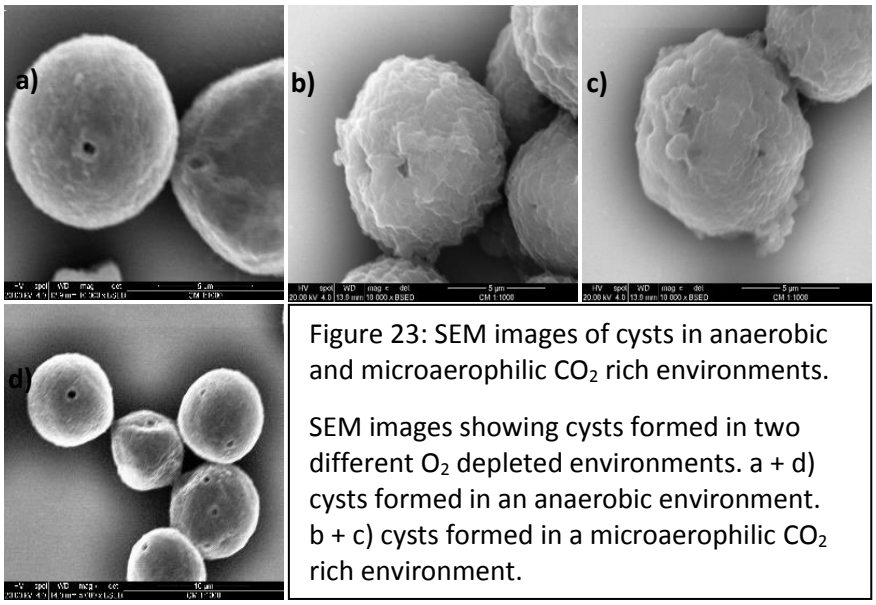

Figure 23: SEM images of cysts in anaerobic and microaerophilic CO_2 rich environments.

SEM images showing cysts formed in two different O_2 depleted environments. a + d) cysts formed in an anaerobic environment. b + c) cysts formed in a microaerophilic CO_2 rich environment.

3.3.4 - Nitrate + Nitrite rich environments

Almost all of the cysts imaged in both the nitrate rich and nitrite rich environments were collapsed inwards as shown in figures 24a and 24b. There were some smaller spherical cyst-like structures visible with what appeared to be ostioles, however these structures were roughly one third to one fourth of the size of a normal cyst as seen in figures 24c and 24e).

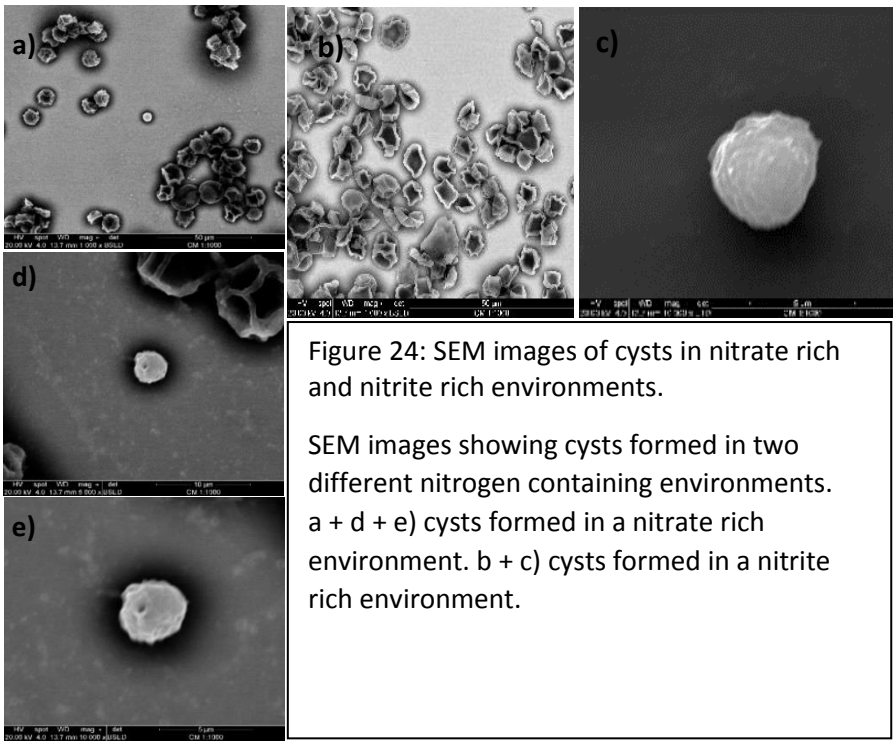

Figure 24: SEM images of cysts in nitrate rich and nitrite rich environments.

SEM images showing cysts formed in two different nitrogen containing environments. a + d + e) cysts formed in a nitrate rich environment. b + c) cysts formed in a nitrite rich environment.

3.4 - Synthesis and purification of proteins of interest

As previously discussed, *Naegleria* contains an expansive intracellular signalling network, including a large number of kinases, cyclases, and proteins with sensory domains (Fritz-Laylin et al., 2010). These proteins are significant components of sensory perception (Fritz-Laylin et al., 2010; Garcia, Orillard, Johnson & Watts, 2017; Söderbäck et al., 2002; Rebbapragada et al., 1997; Ryo et al., 2018; Möglich, Ayers & Moffat, 2009).

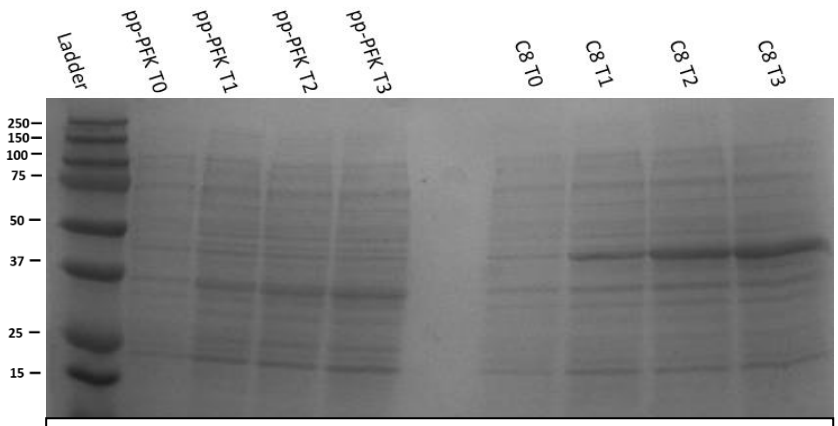

Figure 25: Small scale pp-PFK and C8 induction SDS PAGE.

An image of an SDS PAGE gel showing the results of the small-scale induction of proteins pp-PFK (37kD) and C8 (50kD). The proteins produced are seen as thicker bands, where T0 is the start of induction and T1, T2 and T3 are samples gathered from 1, 2 and 3 hours after induction.

During the course of the MSc, I attempted to purify four signaling proteins of interest. These proteins were an adenylate kinase referred to as AK3, an adenylate/guanylate cyclase referred to as C8, a pyrophosphate-dependent phosphofructo-1-kinase referred to as pp_PFK and a predicted adenylate/guanylate cyclase with PAS domain referred to as PAS1. The sequence encoding each protein insert is shown in the appendix.

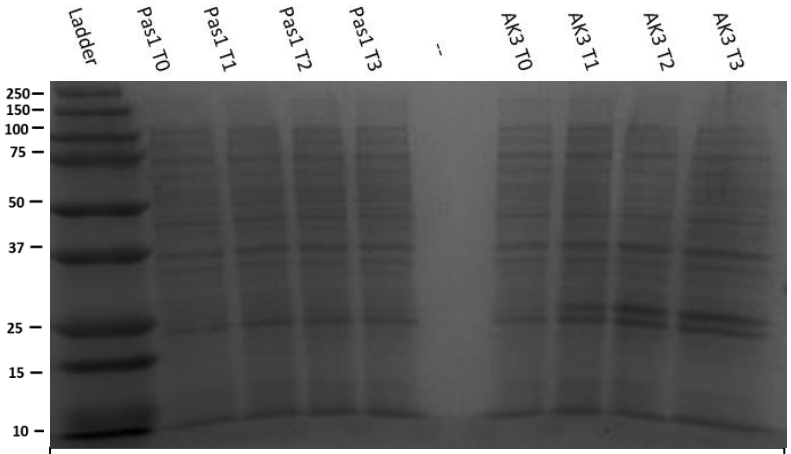

Figure 26: Small scale PAS1 and AK3 induction SDS PAGE.

An image of an SDS PAGE gel showing the results of the small-scale induction of the proteins PAS1 + AK3 (25kD). The AK3 protein produced is seen to be accumulating. T0 is the start of induction and T1, T2 and T3 are samples gathered from 1, 2 and 3 hours after induction.

The protein purification was carried out with the intent of determining protein localisation for each protein during differentiation. The genes encoding the recombinant proteins were ligated into pET28a expression vectors and were first successfully cloned

into chemically competent *E. coli* by another researcher before the MSc work began. A small-scale induction of the cloned cells was the first thing I undertook, in order to check for the presence of the four proteins of interest; AK3, C8, pp-PFK and PAS1. The first small scale induction of the proteins appeared to be largely successful, as shown in figures 25 and 26. However the protein PAS1 was not shown to be expressed in figure 26 so I attempted to troubleshoot this process.

3.4.1 - Troubleshooting PAS1 expression

In order to re-attempt PAS1 expression, troubleshooting methods were employed. Protein from fresh transformants kept in glycerol stock solutions were induced and several colonies were tested for PAS expression. Ultimately this was unsuccessful and eventually PAS1 expression was abandoned in order to continue with expression and purification of the other three proteins.

3.4.2 - Purification of pp-PFK, C8 and AK3

A first attempt at large scale induction was made with the proteins pp-PFK, C8 and AK3 in order to understand whether the protein was soluble or insoluble. This was done by analysing both the resulting pellet and supernatant in an SDS PAGE for each protein, as shown in figure 27. This revealed that pp-PFK and AK3 were insoluble, while C8 was soluble.

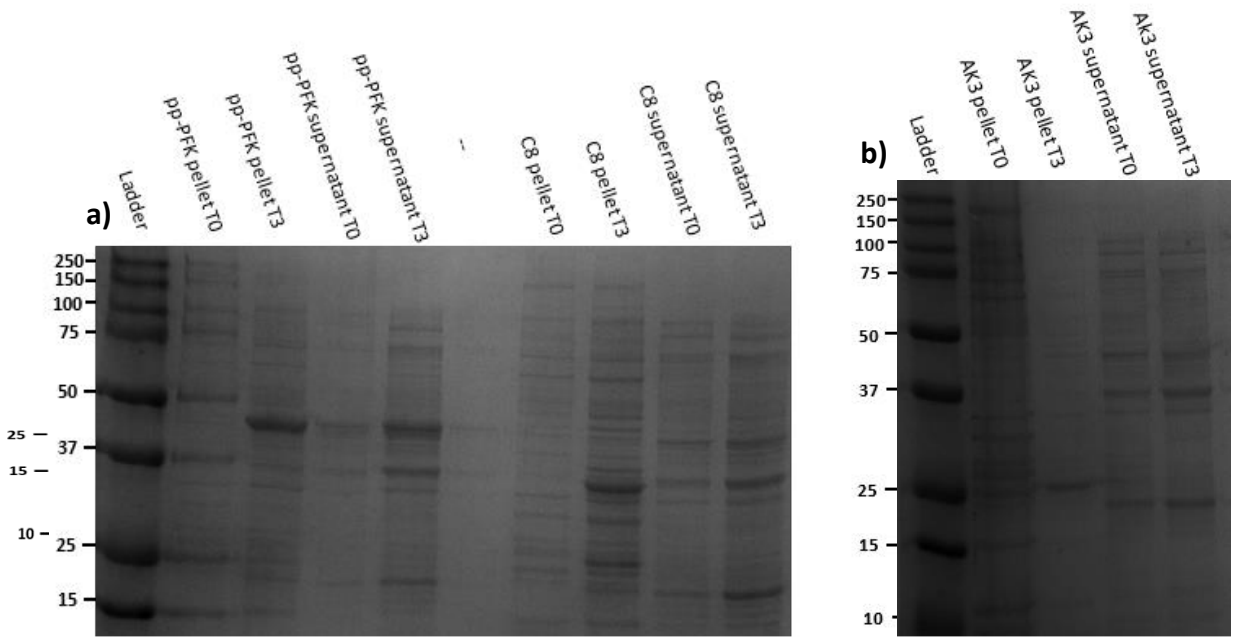

Figure 27: Large scale induction and solubility test.

An SDS PAGE gel of the protein solubility fractions. a) an SDS PAGE gel showing evidence of large-scale soluble pp-PFK (37kD) and insoluble C8 (50kD) inductions. b) an SDS PAGE gel showing evidence of large-scale soluble AK3 (25kD) induction in the supernatant, where T0 is the start of induction and T3 are samples gathered from 3 hours after induction.

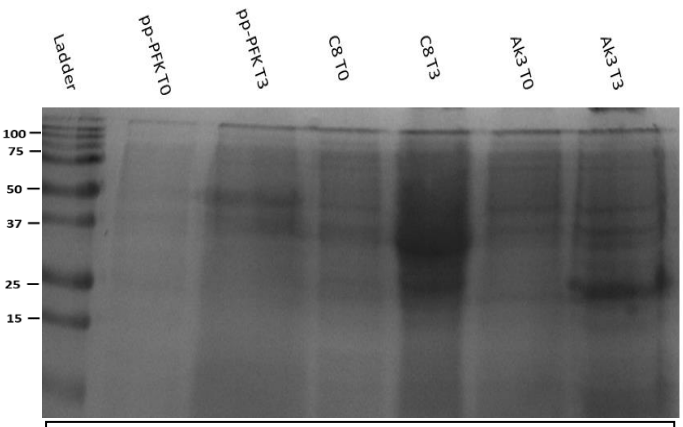

Figure 28: Large scale induction results.

An SDS PAGE gel showing the large induction results for all three different proteins. A trace of each protein is visible. T0 is the start of induction and T3 denotes samples from 3 hours after induction.

A lysis buffer, a wash buffer and an elution buffer were then prepared for protein purification in both denaturing and native conditions. A large-scale induction was carried out for each of the remaining three proteins and 100 µl of each of the protein samples were kept in order to carry out an SDS PAGE as shown in figure 28.

This showed varying traces of each of the three proteins, so the three protein samples were then purified using affinity chromatography with a Ni-NTA agarose affinity resin. Some of each fraction was observed by SDS PAGE and each of the three proteins were shown to have been produced and purified as shown in figure 29.

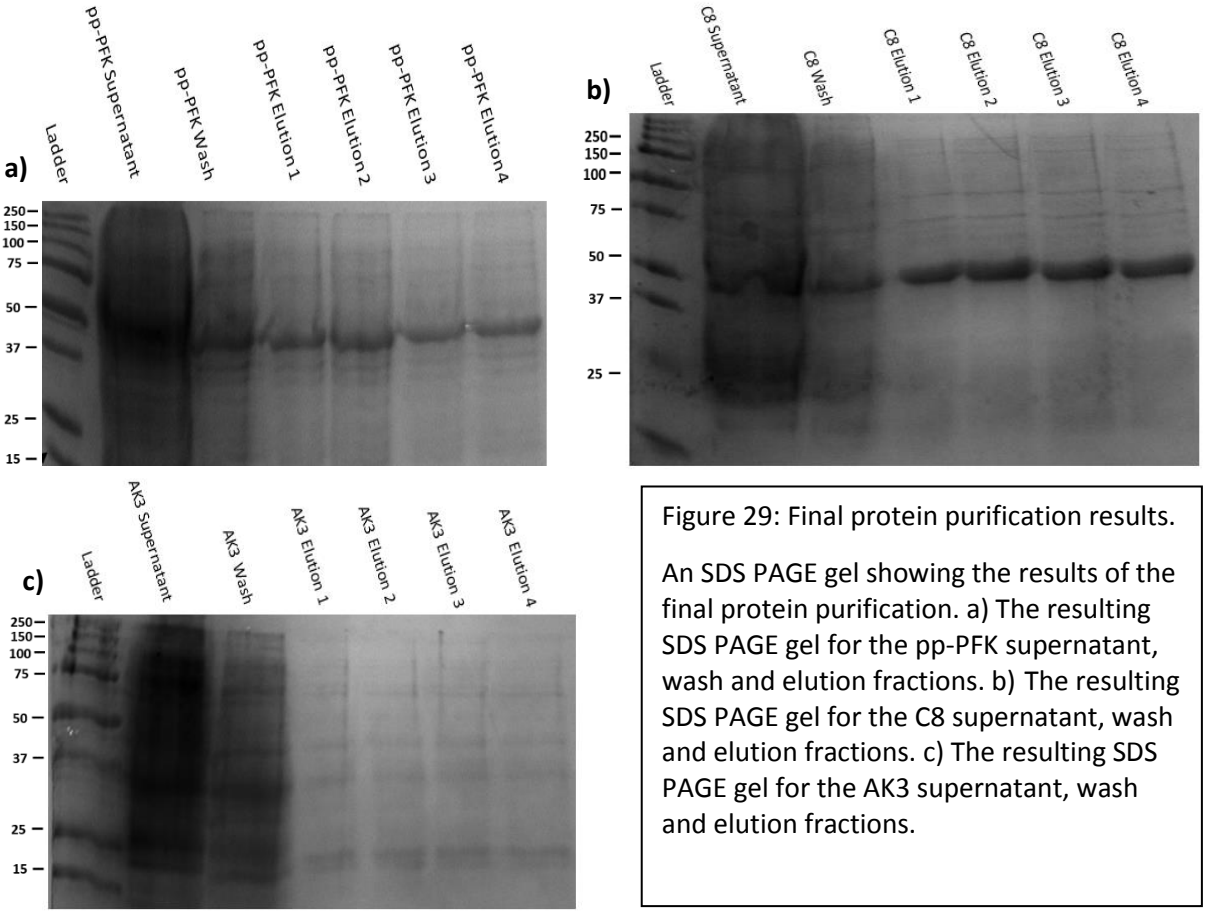

Figure 29: Final protein purification results.

An SDS PAGE gel showing the results of the final protein purification. a) The resulting SDS PAGE gel for the pp-PFK supernatant, wash and elution fractions. b) The resulting SDS PAGE gel for the C8 supernatant, wash and elution fractions. c) The resulting SDS PAGE gel for the AK3 supernatant, wash and elution fractions.

Chapter 4: Discussion

As previously mentioned in the introduction, the presence of flagella in eukaryotes is often vital to survival and proliferation (Moran, McKean & Ginger, 2014; Wood, Huang, Diener & Rosenbaum, 2013). In complex eukaryotes they play roles in intricate systems such as the renal, digestive and nervous systems and are found throughout the human body (Ostrowski, Dutcher & Lo, 2011). More recently, focus has shifted to the sensory capabilities of flagella and cilia in eukaryotes which permits both recognition and response to external stimuli. Genetic syndromes known as ciliopathies are a result of defective flagellar and ciliary function and have previously been shown to predispose individuals to chronic health conditions, including cancer, obesity and diabetes.

Naegleria gruberi is a model organism, which is related to the often fatally pathogenic *N. fowleri* and can be both safely and easily grown in xenic conditions. The rise of whole genome sequencing has led to the discovery and identification of a signalling protein cohort which is much larger than that of neighbouring eukaryotes. This protein cohort, in combination with the natural life cycle and ameboflagellate capabilities of *N. gruberi*, offer a model organism with a host of unexplored, flagellate stage-specific, sensory proteins. This leaves *N. gruberi* well-positioned as a model in which to study the sensory capabilities of flagella, due to the sensory perception and function of the flagellate form.

My project initially began with the aim of localising flagellate specific signalling proteins, in an attempt to determine whether they act as sensory antennae, such as that of *Chlamydomonas* (Collingridge, Wheeler & Brownlee, 2012; Omoto & Brokaw, 1985). However, over the course of the MSc, other experiments replaced this singular focus. The novel experiments concerning environmental sensory perception during differentiation, yielded several results, with the more prominent results reinforcing more recent published material (Bexkens et al., 2018). Meanwhile, although the protein PAS1 could not be purified, even after many different troubleshooting attempts, the other three proteins were shown to be successfully purified.

4.1 - Differentiation

During the differentiation experiments, I had expected glucose to be catalysed in the event of food deprivation, due to the previously indicated potential capacity for aerobic degradation of glucose (Fritz-Laylin et al., 2010; Ginger et al., 2010; Opperdoes et al., 2011) and the fact that it is an essential component of the defined media of *Naegleria* (Nerad, Visvesvara & Daggett, 1983). It came as some surprise to find that freely available glucose remained undisturbed as cells underwent starvation, and eventually, differentiation. The fact that glucose is not recognised as a nutritional carbon source is interesting, considering that glucose is the most widely accepted energy source of microbial eukaryotes (Bunn & Higgins, 1981). These findings do conform with previous studies, which show that although glucose is an essential addition to the defined media for *Naegleria*, glucose within the media is not consumed by *N. gruberi* cultures (Weik & John, 1977). In addition, other experiments during the MSc suggest that *N. gruberi* appears to use lipids as a preferred carbon source for ATP production and proliferation.

Some results concerning the mitochondrial respiratory chain inhibitor sodium azide showed that small concentrations of sodium azide appeared to slightly improve differentiation, possibly due to an adaptive response (Kaiser, 2003; Calabrese et al., 2007; Mattson, 2015). However, generally the results showed that the extent of differentiation increases as O_2 levels are depleted and that the presence of lower concentrations of sodium azide did not present a barrier to differentiation. In fact, strong concentrations of sodium azide had an inhibitory effect upon differentiation that was compounded in an anaerobic atmosphere. These results provide evidence indicating that mitochondrial ATP production via oxidative phosphorylation may not be necessary during differentiation. This would suggest that substrate level phosphorylation may be sufficient to produce the ATP necessary to differentiate and swim, which is surprising, considering that the presence of glucose does not prevent differentiation.

Experiments carried out investigating different nutrient sources showed that cells did not differentiate as readily in the presence of FBS and TWEEN20, with the effect of TWEEN20 upon differentiation being particularly noticeable. This is consistent with recently published data suggesting that *N. gruberi* actively selectively metabolises lipids over other carbon sources (Bexkens et al., 2018). Differentiation does occur in most cases if cells are placed in low oxygen environments, however upon reintroduction of O_2, the cells quickly revert to flagellate form. This also provides some evidence that mitochondrial respiratory chain oxidative phosphorylation is not necessary for ameboflagellate differentiation as the

lipids and amino acids within these substrates are more likely catabolized via the tricarboxylic acid cycle to produce ATP.

As a general trend, the presence of an anaerobic or microaerophilic CO_2 rich atmosphere usually enhanced the amount of differentiation observed, even when lipid nutrient sources were present, which in tandem with the anaerobic results, suggested that a habitat with a lack of atmospheric oxygen is sufficiently inhospitable to trigger the differentiation process. This response, combined with evidence that oxidative phosphorylation may not be utilised in differentiation, raises the question of where *N. gruberi* procures the energy for differentiation, and whether it is stored within the cell or generated on demand. To conclude this research, further experiments assessing differentiation in the presence of only amino acids should be carried out, this would reveal whether only lipids are selectively sought as a source of nutrition.

4.2 - Bioinformatics

What emerges from the bioinformatic analysis, is a sequential ordering of gene expression relating to; centriole assembly, Intraflagellar transport system establishment, BBSome formation and flagellar assembly in *N. gruberi,* as shown more clearly in figure 15. The result of this analysis also shows that there are a number of complex sensory serpentine receptors which show flagellate specific expression, that coincides with the event of flagellate motion as seen in tables 1, 2 and 3. These proteins are in a prime position to act as environmental sensory proteins and leave the open question as to whether they are localised to the flagella within the flagellate form.

It is not yet clear how these proteins are used by the microbial eukaryotes in which they are found. In *N. gruberi*, analysis of the microarray dataset indicates clear differences in the way the extensive repertoire of predicted environmental signaling proteins are upregulated. The recently discovered histidine kinases and adenyl cyclases have a predominantly flagellate specific expression, amidst a more complex pattern of serpentine receptor expression. Future research could be carried out by creating a phylogeny of the *N. gruberi* serpentine receptors to identify which of these proteins have genuine orthologues in *N. fowleri*. This phylogeny would indicate how frequent paralogous gene duplication was during evolution of these receptors in *Naegleria* and whether these paralogues undergo similar patterns of stage specific gene regulation.

4.3 - SEM

As part of the experiments to look at the environmental response of *Naegleria* to O_2 deprivation, I found identical results to earlier studies (Tsaousis, Nývltová, Šuták, Hrdý & Tachezy, 2014; Bexkens et al., 2018), in the fact that xenically grown *Naegleria* failed to grow in an anaerobic environment.

Although a previously published method existed, which should have made the preparation of samples straight forward, I had to carry out several independent troubleshooting exercises in the absence of any available expertise within the lab. Due to the inability to prepare samples with critical point drying, I adjusted the protocols in an attempt to circumvent this.

The resulting images obtained from scanning electron microscopy showed control samples that were morphologically similar to previously published SEM cyst images. Cells cultivated in the microaerophilic CO_2 rich environments also matched the morphology of the controls, while cells grown in an anaerobic environment had a slightly altered morphology, similar to previously published images (Lastovica, 1974).

The presence of a nirK enzyme in *Naegleria* that localises to the mitochondria when heterologously expressed in *Trypanosoma brucei,* has been confirmed in currently unpublished material which suggests that anaerobic respiration may be possible. To explore this, cells were left to encyst in amoebasaline solutions or on agar plates containing a range of NO^-_3 or NO^-_2 concentrations. This resulted in the formation of rounded bodies, which we assumed to be cysts due to a visible ostiole-like structure.

4.4 - Protein purification

During the MSc I originally set out to localise four flagellate specific signalling proteins, of interest. The first was a candidate phosphate dependent fructokinase, which would act as a control as it is constitutively expressed in the cytosol. The second was the adenosine kinase domain of an intriguing fusion of an adenylate kinase with a pyruvate phosphate dikinase which is upregulated during flagellate differentiation. The third was a putative adenylate/guanylate cyclase with a nitrate/nitrite sensory domain which is shown to be upregulated during differentiation at the point where *N. gruberi* would begin to swim, but is then shown to be less expressed over time. And finally, the fourth was a PAS domain from a candidate, flagellate specific, adenyl cyclase.

The progress from each of these purifications is shown in figures 27 to 29 and while the localization of the proteins of interest could not be brought to completion, three of the four recombinant proteins are thought to have been successfully purified.

Further research is still required to reveal the location of these sensory proteins in the flagellate form and could provide a potential starting point for a subsequent project. One way to address this would be to derive antibodies recognising the *Naegleria* signalling proteins and to use immunolocalization to track protein congregation in vivo.

4.5 - Closing remarks

While my project may have begun with the aim of localising flagellate specific signalling proteins, throughout the course of my MSc thesis this aim has shifted and expanded. Throughout this year I have carried out several different independent and intersecting experiments, in an attempt to further elucidate the mechanisms of sensory proteins believed to reside within the flagellum of *Naegleria gruberi*.

The differentiation results and the results of other recently published work (Bexkens et al., 2018) showed evidence that Naegleria did not undergo oxidative phosphorylation when undergoing differentiation, but instead metabolised lipids preferentially. Due to this, a search for the regulation of sensory lipid-detecting proteins may reveal new insights into the differentiation process and flagellar sensory ability.

The localisation of the purified proteins of interest from the serpentine receptor cohort may be confirmed to reside within the flagellum. Further documentation would allow for an easy working model of a sensory flagella, which may be useful for therapeutic research.
The results of the bioinformatic analysis presented a number of sensory serpentine receptors which are now thought to be flagellate specific environmental sensory proteins. Localisation of these proteins will show whether they are actively bound to the flagella. If this is the case, these proteins may also hold value as model flagellate sensory proteins.

While there is much more to be done, this research in context, contributes to a greater understanding of *Naegleria* and early branching eukaryotes, as well as the flagellum as a whole. Conjunctively, these two topics are of significance to further understanding of two separate branches of human disease.

References

Adl, S., Leander, B., Simpson, A., Archibald, J., Anderson, O., & Bass, D. Et al. (2007). Diversity, nomenclature, and taxonomy of protists. Systematic Biology, 56(4), 684-689. Doi: 10.1080/10635150701494127

Ainsworth, C. (2007). Tails of the unexpected. Nature, 448(7154), 638-641. doi: 10.1038/448638a

Alcántar-Curiel, M., Blackburn, D., Saldaña, Z., Gayosso-Vázquez, C., Iovine, N., De la Cruz, M., & Girón, J. (2013). Multi-functional analysis of *Klebsiella pneumoniae* fimbrial types in adherence and biofilm formation. Virulence, 4(2), 129-138. Doi: 10.4161/viru.22974

Altschul, S., Gish, W., Miller, W., Myers, E., & Lipman, D. (1990). Basic local alignment search tool. Journal Of Molecular Biology, 215(3), 403-410. Doi: 10.1016/s0022-2836(05)80360-2

Antony van Leeuwenhoek. (2019). Retrieved from http://www.ucmp.berkeley.edu/history/leeuwenhoek.html

Archibald, J. (2017). Handbook of the protists (2nd ed., pp. 973-1003). New York: Springer.

Arizmendi, N., & Kulka, M. (2018). Adenosine activates Gαs proteins and inhibits c3a-induced activation of human mast cells. Biochemical Pharmacology, 156, 157-167. Doi: 10.1016/j.bcp.2018.08.011

Bardele, C. (1997). On the symbiotic origin of protists, their diversity, and their pivotal role in teaching systematic biology. Italian Journal Of Zoology, 64(2), 107-113. Doi: 10.1080/11250009709356181

Bargmann, C. (2006). Chemosensation in C. Elegans. Wormbook, 8-13. Doi: 10.1895/wormbook.1.123.1

Barker, A., Thomas, R., & Dawe, H. (2013). Meckel-Gruber syndrome and the role of primary cilia in kidney, skeleton, and central nervous system development. Organogenesis, 10(1), 96-107. Doi: 10.4161/org.27375

Beisson, J., & Wright, M. (2003). Basal body/centriole assembly and continuity. Current Opinion In Cell Biology, 15(1), 96-104. Doi: 10.1016/s0955-0674(02)00017-0

Berbari, N., Lewis, J., Bishop, G., Askwith, C., & Mykytyn, K. (2008). Bardet-Biedl syndrome proteins are required for the localization of G protein-coupled receptors to primary cilia. Proceedings Of The National Academy Of Sciences, 105(11), 4242-4246. Doi: 10.1073/pnas.0711027105

Berbari, N., Malarkey, E., Yazdi, S., McNair, A., Kippe, J., & Croyle, M. Et al. (2014). Hippocampal and cortical primary cilia are required for aversive memory in mice. Plos ONE, 9(9), e106576. Doi: 10.1371/journal.pone.0106576

Berndt, J., Callaway, N., & Gonzalez-Lima, F. (2001). Effects of chronic sodium azide on brain and muscle cytochrome oxidase activity: a potential model to investigate environmental contributions to neurodegenerative diseases. Journal Of Toxicology And Environmental Health, Part A, 63(1), 67-77. Doi: 10.1080/152873901750128380

Bernstein, M., Beech, P., Katz, S., & Rosenbaum, J. (1994). A new kinesin-like protein (Klp1) localized to a single microtubule of the *Chlamydomonas* flagellum. The Journal Of Cell Biology, 125(6), 1313-1326. Doi: 10.1083/jcb.125.6.1313

Beste, K., Spangler, C., Burhenne, H., Koch, K., Shen, Y., & Tang, W. Et al. (2013). Nucleotidyl cyclase activity of particulate guanylyl cyclase a: comparison with particulate guanylyl cyclases e and f, soluble guanylyl cyclase and bacterial adenylyl cyclases cyaa and edema factor. Plos ONE, 8(7), e70223. Doi: 10.1371/journal.pone.0070223

Bexkens, M., Zimorski, V., Sarink, M., Wienk, H., Brouwers, J., & De Jonckheere, J. Et al. (2018). Lipids are the preferred substrate of the protist *Naegleria gruberi*, relative of a human brain pathogen. Cell Reports, 25(3), 537-543.e3. Doi: 10.1016/j.celrep.2018.09.055

Bieger, B. (2001). Structural analysis of adenylate cyclases from *Trypanosoma brucei* in their monomeric state. The EMBO Journal, 20(3), 433-445. Doi: 10.1093/emboj/20.3.433

Bilwes, A., Alex, L., Crane, B., & Simon, M. (1999). Structure of chea, a signal-transducing histidine kinase. Cell, 96(1), 131-141. Doi: 10.1016/s0092-8674(00)80966-6

Blackler, S. And Sommerville, R. (1988). Carbonic acid and the excystment of *Naegleria gruberi* (Heterolobosea:Vahlkampfiidae). International Journal for Parasitology, [online] 18(6), pp.785-791. Available at: https://www.sciencedirect.com/science/article/pii/0020751988901208?Via%3Dihub

Bloodgood, R. (2010). Sensory reception is an attribute of both primary cilia and motile cilia. Journal Of Cell Science, 123(4), 505-509. Doi: 10.1242/jcs.066308

Bockaert, J. (1999). Molecular tinkering of G protein-coupled receptors: an evolutionary success. The EMBO Journal, 18(7), 1723-1729. Doi: 10.1093/emboj/18.7.1723

Bockaert, J., & Pin, J. (1999). Molecular tinkering of G protein-coupled receptors: an evolutionary success. The EMBO Journal, 18(7), 1723-1729. Doi: 10.1093/emboj/18.7.1723

Brazill, D., Lindsey, D., Bishop, J., & Gomer, R. (1998). Cell density sensing mediated by a g protein-coupled receptor activating phospholipase C. Journal Of Biological Chemistry, 273(14), 8161-8168. Doi: 10.1074/jbc.273.14.8161

Breugel, M., Wilcken, R., Mclaughlin, S., Rutherford, T., & Johnson, C. (2014). Structure of the SAS-6 cartwheel hub from Leishmania major. Elife, 3. Doi: 10.7554/elife.01812

Briggs, L., Davidge, J., Wickstead, B., Ginger, M., & Gull, K. (2004). More than one way to build a flagellum: comparative genomics of parasitic protozoa. Current Biology, 14(15), R611-R612. Doi: 10.1016/j.cub.2004.07.041

Brown, J., & Witman, G. (2014). Cilia and Diseases. Bioscience, 64(12), 1126-1137. Doi: 10.1093/biosci/biu174

Brown, T. (1979). Observations by immunofluorescence microscopy and electron microscopy on the cytopathogenicity of *Naegleria fowleri* in mouse embryo-cell cultures. Journal Of Medical Microbiology, 12(3), 363-371. Doi: 10.1099/00222615-12-3-363

Brown, T., Cursons, R., Keys, E., Marks, M., & Miles, M. (1983). The occurrence and distribution of pathogenic free-living amoebae in thermal areas of the North Island of New Zealand. New Zealand Journal Of Marine And Freshwater Research, 17(1), 59-69. Doi: 10.1080/00288330.1983.9515987

Bunn, H., & Higgins, P. (1981). Reaction of monosaccharides with proteins: possible evolutionary significance. Science, 213(4504), 222-224. Doi: 10.1126/science.12192669

Butt, C. (1966). Primary amebic meningoencephalitis. New England Journal Of Medicine, 274(26), 1473-1476. Doi: 10.1056/nejm196606302742605

C. Diniz, M., C. Pacheco, A., M. Farias, K., & M. De Oliveira, D. (2012). The eukaryotic flagellum makes the day: novel and unforeseen roles uncovered after post-genomics and proteomics data. Current Protein & Peptide Science, 13(6), 524-546. Doi: 10.2174/138920312803582951

Calabrese, E., Bachmann, K., Bailer, A., Bolger, P., Borak, J., & Cai, L. Et al. (2007). Biological stress response terminology: Integrating the concepts of adaptive response and preconditioning stress within a hormetic dose–response framework. Toxicology And Applied Pharmacology, 222(1), 122-128. Doi: 10.1016/j.taap.2007.02.015

Cao, Y., Park, A., & Sun, Z. (2010). Intraflagellar transport proteins are essential for cilia formation and for planar cell polarity. Journal Of The American Society Of Nephrology, 21(8), 1326-1333. Doi: 10.1681/asn.2009091001

Carter, R. (1970). Description of a *naegleria* sp. Isolated from two cases of primary amoebic meningo-encephalitis, and of the experimental pathological changes induced by it. The Journal Of Pathology, 100(4), 217-244. Doi: 10.1002/path.1711000402

Casino, P., Miguel-Romero, L., & Marina, A. (2014). Visualizing autophosphorylation in histidine kinases. Nature Communications, 5(1). Doi: 10.1038/ncomms4258

Červa, L. (1971). Studies of limax amoebae in a Swimming Pool. Hydrobiologia, 38(1), 141-161. Doi: 10.1007/bf00036798

Cervantes-Sandoval, I., Serrano-Luna, J., García-Latorre, E., Tsutsumi, V., & Shibayama, M. (2008). Characterization of brain inflammation during primary amoebic meningoencephalitis. Parasitology International, 57(3), 307-313. Doi: 10.1016/j.parint.2008.01.006

Chao, Y., Chen, C., Lin, Y., Breer, H., Fleischer, J., & Yang, R. (2014). Receptor guanylyl cyclase-G is a novel thermosensory protein activated by cool temperatures. The EMBO Journal, 34(3), 294-306. Doi: 10.15252/embj.201489652

Chatterjee, D., Eckert, C., Slavov, C., Saxena, K., Fürtig, B., & Sanders, C. Et al. (2015). Influence of arrestin on the photodecay of bovine rhodopsin. Angewandte Chemie International Edition, 54(46), 13555-13560. Doi: 10.1002/anie.201505798

Chauhan, S., Chandel, L., Jaryal, S., & Sood, A. (2014). Prompt diagnosis and extraordinary survival from *Naegleria fowleri* meningitis: A rare case report. Indian Journal Of Medical Microbiology, 32(2), 193. Doi: 10.4103/0255-0857.129834

Chiovetti, R. (1976). Re-encystment of the amoeboflagellate *Naegleria gruberi*. Transactions Of The American Microscopical Society, 95(1), 122. Doi: 10.2307/3225363

Chung, K., & Liu, J. (2017). Pioneers in microbiology. Singapore: World Scientific Publishing Co. Pte. Ltd.

Cilia. (2010). Retrieved from http://www.ciliopathyalliance.org/cilia.html

Clark, C., & Cross, G. (1987). rRNA genes of *Naegleria gruberi* are carried exclusively on a 14-kilobase-pair plasmid. Molecular And Cellular Biology, 7(9), 3027-3031. Doi: 10.1128/mcb.7.9.3027

Clark, C., & Cross, G. (1988). Circular ribosomal RNA genes are a general feature of Schizopyrenid amoebae. The Journal Of Protozoology, 35(2), 326-329. Doi: 10.1111/j.1550-7408.1988.tb04352.x

Cogo, P., Scaglia, M., Gatti, S., Rossetti, F., Alaggio, R., & Laverda, A. Et al. (2004). Fatal N*aegleria fowleri* meningoencephalitis, Italy. Emerging Infectious Diseases, 10(10), 1835-1837. Doi: 10.3201/eid1010.040273

Collingridge, P., Wheeler, G., & Brownlee, C. (2012). The molecular mechanisms of calcium signalling in *Chlamydomonas* flagella. Cilia, 1(1), 19.

Culbertson, C., Ensminger, P., & Overton, W. (1968). Pathogenic *naegleria* sp. Study of a strain isolated from human cerebrospinal fluid. The Journal Of Protozoology, 15(2), 353-363. Doi: 10.1111/j.1550-7408.1968.tb02136.x

Curry, A., Williams, B., & Rosenbaum, J. (1992). Sequence analysis reveals homology between two proteins of the flagellar radial spoke. Molecular And Cellular Biology, 12(9), 3967-3977. Doi: 10.1128/mcb.12.9.3967

Dando, S., Mackay-Sim, A., Norton, R., Currie, B., St. John, J., & Ekberg, J. Et al. (2014). Pathogens penetrating the central nervous system: infection pathways and the cellular and molecular mechanisms of invasion. Clinical Microbiology Reviews, 27(4), 691-726. Doi: 10.1128/cmr.00118-13

D'Angelo, M., Montagna, A., Sanguineti, S., Torres, H., & Flawiá, M. (2002). A novel calcium-stimulated adenylyl cyclase from T*rypanosoma cruzi*, which interacts with the structural flagellar protein paraflagellar rod. Journal Of Biological Chemistry, 277(38), 35025-35034. Doi: 10.1074/jbc.m204696200

De Jonckheere, J. (1981). Pathogenic and non-pathogenic *Acanthamoeba* spp. In thermally polluted discharges and surface waters. The Journal Of Protozoology, 28(1), 56-59. Doi: 10.1111/j.1550-7408.1981.tb02804.x

De Jonckheere, J. (2002). A century of research on the amoeboflagellate genus *Naegleria* (pp. 309 - 342). Brussels: Acta Protozool.

De Jonckheere, J. (2004). Molecular definition and the ubiquity of species in the genus. Protist, 155(1), 89-103. Doi: 10.1078/1434461000167

De Jonckheere, J. (2011). Origin and evolution of the worldwide distributed pathogenic amoeboflagellate *Naegleria* f*owleri*. Infection, Genetics And Evolution, 11(7), 1520-1528. Doi: 10.1016/j.meegid.2011.07.023

De Jonckheere, J. (2012). The impact of man on the occurrence of the pathogenic free-living amoeboflagellate *Naegleria fowleri*. Future Microbiology, 7(1), 5-7. Doi: 10.2217/fmb.11.141

De Jonckheere, J. (2014). What do we know by now about the genus *Naegleria*?. Experimental Parasitology, 145, S2-S9. Doi: 10.1016/j.exppara.2014.07.011

De March, C., Kim, S., Antonczak, S., Goddard, W., & Golebiowski, J. (2015). G protein-coupled odorant receptors: From sequence to structure. Protein Science, 24(9), 1543-1548. Doi: 10.1002/pro.2717

De Souza, W., Morais, E., Krohn, N., Savoldi, M., Goldman, M., & Rodrigues, F. Et al. (2013). Identification of metabolic pathways influenced by the G-protein coupled receptors gprb and gprd in *Aspergillus nidulans*. Plos ONE, 8(5), e62088. Doi: 10.1371/journal.pone.0062088

Deane, J., Verghese, E., Martelotto, L., Cain, J., Galtseva, A., & Rosenblum, N. Et al. (2013). Visualizing renal primary cilia. Nephrology, 18(3), 161-168. Doi: 10.1111/nep.12022

Denet, E., Coupat-Goutaland, B., Nazaret, S., Pélandakis, M., & Favre-Bonté, S. (2017). Diversity of free-living amoebae in soils and their associated human opportunistic bacteria. Parasitology Research, 116(11), 3151-3162. Doi: 10.1007/s00436-017-5632-6

Devree, B., Mahoney, J., Vélez-Ruiz, G., Rasmussen, S., Kuszak, A., & Edwald, E. Et al. (2016). Allosteric coupling from G protein to the agonist-binding pocket in gpcrs. Nature, 535(7610), 182-186. Doi: 10.1038/nature18324

Diagnosis & Detection | *Naegleria fowleri* | CDC. (2018). Retrieved from https://www.cdc.gov/parasites/*Naegleria*/diagnosis.html

Diener, D., Yang, P., Geimer, S., Cole, D., Sale, W., & Rosenbaum, J. (2011). Sequential assembly of flagellar radial spokes. Cytoskeleton, 68(7), 389-400. Doi: 10.1002/cm.20520

Discovery Of Bacteria - by Antony van Leeuwenhoek. (2019). Retrieved from https://explorable.com/discovery-of-bacteria

Dosil, M., Giot, L., Davis, C., & Konopka, J. (1998). Dominant-negative mutations in the G-protein-coupled α-factor receptor map to the extracellular ends of the transmembrane segments. Molecular And Cellular Biology, 18(10), 5981-5991. Doi: 10.1128/mcb.18.10.5981

Dyková, I., Kyselová, I., Pecková, H., Oborník, M., & Lukes, J. (2001). Identity of Naegleria strains isolated from organs of freshwater fishes. Diseases Of Aquatic Organisms, 46, 115-121. doi: 10.3354/dao046115

Ebenezer, T., Carrington, M., Lebert, M., Kelly, S., & Field, M. (2017). *Euglena gracilis* genome and transcriptome: organelles, nuclear genome assembly strategies and initial features. Advances In Experimental Medicine And Biology, 125-140. Doi: 10.1007/978-3-319-54910-1_7

Embley, M., der Giezen, M., Horner, D., Dyal, P., & Foster, P. (2003). Mitochondria and hydrogenosomes are two forms of the same fundamental organelle. Philosophical Transactions Of The Royal Society B: Biological Sciences, 358(1429), 191-203. Doi: 10.1098/rstb.2002.1190

Embley, T. (2006). Multiple secondary origins of the anaerobic lifestyle in eukaryotes. Philosophical Transactions Of The Royal Society B: Biological Sciences, 361(1470), 1055-1067. Doi: 10.1098/rstb.2006.1844

Embley, T., van der Giezen, M., Horner, D., Dyal, P., Bell, S., & Foster, P. (2003). Hydrogenosomes, mitochondria and early eukaryotic evolution. IUBMB Life (International Union Of Biochemistry And Molecular Biology: Life), 55(7), 387-395. Doi: 10.1080/15216540310001592834

Farrar, J., & Manson, P. (2014). Manson's tropical diseases (23rd ed., pp. 683-691). [London u.a.]: Elsevier Saunders.

Flock, T., Ravarani, C., Sun, D., Venkatakrishnan, A., Kayikci, M., & Tate, C. Et al. (2015). Universal allosteric mechanism for Gα activation by gpcrs. Nature, 524(7564), 173-179. Doi: 10.1038/nature14663

Fojo, T. (2008). The role of microtubules in cell biology, neurobiology, and oncology (1st ed., pp. 177-191). Totowa, NJ: Humana Press.

Fritz-Laylin, L. (2010). The genome and cytoskeleton of *Naegleria gruberi*, an amoeboflagellate (Ph.D). University of California, Berkeley.

Fritz-Laylin, L., & Cande, W. (2010). Ancestral centriole and flagella proteins identified by analysis of *Naegleria* differentiation. Journal Of Cell Science, 123(23), 4024-4031. Doi: 10.1242/jcs.077453

Fritz-Laylin, L., & Fulton, C. (2016). *Naegleria*: a classic model for de novo basal body assembly. Cilia, 5(1). Doi: 10.1186/s13630-016-0032-6

Fritz-Laylin, L., Ginger, M., Walsh, C., Dawson, S., & Fulton, C. (2011). The *Naegleria* genome: a free-living microbial eukaryote lends unique insights into core eukaryotic cell biology. Research In Microbiology, 162(6), 607-618. Doi: 10.1016/j.resmic.2011.03.003

Fritz-Laylin, L., Prochnik, S., Ginger, M., Dacks, J., Carpenter, M., & Field, M. Et al. (2010). The Genome of *Naegleria gruberi* Illuminates Early Eukaryotic Versatility. Cell, 140(5), 631-642. Doi: 10.1016/j.cell.2010.01.032

Fukuto, H., Ferkey, D., Apicella, A., Lans, H., Sharmeen, T., & Chen, W. Et al. (2004). G protein-coupled receptor kinase function is essential for chemosensation in *C. elegans*. Neuron, 42(4), 581-593. Doi: 10.1016/s0896-6273(04)00252-1

Fulton C (1970) Amebo-flagellates as research partners: The laboratory biology of *Naegleria* and Tetramitus. Meth Cell Physiol 4: 341–476.

Fulton, C. (1993). *Naegleria*: a research partner for cell and developmental biology. The Journal Of Eukaryotic Microbiology, 40(4), 520-532. Doi: 10.1111/j.1550-7408.1993.tb04945.x

Fulton, C., and Dingle, A. D., 1967, Appearance of the flagellate phenotype in populations of *Naegleria* amebae, Develop. Biol., in press.

Gao, Y., Westfield, G., Erickson, J., Cerione, R., Skiniotis, G., & Ramachandran, S. (2017). Isolation and structure–function characterization of a signaling-active rhodopsin–G protein complex. Journal Of Biological Chemistry, 292(34), 14280-14289. Doi: 10.1074/jbc.m117.797100

Garcia, D., Orillard, E., Johnson, M., & Watts, K. (2017). Gas sensing and signaling in the PAS-heme domain of the *Pseudomonas aeruginosa* Aer2 Receptor. Journal Of Bacteriology, 199(18). Doi: 10.1128/jb.00003-17

General Information | *Naegleria Fowleri* | CDC. (2018). Cdc.gov. Retrieved 30 January 2018, from https://www.cdc.gov/parasites/*Naegleria*/general.html

Gillespie, P., & Müller, U. (2009). Mechanotransduction by hair cells: models, molecules, and mechanisms. Cell, 139(1), 33-44. Doi: 10.1016/j.cell.2009.09.010

Gilmartin, A., & Petri, W. (2018). Exploring the mechanism of amebic trogocytosis: the role of amebic lysosomes. Microbial Cell, 5(1), 1-3. Doi: 10.15698/mic2018.01.606

Ginger, M., Fritz-Laylin, L., Fulton, C., Cande, W., & Dawson, S. (2010). Intermediary metabolism in protists: a sequence-based view of facultative anaerobic metabolism in evolutionarily diverse eukaryotes. Protist, 161(5), 642-671. Doi: 10.1016/j.protis.2010.09.001

Gluenz, E., Höög, J., Smith, A., Dawe, H., Shaw, M., & Gull, K. (2010). Beyond 9+0: noncanonical axoneme structures characterize sensory cilia from protists to humans. The FASEB Journal, 24(9), 3117-3121. Doi: 10.1096/fj.09-151381

Gookin, T., Kim, J., & Assmann, S. (2008). Whole proteome identification of plant candidate G-protein coupled receptors in *Arabidopsis*, rice, and poplar: computational prediction and in-vivo protein coupling. Genome Biology, 9(7), R120. Doi: 10.1186/gb-2008-9-7-r120

Goujon, M. (2010). A new bioinformatics analysis tools framework at EMBL-EBI. Nucleic Acids Research, 38(Web Server), W695-W699. Doi: 10.1093/nar/gkq313

Grace, E., Asbill, S., & Virga, K. (2015). *Naegleria fowleri*: pathogenesis, diagnosis, and treatment options. Antimicrobial Agents And Chemotherapy, 59(11), 6677-6681. Doi: 10.1128/aac.01293-15

Griffin, J. (1983). The pathogenic amoeboflagellate *Naegleria fowleri*: environmental isolations, competitors, ecologic interactions, and the flagellate-empty habitat hypothesis. The Journal Of Protozoology, 30(2), 403-409. Doi: 10.1111/j.1550-7408.1983.tb02939.x

Grigoriev, I., Nordberg, H., Shabalov, I., Aerts, A., Cantor, M., & Goodstein, D. Et al. (2011). The genome portal of the department of energy joint genome institute. Nucleic Acids Research, 40(D1), D26-D32. Doi: 10.1093/nar/gkr947

Guéguinou, M., Gambade, A., Félix, R., Chantôme, A., Fourbon, Y., & Bougnoux, P. Et al. (2015). Lipid rafts, kca/clca/Ca2+ channel complexes and EGFR signaling: Novel targets to reduce tumor development by lipids?. Biochimica Et Biophysica Acta (BBA) - Biomembranes, 1848(10), 2603-2620. Doi: 10.1016/j.bbamem.2014.10.036

Haimo, L., & Rosenbaum, J. (1981). Cilia, flagella, and microtubules. The Journal Of Cell Biology, 91(3), 125s-130. Doi: 10.1083/jcb.91.3.125s

Hampl, V., Hug, L., Leigh, J., Dacks, J., Lang, B., Simpson, A., & Roger, A. (2009). Phylogenomic analyses support the monophyly of Excavata and resolve relationships among eukaryotic "supergroups". Proceedings Of The National Academy Of Sciences, 106(10), 3859-3864. Doi: 10.1073/pnas.0807880106

Hancock, J. (2010). Cell signalling (3rd ed., pp. 189–195). Oxford: Oxford University Press.

Hanousková, P., Táborský, P., & Čepička, I. (2018). Dactylomonas gen. Nov., a Novel Lineage of Heterolobosean Flagellates with Unique Ultrastructure, Closely Related to the Amoeba Selenaion koniopes Park, De Jonckheere & Simpson, 2012. Journal Of Eukaryotic Microbiology. Doi: 10.1111/jeu.12637

Hayes, W., & Laws, E. (1991). Handbook of pesticide toxicology. San Diego, Calif.: Academic Press.

Hazell, G., Hindmarch, C., Pope, G., Roper, J., Lightman, S., & Murphy, D. Et al. (2012). G protein-coupled receptors in the hypothalamic paraventricular and supraoptic nuclei – serpentine gateways to neuroendocrine homeostasis. Frontiers In Neuroendocrinology, 33(1), 45-66. Doi: 10.1016/j.yfrne.2011.07.002

He, Q., Zhu, Y., Corbin, B., Plagge, A., & Bastepe, M. (2015). The G protein α subunit variant xlαs promotes inositol 1,4,5-trisphosphate signaling and mediates the renal actions of parathyroid hormone in vivo. Science Signaling, 8(391), ra84-ra84. Doi: 10.1126/scisignal.aaa9953

Herbst, S., Masada, N., Pfennig, S., Ihling, C., Cooper, D., & Sinz, A. (2013). Structural insights into calmodulin/adenylyl cyclase 8 interaction. Analytical And Bioanalytical Chemistry, 405(29), 9333-9342. Doi: 10.1007/s00216-013-7358-3

Hildebrandt, F., Benzing, T., & Katsanis, N. (2011). Ciliopathies. New England Journal Of Medicine, 364(16), 1533-1543. Doi: 10.1056/nejmra1010172

Hisanaga, S., & Pratt, M. (1984). Calmodulin interaction with cytoplasmic and flagellar dynein: calcium-dependent binding and stimulation of adenosine triphosphatase activity. Biochemistry, 23(13), 3032-3037. Doi: 10.1021/bi00308a029

Höhfeld, I., Otten, J., & Melkonian, M. (1988). Contractile eukaryotic flagella: Centrin is involved. Protoplasma, 147(1), 16-24. Doi: 10.1007/bf01403874

Home - Taxonomy - NCBI. (2018). Ncbi.nlm.nih.gov. Retrieved 28 January 2018, from https://www.ncbi.nlm.nih.gov/taxonomy

Hooke, R. (1665). Micrographia: or some physiological descriptions of minute bodies made by magnifying glasses, with observations and inquiries thereupon. London.

Hou, Y., Pazour, G., & Witman, G. (2004). A dynein light intermediate chain, d1blic, is required for retrograde intraflagellar transport. Molecular Biology Of The Cell, 15(10), 4382-4394. Doi: 10.1091/mbc.e04-05-0377

Huang, C., Hepler, J., Chen, L., Gilman, A., Anderson, R., & Mumby, S. (1997). Organization of G proteins and adenylyl cyclase at the plasma membrane. Molecular Biology Of The Cell, 8(12), 2365-2378. Doi: 10.1091/mbc.8.12.2365

Hülsmann, N. (1992). Undulipodium: End of a useless discussion. European Journal Of Protistology, 28(3), 253-257. Doi: 10.1016/s0932-4739(11)80231-2

Ikeda, K., Brown, J., Yagi, T., Norrander, J., Hirono, M., & Eccleston, E. Et al. (2002). Rib72, a conserved protein associated with the ribbon compartment of flagellar a-microtubules and potentially involved in the linkage between outer doublet microtubules. Journal Of Biological Chemistry, 278(9), 7725-7734. Doi: 10.1074/jbc.m210751200

Ikeda, K., Ikeda, T., Morikawa, K., & Kamiya, R. (2007). Axonemal localization of *Chlamydomonas* pacrg, a homologue of the humanparkin-coregulated gene product. Cell Motility And The Cytoskeleton, 64(11), 814-821. Doi: 10.1002/cm.20225

Ikeda, T. (2008). Parkin-co-regulated gene (PACRG) product interacts with tubulin and microtubules. FEBS Letters, 582(10), 1413-1418. Doi: 10.1016/j.febslet.2008.02.081

Inaba, K. (2015). Calcium sensors of ciliary outer arm dynein: functions and phylogenetic considerations for eukaryotic evolution. Cilia, 4(1). Doi: 10.1186/s13630-015-0015-z

Iseki, M., Matsunaga, S., Murakami, A., Ohno, K., Shiga, K., & Yoshida, K. Et al. (2002). A blue-light-activated adenylyl cyclase mediates photoavoidance in Euglena gracilis. Nature, 415(6875), 1047-1051. Doi: 10.1038/4151047a

Jamerson, M., da Rocha-Azevedo, B., Cabral, G., & Marciano-Cabral, F. (2012). Pathogenic *Naegleria fowleri* and non-pathogenic *Naegleria lovaniensis* exhibit differential adhesion to, and invasion of, extracellular matrix proteins. Microbiology, 158(Pt_3), 791-803. Doi: 10.1099/mic.0.055020-0

Jarolim, K., McCosh, J., Howard, M., & John, D. (2000). A light microscopy study of the migration of *Naegleria fowleri* from the nasal submucosa to the central nervous system during the early stage of primary amebic meningoencephalitis in mice. Journal Of Parasitology, 86(1), 50-55. Doi: 10.1645/0022-3395(2000)086[0050:almsot]2.0.co;2

Jarrell, K., & McBride, M. (2008). The surprisingly diverse ways that prokaryotes move. Nature Reviews Microbiology, 6(6), 466-476. Doi: 10.1038/nrmicro1900

Jiang, B., Zhang, W., Yang, T., Guo, C., Cao, D., Zhang, Z., & Gao, Y. (2018). Demethylation of G protein-coupled receptor 151 promoter facilitates the binding of Kruppel-like factor 5 and enhances neuropathic pain after nerve injury in mice. The Journal Of Neuroscience, 0702-18. Doi: 10.1523/jneurosci.0702-18.2018

Jin, H., & Nachury, M. (2009). The bbsome. Current Biology, 19(12), R472-R473. Doi: 10.1016/j.cub.2009.04.015

Jin, H., White, S., Shida, T., Schulz, S., Aguiar, M., & Gygi, S. Et al. (2010). The conserved bardet-biedl syndrome proteins assemble a coat that traffics membrane proteins to cilia. Cell, 141(7), 1208-1219. Doi: 10.1016/j.cell.2010.05.015

John, D., Cole, T., & Bruner, R. (1985). Amebostomes of *Naegleria fowleri*. The Journal Of Protozoology, 32(1), 12-19. Doi: 10.1111/j.1550-7408.1985.tb03006.x

John, D., Cole, T., & Marciano-Cabral, F. (1984). Sucker-like structures on the pathogenic amoeba *Naegleria fowleri*. Appl. Environ. Microbiol. 47(1), 12-14.

John, D., Petri, W., Markell, E., & Voge, M. (2006). Markell and Voge's medical parasitology (9th ed., pp. 152-157). St. Luis: Saunders Elsevier.

Jones, C., & Chen, P. (2008). Chapter eight primary cilia in planar cell polarity regulation of the inner ear. Ciliary Function In Mammalian Development, 197-224. Doi: 10.1016/s0070-2153(08)00808-9

Kabbara, S., Hérivaux, A., Dugé De Bernonville, T., Courdavault, V., Clastre, M., & Gastebois, A. Et al. (2018). Diversity and evolution of sensor histidine kinases in eukaryotes. Genome Biology And Evolution. Doi: 10.1093/gbe/evy213

Kaiser, J. (2003). Hormesis: sipping from a poisoned chalice. Science, 302(5644), 376-379. Doi: 10.1126/science.302.5644.376

Karunanithi, S., Xiong, T., Uhm, M., Leto, D., Sun, J., Chen, X., & Saltiel, A. (2014). A Rab10:rala G protein cascade regulates insulin-stimulated glucose uptake in adipocytes. Molecular Biology Of The Cell, 25(19), 3059-3069. Doi: 10.1091/mbc.e14-06-1060

Keeling, P., Burger, G., Durnford, D., Lang, B., Lee, R., & Pearlman, R. Et al. (2005). The tree of eukaryotes. Trends In Ecology & Evolution, 20(12), 670-676. Doi: 10.1016/j.tree.2005.09.005

Kelly, J. (2013). Unusual aspects of *Trypanosoma* and *naegleria* metabolism (M.Sc.). The University of Lancaster.

Khan, S., & Scholey, J. (2018). Assembly, functions and evolution of archaella, flagella and cilia. Current Biology, 28(6), R278-R292. Doi: 10.1016/j.cub.2018.01.085

Kim, J., Ahuja, L., Chao, F., Xia, Y., Mclendon, C., & Kornev, A. Et al. (2017). A dynamic hydrophobic core orchestrates allostery in protein kinases. Science Advances, 3(4), e1600663. Doi: 10.1126/sciadv.1600663

Kim, S., Dangelmaier, C., Bhavanasi, D., Meng, S., Wang, H., Goldfinger, L., & Kunapuli, S. (2013). Rhog protein regulates glycoprotein vi-fc receptor γ-chain complex-mediated platelet activation and

thrombus formation. Journal Of Biological Chemistry, 288(47), 34230-34238. Doi: 10.1074/jbc.m113.504928

Klink, B., Zent, E., Juneja, P., Kuhlee, A., Raunser, S., & Wittinghofer, A. (2017). A recombinant bbsome core complex and how it interacts with ciliary cargo. Elife, 6. Doi: 10.7554/elife.27434

Koretke, K., Lupas, A., Warren, P., Rosenberg, M., & Brown, J. (2000). Evolution of two-component signal transduction. Molecular Biology And Evolution, 17(12), 1956-1970. Doi: 10.1093/oxfordjournals.molbev.a026297

Koumandou, V., Wickstead, B., Ginger, M., van der Giezen, M., Dacks, J., & Field, M. (2013). Molecular paleontology and complexity in the last eukaryotic common ancestor. Critical Reviews In Biochemistry And Molecular Biology, 48(4), 373-396. Doi: 10.3109/10409238.2013.821444

Kozminski, K., Johnson, K., Forscher, P., & Rosenbaum, J. (1993). A motility in the eukaryotic flagellum unrelated to flagellar beating. Proceedings Of The National Academy Of Sciences, 90(12), 5519-5523. Doi: 10.1073/pnas.90.12.5519

Lai, E. (1988). The alpha-tubulin gene family expressed during cell differentiation in *Naegleria gruberi*. The Journal Of Cell Biology, 106(6), 2035-2046. Doi: 10.1083/jcb.106.6.2035

Lane, N. (2015). The unseen world: reflections on Leeuwenhoek (1677) Concerning little animals. Philosophical Transactions Of The Royal Society B: Biological Sciences, 370(1666), 20140344-20140344. Doi: 10.1098/rstb.2014.0344

Lara, E., Chatzinotas, A., & Simpson, A. (2006). Andalucia (n. Gen.) the deepest branch within Jakobids (Jakobida; Excavata), based on morphological and molecular study of a new flagellate from soil. The Journal Of Eukaryotic Microbiology, 53(2), 112-120. Doi: 10.1111/j.1550-7408.2005.00081.x

Lastovica, A. (1974). Scanning electron microscopy of pathogenic and non-pathogenic *Naegleria* cysts. International Journal For Parasitology, 4(2), 139-142. Doi: 10.1016/0020-7519(74)90096-4

Lechtreck, K. (2015). IFT cargo interactions and protein transport in cilia. Trends In Biochemical Sciences, 40(12), 765-778. Doi: 10.1016/j.tibs.2015.09.003

Li, L., Anand, M., Rao, K., & Khanna, H. (2015). Cilia in photoreceptors. Methods In Cilia & Flagella, 75-92. Doi: 10.1016/bs.mcb.2014.12.005

Li, S., Fernandez, J., Marshall, W., & Agard, D. (2011). Three-dimensional structure of basal body triplet revealed by electron cryo-tomography. The EMBO Journal, 31(3), 552-562. Doi: 10.1038/emboj.2011.460

Li, Z. (2014). A novel role of centrin in flagellar motility: stabilizing an inner-arm dynein motor in the flagellar axoneme. Microbial Cell, 1(8), 267-269. Doi: 10.15698/mic2014.08.161

Lichstein, H. C., & Soule, M. H. (1944). Studies of the effect of sodium azide on microbic growth and respiration: i. The action of sodium azide on microbic growth. Journal of bacteriology, 47(3), 221-30.

Linam, W., Ahmed, M., Cope, J., Chu, C., Visvesvara, G., & da Silva, A. Et al. (2015). Successful treatment of an adolescent with *Naegleria fowleri* primary amebic meningoencephalitis. Pediatrics, 135(3), e744-e748. Doi: 10.1542/peds.2014-2292

Lodish, H., Berk, A., Zipursky, L., Matsudaira, P., Baltimore, D., & Darnell, J. (2000). Molecular cell biology (4th ed.). New York: W.H. Freeman.

Lopez, M., Saada, E., & Hill, K. (2014). Insect stage-specific adenylate cyclases regulate social motility in african trypanosomes. Eukaryotic Cell, 14(1), 104-112. Doi: 10.1128/ec.00217-14

López-Elizalde, R., Campero, A., Sánchez-Delgadillo, T., Lemus-Rodríguez, Y., López-González, M., & Godínez-Rubí, M. (2017). Anatomy of the olfactory nerve: A comprehensive review with cadaveric dissection. Clinical Anatomy, 31(1), 109-117. Doi: 10.1002/ca.23003

Loucks, C., Bialas, N., Dekkers, M., Walker, D., Grundy, L., & Li, C. Et al. (2016). PACRG, a protein linked to ciliary motility, mediates cellular signaling. Molecular Biology Of The Cell, 27(13), 2133-2144. Doi: 10.1091/mbc.e15-07-0490

Macneil, S., Lakey, T., & Tomlinson, S. (1985). Calmodulin regulation of adenylate cyclase activity. Cell Calcium, 6(3), 213-226. Doi: 10.1016/0143-4160(85)90007-7

Marciano-Cabral, F. & Fulford, D. (1986). Cytopathology of pathogenic and non pathogenic *Naegleria* species for cultured rat neuroblastoma cells. Appl. Environ. Microbiol. 51(5), 1133-1137.

Marciano-Cabral, F. (1988). Biology of *Naegleria* spp. Microbiol. Rev., 52(1), 114-133.

Marciano-Cabral, F., & Cabral, G. (2007). The immune response to *Naegleria fowleri* amebae and pathogenesis of infection. FEMS Immunology & Medical Microbiology, 51(2), 243-259. Doi: 10.1111/j.1574-695x.2007.00332.x

Marciano-Cabral, F., & John, D. (1983). Cytopathogenicity of *Naegleria fowleri* for rat neuroblastoma cell cultures: scanning electron microscopy study. Infect. Immun. 40(3), 1214-1217.

Marciano-Cabral, F., maclean, R., Mensah, A., & lapat-Polasko, L. (2003). Identification of *Naegleria fowleri* in domestic water sources by nested PCR. Applied And Environmental Microbiology, 69(10), 5864-5869. Doi: 10.1128/aem.69.10.5864-5869.2003

Margulis, L. (1980). Undulipodia, flagella and cilia. Biosystems, 12(1-2), 105-108. Doi: 10.1016/0303-2647(80)90041-6

Martin, W., & Müller, M. (1998). The hydrogen hypothesis for the first eukaryote. Nature, 392(6671), 37-41. Doi: 10.1038/32096

Masuda, S., & Bauer, C. (2002). Appa is a blue light photoreceptor that antirepresses photosynthesis gene expression in *Rhodobacter sphaeroides*. Cell, 110(5), 613-623. Doi: 10.1016/s0092-8674(02)00876-0

Mattson, M. (2008). Hormesis defined. Ageing Research Reviews, 7(1), 1-7. Doi: 10.1016/j.arr.2007.08.007

Mattson, M. (2015). What doesn't kill you ... Scientific American, 313(1), 40-45. Doi: 10.1038/scientificamerican0715-40

Mechaly, A., Soto Diaz, S., Sassoon, N., Buschiazzo, A., Betton, J., & Alzari, P. (2017). Structural coupling between autokinase and phosphotransferase reactions in a bacterial histidine kinase. Structure, 25(6), 939-944.e3. Doi: 10.1016/j.str.2017.04.011

Merchant, S., Prochnik, S., Vallon, O., Harris, E., Karpowicz, S., & Witman, G. Et al. (2007). The *Chlamydomonas* genome reveals the evolution of key animal and plant functions. Science, 318(5848), 245-250. Doi: 10.1126/science.1143609

Michel, R., & Jonckheere, J. (1983). Isolation and identification of pathogenic *Naegleria australiensis* (De Jonckheere, 1981) from pond water in India. Transactions Of The Royal Society Of Tropical Medicine And Hygiene, 77(6), 878. Doi: 10.1016/0035-9203(83)90317-6

Minamino, T., Imada, K., & Namba, K. (2008). Molecular motors of the bacterial flagella. Current Opinion In Structural Biology, 18(6), 693-701. Doi: 10.1016/j.sbi.2008.09.006

Misook, K., & Joo Hun, L. (2001). Regulation of actin gene expression during the differentiation of *Naegleria gruberi*. Journaljournal Of Microbiology, 39(1), 42-48.

Mitchell, D. (2004). Speculations on the evolution of 9+2 organelles and the role of central pair microtubules. Biology Of The Cell, 96(9), 691-696. Doi: 10.1016/j.biolcel.2004.07.004

Mitchell, D. (2007). The evolution of eukaryotic cilia and flagella as motile and sensory organelles. Advances In Experimental Medicine And Biology, 130-140. Doi: 10.1007/978-0-387-74021-8_11

Mizuno, K., Dymek, E., & Smith, E. (2016). Microtubule binding protein PACRG plays a role in regulating specific ciliary dyneins during microtubule sliding. Cytoskeleton, 73(12), 703-711. Doi: 10.1002/cm.21340

Möglich, A., Ayers, R., & Moffat, K. (2009). Structure and signaling mechanism of Per-ARNT-Sim domains. Structure, 17(10), 1282-1294. Doi: 10.1016/j.str.2009.08.011

Moon, Y., Kim, S., & Chung, Y. (2012). sensing and responding to UV-A in cyanobacteria. International Journal Of Molecular Sciences, 13(12), 16303-16332. Doi: 10.3390/ijms131216303

Moran, J., McKean, P., & Ginger, M. (2014). Eukaryotic flagella: variations in form, function, and composition during evolution. Bioscience, 64(12), 1103-1114. Doi: 10.1093/biosci/biu175

Morimoto, Y., & Minamino, T. (2014). Structure and function of the bi-directional bacterial flagellar motor. Biomolecules, 4(1), 217-234. Doi: 10.3390/biom4010217

Mulukutla, B., Yongky, A., Le, T., Mashek, D., & Hu, W. (2016). Regulation of glucose metabolism – a perspective from cell bioprocessing. Trends In Biotechnology, 34(8), 638-651. Doi: 10.1016/j.tibtech.2016.04.012

Mykytyn, K., & Askwith, C. (2017). G-protein-coupled receptor signaling in cilia. Cold Spring Harbor Perspectives In Biology, 9(9), a028183. Doi: 10.1101/cshperspect.a028183

Naegleria Page. (2018). Retrieved from http://www.pitt.edu/~cwalsh/*Naegleria*.html

Nakazawa, Y., Hiraki, M., Kamiya, R., & Hirono, M. (2007). SAS-6 is a cartwheel protein that establishes the 9-fold symmetry of the centriole. Current Biology, 17(24), 2169-2174. Doi: 10.1016/j.cub.2007.11.046

NCBI Resource Coordinators. (2016). Database resources of the National Center for Biotechnology Information. Nucleic Acids Research, 44(Database issue), D7–D19. Doi: 10.1093/nar/gkv1290

Nechipurenko, I., Doroquez, D., & Sengupta, P. (2013). Primary cilia and dendritic spines: Different but similar signaling compartments. Molecules And Cells, 36(4), 288-303. Doi: 10.1007/s10059-013-0246-z

Nerad, T., Visvesvara, G., & Daggett, P. (1983). Chemically defined media for the cultivation of *Naegleria*: pathogenic and high temperature tolerant species. The Journal Of Protozoology, 30(2), 383-387. Doi: 10.1111/j.1550-7408.1983.tb02935.x

Neves, S. (2002). G protein pathways. Science, 296(5573), 1636-1639. Doi: 10.1126/science.1071550

Nogales, E., Wolf, S., & Downing, K. (1998). Structure of the αβ tubulin dimer by electron crystallography. Nature, 391(6663), 199-203. Doi: 10.1038/34465

Norrander, J., decathelineau, A., Brown, J., Porter, M., & Linck, R. (2000). The Rib43a protein is associated with forming the specialized protofilament ribbons of flagellar microtubules in *Chlamydomonas*. Molecular Biology Of The Cell, 11(1), 201-215. Doi: 10.1091/mbc.11.1.201

Ntefidou, M. (2003). Photoactivated adenylyl cyclase controls phototaxis in the flagellate *Euglena gracilis*. PLANT PHYSIOLOGY, 133(4), 1517-1521. Doi: 10.1104/pp.103.034223

Oakley, B. (2000). An abundance of tubulins. Trends In Cell Biology, 10(12), 537-542. Doi: 10.1016/s0962-8924(00)01857-2

Oliveira, L., Paiva, P., Paiva, A., & Vriend, G. (2003). Sequence analysis reveals how G protein-coupled receptors transduce the signal to the G protein. Proteins: Structure, Function, And Bioinformatics, 52(4), 553-560. Doi: 10.1002/prot.10489

Omoto, C., & Brokaw, C. (1985). Bending patterns of *Chlamydomonas* flagella: II. Calcium effects on reactivated *Chlamydomonas* flagella. Cell Motility, 5(1), 53-60. Doi: 10.1002/cm.970050105

Opperdoes, F., De Jonckheere, J., & Tielens, A. (2011). *Naegleria gruberi* metabolism. International Journal For Parasitology, 41(9), 915-924. Doi: 10.1016/j.ijpara.2011.04.004

Ostrowski, L., Dutcher, S., & Lo, C. (2011). Cilia and models for studying structure and function. Proceedings Of The American Thoracic Society, 8(5), 423-429. Doi: 10.1513/pats.201103-027sd

O'Toole, E., Greenan, G., Lange, K., Srayko, M., & Müller-Reichert, T. (2012). The role of γ-Tubulin in centrosomal microtubule organization. Plos ONE, 7(1), e29795. Doi: 10.1371/journal.pone.0029795

Page, F. (1967). Taxonomic Criteria for Limax Amoebae, with Descriptions of 3 New Species of Hartmannella and 3 of Vahlkampfia. The Journal Of Protozoology, 14(3), 499-521. Doi: 10.1111/j.1550-7408.1967.tb02036.x

Pandey, S., Nelson, D., & Assmann, S. (2009). Two novel GPCR-Type G proteins are abscisic acid receptors in arabidopsis. Cell, 136(1), 136-148. Doi: 10.1016/j.cell.2008.12.026

Pánek, T., Ptáčková, E., & Čepička, I. (2014). Survey on diversity of marine/saline anaerobic Heterolobosea (Excavata: Discoba) with description of seven new species. International Journal Of Systematic And Evolutionary Microbiology, 64(Pt 7), 2280-2304. Doi: 10.1099/ijs.0.063487-0

Park, S., & Tame, J. (2017). Seeing the light with BLUF proteins. Biophysical Reviews, 9(2), 169-176. Doi: 10.1007/s12551-017-0258-6

Patterson, D. (1999). The diversity of eukaryotes. The American Naturalist, 154(S4), S96-S124. Doi: 10.1086/303287

Pazour, G., Koutoulis, A., Benashski, S., Dickert, B., Sheng, H., & Patel-King, R. Et al. (1999). LC2, the *Chlamydomonas* homologue of the T complex-encoded protein Tctex2, is essential for outer dynein arm assembly. Molecular Biology Of The Cell, 10(10), 3507-3520. Doi: 10.1091/mbc.10.10.3507

Percival, S. (2014). Microbiology of waterborne diseases (2nd ed., pp. 407-416). London: Elsevier.

Pereira, S., Goss, L., & Dworkin, J. (2011). Eukaryote-like serine/threonine kinases and phosphatases in bacteria. Microbiology And Molecular Biology Reviews, 75(1), 192-212. Doi: 10.1128/mmbr.00042-10

Pierce, K., Premont, R., & Lefkowitz, R. (2002). Seven-transmembrane receptors. Nature Reviews Molecular Cell Biology, 3(9), 639-650. Doi: 10.1038/nrm908

Pijper, A. (1948). Bacterial flagella and motility. Nature, 161(4084), 200-201. Doi: 10.1038/161200b0

Pluznick, J., & Caplan, M. (2014). Chemical and physical sensors in the regulation of renal function. Clinical Journal Of The American Society Of Nephrology, 10(9), 1626-1635. Doi: 10.2215/cjn.00730114

Potter, L. (2011). Guanylyl cyclase structure, function and regulation. Cellular Signalling, 23(12), 1921-1926. Doi: 10.1016/j.cellsig.2011.09.001

Praetorius, H., & Leipziger, J. (2013). Primary cilium-dependent sensing of urinary flow and paracrine purinergic signaling. Seminars In Cell & Developmental Biology, 24(1), 3-10. Doi: 10.1016/j.semcdb.2012.10.003

Preininger, A., & Hamm, H. (2004). G Protein Signaling: Insights from New Structures. Science Signaling, 2004(218), re3-re3. Doi: 10.1126/stke.2182004re3

Preston, T., & O'Dell, D. (1980). The cell surface in amoeboid locomotion: behaviour of *Naegleria gruberi* on an adhesive lectin substrate. Microbiology, 116(2), 515-520. Doi: 10.1099/00221287-116-2-515

Preston, T.M. & O'Dell, D.S. & King, C.A. (1975). Fluorescence microscope observations of some surface components of the amoeboflagellate *Naegleria gruberi* during amoeboid locomotion. Cytobios. 13. 207-216.

Prevo, B., Scholey, J., & Peterman, E. (2017). Intraflagellar transport: mechanisms of motor action, cooperation, and cargo delivery. The FEBS Journal, 284(18), 2905-2931. Doi: 10.1111/febs.14068

Psi Wavefunction. (2009). Skeptic wonder. Retrieved from http://skepticwonder.fieldofscience.com/search?Q=*Naegleria*

Rajeshwari, H., Nagveni, S., Oli, A., Parashar, D., & Chandrakanth, K. (2009). Morphological changes of *Klebsiella pneumoniae* in response to cefotaxime: a scanning electron microscope study. World Journal Of Microbiology And Biotechnology, 25(12), 2263-2266. Doi: 10.1007/s11274-009-0126-z

Ramesh, M., Malik, S., & Logsdon, J. (2005). A phylogenomic inventory of meiotic genes. Current Biology, 15(2), 185-191. Doi: 10.1016/j.cub.2005.01.003

Rauch, A., Leipelt, M., Russwurm, M., & Steegborn, C. (2008). Crystal structure of the guanylyl cyclase Cya2. Proceedings Of The National Academy Of Sciences, 105(41), 15720-15725. Doi: 10.1073/pnas.0808473105

Rebbapragada, A., Johnson, M., Harding, G., Zuccarelli, A., Fletcher, H., Zhulin, I., & Taylor, B. (1997). The Aer protein and the serine chemoreceptor Tsr independently sense intracellular energy levels and transduce oxygen, redox, and energy signals for Escherichia coli behavior. Proceedings Of The National Academy Of Sciences, 94(20), 10541-10546. Doi: 10.1073/pnas.94.20.10541

Reyes-Batlle, M., Wagner, C., López-Arencibia, A., Sifaoui, I., Martínez-Carretero, E., & Valladares, B. Et al. (2017). Isolation and molecular characterization of a *Naegleria* strain from a recreational water fountain in Tenerife, Canary Islands, Spain. Acta Parasitologica, 62(2). Doi: 10.1515/ap-2017-0033

Rhee, S., Kirschen, G., Gu, Y., & Ge, S. (2016). Depletion of primary cilia from mature dentate granule cells impairs hippocampus-dependent contextual memory. Scientific Reports, 6(1). Doi: 10.1038/srep34370

Robichaux, W., Branham-O'Connor, M., Hwang, I., Vural, A., Kehrl, J., & Blumer, J. (2017). Regulation of chemokine signal integration by activator of G-protein signaling 4 (AGS4). Journal Of Pharmacology And Experimental Therapeutics, 360(3), 424-433. Doi: 10.1124/jpet.116.238436

Robinson, B., Christy, P., Hayes, S., & Dobson, P. (1992). Discontinuous genetic variation among mesophilic *Naegleria* isolates: further evidence that *N. Gruberi* is not a single species. The Journal Of Protozoology, 39(6), 702-712. Doi: 10.1111/j.1550-7408.1992.tb04452.x

Roger, A., & Simpson, A. (2009). Evolution: revisiting the root of the eukaryote tree. Current Biology, 19(4), R165-R167. Doi: 10.1016/j.cub.2008.12.032

Rolland, F., Winderickx, J., & Thevelein, J. (2001). Glucose-sensing mechanisms in eukaryotic cells. Trends In Biochemical Sciences, 26(5), 310-317. Doi: 10.1016/s0968-0004(01)01805-9

Romero-Castillo, R., Roy Choudhury, S., León-Félix, J., & Pandey, S. (2015). Characterization of the heterotrimeric G-protein family and its transmembrane regulator from *Capsicum* (*Capsicum annuum* L.). Plant Science, 234, 97-109. Doi: 10.1016/j.plantsci.2015.02.007

Rosenbaum, D., Rasmussen, S., & Kobilka, B. (2009). The structure and function of G-protein-coupled receptors. Nature, 459(7245), 356-363. Doi: 10.1038/nature08144

Ryo, M., Yamashino, T., Nomoto, Y., Goto, Y., Ichinose, M., & Sato, K. Et al. (2018). Light-regulated PAS-containing histidine kinases delay gametophore formation in the moss *Physcomitrella* patens. Journal Of Experimental Botany, 69(20), 4839-4851. Doi: 10.1093/jxb/ery257

Ryo, M., Yamashino, T., Yamakawa, H., Fujita, Y., & Aoki, S. (2018). PAS-histidine kinases PHK1 and PHK2 exert oxygen-dependent dual and opposite effects on gametophore formation in the moss *Physcomitrella* patens. Biochemical And Biophysical Research Communications, 503(4), 2861-2865. Doi: 10.1016/j.bbrc.2018.08.056

Saada, E., demarco, S., Shimogawa, M., & Hill, K. (2015). "With a Little Help from My Friends"— social motility in *Trypanosoma brucei*. PLOS Pathogens, 11(12), e1005272. Doi: 10.1371/journal.ppat.1005272

Sanders, R. (2018). Genome sequenced for amoeba that flips into free-swimming cell.

Satisbury, J. (1995). Centrin, centrosomes, and mitotic spindle poles. Current Opinion In Cell Biology, 7(1), 39-45. Doi: 10.1016/0955-0674(95)80043-3

Schardinger, F. (1899). Entwicklungskreis einer amoeba lobosa (gymnamoeba): Amoeba *gruberi*. S.K.Akad.Wiss.Wien., 108, 713-734.

Shalaeva, D., Galperin, M., & Mulkidjanian, A. (2015). Eukaryotic G protein-coupled receptors as descendants of prokaryotic sodium-translocating rhodopsins. Biology Direct, 10(1). Doi: 10.1186/s13062-015-0091-4

Shea, D. (1987). mRNAs for alpha- and beta-tubulin and flagellar calmodulin are among those coordinately regulated when *Naegleria gruberi* amebae differentiate into flagellates. The Journal Of Cell Biology, 105(3), 1303-1309. Doi: 10.1083/jcb.105.3.1303

Shu, C., Ulrich, L., & Zhulin, I. (2003). The NIT domain: a predicted nitrate-responsive module in bacterial sensory receptors. Trends In Biochemical Sciences, 28(3), 121-124. Doi: 10.1016/s0968-0004(03)00032-x

Silflow, C., & Lefebvre, P. (2001). Assembly and motility of eukaryotic cilia and flagella. lessons from *Chlamydomonas reinhardtii*. PLANT PHYSIOLOGY, 127(4), 1500-1507. Doi: 10.1104/pp.010807

Simon, M., Strathmann, M., & Gautam, N. (1991). Diversity of G proteins in signal transduction. Science, 252(5007), 802-808. Doi: 10.1126/science.1902986

Simonds, W. (1999). G protein regulation of adenylate cyclase. Trends In Pharmacological Sciences, 20(2), 66-73. Doi: 10.1016/s0165-6147(99)01307-3

Simpson, A., & Patterson, D. (1999). The ultrastructure of *Carpediemonas membranifera* (Eukaryota) with reference to the "excavate hypothesis". European Journal Of Protistology, 35(4), 353-370. Doi: 10.1016/s0932-4739(99)80044-3

Simpson, A., & Patterson, D. (2001). On core jakobids and excavate taxa: the ultrastructure of jakoba incarcerata. The Journal Of Eukaryotic Microbiology, 48(4), 480-492. Doi: 10.1111/j.1550-7408.2001.tb00183.x

Slapeta, J., Moreira, D., & Lopez-Garcia, P. (2005). The extent of protist diversity: insights from molecular ecology of freshwater eukaryotes. Proceedings Of The Royal Society B: Biological Sciences, 272(1576), 2073-2081. Doi: 10.1098/rspb.2005.3195

Sloboda, R., & Rosenbaum, J. (2007). Making sense of cilia and flagella. The Journal Of Cell Biology, 179(4), 575-582. Doi: 10.1083/jcb.200709039

Smith, E. (2002). Regulation of flagellar dynein by calcium and a role for an axonemal calmodulin and calmodulin-dependent kinase. Molecular Biology Of The Cell, 13(9), 3303-3313. Doi: 10.1091/mbc.e02-04-0185

Smith, E., & Lefebvre, P. (1996). PF16 encodes a protein with armadillo repeats and localizes to a single microtubule of the central apparatus in *Chlamydomonas* flagella. The Journal Of Cell Biology, 132(3), 359-370. Doi: 10.1083/jcb.132.3.359

Smith, E., & Lefebvre, P. (1997). PF20 gene product contains WD repeats and localizes to the intermicrotubule bridges in *Chlamydomonas* flagella. Molecular Biology Of The Cell, 8(3), 455-467. Doi: 10.1091/mbc.8.3.455

Söderbäck, E., Reyes-Ramirez, F., Eydmann, T., Austin, S., Hill, S., & Dixon, R. (2002). The redox- and fixed nitrogen-responsive regulatory protein NIFL from *Azotobacter vinelandii* comprises discrete flavin and nucleotide-binding domains. Molecular Microbiology, 28(1), 179-192. Doi: 10.1046/j.1365-2958.1998.00788.x

Sohn, H., Kim, J., Shin, M., Song, K., & Shin, H. (2010). The Nf-actin gene is an important factor for food-cup formation and cytotoxicity of pathogenic *Naegleria fowleri*. Parasitology Research, 106(4), 917-924. Doi: 10.1007/s00436-010-1760-y

Szymanska, K., & Johnson, C. (2012). The transition zone: an essential functional compartment of cilia. Cilia, 1(1), 10. Doi: 10.1186/2046-2530-1-10

Takada, S., Wilkerson, C., Wakabayashi, K., Kamiya, R., & Witman, G. (2002). The outer dynein arm-docking complex: composition and characterization of a subunit (Oda1) necessary for outer arm assembly. Molecular Biology Of The Cell, 13(3), 1015-1029. Doi: 10.1091/mbc.01-04-0201

Takao, D., & Verhey, K. (2015). Gated entry into the ciliary compartment. Cellular And Molecular Life Sciences, 73(1), 119-127. Doi: 10.1007/s00018-015-2058-0

Tang, Y., Wu, Y., Herlihy, S., Brito-Aleman, F., Ting, J., Janetopoulos, C., & Gomer, R. (2018). An autocrine proliferation repressor regulates dictyostelium discoideum proliferation and chemorepulsion using the G protein-coupled receptor grlh. Mbio, 9(1). Doi: 10.1128/mbio.02443-17

Taxonomy Browser. (2018). Retrieved from https://www.ncbi.nlm.nih.gov/Taxonomy/Browser/wwwtax.cgi?Mode=Undef&id=5765&lvl=3&lin=f&keep=1&srchmode=1&unlock

Team:Chalmers-Gothenburg/Theory - 2012.igem.org. (2018). Retrieved from http://2012.igem.org/Team:Chalmers-Gothenburg/Theory

Terashima, H., Kojima, S., & Homma, M. (2008). Chapter 2 flagellar motility in bacteria. International Review Of Cell And Molecular Biology, 270, 39-85. Doi: 10.1016/s1937-6448(08)01402-0

Thermo Fisher Scientific - UK. (2018). Retrieved from https://www.thermofisher.com/uk/en/home.html

Trusov, Y., & Botella, J. (2016). Plant G-proteins come of age: breaking the bond with animal models. Frontiers In Chemistry, 4. Doi: 10.3389/fchem.2016.00024

Trzaskowski, B., Latek, D., Yuan, S., Ghoshdastider, U., Debinski, A., & Filipek, S. (2012). Action of molecular switches in gpcrs - theoretical and experimental studies. Current Medicinal Chemistry, 19(8), 1090-1109. Doi: 10.2174/092986712799320556

Tsaousis, A., Nývltová, E., Šuták, R., Hrdý, I., & Tachezy, J. (2014). A nonmitochondrial hydrogen production in *Naegleria gruberi*. Genome Biology And Evolution, 6(4), 792-799. Doi: 10.1093/gbe/evu065

Tucker, K., Caspary, T., Grimsley-Myers, C., & Chen, P. (2013). Cilia and nervous system development and function (pp. 131-163). Dordrecht: Springer.

Tuszynski, J. (2007). Introduction to molecular and cellular biophysics (pp. 202-203). Boca Raton, Fla.: Chapman & Hall/CRC.

Vickerman, K. (1962). Patterns of cellular organisation in limax amoebae. Experimental Cell Research, 26(3), 497-519. Doi: 10.1016/0014-4827(62)90155-6

Vignais, P., & Billoud, B. (2007). Occurrence, classification, and biological function of hydrogenases: an overview. Chemical Reviews, 107(10), 4206-4272. Doi: 10.1021/cr050196r

Visvesvara, G., Moura, H., & Schuster, F. (2007). Pathogenic and opportunistic free-living amoebae: *Acanthamoeba* spp., *Balamuthia mandrillaris*, *Naegleria fowleri*, *Andsappinia diploidea*. FEMS Immunology & Medical Microbiology, 50(1), 1-26. Doi: 10.1111/j.1574-695x.2007.00232.x

Walsh, C. (1984). Synthesis and assembly of the cytoskeleton of *Naegleria gruberi* flagellates. The Journal Of Cell Biology, 98(2), 449-456. Doi: 10.1083/jcb.98.2.449

Walsh, C. (2007). The role of actin, actomyosin and microtubules in defining cell shape during the differentiation of *Naegleria* amebae into flagellates. European Journal Of Cell Biology, 86(2), 85-98. Doi: 10.1016/j.ejcb.2006.10.003

Wang, F., Cheng, S., Wu, Y., Ren, B., & Qian, W. (2017). A bacterial receptor pcrk senses the plant hormone cytokinin to promote adaptation to oxidative stress. Cell Reports, 21(10), 2940-2951. Doi: 10.1016/j.celrep.2017.11.017

Wang, J., & Xiao, R. (2014). G protein-coupled receptors in energy homeostasis. Science China Life Sciences, 57(7), 672-680. Doi: 10.1007/s11427-014-4694-2

Wang, S., & Dong, Z. (2013). Primary cilia and kidney injury: current research status and future perspectives. American Journal Of Physiology-Renal Physiology, 305(8), F1085-F1098. Doi: 10.1152/ajprenal.00399.2013

Wargo, M. (2005). Calmodulin and PF6 are components of a complex that localizes to the C1 microtubule of the flagellar central apparatus. Journal Of Cell Science, 118(20), 4655-4665. Doi: 10.1242/jcs.02585

Weik, R., & John, D. (1977). Agitated mass cultivation of *Naegleria fowleri*. The Journal Of Parasitology, 63(5), 868. Doi: 10.2307/3279896

Wellings, F., Amuso, P., Chang, S., & Lewis, A. (1977). Isolation and identification of pathogenic *Naegleria* from Florida lakes. Appl Environ Microbiol., 34(6), 661–667.

Wellings, F., Amuso, P., Lewis, A., Farmelo, M., & Moody. D. (1979). Pathogenic '*Naegleria*': distribution in nature. U.S. Environmental Protection Agency, Washington, D.C., EPA/600/1-79/018.

Wemmer, K., & Marshall, W. (2004). Flagellar motility: all pull together. Current Biology, 14(23), R992-R993. Doi: 10.1016/j.cub.2004.11.019

Wheway, G., Parry, D., & Johnson, C. (2013). The role of primary cilia in the development and disease of the retina. Organogenesis, 10(1), 69-85. Doi: 10.4161/org.26710

Wilkerson, C., King, S., Koutoulis, A., Pazour, G., & Witman, G. (1995). The 78,000 M(r) intermediate chain of *Chlamydomonas* outer arm dynein isa WD-repeat protein required for arm assembly. The Journal Of Cell Biology, 129(1), 169-178. Doi: 10.1083/jcb.129.1.169

Willett, J., & Crosson, S. (2016). Atypical modes of bacterial histidine kinase signaling. Molecular Microbiology, 103(2), 197-202. Doi: 10.1111/mmi.13525

Williams, C., Li, C., Kida, K., Inglis, P., Mohan, S., & Semenec, L. Et al. (2011). MKS and NPHP modules cooperate to establish basal body/transition zone membrane associations and ciliary gate function during ciliogenesis. The Journal Of Cell Biology, 192(6), 1023-1041. Doi: 10.1083/jcb.201012116

Williams, J., Noegel, A., & Eichinger, L. (2005). Manifestations of multicellularity: *Dictyostelium* reports in. Trends In Genetics, 21(7), 392-398. Doi: 10.1016/j.tig.2005.05.002

Willmer, E. (1956). Factors which influence the acquisition of flagella by the amoeba, *Naegleria gruberi*.

Winey, M., & O'Toole, E. (2014). Centriole structure. Philosophical Transactions Of The Royal Society B: Biological Sciences, 369(1650), 20130457-20130457. Doi: 10.1098/rstb.2013.0457

Winger, J., Derbyshire, E., Lamers, M., Marletta, M., & Kuriyan, J. (2008). The crystal structure of the catalytic domain of a eukaryotic guanylate cyclase. BMC Structural Biology, 8(1), 42. Doi: 10.1186/1472-6807-8-42

Wiwanitkit, V. (2016). Primary amebic meningoencephalitis: Summarization on cases with early diagnosis by identification of amebae trophozoite in the cerebrospinal fluid. Journal Of Pediatric Neurosciences, 11(1), 90. Doi: 10.4103/1817-1745.181256

Wollman, A., Nudd, R., Hedlund, E., & Leake, M. (2015). From Animaculum to single molecules: 300 years of the light microscope. Open Biology, 5(4), 150019-150019. Doi: 10.1098/rsob.150019

Wood, C., Huang, K., Diener, D., & Rosenbaum, J. (2013). The cilium secretes bioactive ectosomes. Current Biology, 23(10), 906-911. Doi: 10.1016/j.cub.2013.04.019

Xie, K., Masuho, I., Shih, C., Cao, Y., Sasaki, K., & Lai, C. Et al. (2015). Stable G protein-effector complexes in striatal neurons: mechanism of assembly and role in neurotransmitter signaling. Elife, 4. Doi: 10.7554/elife.10451

Xu, L., Venkataramani, P., Ding, Y., Liu, Y., Deng, Y., & Yong, G. Et al. (2016). A cyclic di-GMP-binding adaptor protein interacts with histidine kinase to regulate two-component signaling. Journal Of Biological Chemistry, 291(31), 16112-16123. Doi: 10.1074/jbc.m116.730887

Xu, X., & Jin, T. (2017). ELMO proteins transduce G protein-coupled receptor signal to control reorganization of actin cytoskeleton in chemotaxis of eukaryotic cells. Small Gtpases, 1-9. Doi: 10.1080/21541248.2017.1318816

Yang, J., Harding, T., Kamikawa, R., Simpson, A., & Roger, A. (2017). Mitochondrial genome evolution and a novel RNA editing system in deep-branching Heteroloboseids. Genome Biology And Evolution, 9(5), 1161-1174. Doi: 10.1093/gbe/evx086

Yang, P., Diener, D., Rosenbaum, J., & Sale, W. (2001). Localization of calmodulin and dynein light chain Lc8 in flagellar radial spokes. The Journal Of Cell Biology, 153(6), 1315-1326. Doi: 10.1083/jcb.153.6.1315

Yang, P., Yang, C., & Sale, W. (2004). Flagellar radial spoke protein 2 is a calmodulin binding protein required for motility in *chlamydomonas* reinhardtii. Eukaryotic Cell, 3(1), 72-81. Doi: 10.1128/ec.3.1.72-81.2004

Yokoyama, R., O'Toole, E., Ghosh, S., & Mitchell, D. (2004). Regulation of flagellar dynein activity by a central pair kinesin. Proceedings Of The National Academy Of Sciences, 101(50), 17398-17403. Doi: 10.1073/pnas.0406817101

Yoshikawa, S., & Orii, Y. (1972). The inhibition mechanism of the cytochrome oxidase reaction. The Journal Of Biochemistry, 71(5), 859-872. Doi: 10.1093/oxfordjournals.jbchem.a129835

Zhang, G., Liu, Y., Ruoho, A., & Hurley, J. (1997). Structure of the adenylyl cyclase catalytic core. Nature, 386(6622), 247-253. Doi: 10.1038/386247a0

Zhou, X., Gao, X., Barty, A., Kang, Y., He, Y., & Liu, W. Et al. (2016). X-ray laser diffraction for structure determination of the rhodopsin-arrestin complex. Scientific Data, 3, 160021. Doi: 10.1038/sdata.2016.21

Zschiedrich, C., Keidel, V., & Szurmant, H. (2016). Molecular mechanisms of two-component signal transduction. Journal Of Molecular Biology, 428(19), 3752-3775. Doi: 10.1016/j.jmb.2016.08.003

Zysset-Burri, D., Müller, N., Beuret, C., Heller, M., Schürch, N., Gottstein, B., & Wittwer, M. (2014). Genome-wide identification of pathogenicity factors of the free-living amoeba *Naegleria Fowleri*. BMC Genomics, 15(1), 496. Doi: 10.1186/1471-2164-15-496

Appendix

I. Reagents and materials used

Chemicals + Equipment	Provider
Glass wool	ACROS Organics
Taq polymerase	Bioline
T100 Thermal cycler	Bio-Rad Laboratories, Inc.
Gene Pulser Xcell Electroporation System	Bio-Rad Laboratories, Inc.
PowerPac™ Basic Power Supply	Bio-Rad Laboratories, Inc.
Mini Centrifuge	Bio-Rad Laboratories, Inc.
Mini-PROTEAN® Tetra System Kit	Bio-Rad Laboratories, Inc.
Instant Blue™	Expedeon Ltd.
Discovery Comfort Pipettes	HTL Lab Solutions
Heat Accublock Dry Block Heater	Labnet
Tris	Melford Biolaboratories Ltd.
Boric Acid	Melford Biolaboratories Ltd.
Agarose powder	Melford Biolaboratories Ltd.
Sodium Phosphate – Monobasic	Melford Biolaboratories Ltd.
Calcium Acetate	Melford Biolaboratories Ltd.
Sodium acetate	Melford Biolaboratories Ltd.
Glycine	Melford Biolaboratories Ltd.
Acrylamide Solution	Melford Biolaboratories Ltd.
Dithiothreitol	Melford Biolaboratories Ltd.
Ammonium Persulfate	Melford Biolaboratories Ltd.
Primers	MWG Eurofins Genomics
Gel Extraction Kit	Neo Biotech
Digital Stop clock	New England Biolabs, Inc.
1kb ladder	New England Biolabs, Inc.
T4 DNA Ligase	New England Biolabs, Inc.

2.1 buffer	New England Biolabs, Inc.
EcoR1	New England Biolabs, Inc.
XhoI	New England Biolabs, Inc.
HindIII	New England Biolabs, Inc.
Orange G 6x loading buffer	New England Biolabs, Inc.
Brain-Heart Infusion	Oxoid Limited, Thermo Fisher Scientific Inc.
Prestige medical© classic autoclave models 210004 and 210008	Prestige medical + camlab
15ml + 50ml Centrifuge Tubes	SARSTEDT AG & Co
LB agar	Sigma-Aldrich, Inc.
LB Broth, High salt	Sigma-Aldrich, Inc.
Sodium phosphate – dibasic	Sigma-Aldrich, Inc.
SIGMA 1-14 Microfuge	Sigma-Aldrich, Inc.
Hemin	Sigma-Aldrich, Inc.
Sodium hydroxide	Sigma-Aldrich, Inc.
Bovine foetal serum	Sigma-Aldrich, Inc.
Kanamycin powder	Sigma-Aldrich, Inc.
Ampicillin powder	Sigma-Aldrich, Inc.
sodium dodecyl sulfate solution	Sigma-Aldrich, Inc.
Nicotinic acid (98%)	Sigma-Aldrich, Inc.
phenylmethylsulfonyl fluoride	Sigma-Aldrich, Inc.
Swann Morton Disposable Sterile Scalpels	Swann Morton Limited 2017
ultraviolet benchtop transilluminator	Syngene - Synoptics Ltd.
AneroGen™ compact	Thermo Fisher Scientific Inc.
Campygen™ compact	Thermo Fisher Scientific Inc.
LB Agar, Miller	Thermo Fisher Scientific Inc.
10XTBE	Thermo Fisher Scientific Inc.
1XTAE	Thermo Fisher Scientific Inc.
Gene JET PCR purification kit	Thermo Fisher Scientific Inc.
Elution buffer	Thermo Fisher Scientific Inc.
Heratherm Compact Microbiological Incubator	Thermo Fisher Scientific Inc.
Fisherbrand™ L-Shaped Cell Spreaders	Thermo Fisher Scientific Inc.

Hoefer™ Submarine Gel Electrophoresis Units: SUB6 Mini Horizontal	Thermo Fisher Scientific Inc.
GeneJET Plasmid Miniprep Kit	Thermo Fisher Scientific Inc.
GeneJET Gel Extraction Kit	Thermo Fisher Scientific Inc.
2000ml Schott bottle with cap and pouring ring	Thermo Fisher Scientific Inc.
1000ml Schott bottle with cap and pouring ring	Thermo Fisher Scientific Inc.
500ml Schott bottle with cap and pouring ring	Thermo Fisher Scientific Inc.
250ml Schott bottle with cap and pouring ring	Thermo Fisher Scientific Inc.
100ml Schott bottle with cap and pouring ring	Thermo Fisher Scientific Inc.
Heraeus Pico 17 Centrifuge	Thermo Fisher Scientific Inc.
KuroGEL Mini Plus 10 Electrophoresis tank	VWR

Table 5: Appendix of reagents and materials.

This table lists the reagents and materials used throughout the thesis with the provider of each item.

II. Expression patterns of Serpentine receptor EFC44333.1, EFC40821.1 and EFC35362.1 queries.

JGIDB Identifier	Expression	JGIDB Identifier	Expression	JGIDB Identifier	Expression
JGIDB:Naegr1_45907	Flagellate specific	JGIDB:Naegr1_66373	No clear pattern	JGIDB:Naegr1_72875	Amoeba specific
JGIDB:Naegr1_46482	Constitutive	JGIDB:Naegr1_66385	Flagellate specific	JGIDB:Naegr1_73289	No clear pattern
JGIDB:Naegr1_48032	Flagellate specific	JGIDB:Naegr1_66386	Flagellate specific	JGIDB:Naegr1_73295	Constitutive
JGIDB:Naegr1_49902	No clear pattern	JGIDB:Naegr1_66517	No clear pattern	JGIDB:Naegr1_74387	Flagellate specific
JGIDB:Naegr1_51041	No clear pattern	JGIDB:Naegr1_66787	No clear pattern	JGIDB:Naegr1_74523	Constitutive
JGIDB:Naegr1_51839	No clear pattern	JGIDB:Naegr1_67021	Amoeba specific	JGIDB:Naegr1_74614	Amoeba specific
JGIDB:Naegr1_52199	Amoeba specific	JGIDB:Naegr1_67380	No clear pattern	JGIDB:Naegr1_74625	Constitutive
JGIDB:Naegr1_52771	No clear pattern	JGIDB:Naegr1_67552	Amoeba specific	JGIDB:Naegr1_74779	Constitutive
JGIDB:Naegr1_54490	Flagellate specific	JGIDB:Naegr1_67572	Constitutive	JGIDB:Naegr1_74835	No clear pattern
JGIDB:Naegr1_57228	No clear pattern	JGIDB:Naegr1_68613	Constitutive	JGIDB:Naegr1_75738	No clear pattern
JGIDB:Naegr1_57455	No clear pattern	JGIDB:Naegr1_69334	Flagellate specific	JGIDB:Naegr1_75753	Flagellate specific
JGIDB:Naegr1_58957	Constitutive	JGIDB:Naegr1_69573	Amoeba specific	JGIDB:Naegr1_75819	Constitutive
JGIDB:Naegr1_59210	Constitutive	JGIDB:Naegr1_70394	Constitutive	JGIDB:Naegr1_75820	Amoeba specific
JGIDB:Naegr1_59845	Constitutive	JGIDB:Naegr1_70688	Constitutive	JGIDB:Naegr1_75882	No clear pattern
JGIDB:Naegr1_59935	Amoeba specific	JGIDB:Naegr1_71107	No clear pattern	JGIDB:Naegr1_76206	No clear pattern
JGIDB:Naegr1_62535	Constitutive	JGIDB:Naegr1_71707	Constitutive	JGIDB:Naegr1_76418	No clear pattern
JGIDB:Naegr1_62703	Constitutive	JGIDB:Naegr1_71982	Amoeba specific	JGIDB:Naegr1_78910	No clear pattern
JGIDB:Naegr1_63837	Constitutive	JGIDB:Naegr1_71988	Constitutive	JGIDB:Naegr1_80549	No clear pattern
JGIDB:Naegr1_64339	Amoeba specific	JGIDB:Naegr1_72058	Constitutive	JGIDB:Naegr1_81447	Constitutive
JGIDB:Naegr1_64936	Constitutive	JGIDB:Naegr1_72711	No clear pattern	JGIDB:Naegr1_81945	Flagellate specific

Table 6: Query results for protein EFC44333.1.

A table displaying the protein blast results for protein EFC44333.1 carried out on the JGI website. The results are ordered by JGI identifying numbers.

JGIDB Identifier	Expression
JGIDB:Naegr1_71442	No clear pattern
JGIDB:Naegr1_80140	No clear pattern

Table 7: Query results for protein EFC40821.1.

A table displaying the protein blast results for protein EFC40821.1 carried out on the JGI website. The results are ordered by JGI identifying numbers.

JGIDB Identifier	Expression
JGIDB:Naegr1_49784	Flagellate specific
JGIDB:Naegr1_50935	Flagellate specific
JGIDB:Naegr1_54685	Constitutive
JGIDB:Naegr1_54955	Constitutive
JGIDB:Naegr1_56981	Amoeba specific
JGIDB:Naegr1_59834	No clear pattern
JGIDB:Naegr1_63246	No clear pattern
JGIDB:Naegr1_66075	Constitutive
JGIDB:Naegr1_68354	No clear pattern
JGIDB:Naegr1_68612	Constitutive
JGIDB:Naegr1_71995	No clear pattern
JGIDB:Naegr1_73150	Constitutive
JGIDB:Naegr1_74736	Constitutive
JGIDB:Naegr1_74742	No clear pattern
JGIDB:Naegr1_81896	Constitutive

Table 8: Query results for protein EFC35362.1.

A table displaying the protein blast results for protein EFC35362.1 carried out on the JGI website. The results are ordered by JGI identifying numbers.

III. Attached microarray analysis excel sheet

The microarray excel sheet used in the serpentine receptor analysis has been attached with this document and is found on the accompanying USB device.

IV. Serpentine protein expression graphs

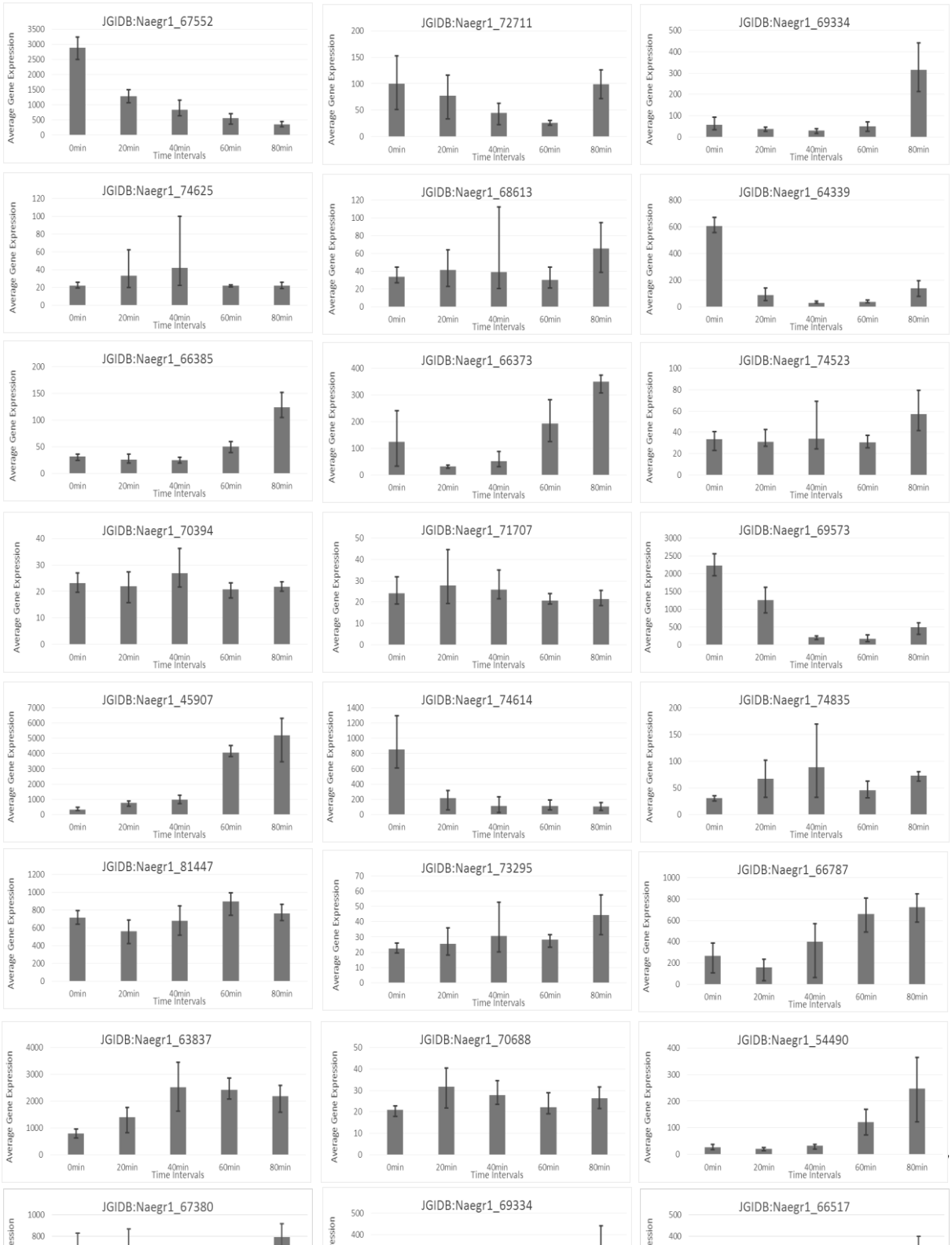

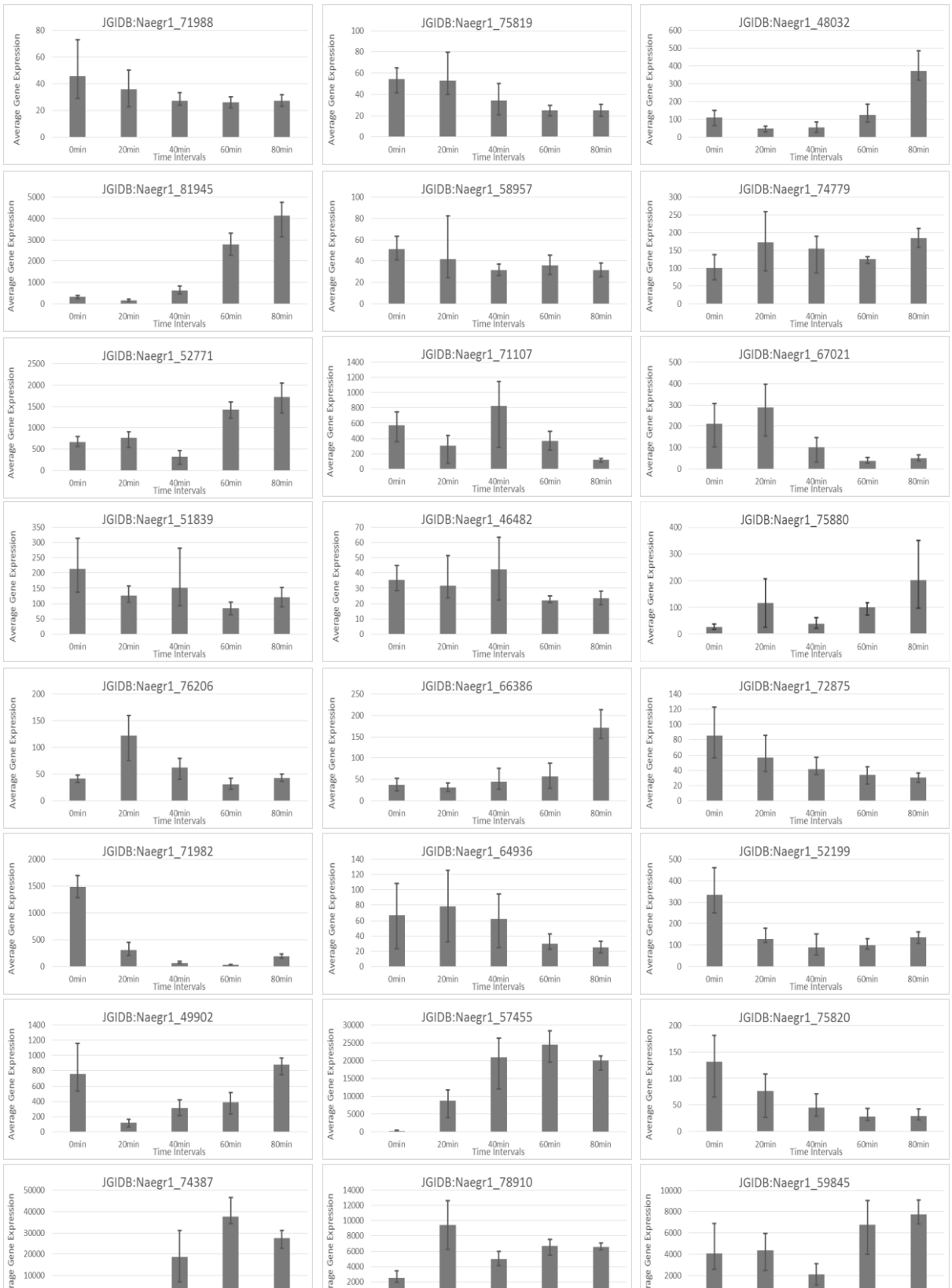
JGIDB:Naegr1_71988
JGIDB:Naegr1_75819
JGIDB:Naegr1_48032
JGIDB:Naegr1_81945
JGIDB:Naegr1_58957
JGIDB:Naegr1_74779
JGIDB:Naegr1_52771
JGIDB:Naegr1_71107
JGIDB:Naegr1_67021
JGIDB:Naegr1_51839
JGIDB:Naegr1_46482
JGIDB:Naegr1_75880
JGIDB:Naegr1_76206
JGIDB:Naegr1_66386
JGIDB:Naegr1_72875
JGIDB:Naegr1_71982
JGIDB:Naegr1_64936
JGIDB:Naegr1_52199
JGIDB:Naegr1_49902
JGIDB:Naegr1_57455
JGIDB:Naegr1_75820
JGIDB:Naegr1_74387
JGIDB:Naegr1_78910
JGIDB:Naegr1_59845
Average Gene Expression
Time Intervals
0min
20min
40min
60min
80min

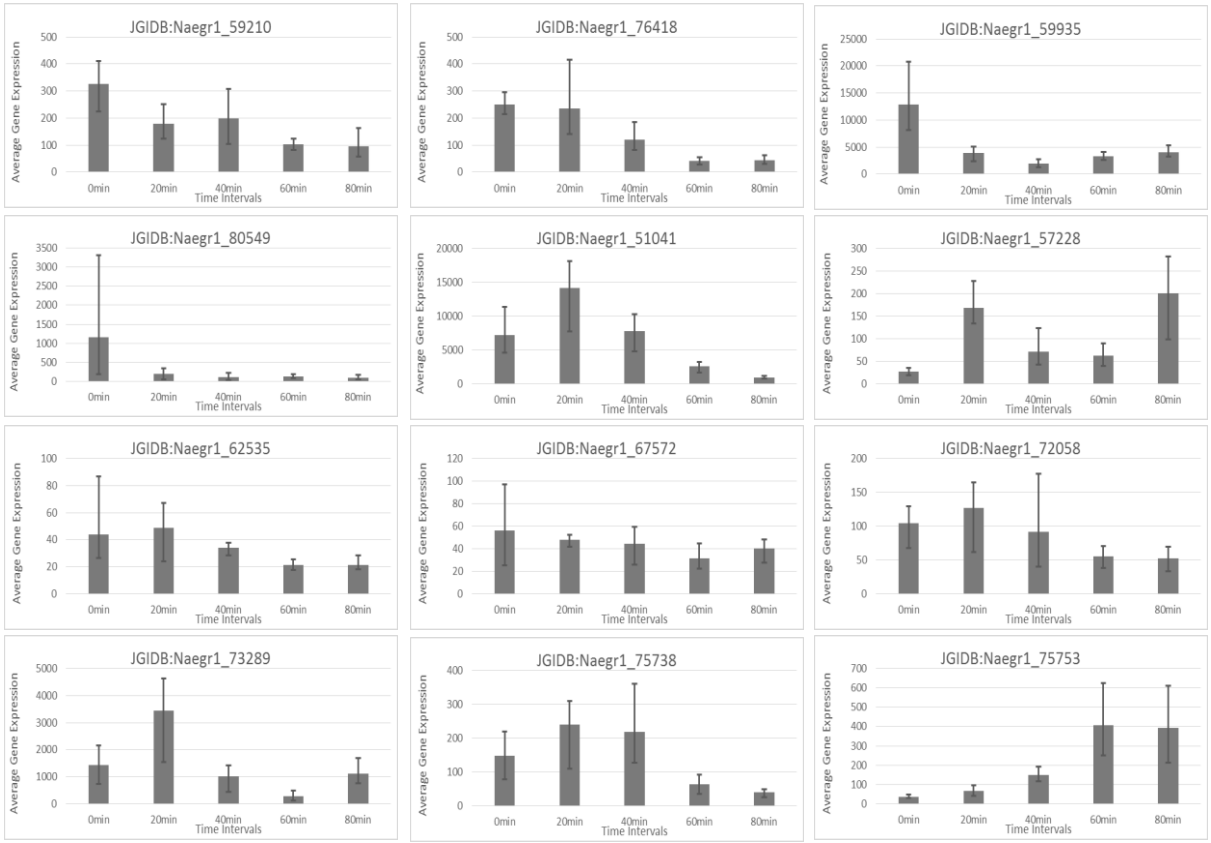

Figure 30: Protein analysis of EFC44333.1.
A collection of all tables constructed of the RNA expression of proteins returned in the BLAST searches of the amino acid sequence of EFC44333.1 ordered by e-value of initial blast search.

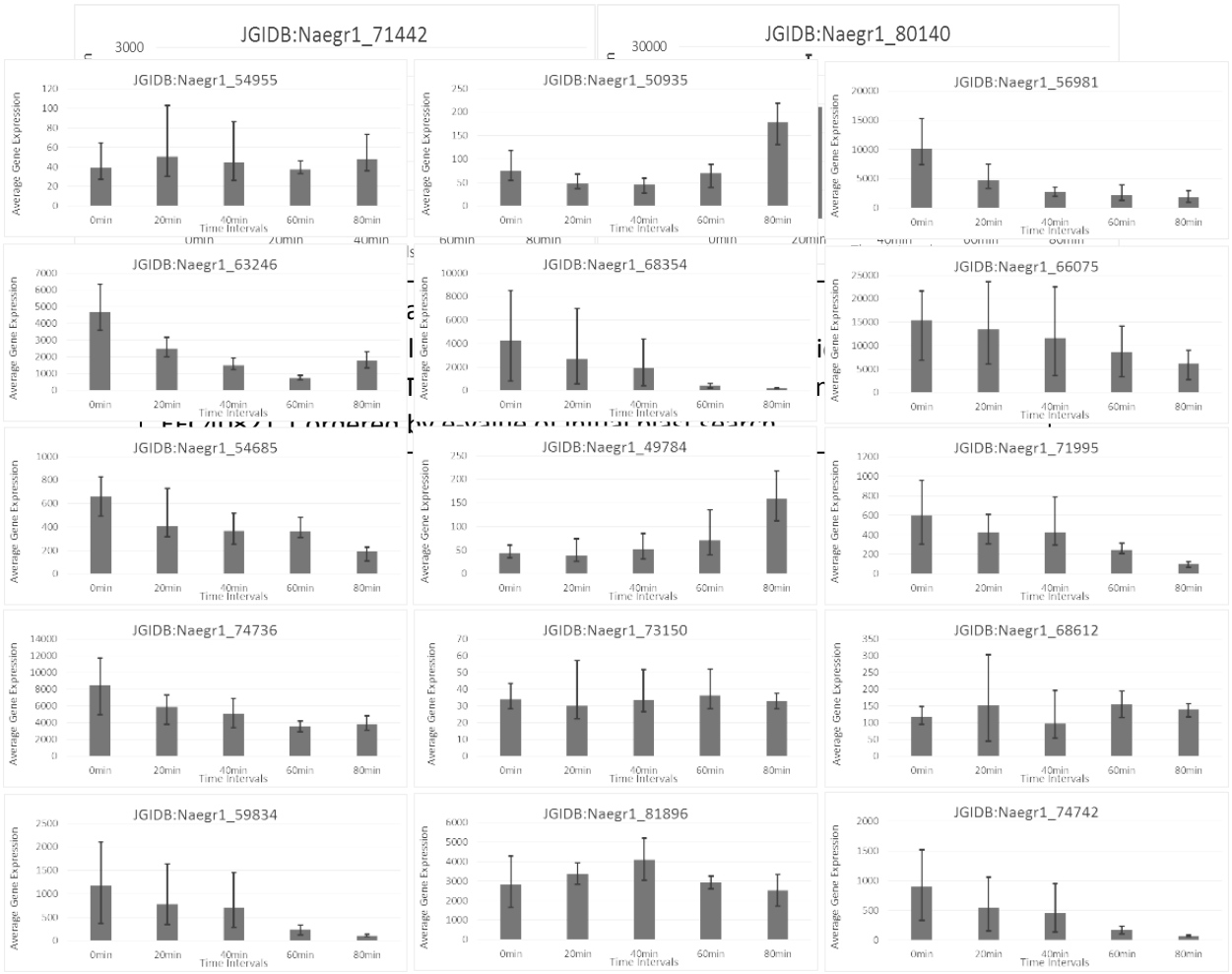

Figure 32: Protein analysis of EFC35362.1.
A collection of all tables constructed of the RNA expression of proteins returned in the BLAST searches of the amino acid sequence of EFC35362.1 ordered by e-value of initial blast search.

V. Bioinformatic Control graphs

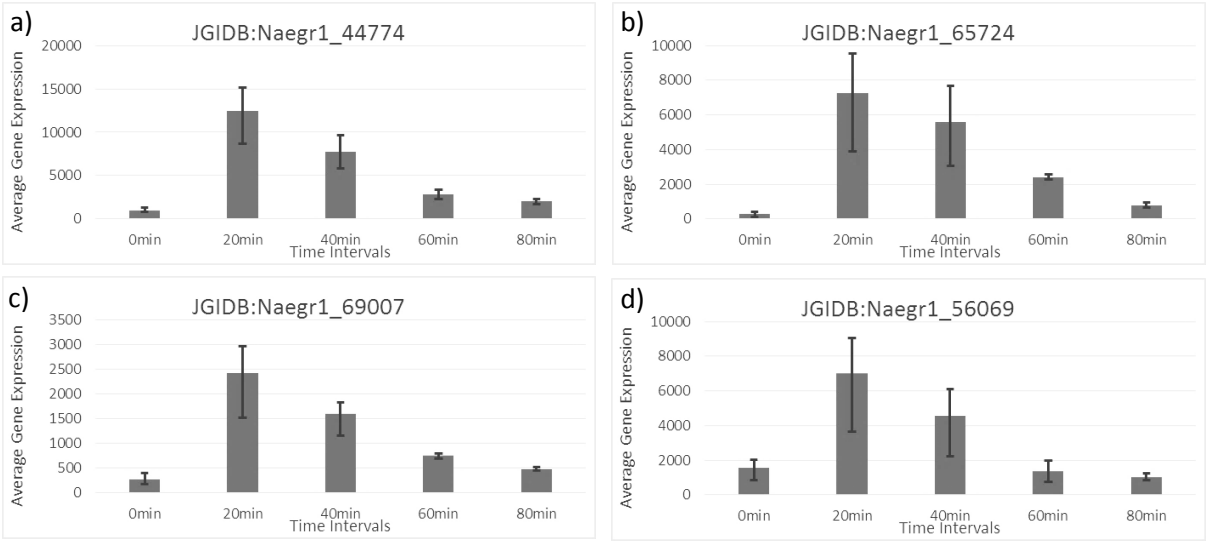

Figure 33: Tubulin mRNA expression during differentiation.

A set of graphs depicting the upregulation of tubulins during differentiation of N. *gruberi*. The graphs show expression of: a) ε-Tubulin; b) η-Tubulin; c) δ-Tubulin; d) γ-Tubulin.

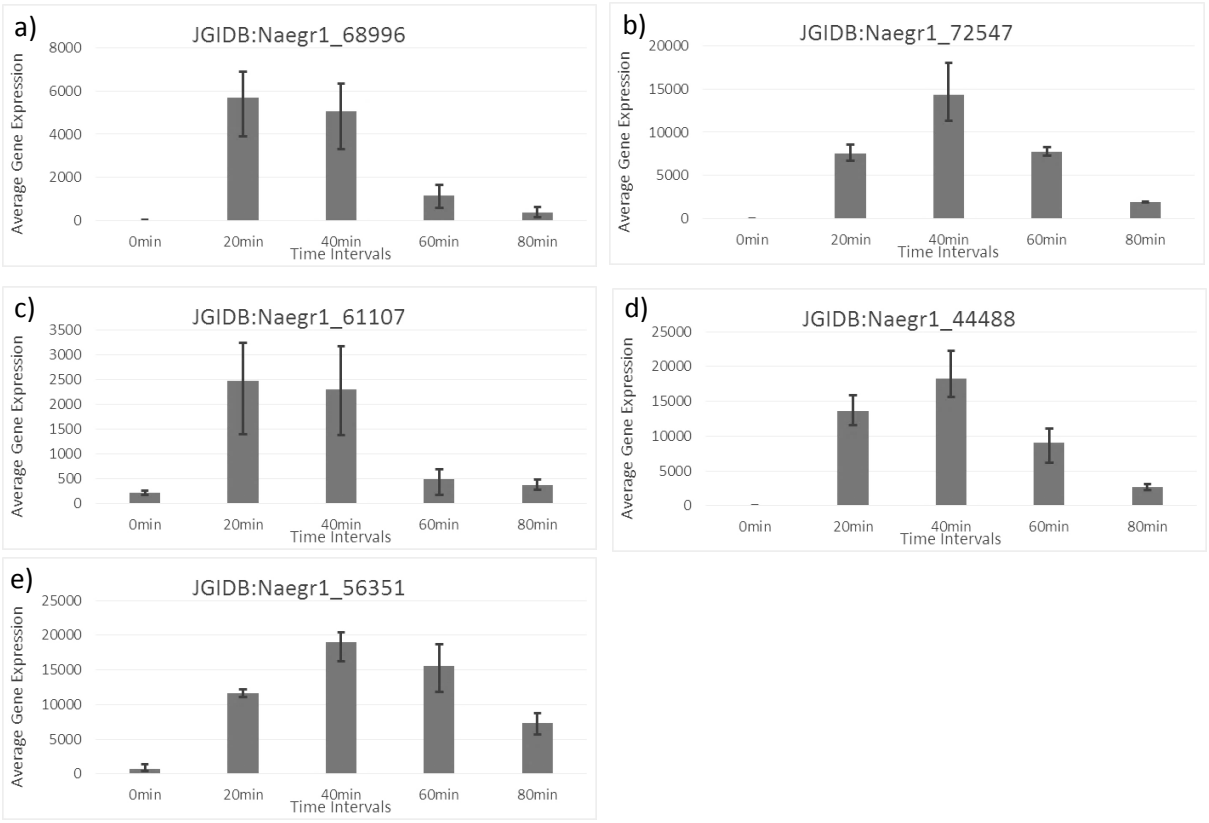

Figure 34: SAS and centrin mRNA expression during differentiation.

A set of graphs depicting the upregulation of SAS and centrin proteins during differentiation of N. *gruberi*. The graphs show expression of: a) + b) two variants of SAS-6; c) SAS-4; d) centrin 1; e) centrin 2.

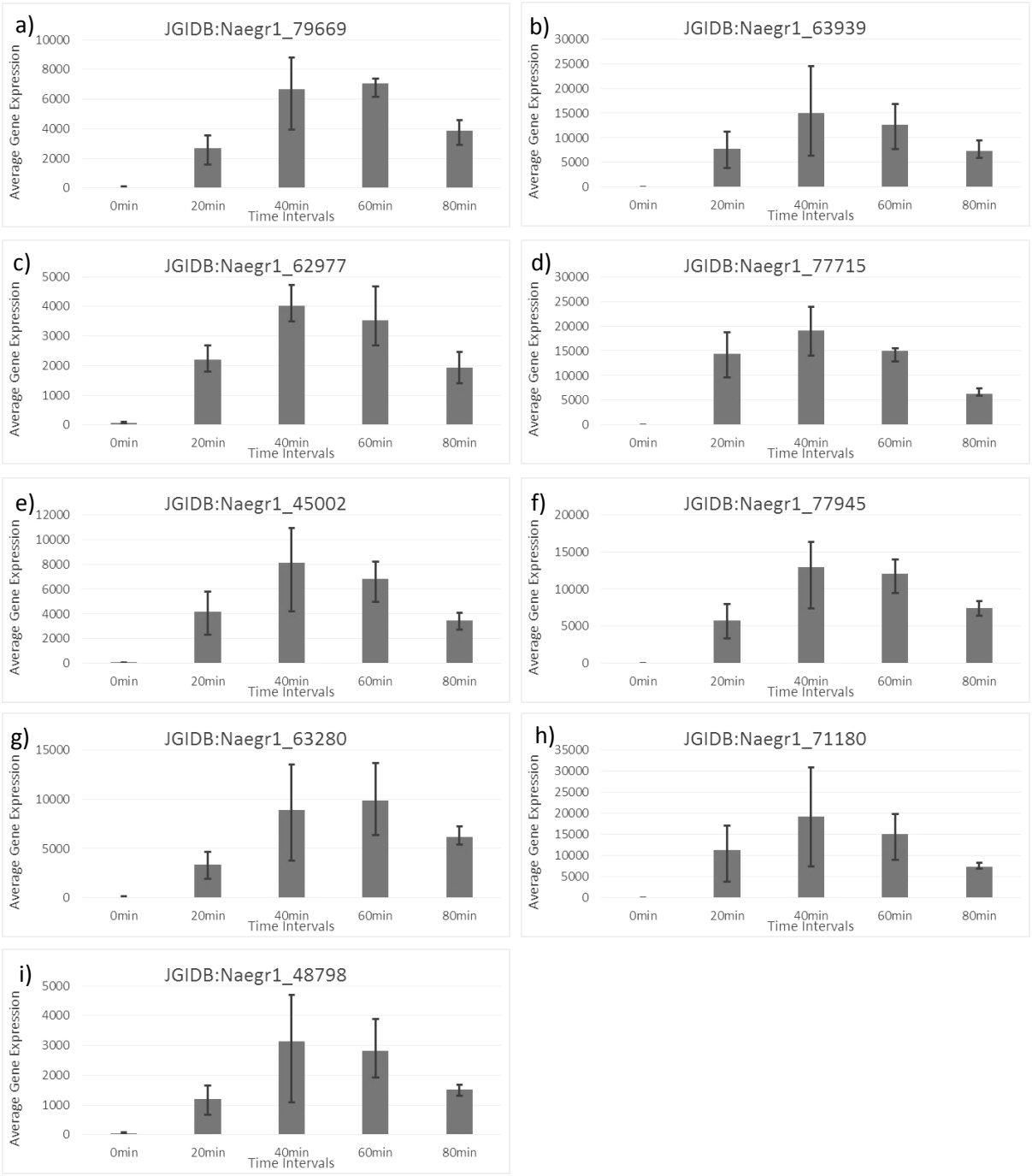

Figure 35: Kinesin and intraflagellar transport protein mRNA expression during differentiation.

A set of graphs depicting the upregulation of Kinesin and intraflagellar transport proteins during differentiation of N. *gruberi*. The graphs show expression of: a) FLA3/Kinesin-associated protein 3; b) FLA2/FLA8 (kinesin 2 homolog); c) IFT20; d) IFT52; e) IFT57; f) of IFT80; g) IFT88; h) IFT122; j) IFT140.

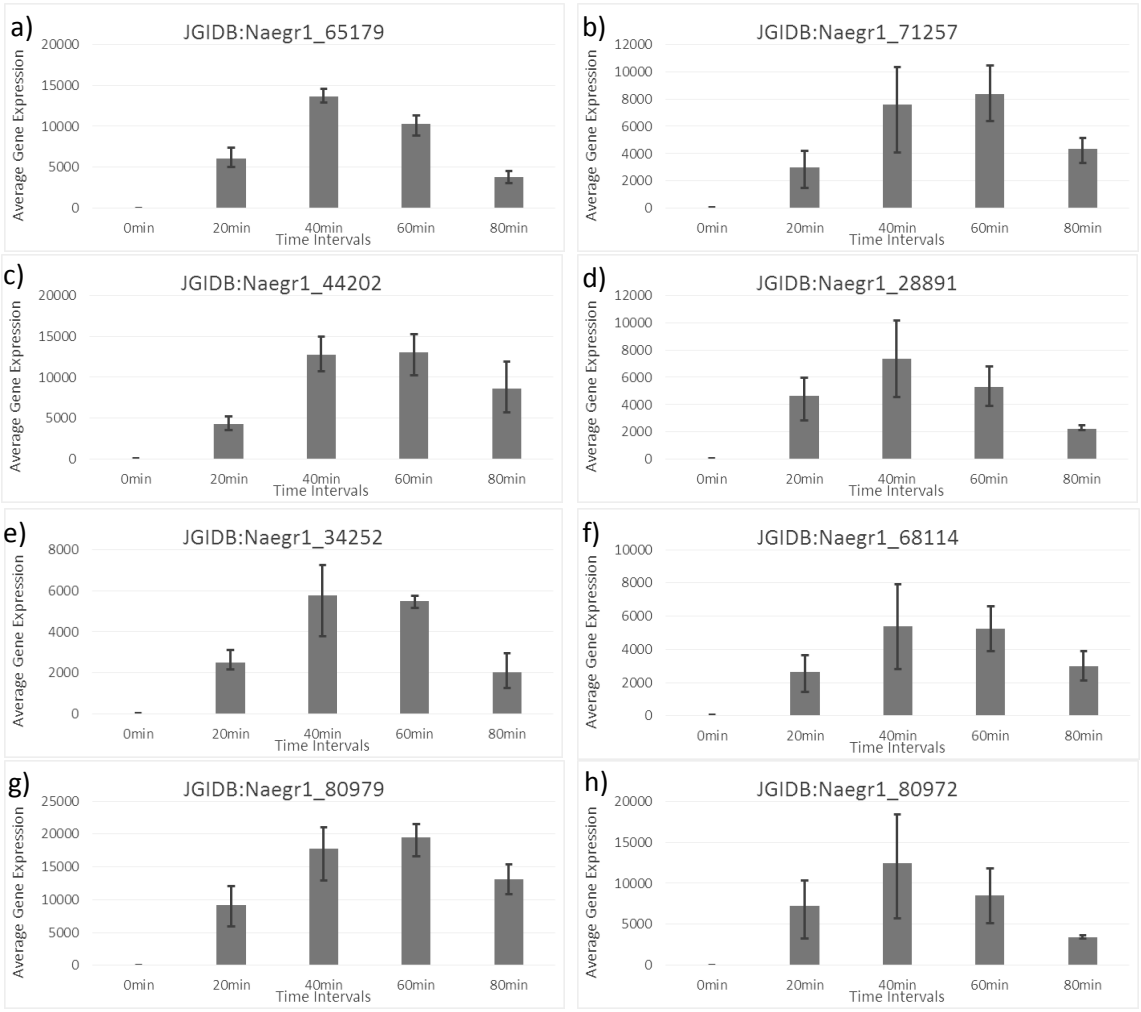

Figure 36: BBS protein mRNA expression during differentiation.

A set of graphs depicting the upregulation of BBS proteins during differentiation of N. *gruberi*. The graphs show expression of: a) BBS1; b) BBS2; c) BBS3; d) BBS4; e) BBS5; f) BBS7; g) BBS8; h) BBS9.

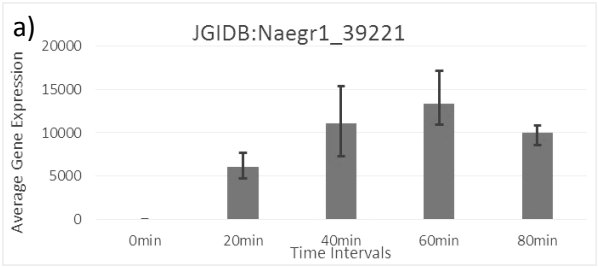
a)
JGIDB:Naegr1_39221
Average Gene Expression
20000
15000
10000
5000
0
0min
20min
40min
60min
80min
Time Intervals

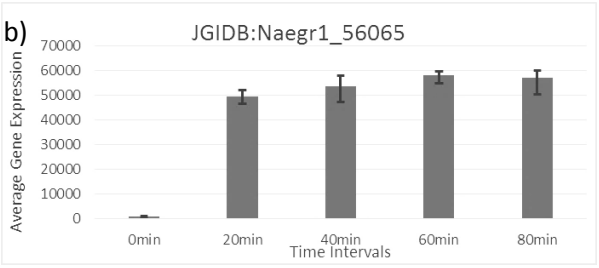
b)
JGIDB:Naegr1_56065
Average Gene Expression
70000
60000
50000
40000
30000
20000
10000
0
0min
20min
40min
60min
80min
Time Intervals

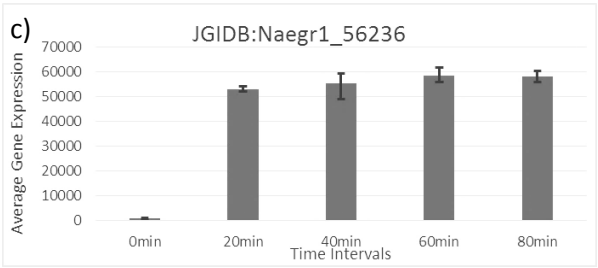
c)
JGIDB:Naegr1_56236
Average Gene Expression
70000
60000
50000
40000
30000
20000
10000
0
0min
20min
40min
60min
80min
Time Intervals

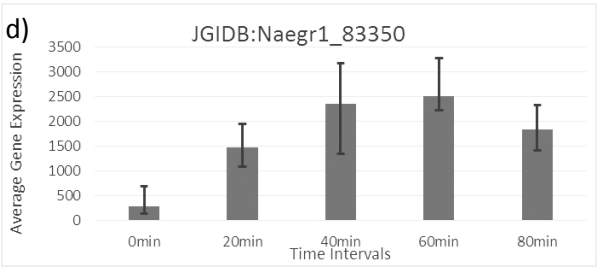
d)
JGIDB:Naegr1_83350
Average Gene Expression
3500
3000
2500
2000
1500
1000
500
0
0min
20min
40min
60min
80min
Time Intervals

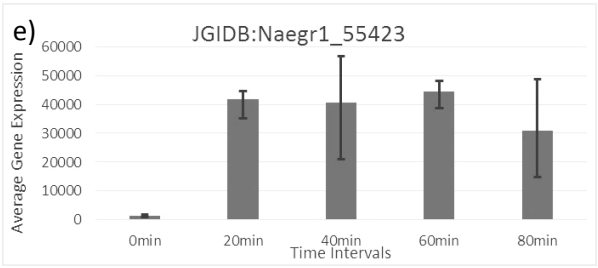
e)
JGIDB:Naegr1_55423
Average Gene Expression
60000
50000
40000
30000
20000
10000
0
0min
20min
40min
60min
80min
Time Intervals

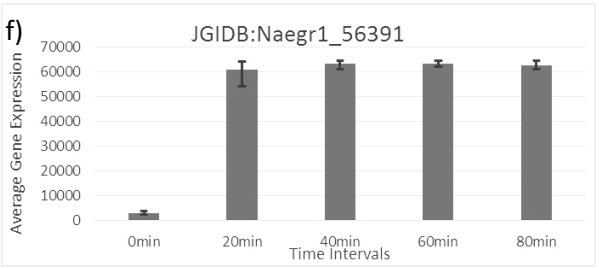
f)
JGIDB:Naegr1_56391
Average Gene Expression
70000
60000
50000
40000
30000
20000
10000
0
0min
20min
40min
60min
80min
Time Intervals

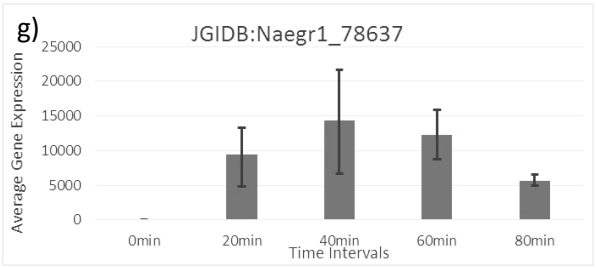
g)
JGIDB:Naegr1_78637
Average Gene Expression
25000
20000
15000
10000
5000
0
0min
20min
40min
60min
80min
Time Intervals

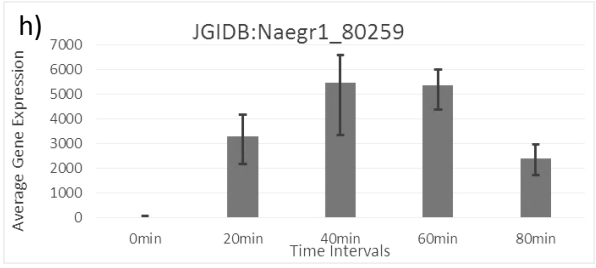
h)
JGIDB:Naegr1_80259
Average Gene Expression
7000
6000
5000
4000
3000
2000
1000
0
0min
20min
40min
60min
80min
Time Intervals

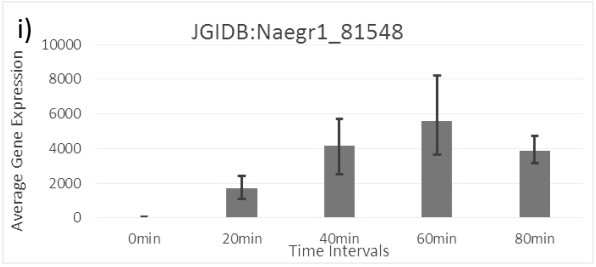
i)
JGIDB:Naegr1_81548
Average Gene Expression
10000
8000
6000
4000
2000
0
0min
20min
40min
60min
80min
Time Intervals

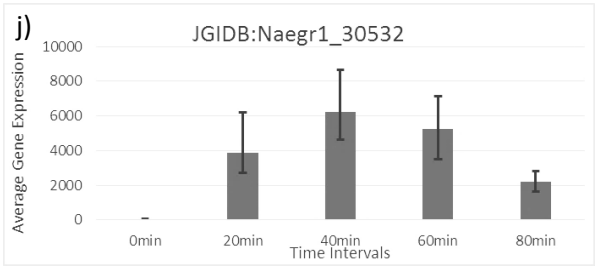
j)
JGIDB:Naegr1_30532
Average Gene Expression
10000
8000
6000
4000
2000
0
0min
20min
40min
60min
80min
Time Intervals

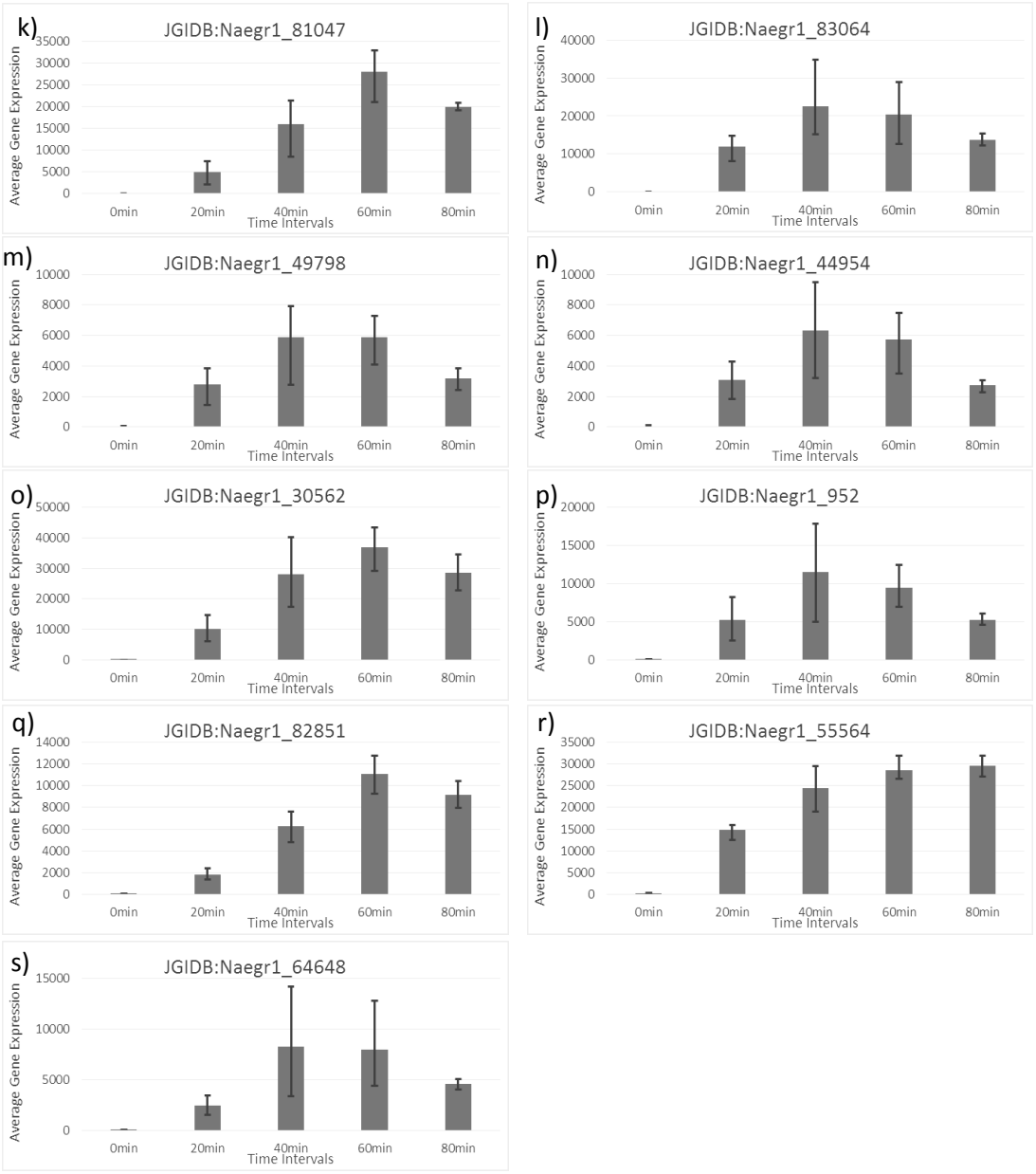

Figure 37: structural control protein analysis.

A collection of graphs depicting the upregulation of the selected structural control proteins during differentiation of N. *gruberi*. The graphs show expression of: a, b and c) different α-tubulins; d, e and f) different β-tubulins; g) ODA9; h) D1bLIC; i) ODA1; j) ODA12; k) RIB72; l) RIB43A-domain containing protein; m) radial spoke protein 4; n) radial spoke-head-like protein; o) PF16; p) PF20/SPG16; q) PACRG; r) flagellar calmodulin (CAM1); s) Expression of KLP1.

VI. Expression visualisation of the serpentine receptor BLAST results

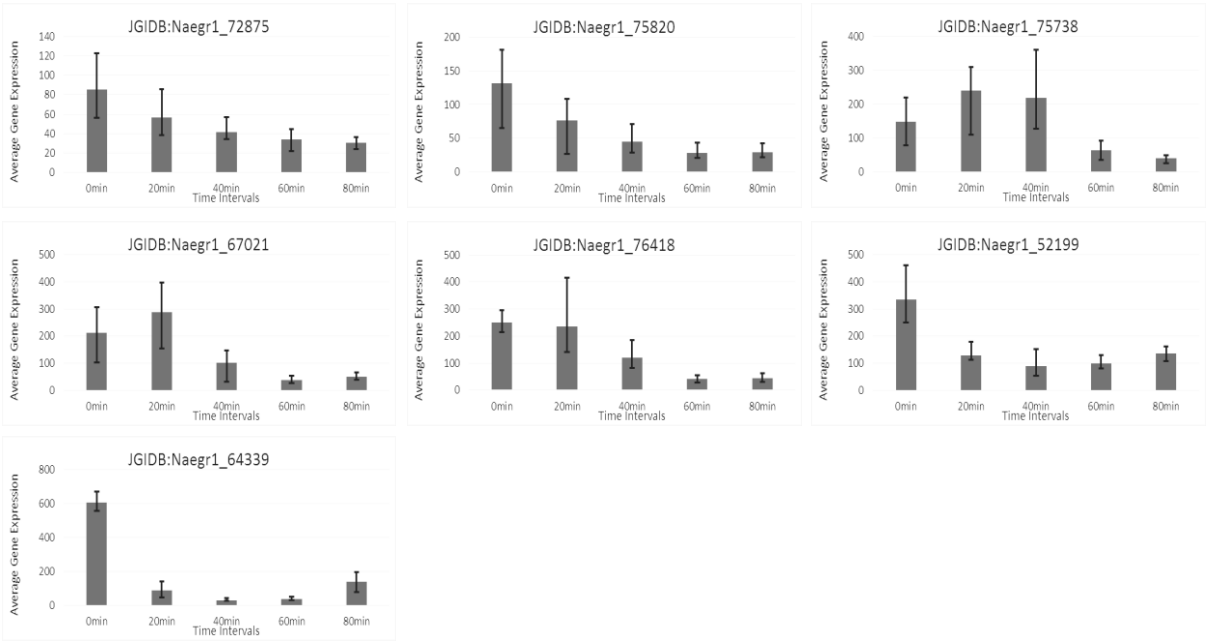

Figure 38: Low expression amoeba specific proteins.

A collection of expression graphs showing the amoeba specific gene expression pattern with an expression of 0-1,000. Graphs are ordered from weakest to highest expression.

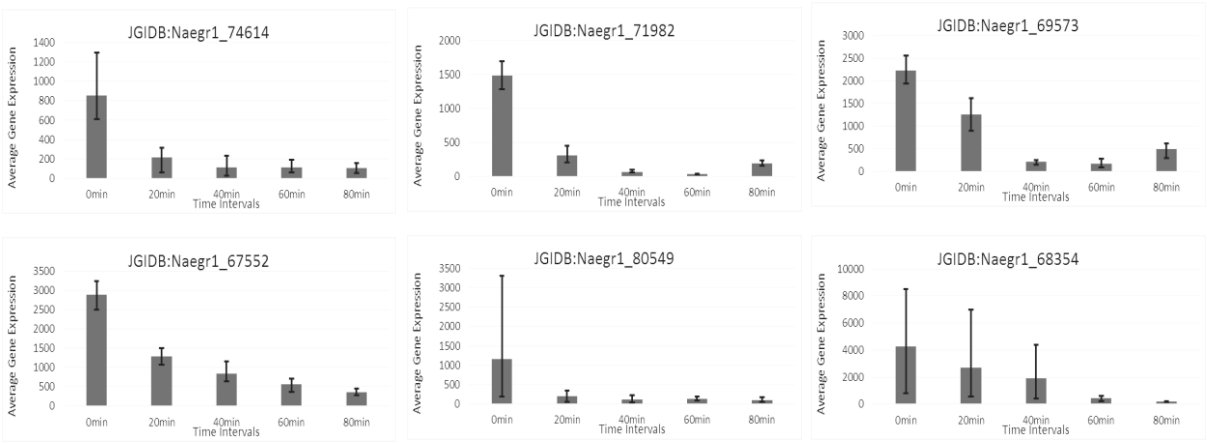

Figure 39: Medium expression amoeba specific proteins.

A collection of expression graphs showing the amoeba specific gene expression pattern with an expression of 1,000-10,000. Graphs are ordered from weakest to highest expression.

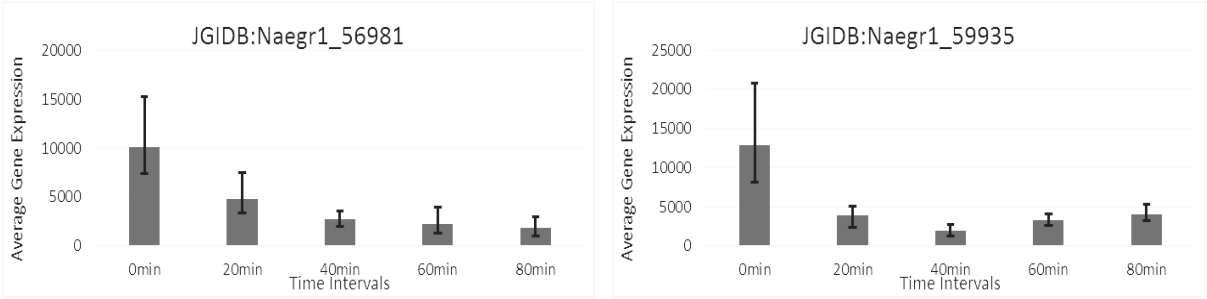

Figure 40: High expression amoeba specific proteins.

Two expression graphs showing the amoeba specific gene expression pattern with an expression of 10,000-100,000. Graphs are ordered from weakest to highest expression.

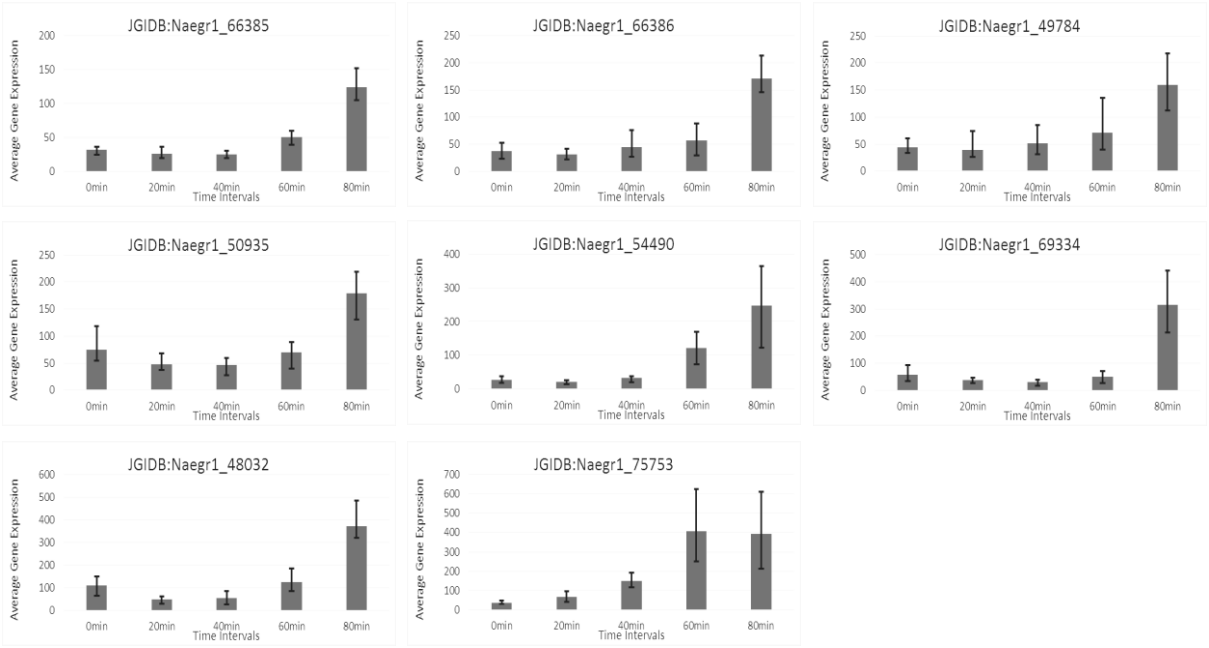

Figure 41: Low expression flagellate specific proteins.

A collection of expression graphs showing the flagellate specific gene expression pattern with an expression of 0-1,000. Graphs are ordered from weakest to highest expression.

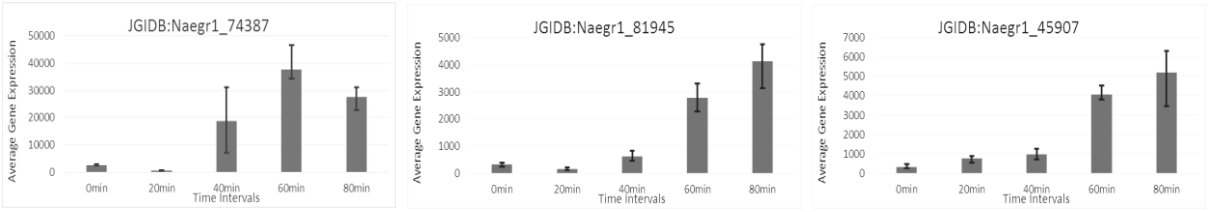

Figure 42: Medium expression flagellate specific proteins.

A collection of expression graphs showing the flagellate specific gene expression pattern with an expression of 1,000-10,000. Graphs are ordered from weakest to highest expression.

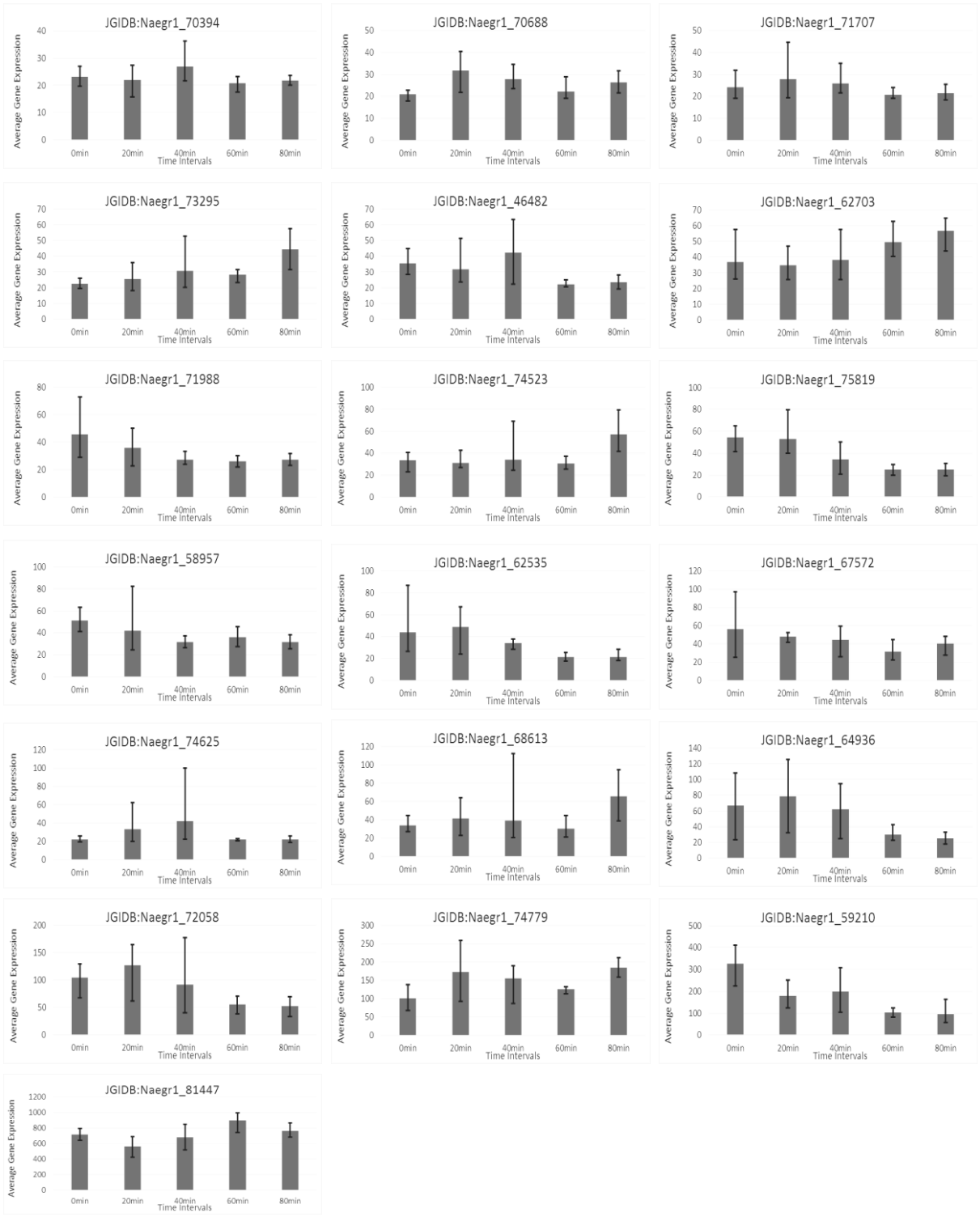

Figure 43: Low expression constitutive proteins.

A collection of expression graphs showing the constitutive gene expression pattern with an expression of 0-1,000. Graphs are ordered from weakest to highest expression.

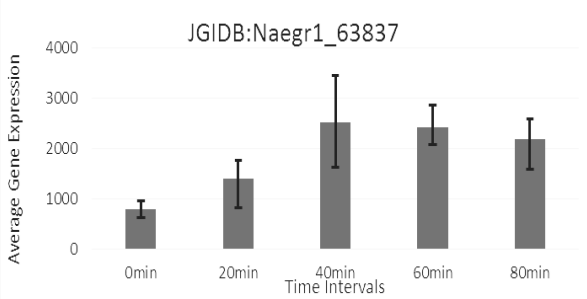

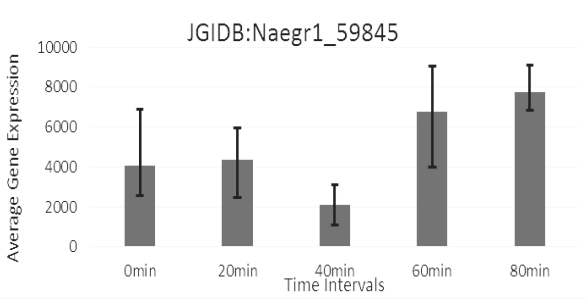

Figure 44: Medium expression constitutive proteins.

A collection of expression graphs showing the constitutive gene expression pattern with an expression of 0-1,000. Graphs are ordered from weakest to highest expression.

VII. Protein expression of proteins homologous to most upregulated amoeba specific proteins

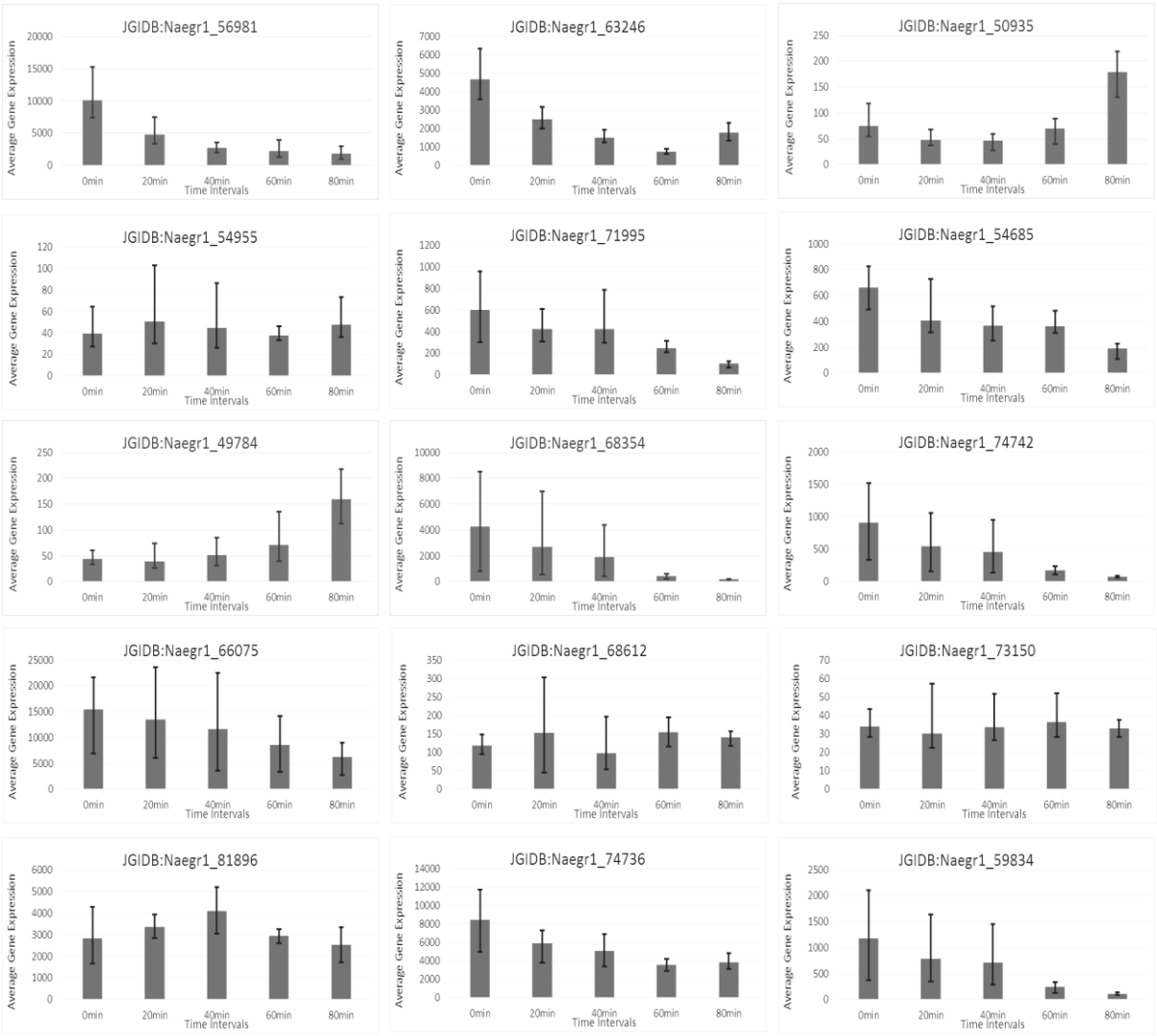

Figure 45: Expression of proteins homologous to upregulated amoeba specific protein XP_002681468.1.

This collection of graphs shows the expression of proteins returned from a protein blast using the sequence of the protein XP_002681468.1 obtained from the NCBI website. The expression graphs are ordered by e-value with the most homologous sequences first.

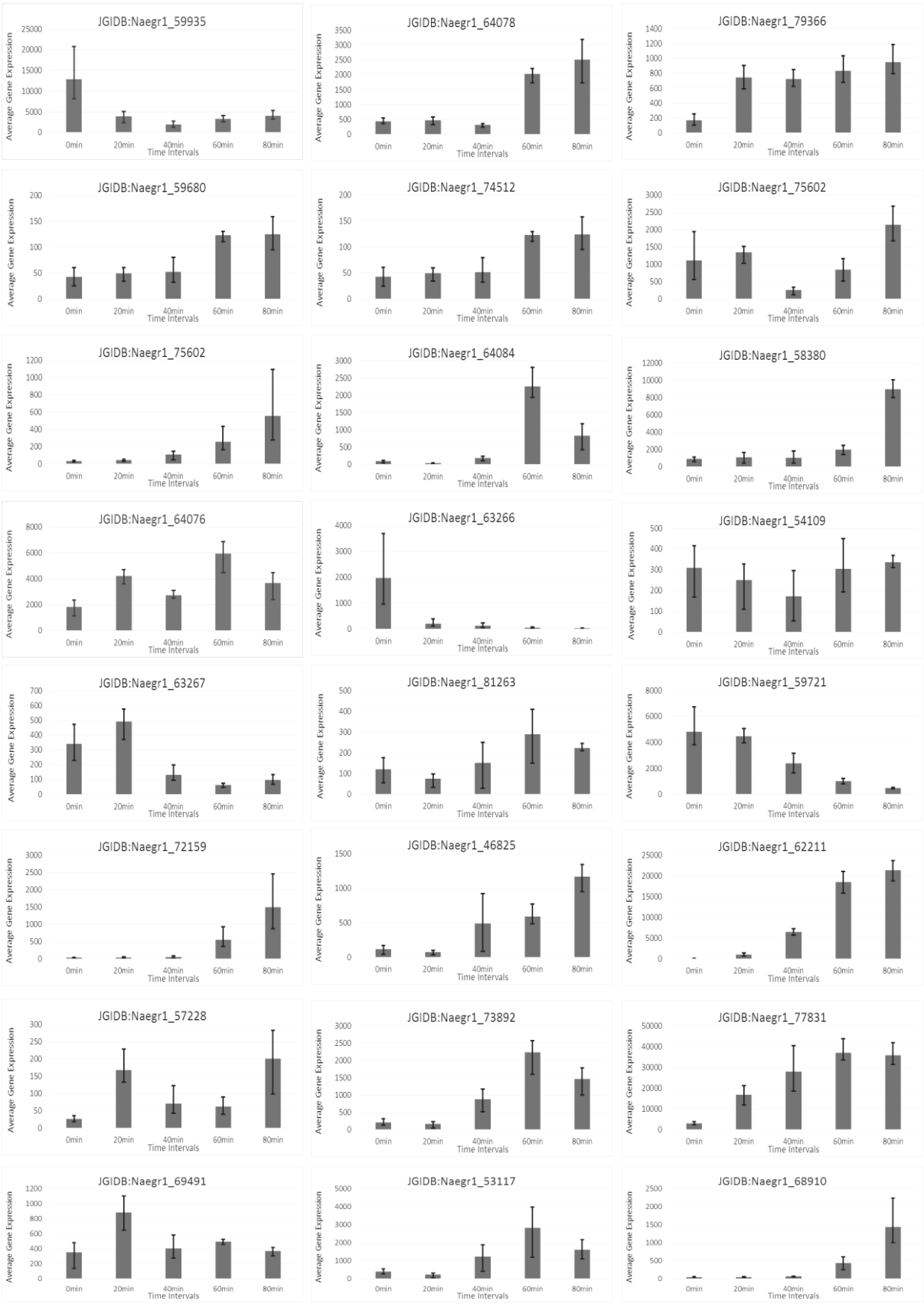
JGIDB:Naegr1_59935
JGIDB:Naegr1_64078
JGIDB:Naegr1_79366
JGIDB:Naegr1_59680
JGIDB:Naegr1_74512
JGIDB:Naegr1_75602
JGIDB:Naegr1_75602
JGIDB:Naegr1_64084
JGIDB:Naegr1_58380
JGIDB:Naegr1_64076
JGIDB:Naegr1_63266
JGIDB:Naegr1_54109
JGIDB:Naegr1_63267
JGIDB:Naegr1_81263
JGIDB:Naegr1_59721
JGIDB:Naegr1_72159
JGIDB:Naegr1_46825
JGIDB:Naegr1_62211
JGIDB:Naegr1_57228
JGIDB:Naegr1_73892
JGIDB:Naegr1_77831
JGIDB:Naegr1_69491
JGIDB:Naegr1_53117
JGIDB:Naegr1_68910
Average Gene Expression
Time Intervals
0min
20min
40min
60min
80min

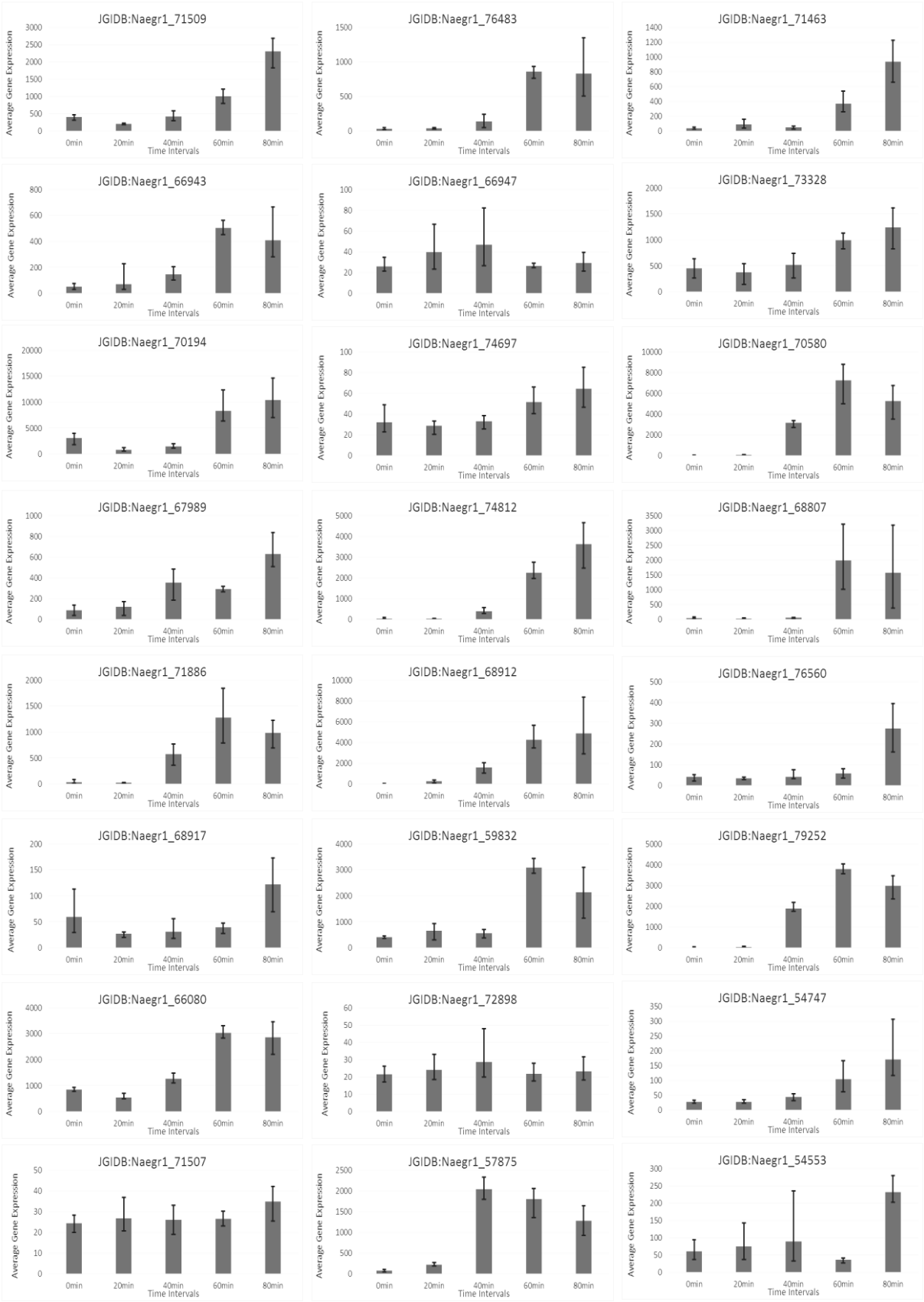
JGIDB:Naegr1_71509
JGIDB:Naegr1_76483
JGIDB:Naegr1_71463
JGIDB:Naegr1_66943
JGIDB:Naegr1_66947
JGIDB:Naegr1_73328
JGIDB:Naegr1_70194
JGIDB:Naegr1_74697
JGIDB:Naegr1_70580
JGIDB:Naegr1_67989
JGIDB:Naegr1_74812
JGIDB:Naegr1_68807
JGIDB:Naegr1_71886
JGIDB:Naegr1_68912
JGIDB:Naegr1_76560
JGIDB:Naegr1_68917
JGIDB:Naegr1_59832
JGIDB:Naegr1_79252
JGIDB:Naegr1_66080
JGIDB:Naegr1_72898
JGIDB:Naegr1_54747
JGIDB:Naegr1_71507
JGIDB:Naegr1_57875
JGIDB:Naegr1_54553
Average Gene Expression
Time Intervals
0min
20min
40min
60min
80min

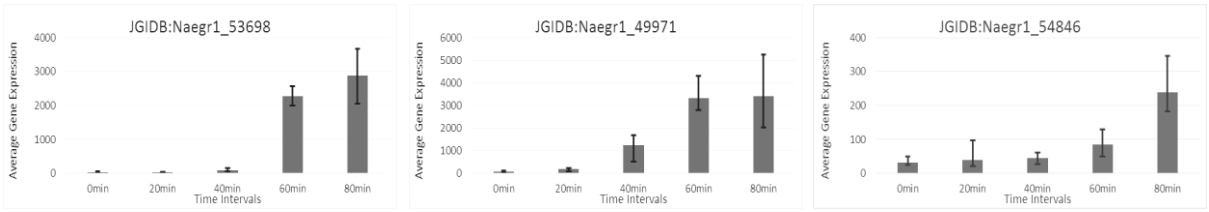

Figure 46: Expression of proteins homologous to upregulated amoeba specific protein XP_002669496.1.

This collection of graphs shows the expression of proteins returned from a protein blast using the sequence of the protein XP_002669496.1 obtained from the NCBI website. The expression graphs are ordered by e-value with the most homologous sequences first.

VIII. Protein expression of proteins homologous to most upregulated flagellate specific proteins

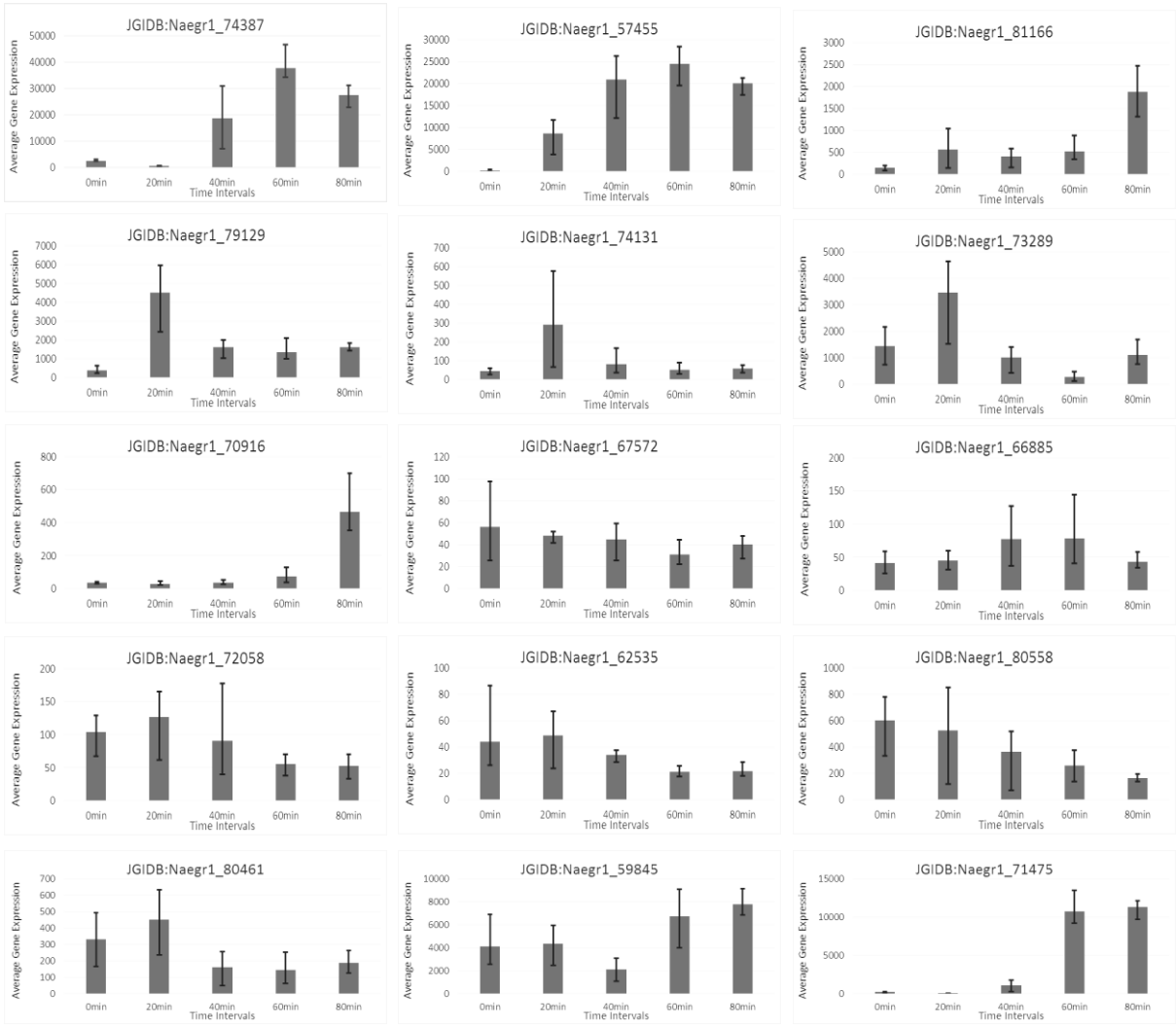

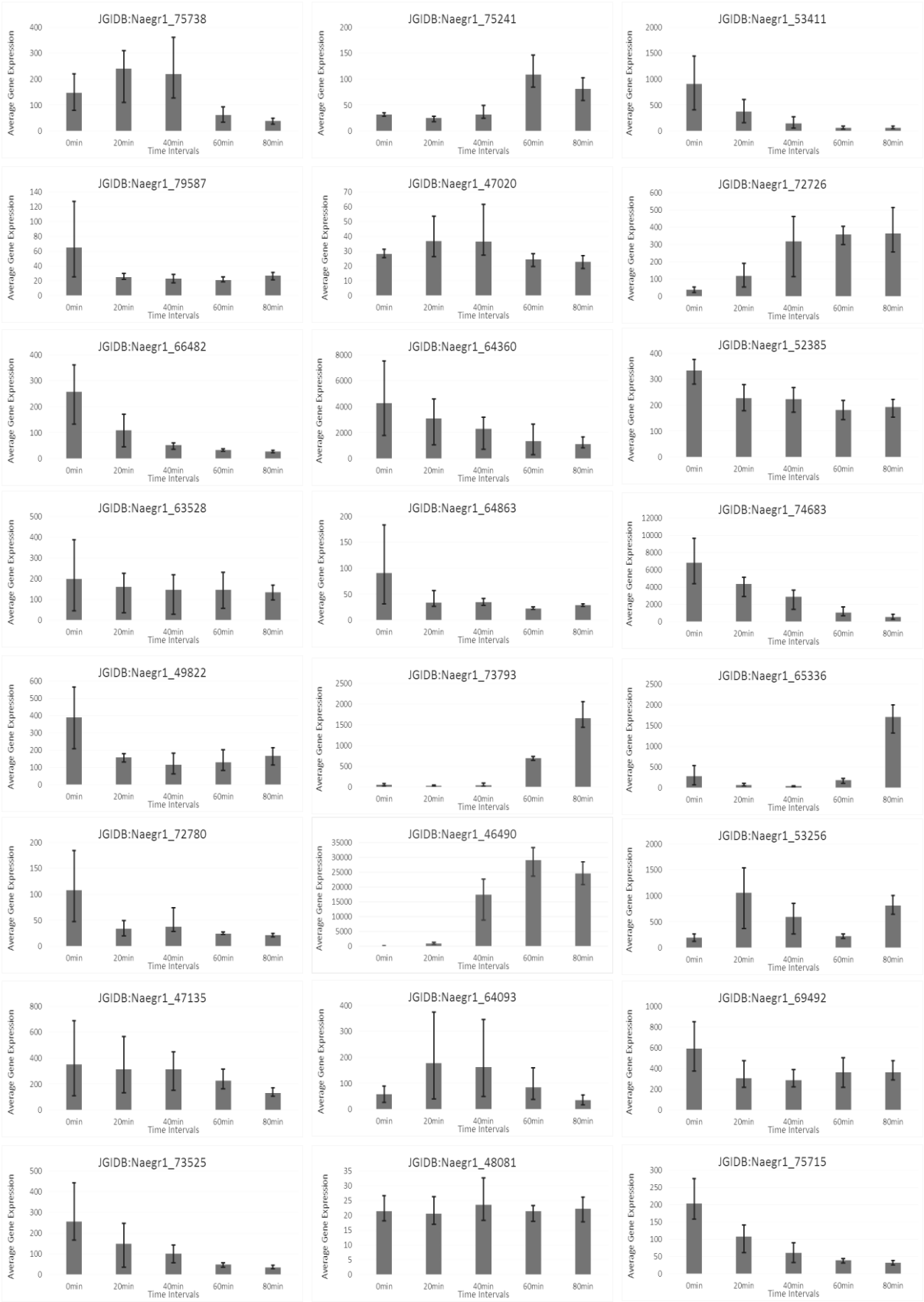
JGIDB:Naegr1_75738
JGIDB:Naegr1_75241
JGIDB:Naegr1_53411
JGIDB:Naegr1_79587
JGIDB:Naegr1_47020
JGIDB:Naegr1_72726
JGIDB:Naegr1_66482
JGIDB:Naegr1_64360
JGIDB:Naegr1_52385
JGIDB:Naegr1_63528
JGIDB:Naegr1_64863
JGIDB:Naegr1_74683
JGIDB:Naegr1_49822
JGIDB:Naegr1_73793
JGIDB:Naegr1_65336
JGIDB:Naegr1_72780
JGIDB:Naegr1_46490
JGIDB:Naegr1_53256
JGIDB:Naegr1_47135
JGIDB:Naegr1_64093
JGIDB:Naegr1_69492
JGIDB:Naegr1_73525
JGIDB:Naegr1_48081
JGIDB:Naegr1_75715
Average Gene Expression
Time Intervals
0min
20min
40min
60min
80min

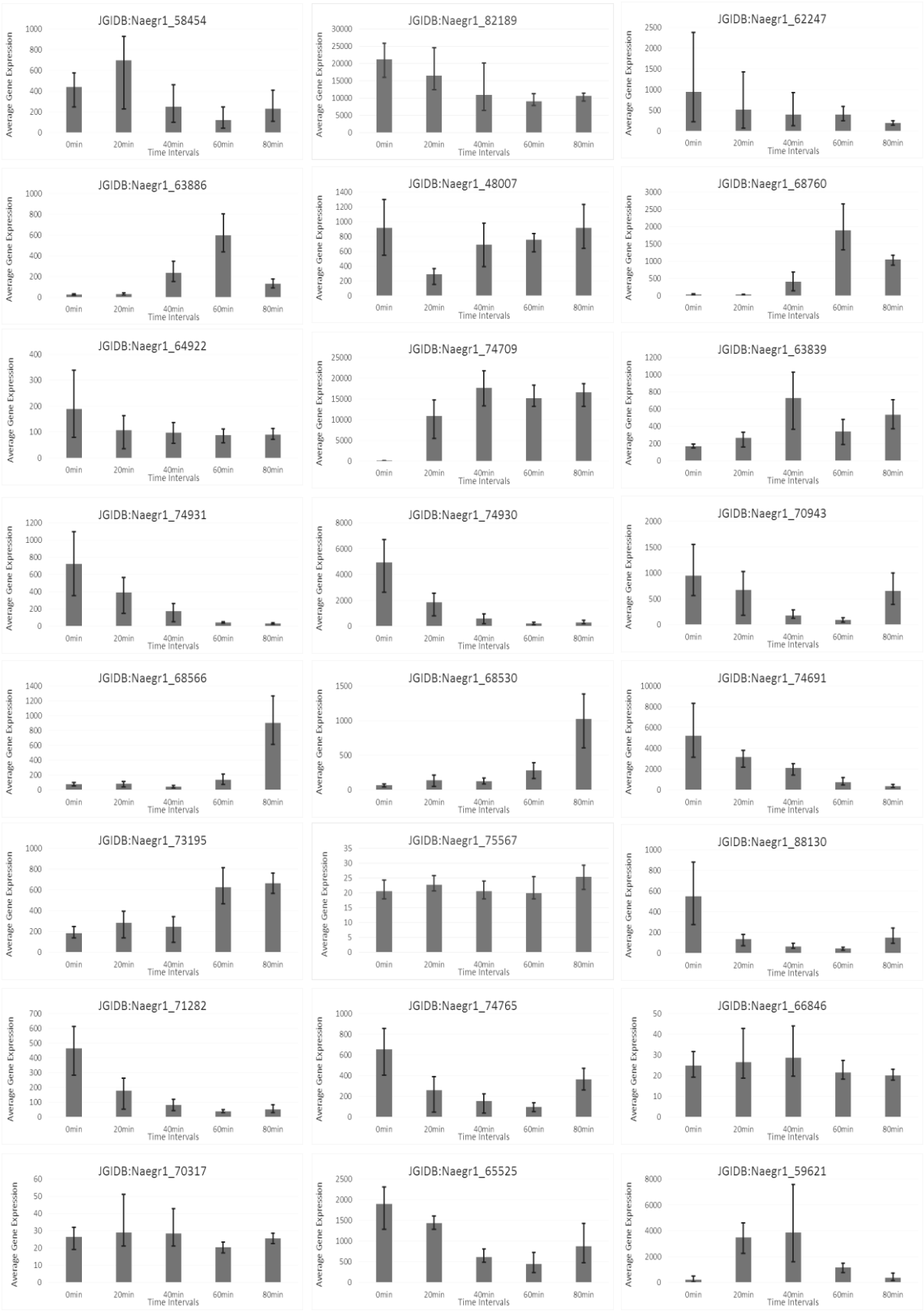
JGIDB:Naegr1_58454
JGIDB:Naegr1_82189
JGIDB:Naegr1_62247
JGIDB:Naegr1_63886
JGIDB:Naegr1_48007
JGIDB:Naegr1_68760
JGIDB:Naegr1_64922
JGIDB:Naegr1_74709
JGIDB:Naegr1_63839
JGIDB:Naegr1_74931
JGIDB:Naegr1_74930
JGIDB:Naegr1_70943
JGIDB:Naegr1_68566
JGIDB:Naegr1_68530
JGIDB:Naegr1_74691
JGIDB:Naegr1_73195
JGIDB:Naegr1_75567
JGIDB:Naegr1_88130
JGIDB:Naegr1_71282
JGIDB:Naegr1_74765
JGIDB:Naegr1_66846
JGIDB:Naegr1_70317
JGIDB:Naegr1_65525
JGIDB:Naegr1_59621
Average Gene Expression
Time Intervals
0min
20min
40min
60min
80min

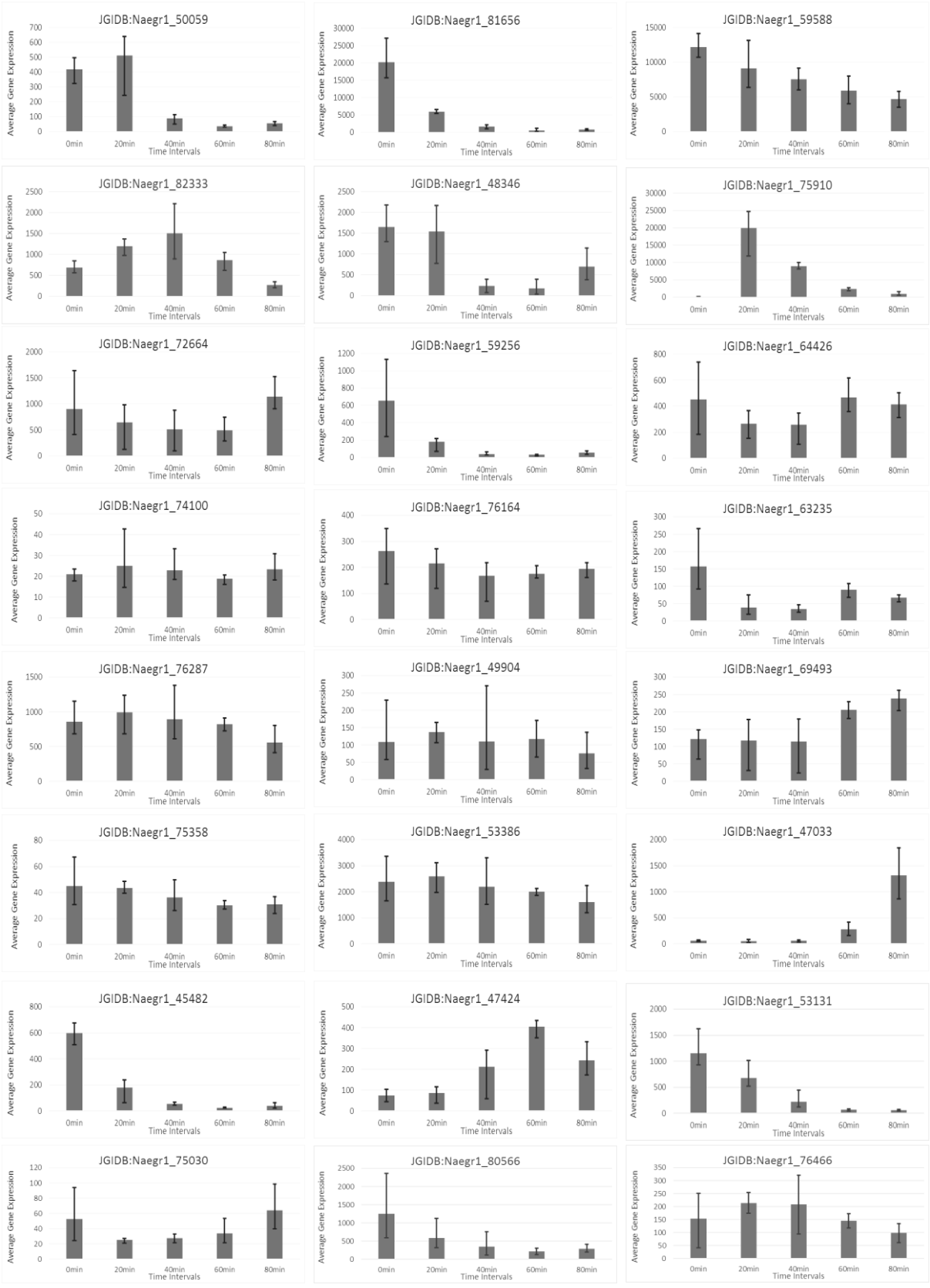
JGIDB:Naegr1_50059
JGIDB:Naegr1_81656
JGIDB:Naegr1_59588
JGIDB:Naegr1_82333
JGIDB:Naegr1_48346
JGIDB:Naegr1_75910
JGIDB:Naegr1_72664
JGIDB:Naegr1_59256
JGIDB:Naegr1_64426
JGIDB:Naegr1_74100
JGIDB:Naegr1_76164
JGIDB:Naegr1_63235
JGIDB:Naegr1_76287
JGIDB:Naegr1_49904
JGIDB:Naegr1_69493
JGIDB:Naegr1_75358
JGIDB:Naegr1_53386
JGIDB:Naegr1_47033
JGIDB:Naegr1_45482
JGIDB:Naegr1_47424
JGIDB:Naegr1_53131
JGIDB:Naegr1_75030
JGIDB:Naegr1_80566
JGIDB:Naegr1_76466
Average Gene Expression
Time Intervals
0min
20min
40min
60min
80min

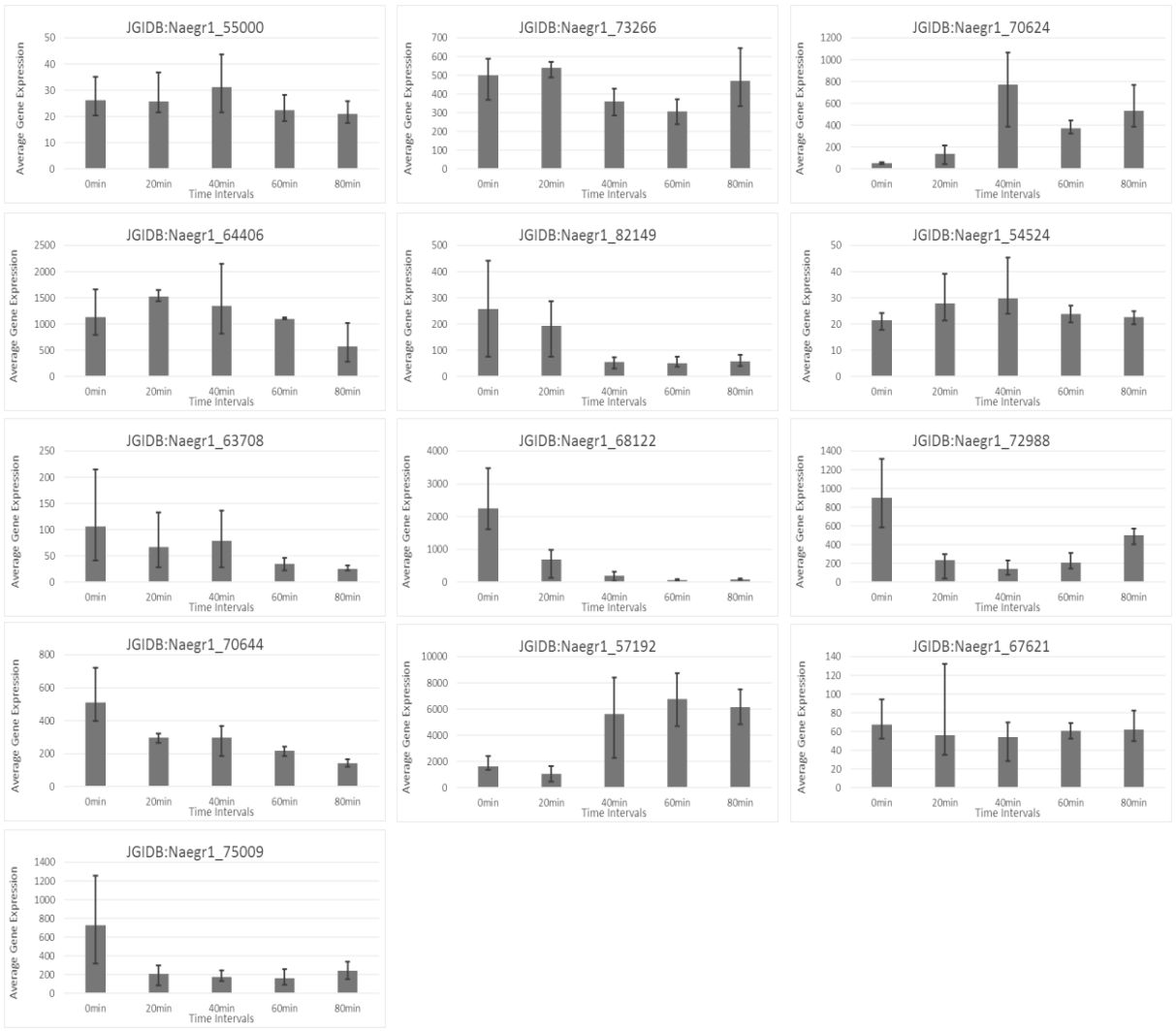

Figure 47: Expression of proteins homologous to upregulated flagellate specific protein XP_002670636.1.

This collection of graphs shows the expression of proteins returned from a protein blast using the sequence of the protein XP_002670636.1 obtained from the NCBI website. The expression graphs are ordered by e-value with the most homologous sequences first.

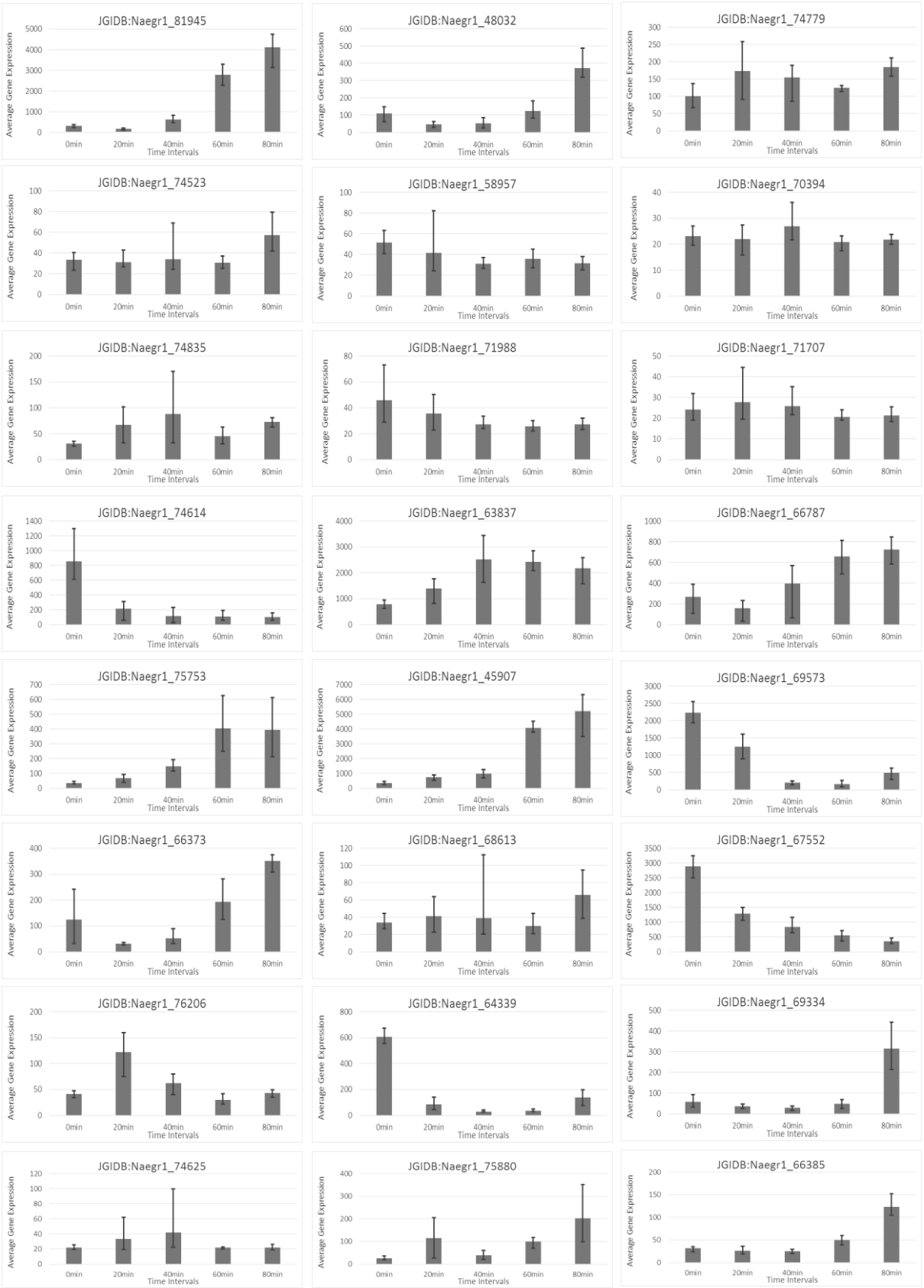
JGIDB:Naegr1_81945
JGIDB:Naegr1_48032
JGIDB:Naegr1_74779
JGIDB:Naegr1_74523
JGIDB:Naegr1_58957
JGIDB:Naegr1_70394
JGIDB:Naegr1_74835
JGIDB:Naegr1_71988
JGIDB:Naegr1_71707
JGIDB:Naegr1_74614
JGIDB:Naegr1_63837
JGIDB:Naegr1_66787
JGIDB:Naegr1_75753
JGIDB:Naegr1_45907
JGIDB:Naegr1_69573
JGIDB:Naegr1_66373
JGIDB:Naegr1_68613
JGIDB:Naegr1_67552
JGIDB:Naegr1_76206
JGIDB:Naegr1_64339
JGIDB:Naegr1_69334
JGIDB:Naegr1_74625
JGIDB:Naegr1_75880
JGIDB:Naegr1_66385
Average Gene Expression
Time Intervals
0min
20min
40min
60min
80min

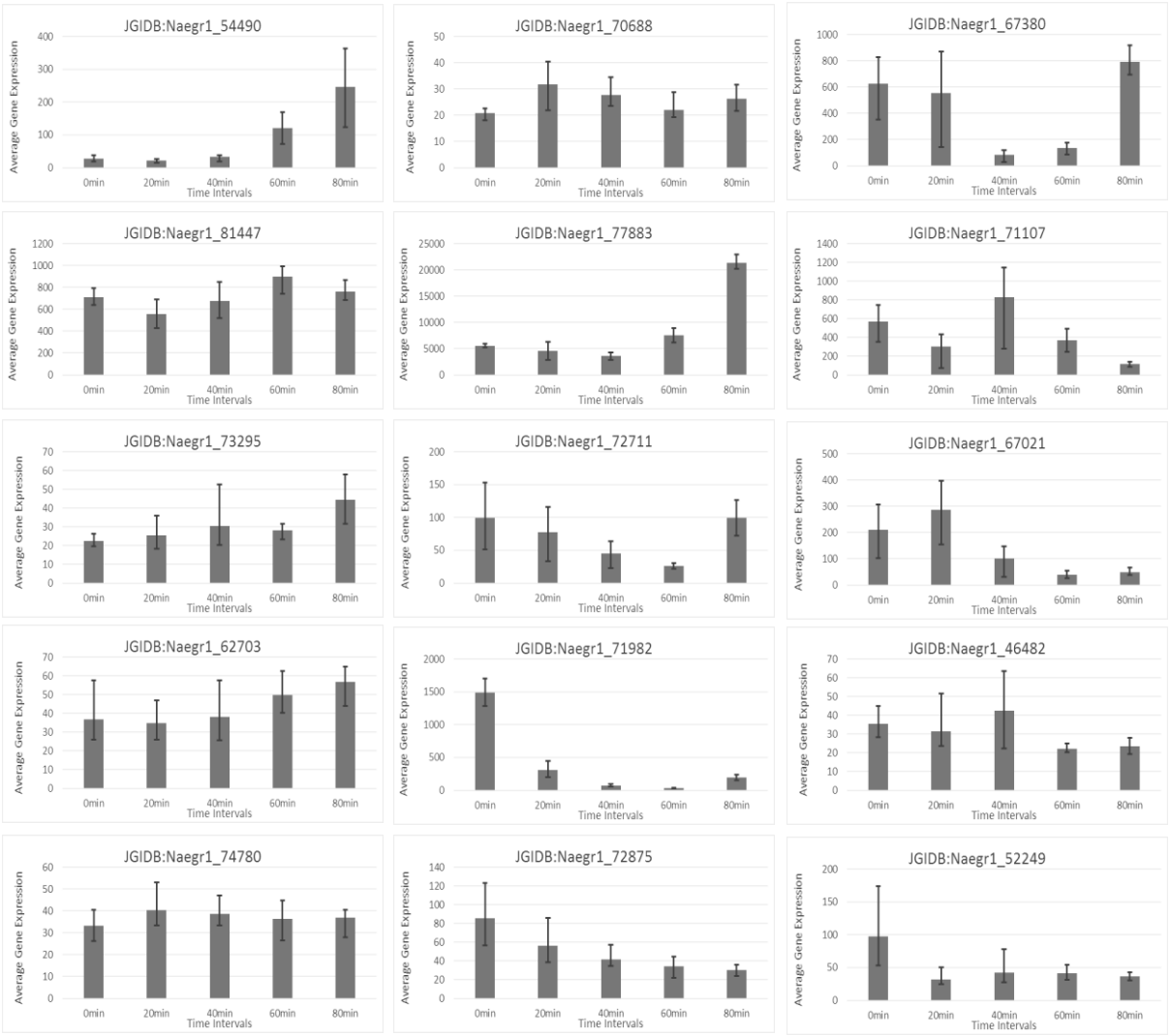

Figure 48: Expression of proteins homologous to upregulated flagellate specific protein XP_002670067.1.

This collection of graphs shows the expression of proteins returned from a protein blast using the sequence of the protein XP_002670067.1 obtained from the NCBI website. The expression graphs are ordered by e-value with the most homologous sequences first.

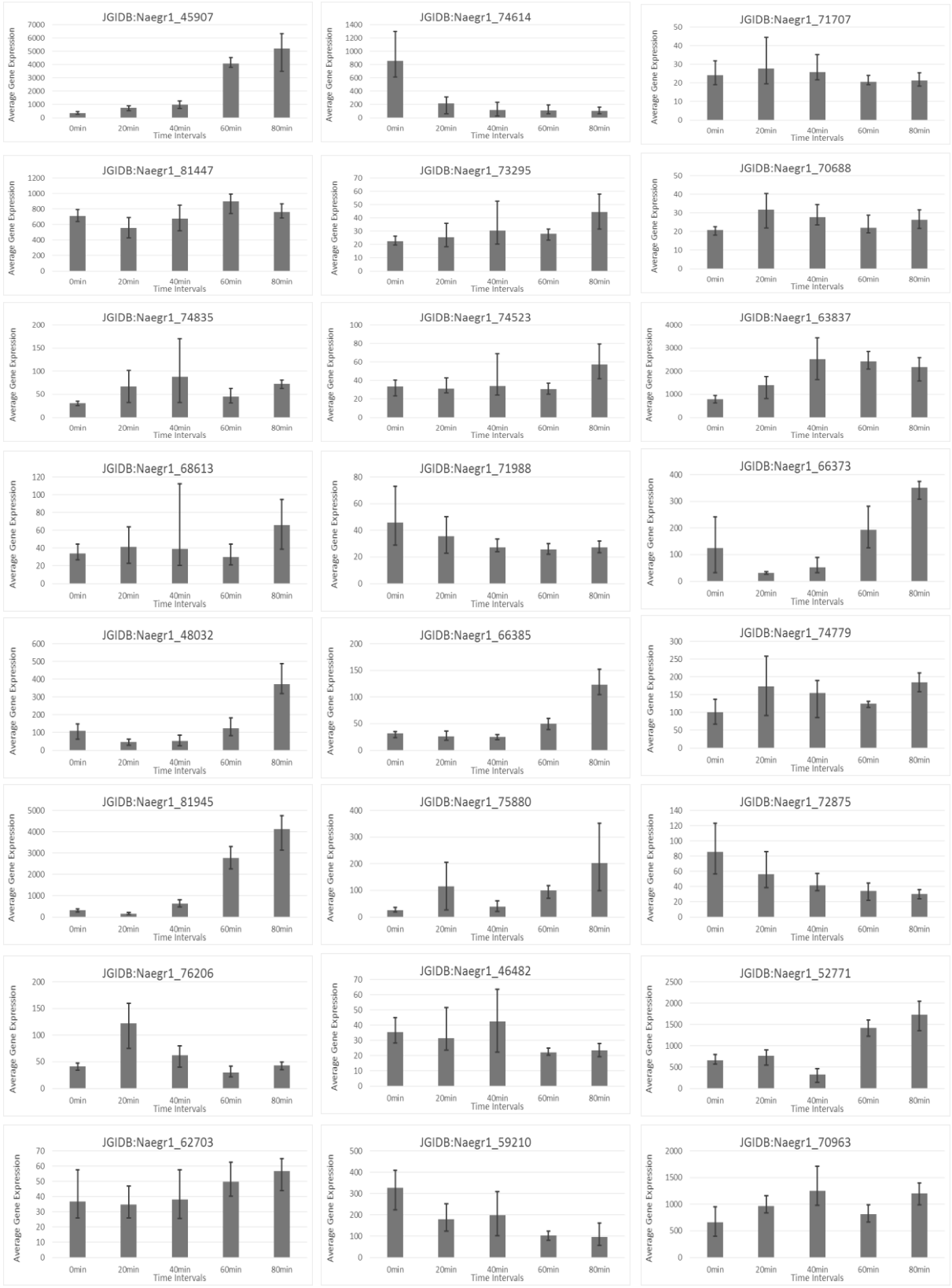
JGIDB:Naegr1_45907
JGIDB:Naegr1_74614
JGIDB:Naegr1_71707
JGIDB:Naegr1_81447
JGIDB:Naegr1_73295
JGIDB:Naegr1_70688
JGIDB:Naegr1_74835
JGIDB:Naegr1_74523
JGIDB:Naegr1_63837
JGIDB:Naegr1_68613
JGIDB:Naegr1_71988
JGIDB:Naegr1_66373
JGIDB:Naegr1_48032
JGIDB:Naegr1_66385
JGIDB:Naegr1_74779
JGIDB:Naegr1_81945
JGIDB:Naegr1_75880
JGIDB:Naegr1_72875
JGIDB:Naegr1_76206
JGIDB:Naegr1_46482
JGIDB:Naegr1_52771
JGIDB:Naegr1_62703
JGIDB:Naegr1_59210
JGIDB:Naegr1_70963
Average Gene Expression
Time Intervals
0min
20min
40min
60min
80min

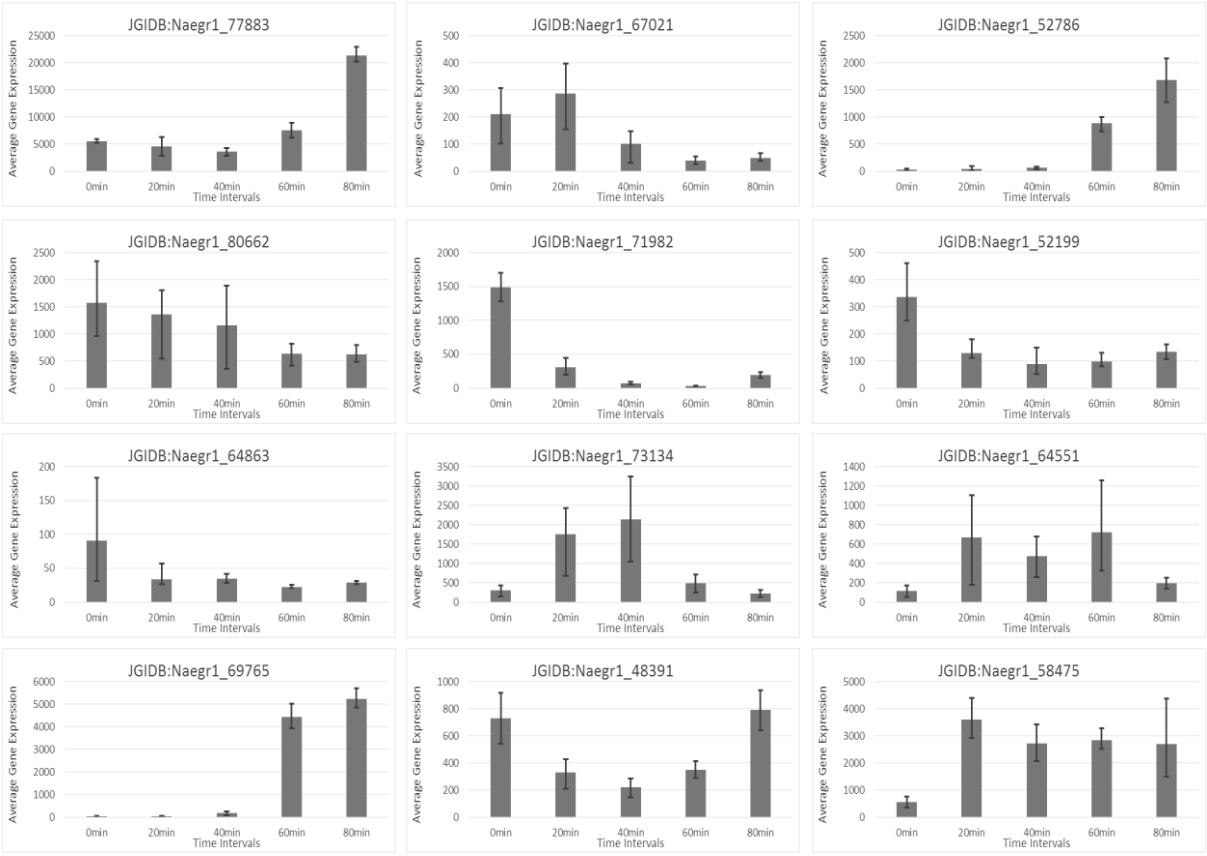

Figure 49: Expression of proteins homologous to upregulated flagellate specific protein XP_002682068.1

This collection of graphs shows the expression of proteins returned from a protein blast using the sequence of the protein XP_002682068.1 obtained from the NCBI website. The expression graphs are ordered by e-value with the most homologous sequences first.

IX. Protein expression of proteins homologous to most upregulated constitutive proteins

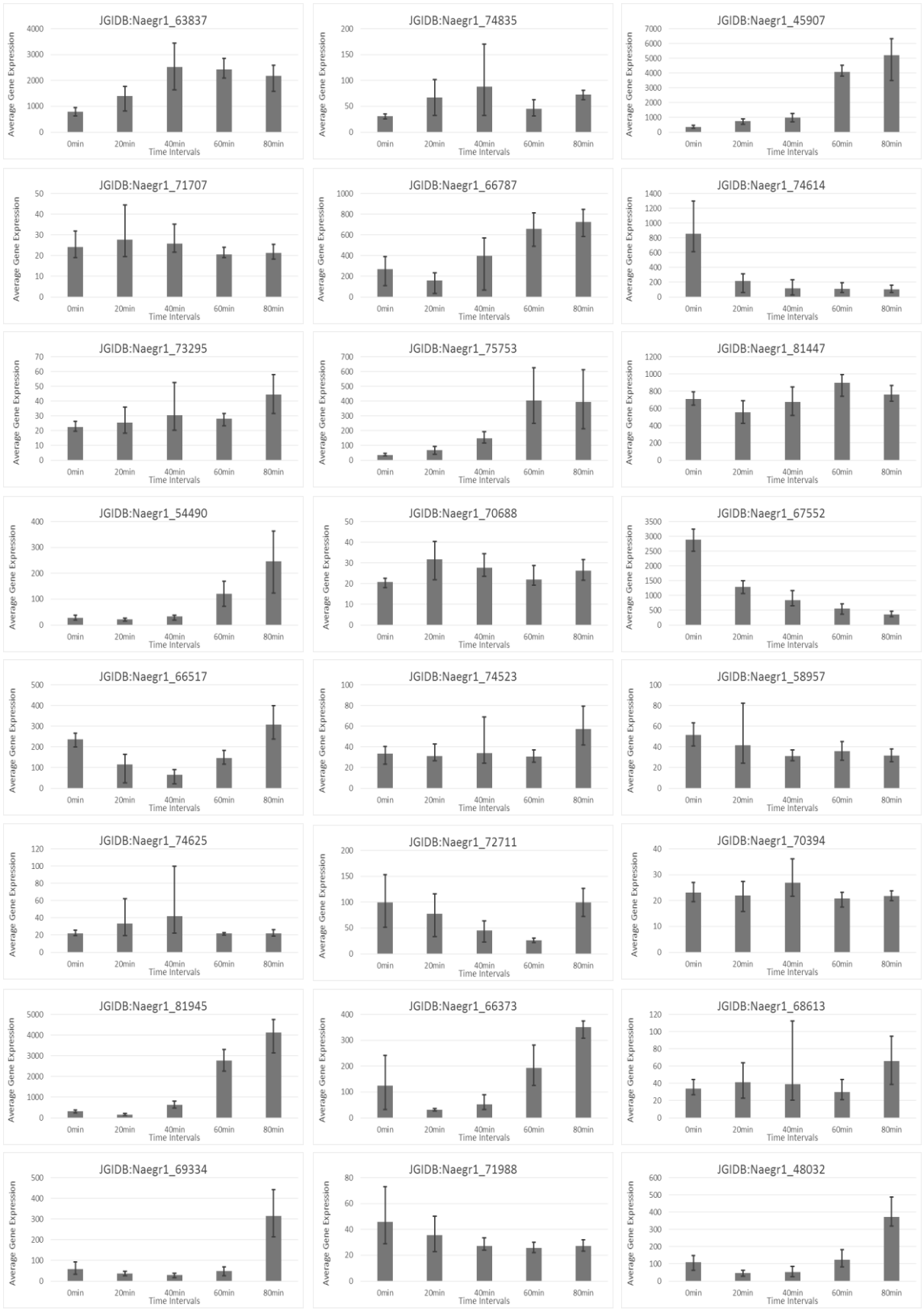

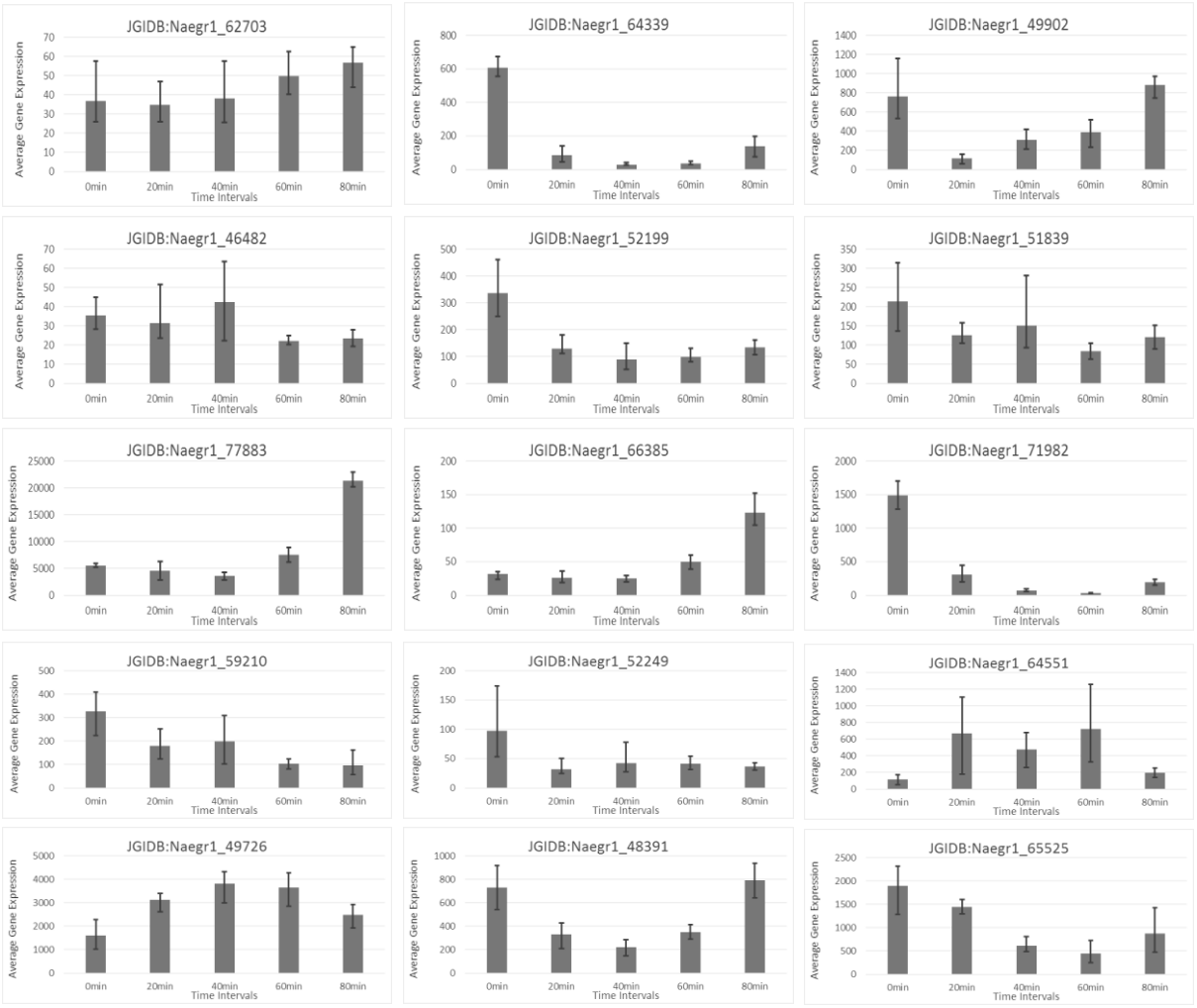

Figure 50: Expression of proteins homologous to the upregulated constitutive protein XP_002680867.1.

This collection of graphs shows the expression of proteins returned from a protein blast using the sequence of the protein XP_002680867.1 obtained from the NCBI website. The expression graphs are ordered by e-value with the most homologous sequences first.

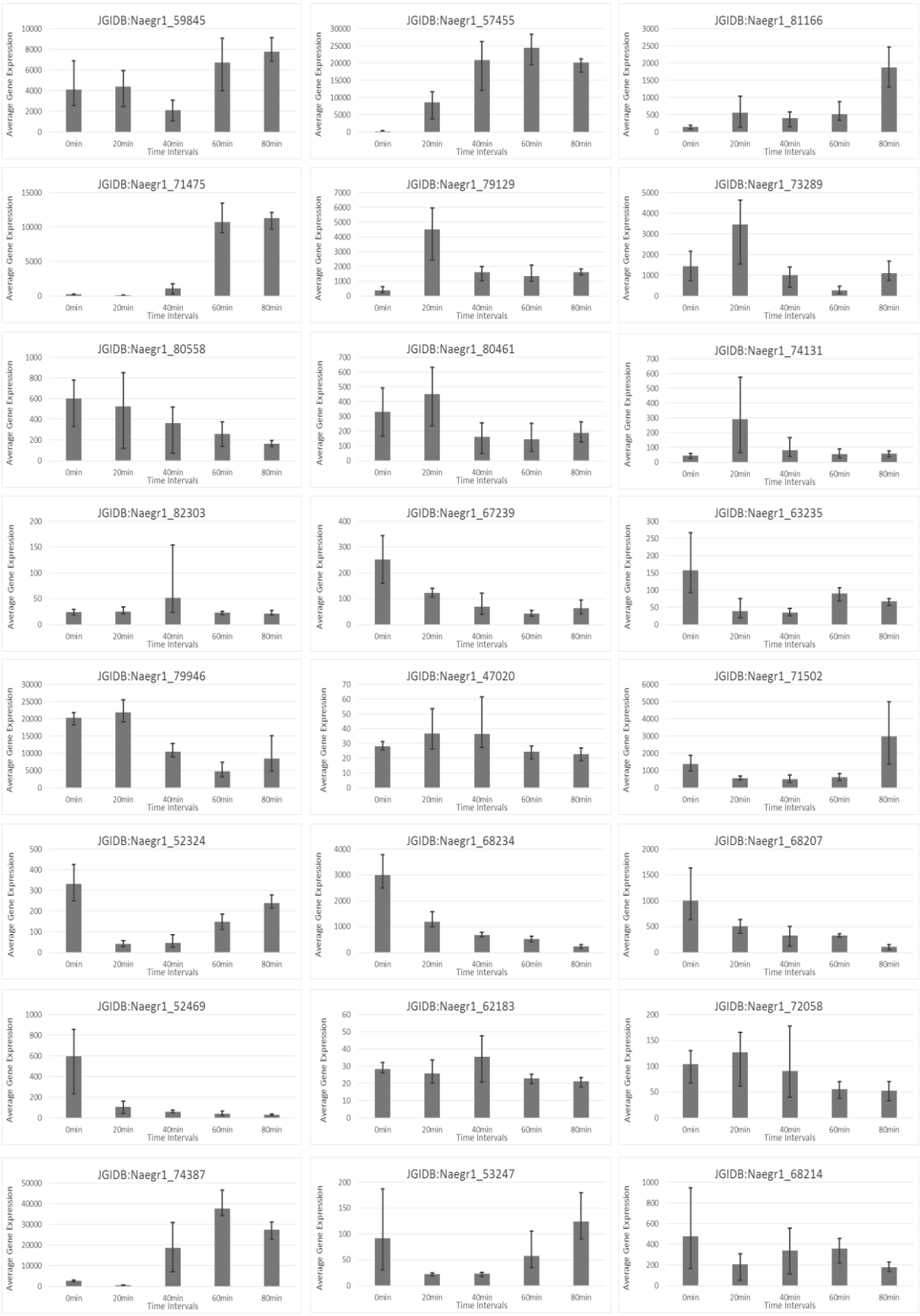
JGIDB:Naegr1_59845
JGIDB:Naegr1_57455
JGIDB:Naegr1_81166
JGIDB:Naegr1_71475
JGIDB:Naegr1_79129
JGIDB:Naegr1_73289
JGIDB:Naegr1_80558
JGIDB:Naegr1_80461
JGIDB:Naegr1_74131
JGIDB:Naegr1_82303
JGIDB:Naegr1_67239
JGIDB:Naegr1_63235
JGIDB:Naegr1_79946
JGIDB:Naegr1_47020
JGIDB:Naegr1_71502
JGIDB:Naegr1_52324
JGIDB:Naegr1_68234
JGIDB:Naegr1_68207
JGIDB:Naegr1_52469
JGIDB:Naegr1_62183
JGIDB:Naegr1_72058
JGIDB:Naegr1_74387
JGIDB:Naegr1_53247
JGIDB:Naegr1_68214
Average Gene Expression
Time Intervals
0min
20min
40min
60min
80min

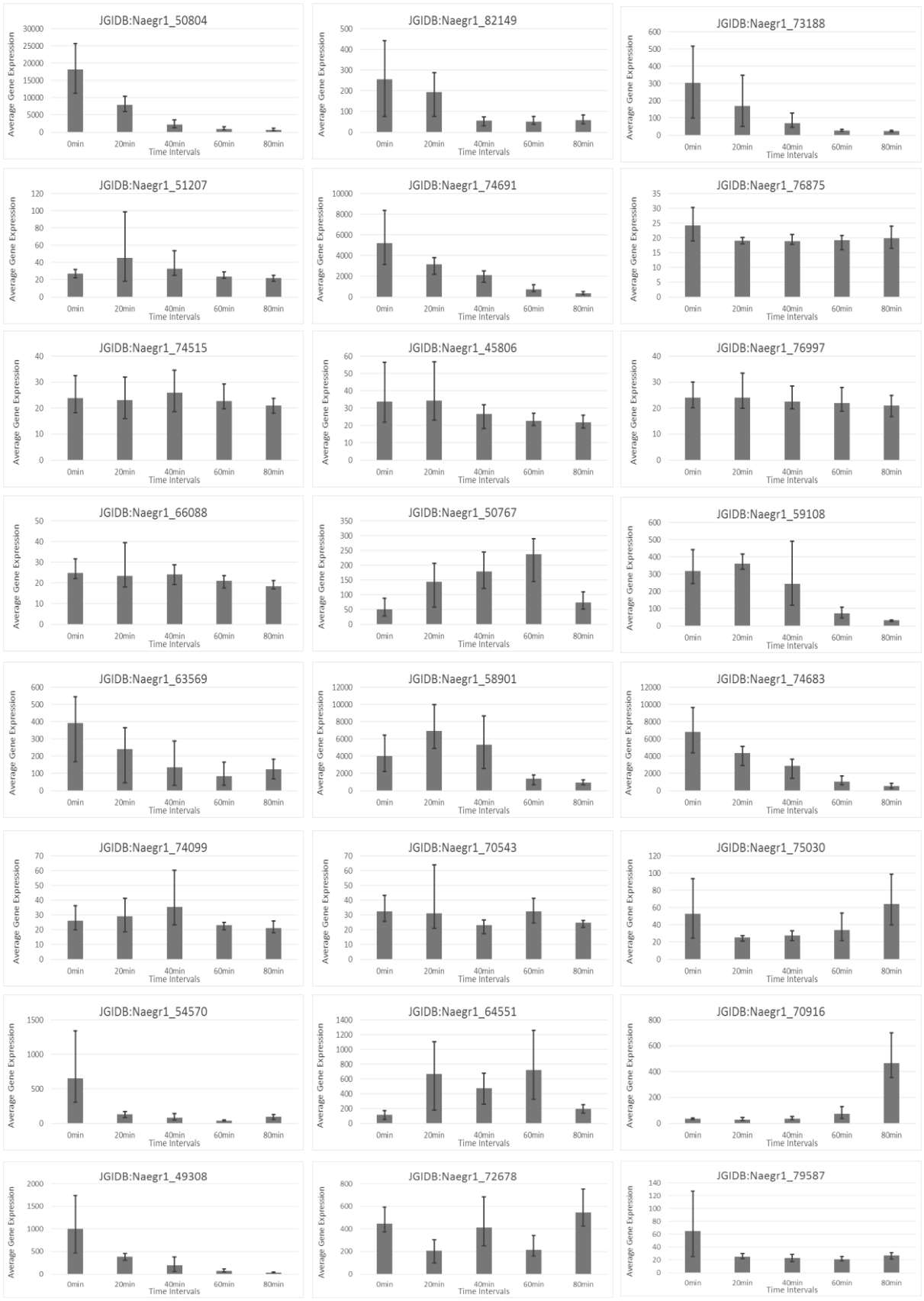
JGIDB:Naegr1_50804
JGIDB:Naegr1_82149
JGIDB:Naegr1_73188
JGIDB:Naegr1_51207
JGIDB:Naegr1_74691
JGIDB:Naegr1_76875
JGIDB:Naegr1_74515
JGIDB:Naegr1_45806
JGIDB:Naegr1_76997
JGIDB:Naegr1_66088
JGIDB:Naegr1_50767
JGIDB:Naegr1_59108
JGIDB:Naegr1_63569
JGIDB:Naegr1_58901
JGIDB:Naegr1_74683
JGIDB:Naegr1_74099
JGIDB:Naegr1_70543
JGIDB:Naegr1_75030
JGIDB:Naegr1_54570
JGIDB:Naegr1_64551
JGIDB:Naegr1_70916
JGIDB:Naegr1_49308
JGIDB:Naegr1_72678
JGIDB:Naegr1_79587
Average Gene Expression
Time Intervals
0min
20min
40min
60min
80min

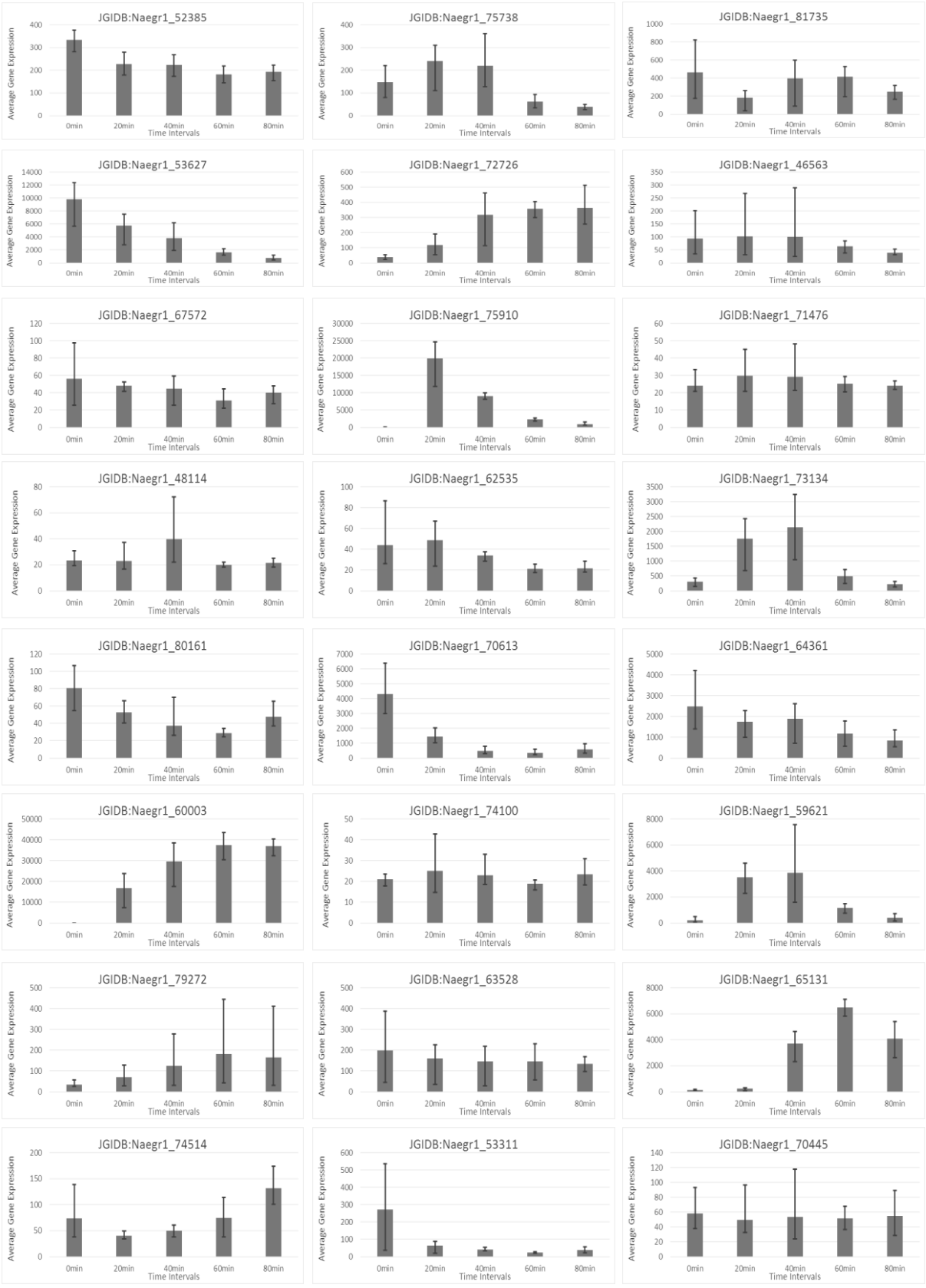
JGIDB:Naegr1_52385
JGIDB:Naegr1_75738
JGIDB:Naegr1_81735
JGIDB:Naegr1_53627
JGIDB:Naegr1_72726
JGIDB:Naegr1_46563
JGIDB:Naegr1_67572
JGIDB:Naegr1_75910
JGIDB:Naegr1_71476
JGIDB:Naegr1_48114
JGIDB:Naegr1_62535
JGIDB:Naegr1_73134
JGIDB:Naegr1_80161
JGIDB:Naegr1_70613
JGIDB:Naegr1_64361
JGIDB:Naegr1_60003
JGIDB:Naegr1_74100
JGIDB:Naegr1_59621
JGIDB:Naegr1_79272
JGIDB:Naegr1_63528
JGIDB:Naegr1_65131
JGIDB:Naegr1_74514
JGIDB:Naegr1_53311
JGIDB:Naegr1_70445
Average Gene Expression
Time Intervals
0min
20min
40min
60min
80min

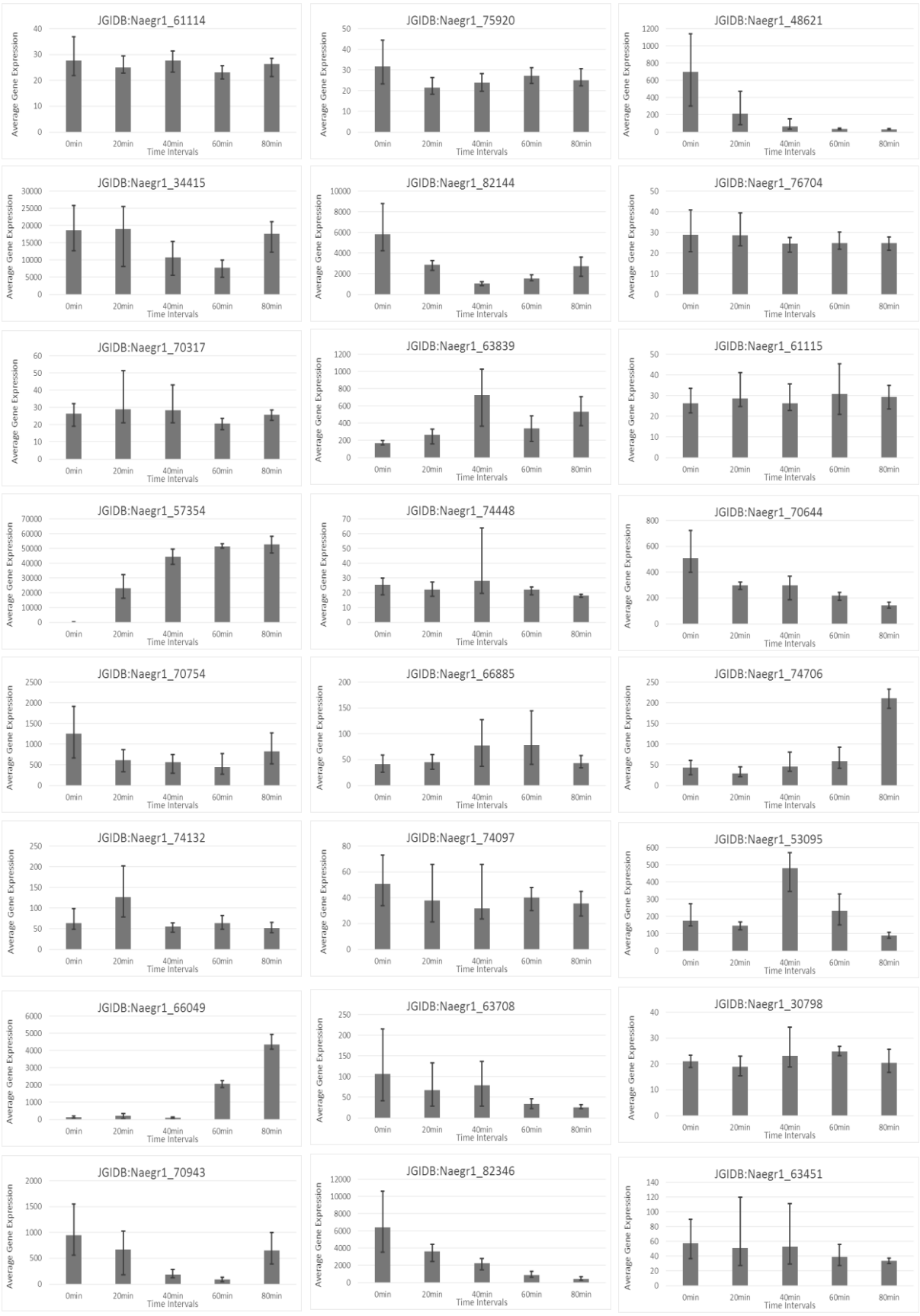
JGIDB:Naegr1_61114
JGIDB:Naegr1_75920
JGIDB:Naegr1_48621
JGIDB:Naegr1_34415
JGIDB:Naegr1_82144
JGIDB:Naegr1_76704
JGIDB:Naegr1_70317
JGIDB:Naegr1_63839
JGIDB:Naegr1_61115
JGIDB:Naegr1_57354
JGIDB:Naegr1_74448
JGIDB:Naegr1_70644
JGIDB:Naegr1_70754
JGIDB:Naegr1_66885
JGIDB:Naegr1_74706
JGIDB:Naegr1_74132
JGIDB:Naegr1_74097
JGIDB:Naegr1_53095
JGIDB:Naegr1_66049
JGIDB:Naegr1_63708
JGIDB:Naegr1_30798
JGIDB:Naegr1_70943
JGIDB:Naegr1_82346
JGIDB:Naegr1_63451
Average Gene Expression
Time Intervals
0min
20min
40min
60min
80min

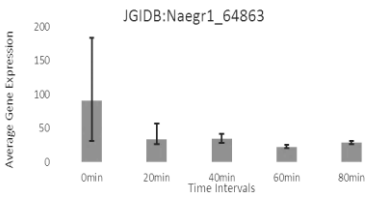

Figure 51: Expression of proteins homologous to upregulated constitutive protein XP_002669791.1.

This collection of graphs shows the expression of proteins returned from a protein blast using the sequence of the protein XP_002669791.1 obtained from the NCBI website. The expression graphs are ordered by e-value with the most homologous sequences first.

X. Differentiation Graphs

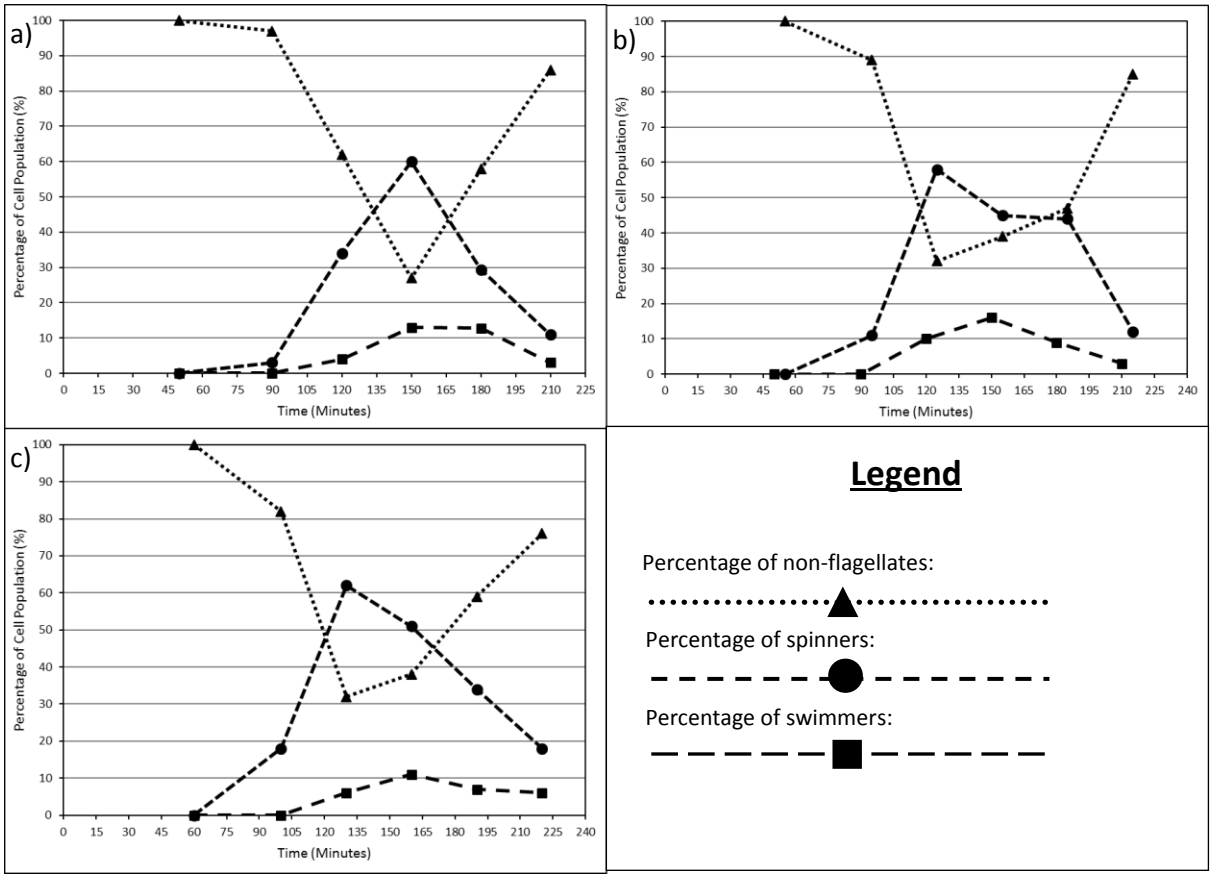

Figure 54: 'amoebasaline-chunk-and-wash' differentiation graphs.

A collection of several graphs, plotting data from the 'amoebasaline-chunk-and-wash' experiment. a) The differentiation results of excised agar washed in 10ml amoeba saline solution. b) The differentiation results of excised agar washed in 1ml amoeba saline solution. c) The differentiation results of cells washed from plate with amoeba saline solution. Nested in the bottom corner is a legend that shows which graph data relates to non-flagellates, spinners and swimmers, this formatting is repeated for all of the differentiation graphs.

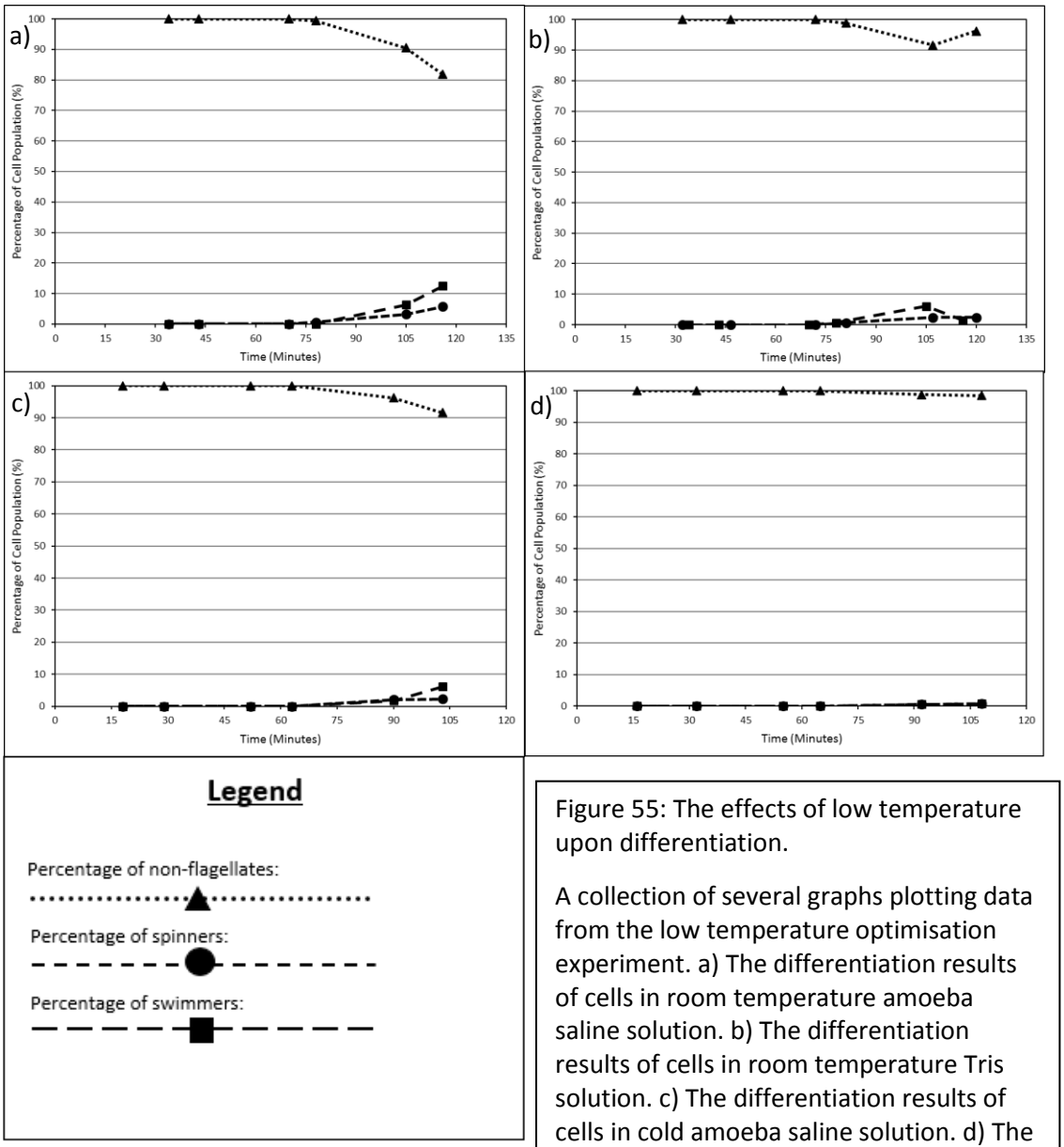

Figure 55: The effects of low temperature upon differentiation.

A collection of several graphs plotting data from the low temperature optimisation experiment. a) The differentiation results of cells in room temperature amoeba saline solution. b) The differentiation results of cells in room temperature Tris solution. c) The differentiation results of cells in cold amoeba saline solution. d) The differentiation results of cells in cold Tris solution. The plot formatting mirrors the formatting in figure 40.

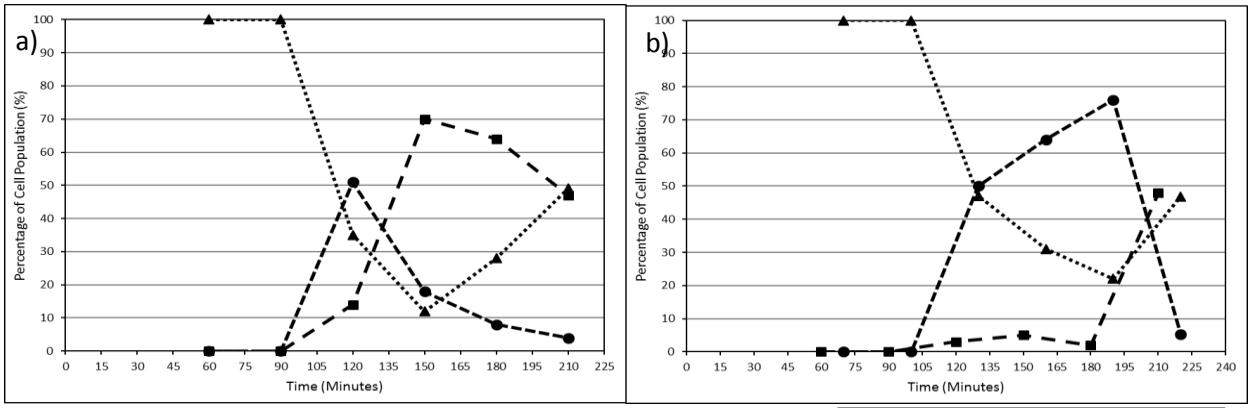

Figure 56: Improving *Klebsiella* nutrient source removal.

Two graphs plotting data from the *Klebsiella* nutrient source removal experiment. a) The differentiation results of cells in the centrifuge removal method. b) The differentiation results of cells in previous wash method. The formatting mirrors the formatting in figure 40.

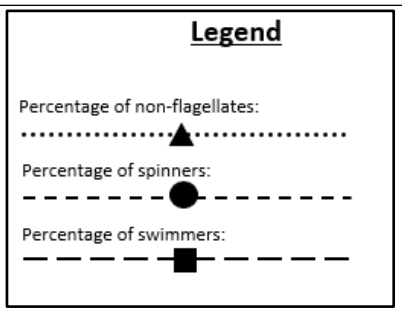

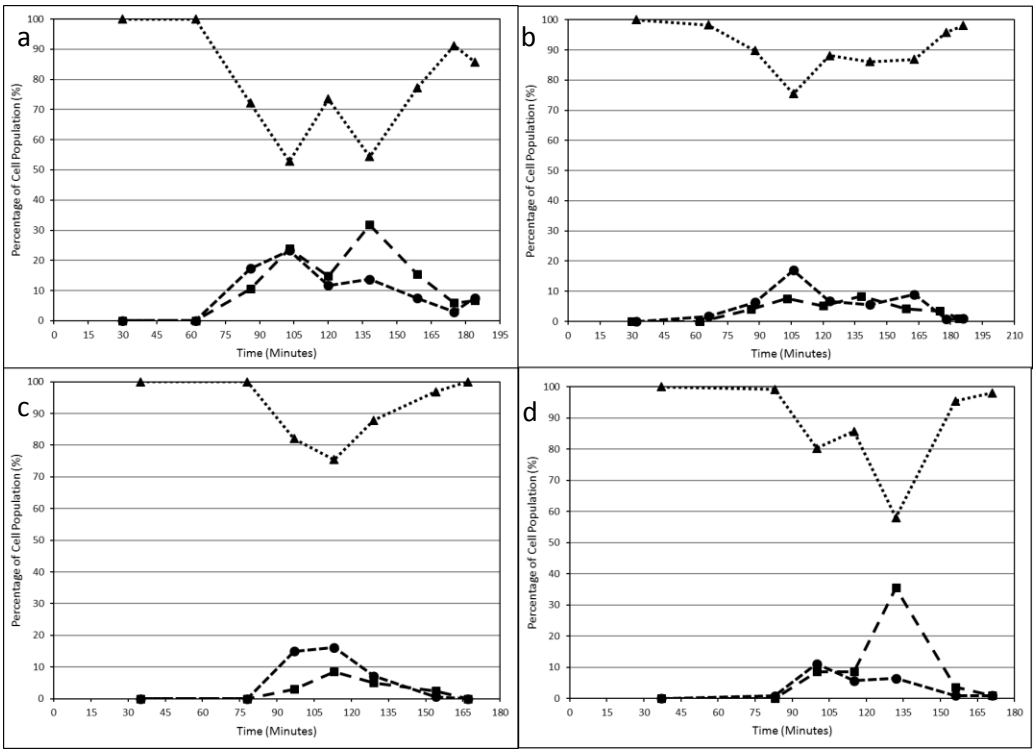

Figure 57: The effect of agitation upon differentiation.

A collection of several graphs plotting data from the agitation optimisation experiment. a) The differentiation results of cells in non-shaken amoeba saline solution. b) The differentiation results of cells in non-shaken Tris solution. c) The differentiation results of cells in shaken amoeba saline solution. d) The differentiation results of cells in shaken Tris solution. The plot formatting mirrors the formatting in figure 40.

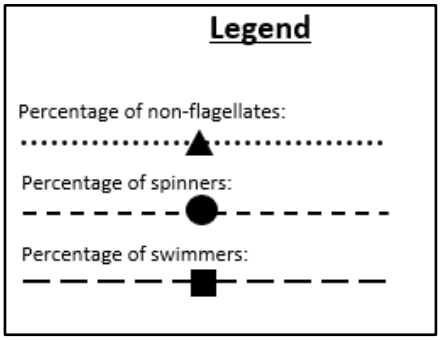

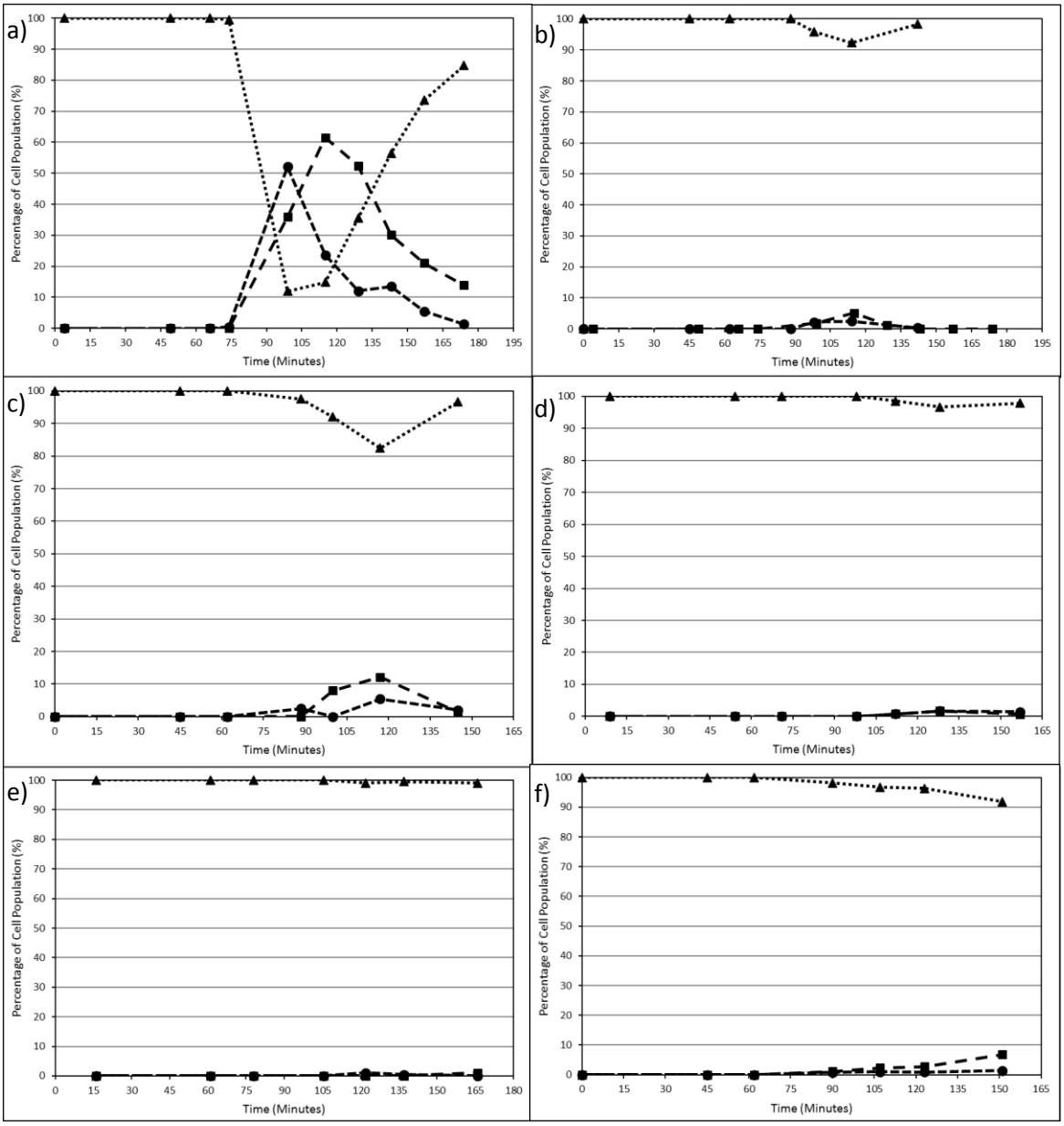

Figure 58: Final optimisation of methods.

A collection of graphs plotting data from the final optimisation experiment which repeated the buffer, centrifugation and temperature tests for a final time. a) The results of cells in centrifuged amoeba saline solution. b) The results of cells in centrifuged Tris solution. c) The results of cells in centrifuged Tris solution. d) The results of cells in centrifuged cold Tris solution. e) The results of cells in cold Tris solution after multiple centrifuge spins to clear nutrient. f) The results of cells in Tris solution after multiple centrifuge spins to clear nutrient. The plot formatting mirrors the formatting in figure 40.

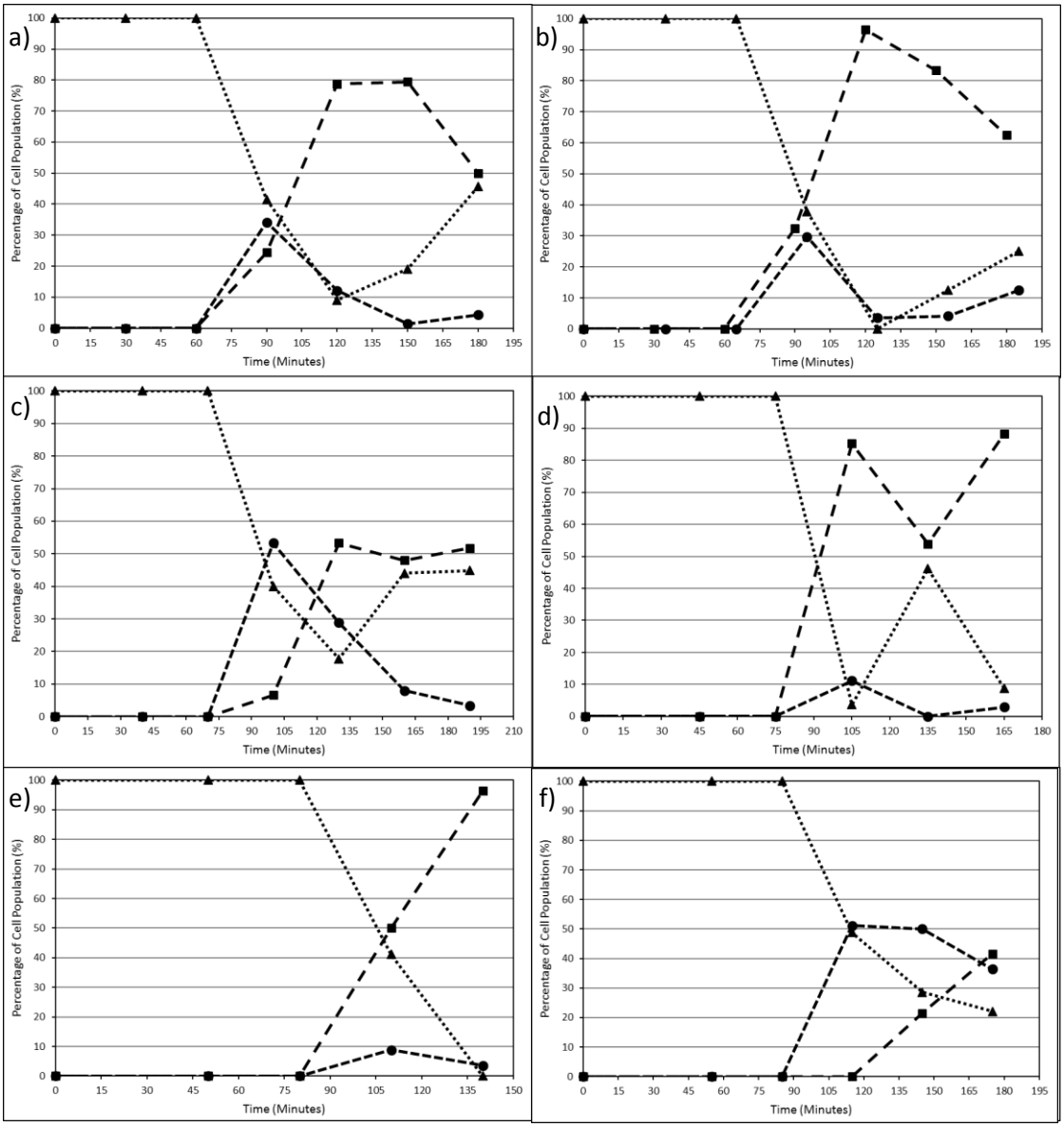

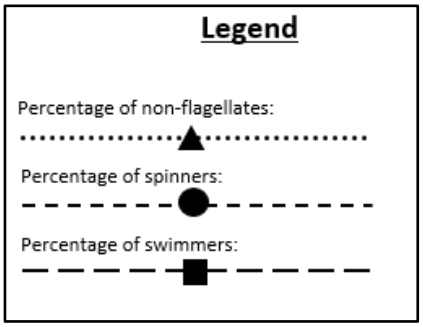

Figure 59: The effects of sodium azide (NaN3) upon differentiation in aerobic and anaerobic environments.

A collection of graphs plotting differentiation data from the first sodium azide experiment. a) The results of a control sample. b) The results of cells mixed with 1 µM azide. c) The results of cells mixed with 10 µM azide. d) The results of cells in anaerobic conditions. e) The results of cells in anaerobic conditions mixed with 1 µM azide. f) The results of cells in anaerobic conditions mixed with 10 µM azide. The plot formatting mirrors the formatting in figure 40.

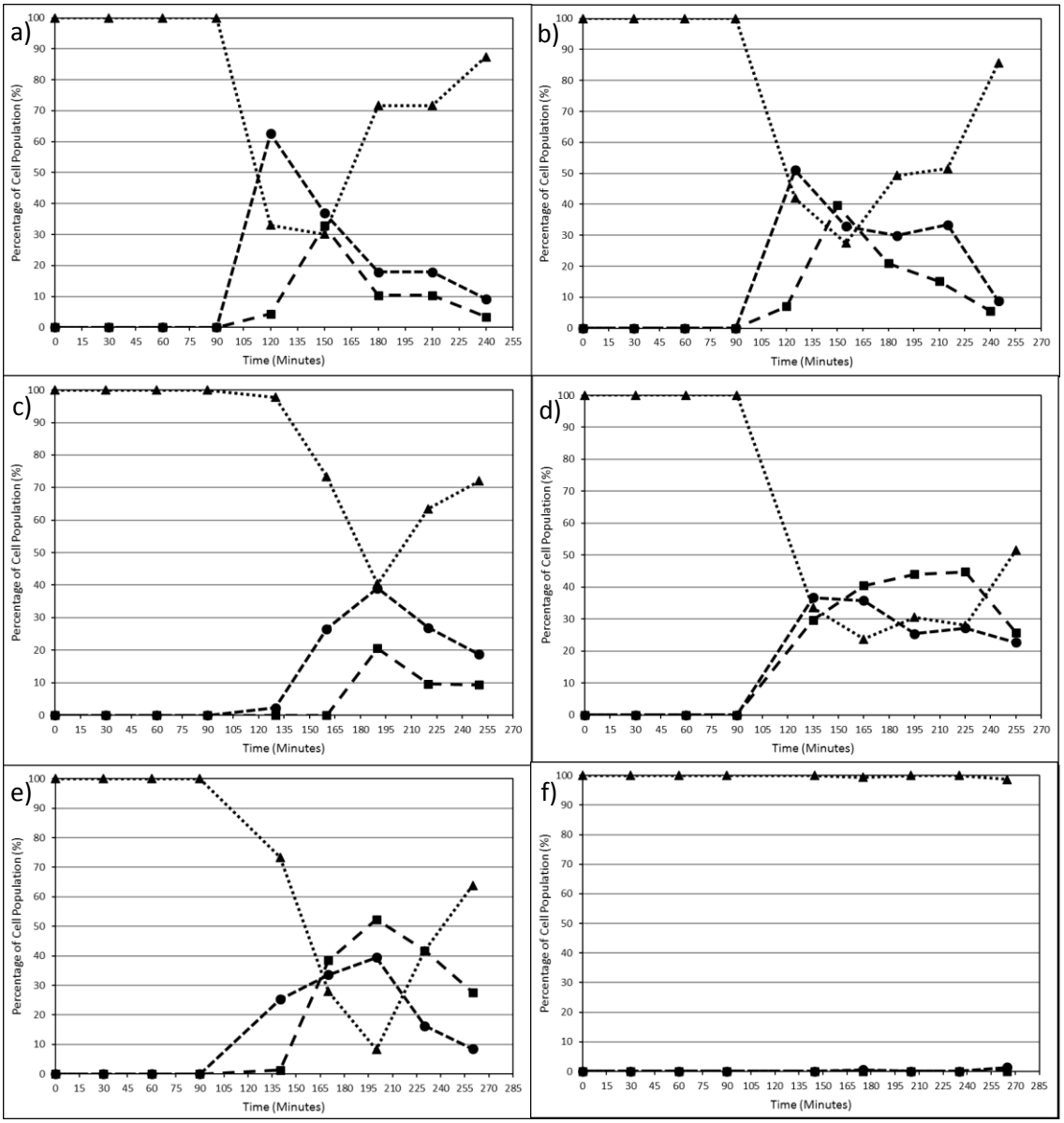

Figure 60: Repeat of sodium azide differentiation in aerobic and anaerobic environments.

A collection of graphs plotting differentiation data from the repeat sodium azide experiment. a) The results of a control sample. b) The results of cells mixed with 1 µM azide. c) The results of cells mixed with 10 µM azide. d) The results of cells in anaerobic conditions. e) The results of cells in anaerobic conditions mixed with 1 µM azide. f) The results of cells in anaerobic conditions mixed with 10 µM azide. The plot formatting mirrors the formatting in figure 40.

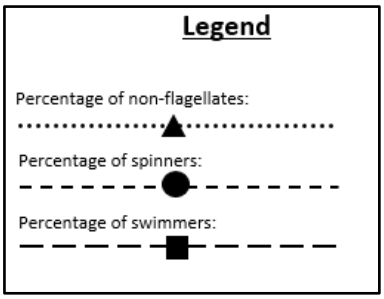

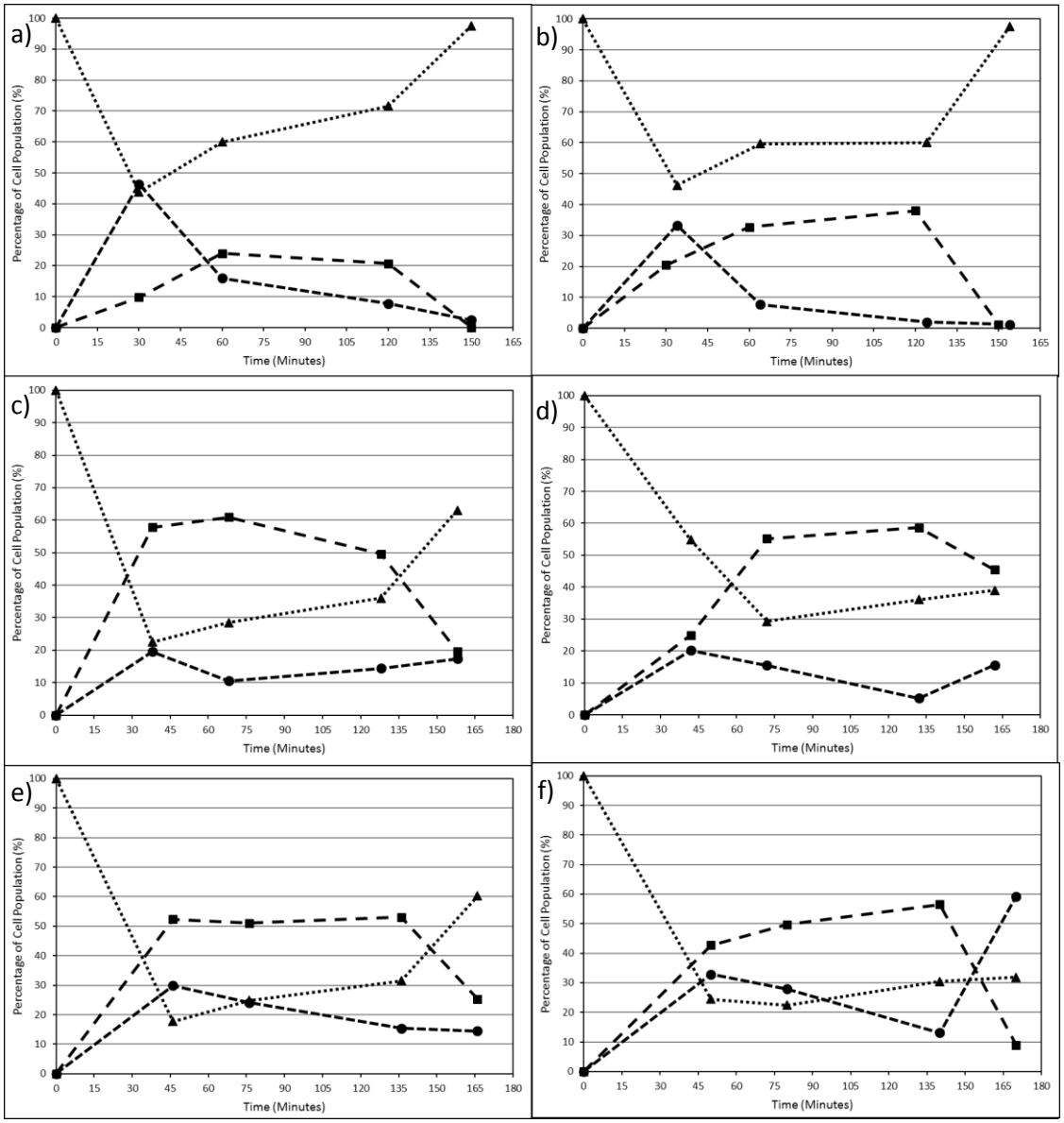

Figure 61: A comparison of the effects of foetal bovine serum (FBS) upon differentiation in anaerobic and microaerophilic CO_2 rich environments.

A collection of graphs plotting differentiation data from the first FBS experiment. a) The results of cells mixed with 0.2% FBS. b) The results of cells mixed with 1% FBS. c) The results of cells in anaerobic conditions mixed with 0.2% FBS. d) The results of cells in anaerobic conditions mixed with 0.2% FBS. e) The results of cells in microaerophilic, CO_2 rich conditions mixed with 0.2% FBS. f) The results of cells in microaerophilic CO_2 rich conditions mixed with 1% FBS. The plot formatting mirrors the formatting in figure 40.

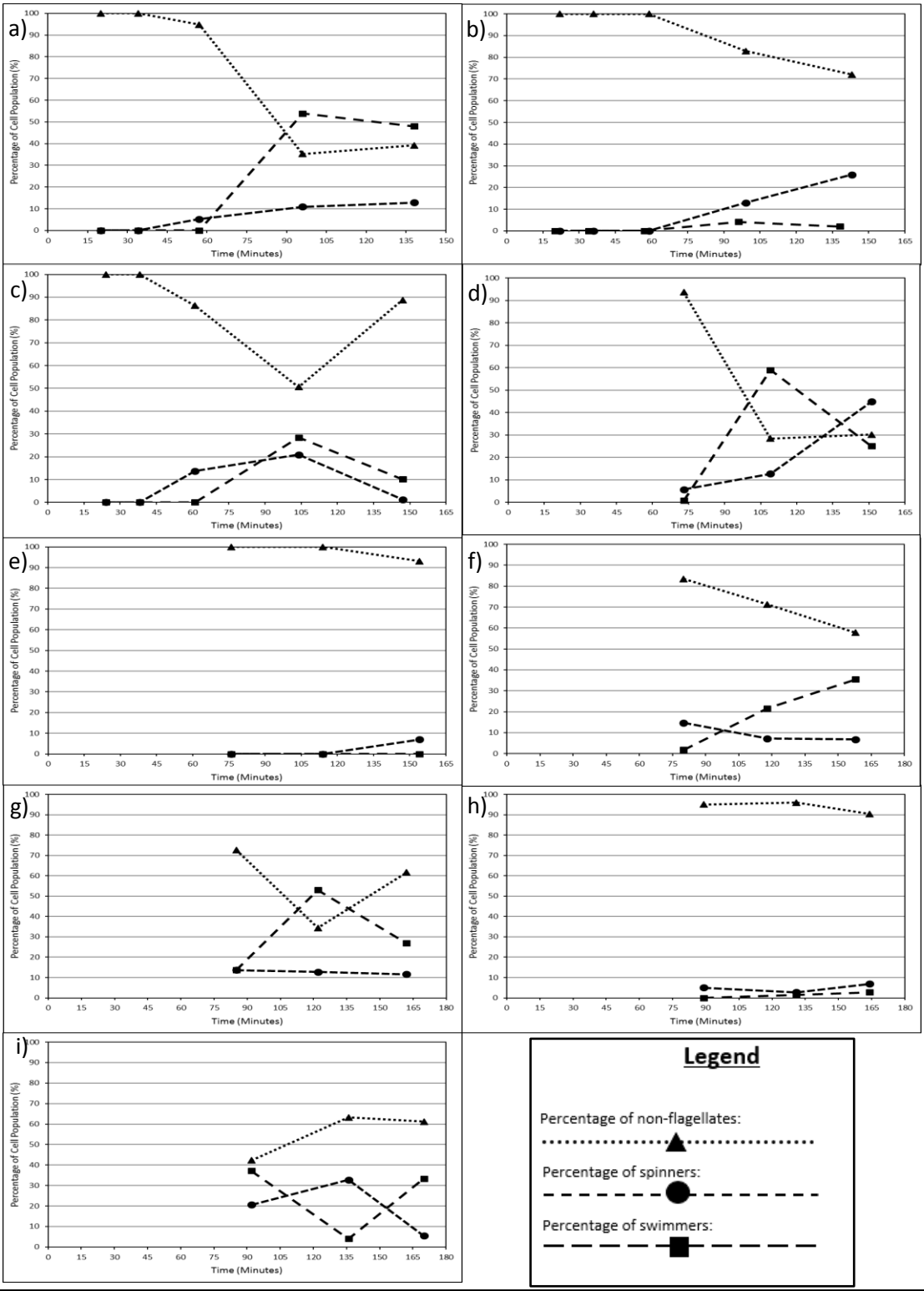

Figure 62: Repeat of FBS experiments in anaerobic and microaerophilic CO_2 rich environments.

A collection of graphs plotting differentiation data from the first FBS experiment. a) The results of a control sample. b) The results of cells mixed with 0.2% FBS. c) The results of cells mixed with 1% FBS. d) The results of control cells in anaerobic conditions. e) The results of cells in anaerobic conditions mixed with 0.2% FBS. f) The results of cells in anaerobic conditions mixed with 1% FBS. g) The results of control cells in microaerophilic, CO_2 rich conditions. h) The results of cells in microaerophilic CO_2 rich conditions mixed with 0.2% FBS. i) The results of cells in microaerophilic CO_2 rich conditions mixed with 1% FBS. The plot formatting mirrors the formatting in figure 40.

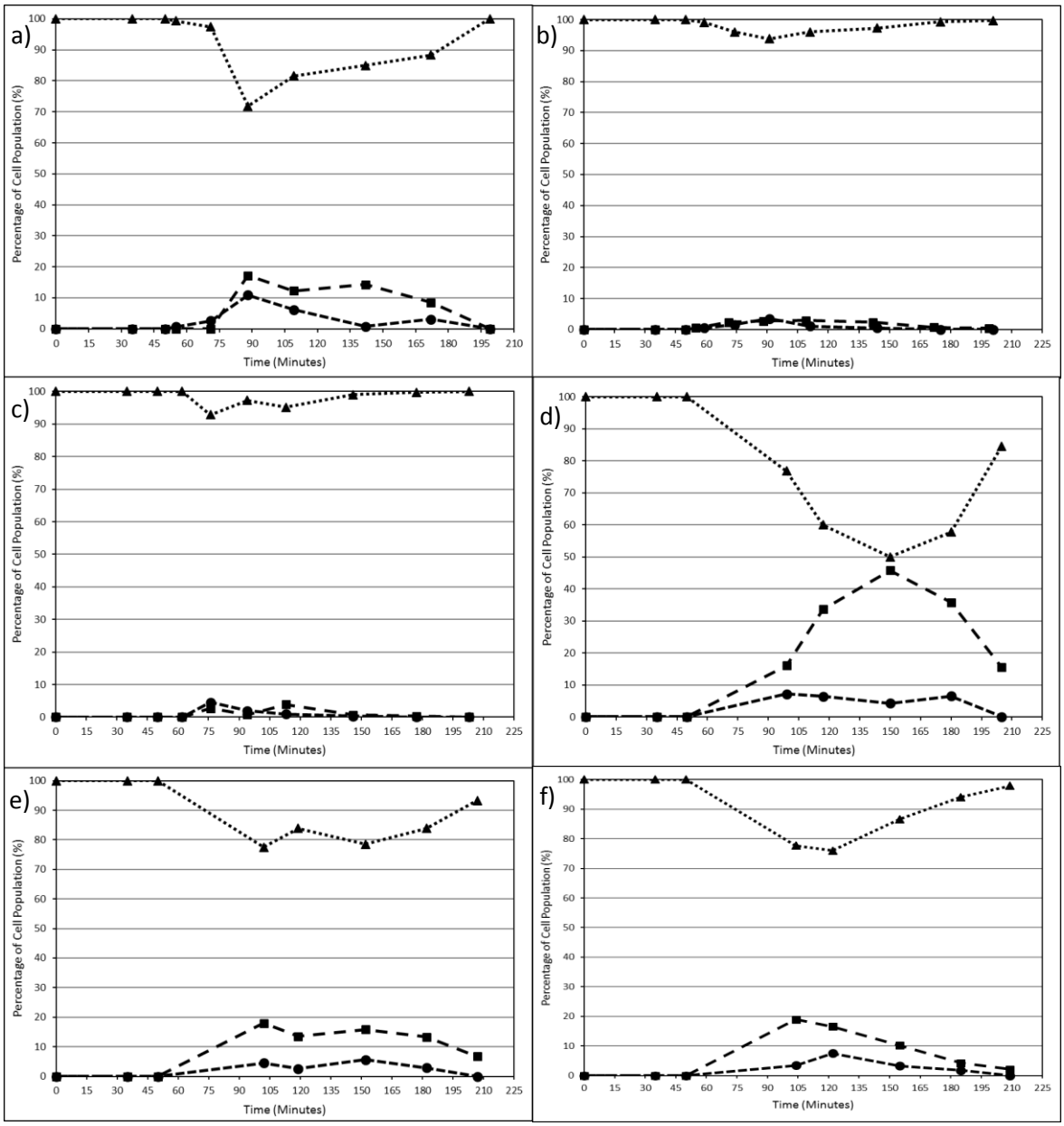

Figure 63: The effect of FBS addition to differentiation in anaerobic environments.

A collection of graphs plotting differentiation data from the first FBS experiment. a) The results of a control sample. b) The results of cells mixed with 1% FBS. c) The results of cells mixed with 0.2% FBS. d) The results of control cells in anaerobic conditions. e) The results of cells in anaerobic conditions mixed with 1% FBS. f) The results of cells in anaerobic conditions mixed with 0.2% FBS. The plot formatting mirrors the formatting in figure 40.

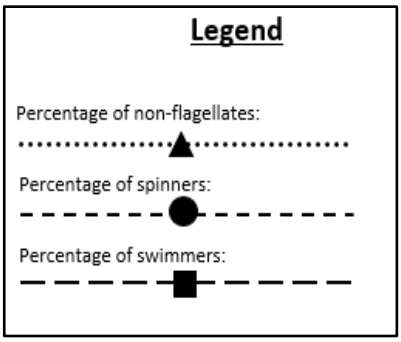

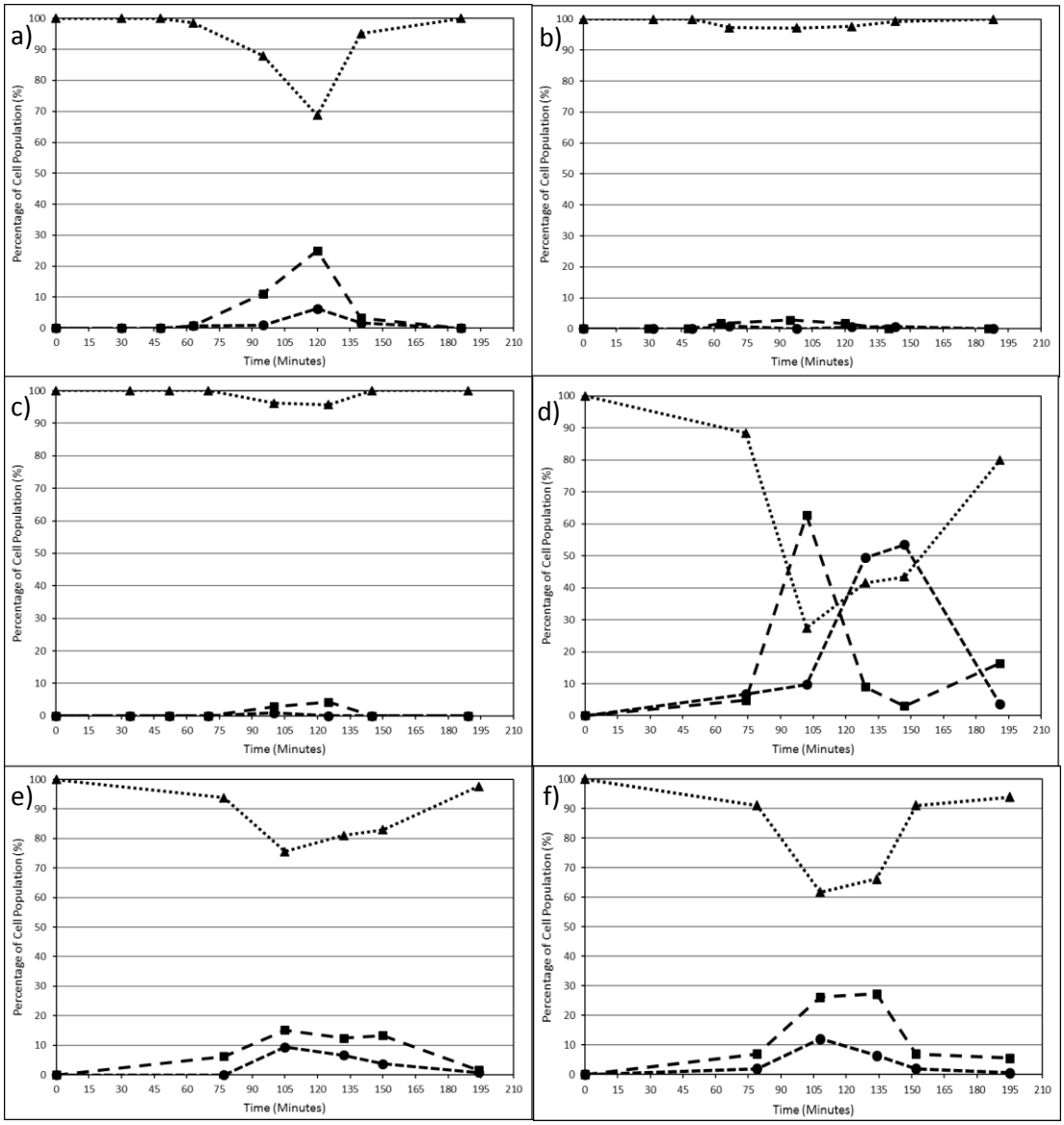

Figure 64: A repeat of effects of FBS addition in anaerobic environments.

A collection of graphs plotting differentiation data from the first FBS experiment. a) The results of a control sample. b) The results of cells mixed with 1% FBS. c) The results of cells mixed with 0.2% FBS. d) The results of control cells in anaerobic conditions. e) The results of cells in anaerobic conditions mixed with 1% FBS. f) The results of cells in anaerobic conditions mixed with 0.2% FBS. The plot formatting mirrors the formatting in figure 40.

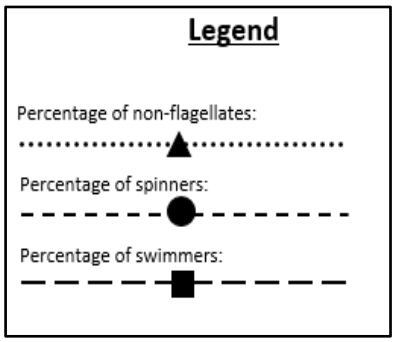

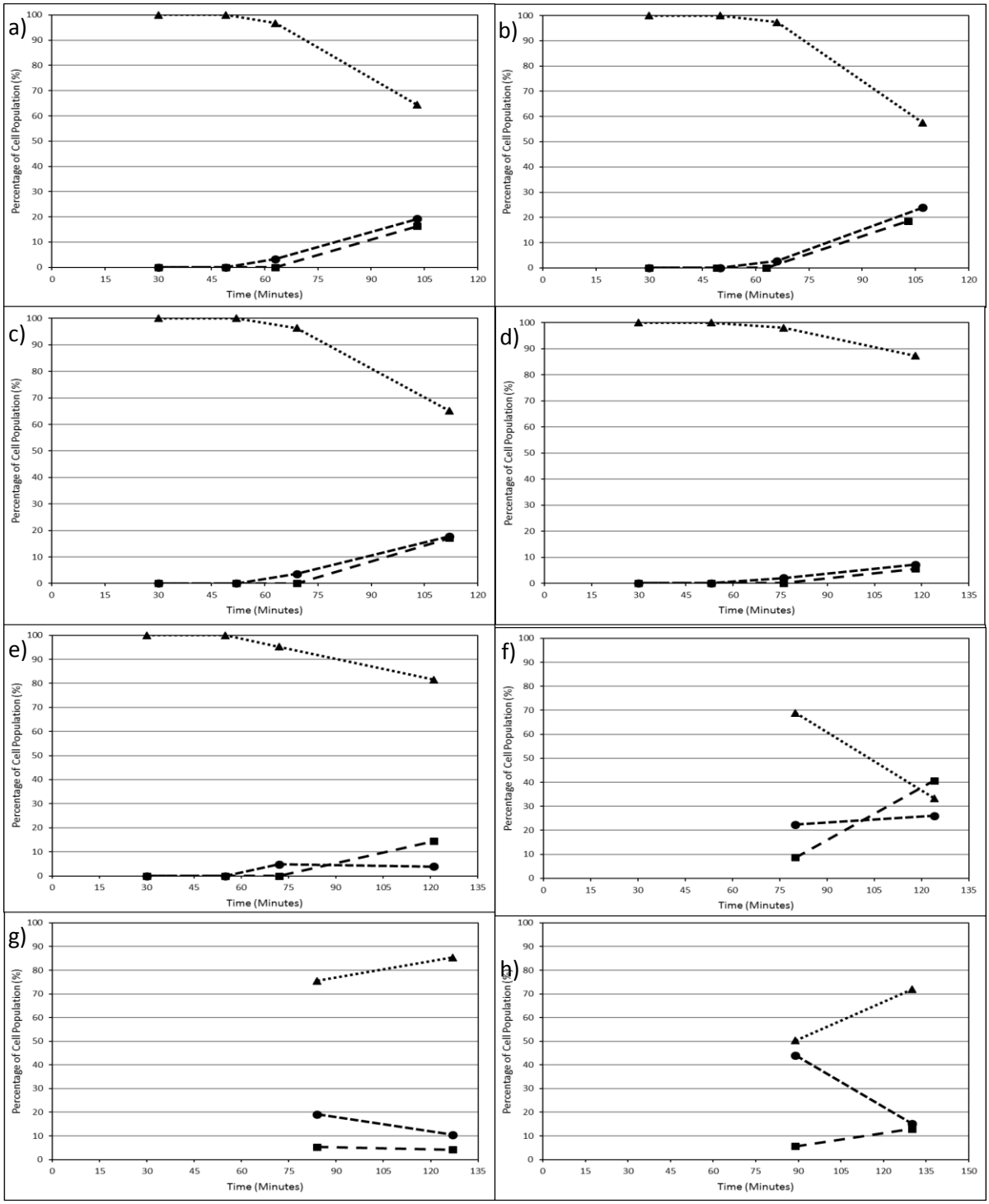

Figure 65: The effect of addition of FBS upon differentiation in microaerophilic CO_2 rich and glucose rich environments.

A collection of graphs plotting differentiation data from the first FBS experiment. a) The results of a control sample. b) The results of cells mixed with 0.2% glucose. c) The results of cells mixed with 1% glucose. d) The results of cells mixed with 1% FBS. e) The results of cells mixed with 0.2% FBS. f) The results of control cells in microaerophilic, CO_2 rich conditions. g) The results of cells in microaerophilic CO_2 rich conditions mixed with 1% FBS. h) The results of cells in microaerophilic CO_2 rich conditions mixed with 1% FBS. The plot formatting mirrors the formatting in figure 40.

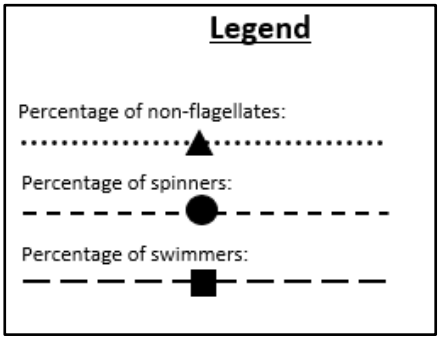

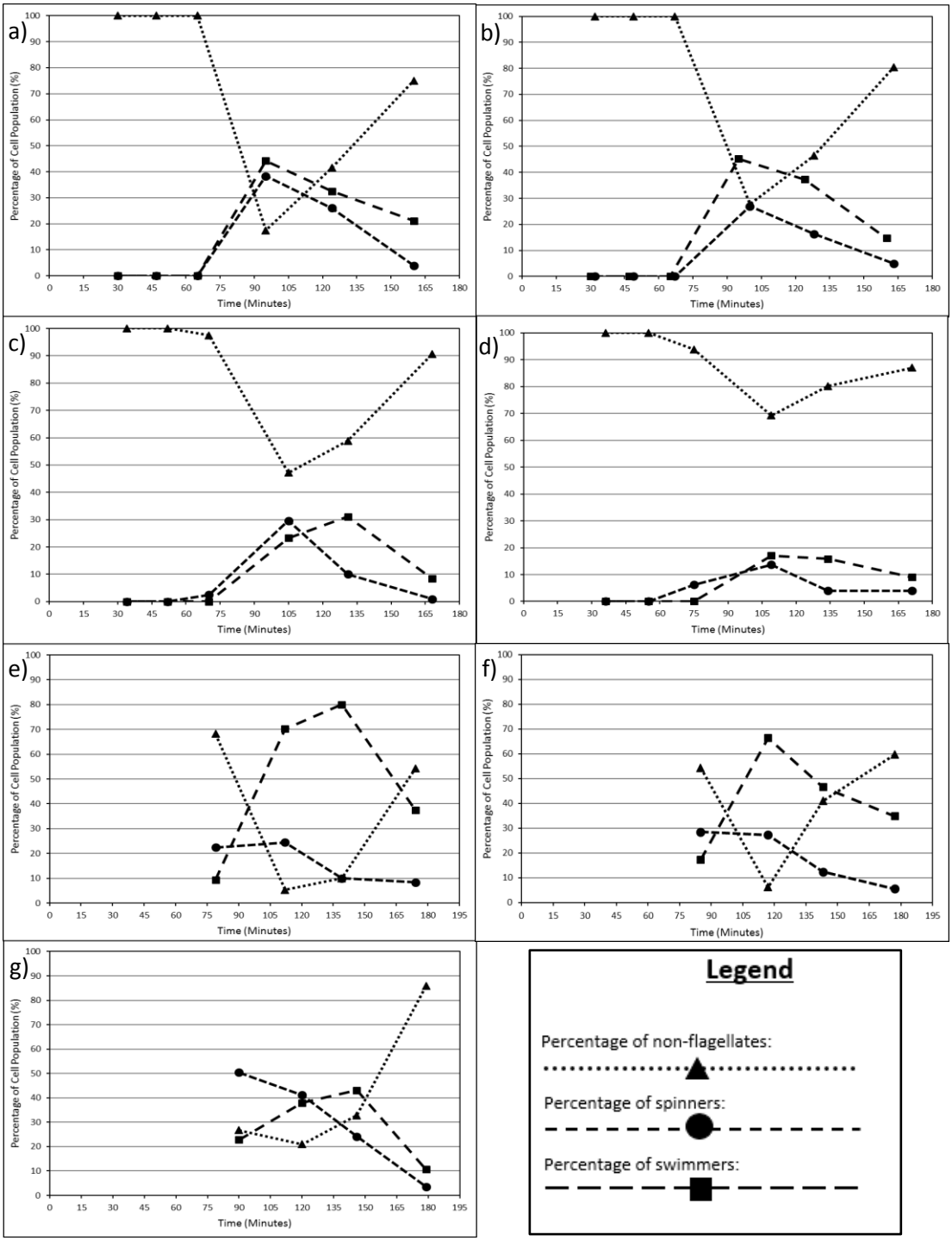

Figure 66: A repeat of the effect of FBS addition to microaerophilic CO_2 rich and glucose rich environments.

A collection of graphs plotting differentiation data from the first FBS experiment. a) The results of a control sample. b) The results of cells mixed with 1% glucose. c) The results of cells mixed with 1% FBS. d) The results of cells mixed with 0.2% FBS. e) The results of control cells in microaerophilic, CO_2 rich conditions. f) The results of cells in microaerophilic CO_2 rich conditions mixed with 1% FBS. g) The results of cells in microaerophilic CO_2 rich conditions mixed with 1% FBS. The plot formatting mirrors the formatting in figure 40.

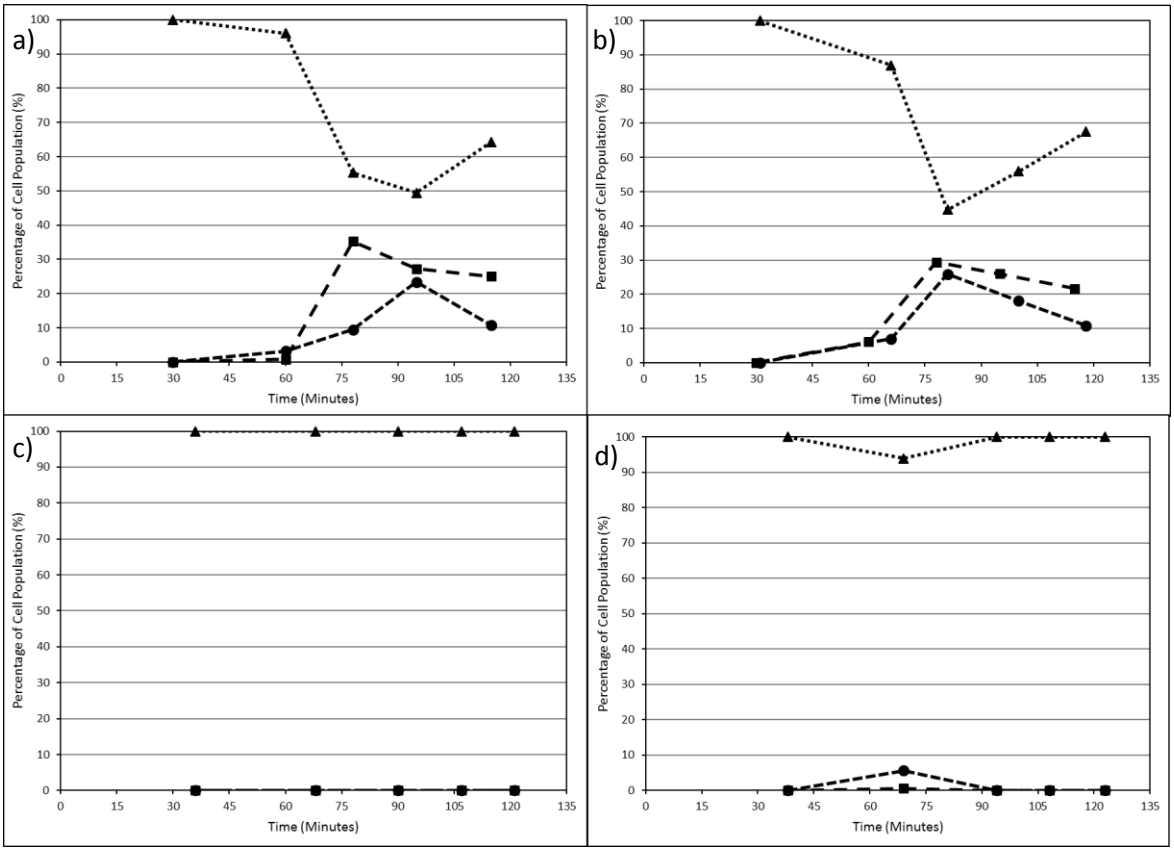

Figure 67: The effect of addition of Polyoxyethylene sorbitan monolaurate (TWEEN20) upon differentiation in comparison to glucose rich environments.

A collection of graphs plotting differentiation data from the first FBS experiment. a) The results of a control sample. b) The results of cells mixed with 1% glucose. c) The results of cells mixed with 1% TWEEN20. d) The results of cells mixed with 0.2% TWEEN20. The plot formatting mirrors the formatting in figure 40.

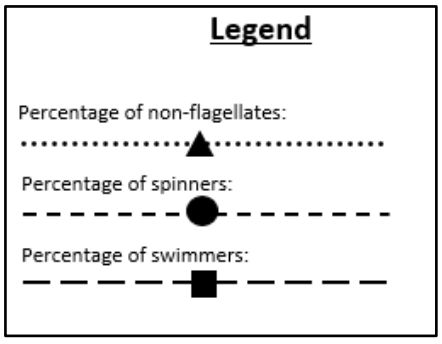

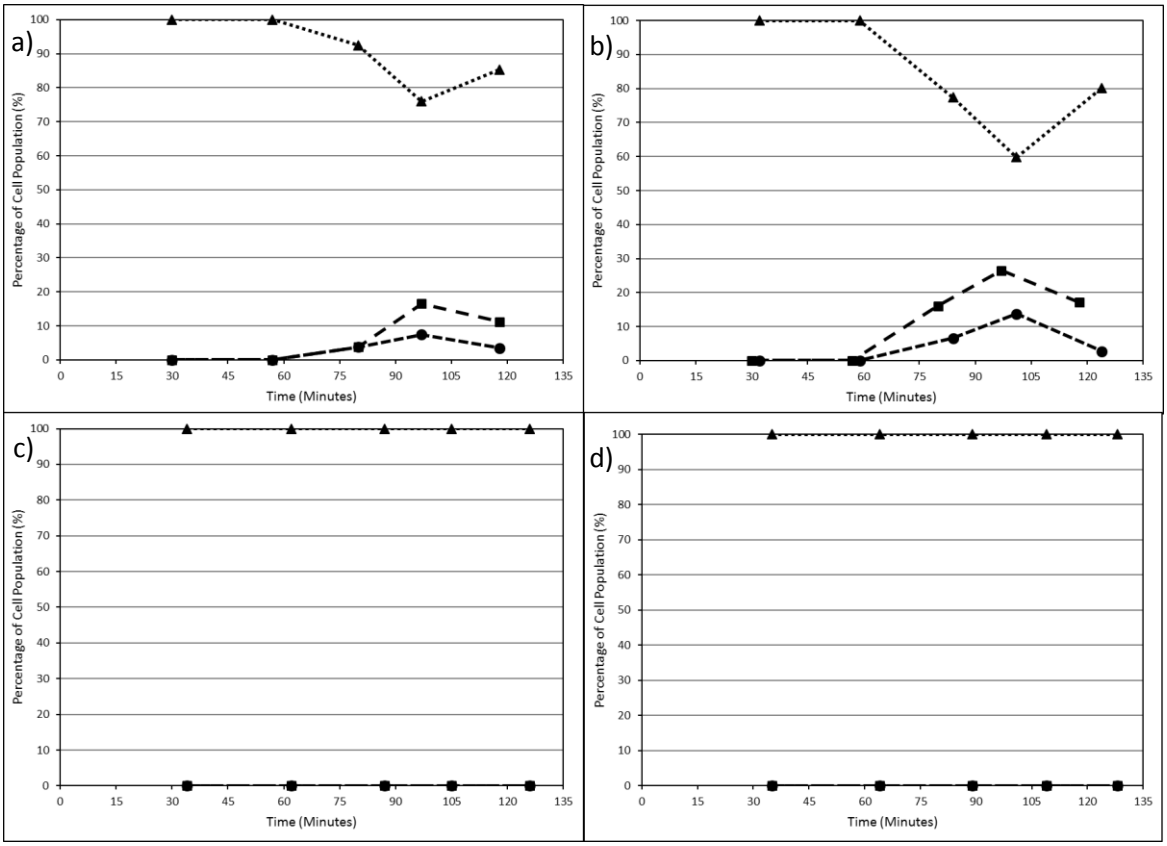

Figure 68: A repeat experiment on the effect of addition of TWEEN20 upon differentiation in comparison to glucose rich environments.

A collection of graphs plotting differentiation data from the first FBS experiment. a) The results of a control sample. b) The results of cells mixed with 1% glucose. c) The results of cells mixed with 1% TWEEN20. d) The results of cells mixed with 0.2% TWEEN20. The plot formatting mirrors the formatting in figure 40.

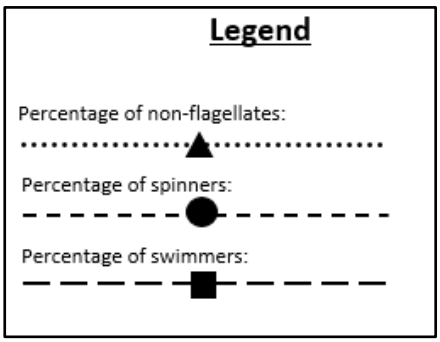

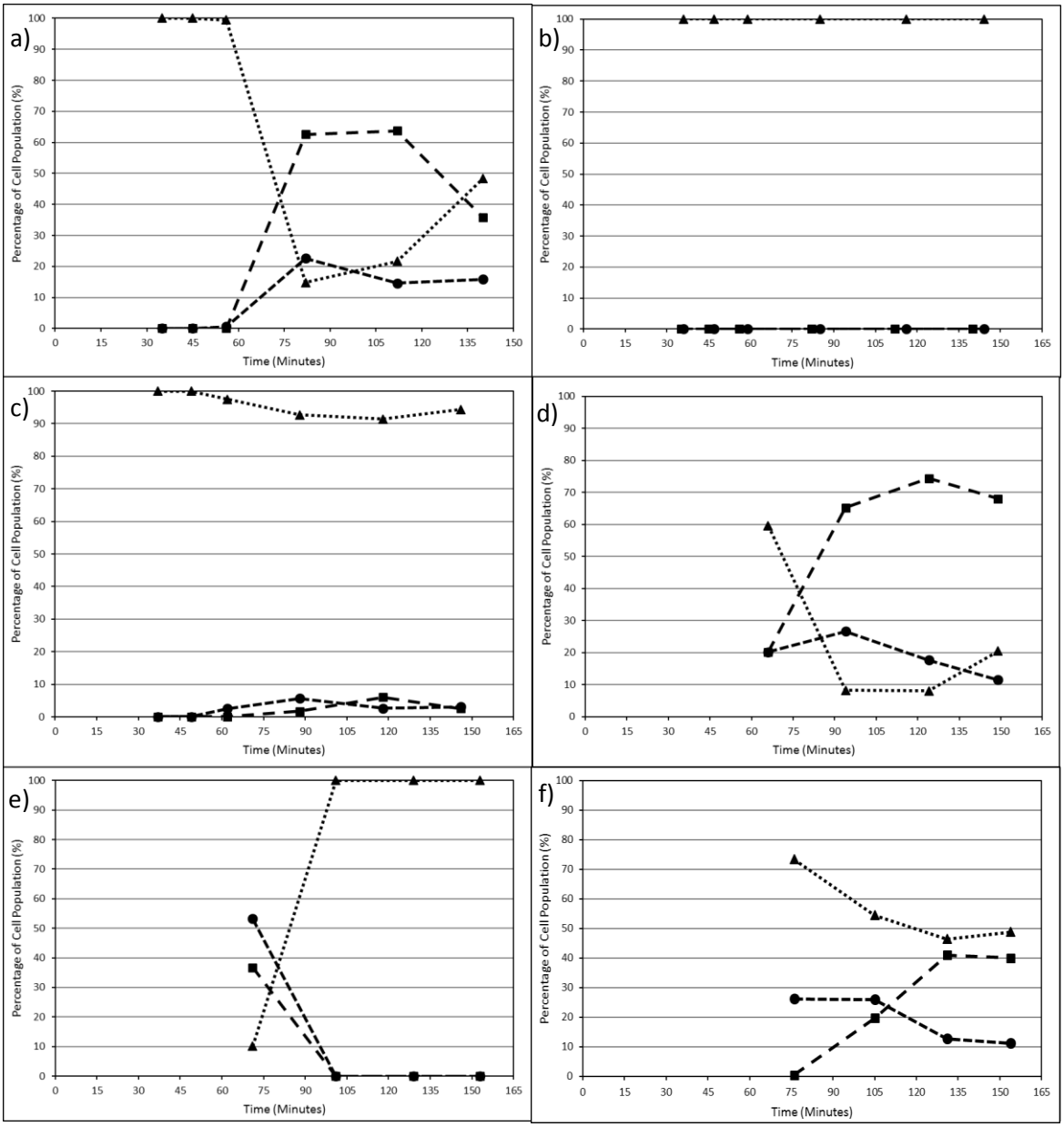

Figure 69: The effect of TWEEN20 upon differentiation in microaerophilic CO_2 rich environments.

A collection of graphs plotting differentiation data from the first FBS experiment. a) The results of a control sample. b) The results of cells mixed with 1% TWEEN20. c) The results of cells mixed with 0.2% TWEEN20. d) The results of control cells in microaerophilic, CO_2 rich conditions. e) The results of cells in microaerophilic CO_2 rich conditions mixed with 1% TWEEN20. f) The results of cells in microaerophilic CO_2 rich conditions mixed with 0.2% TWEEN20. The plot formatting mirrors the formatting in figure 40.

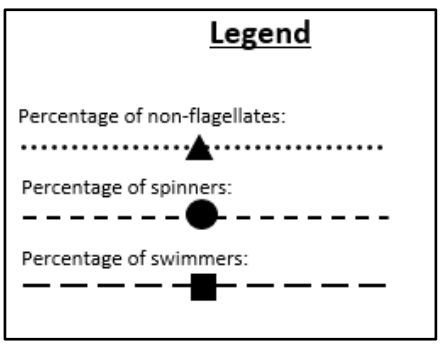

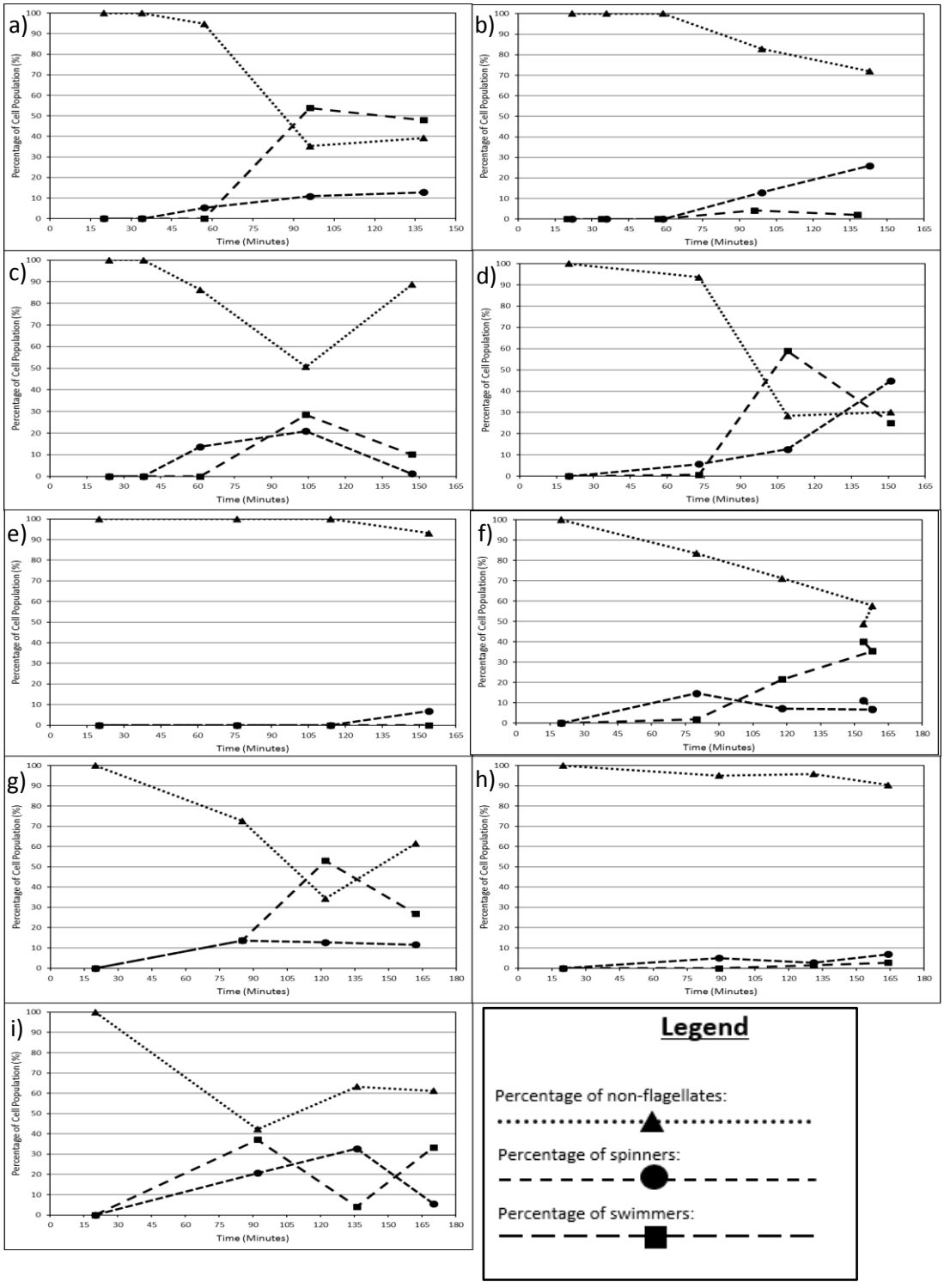

Figure 70: The effect of TWEEN20 addition in anaerobic and microaerophilic CO_2 rich environments.

A collection of graphs plotting differentiation data from the first FBS experiment. a) The results of a control sample. b) The results of cells mixed with 1% TWEEN20. c) The results of cells mixed with 0.2% TWEEN20. d) The results of control cells in microaerophilic, CO_2 rich conditions. e) The results of cells in microaerophilic CO_2 rich conditions mixed with 1% TWEEN20. f) The results of cells in microaerophilic CO_2 rich conditions mixed with 0.2% TWEEN20. g) The results of control cells in anaerobic conditions. e) The results of cells in anaerobic conditions mixed with 1% TWEEN20. f) The results of cells in anaerobic conditions mixed with 0.2% TWEEN20. The plot formatting mirrors the formatting in figure 40.

XI. Sequences of the purification proteins of interest

>AK3

GCTATGCATCCAACGCGTTGGGAGCTCTCCCATATGGTCGACCTGCAGGCGGCCGCGAATTCACTAGTGATTT
GGCTCGAGTTAATCAAATAATTTGCATACTTCAGCAAACACTTCTTCTTGTGTCTTTGAACTATCAATTGTCTTG
ACTCTATCAGTCTTCTTAAAGTATCCAATAACTGGCATTGTTTGGTCGCTATAGGTCTTGAATCTCTTCTTAATA
CTTTCGGCATTGTCATCAGATCTACCACTCGTCTTACCTCTTTCTAACAATCTTTGTTCCAAAATTTCTTCTGGAC
AATCAAAGAAGAGGACAAACTTGAATTTACAGACATGAGCTTCAAAGTCAACAGCTTGTTGCATTTCTCTTGG
GAAGCCATCGATCAAGAACGTAGCATCCTTTTTAGGATGGTTCAAAATAGCATTTCTTAACAAACCAAGAGTA
ACAGCACCAGGCACAATCTTACCTTCCTTAATGTATGACGAGATCATTCTACCCTGTTCTGTATCCTTAGCAGCT
TCAGCTCTCAACAAATCACCTGTACTATAATGGATAAAACCATACTTTTCAACAAGTTTGGCACATTGTGTGCC
CTTTCCTGATCCTGGACCACCATTAACACAAATAACATTTCTCCAATTCTTGACAGATTCTTGAGCAGCAGAAA
GTCTAGCCATATGCCAAATCGAATTCCCGCGGCCGCCATGGCGGCCGGGAGCATGCGACGTCGGGCCCAATT
CGCCCTATAGTGAGTCGTATTACAATTCACTGGCCGTCGTTTTACAACGTCGTGACTGGGAAAACCCTGGCGTT
ACCCAACTTAATCGCCTTGCAGCACATCCCCCTTTCGCCAGCTGGCGTAATAGCGAAGAGGCCCGCACCGATC
GCCCTTCCCAACAGTTGCGCAGCCTGAATGGCGAATGGACGCGCCCTGTAGCGGCGCATTAAGCGCGGCGGG
TGTGGTGGTTACGCGCAGCGTGACCGCTACACTTGCCAGCGCCCTAGCGCCCGCTCCTTTCGCTTTCTTCCCTT
CCTTTCTCGCCACGTTCGCCGGCTTTCCCCGTCAAGCTCTAAATCGGGGGCTCCCTTTAGGGTTCCGATTTAGT
GCTTTACGGCACCTCGACCCCAAAAAACTTGATTAGGGTGATGGTTCACGTA

>C8

CTATAGATACTCAGCTATGCATCCAACGCGTTGGGAGCTCTCCCATATGGTCGACCTGCAGGCGGCCGCGAAT
TCACTAGTGATTTGTCGTTAATCTTTTCGAGGACCATTCAGGACTTGTTAAGATTGCACAATGAGACAGTTCAC
AAATTTGTTCCAAAGGAATTCATGTCGATTGTTCAGAAGGAGAGTGTAATGGACCTTACGCACGGAGATTACT
TTGAAATGGAATTGGATGTGTTGTTTGCTGACATTAGAGGTTATACAAGTATTTGTGAAAAGATGACACCAGA
TGAAACTTTTGAATTTTTGAATAATTATTTGTCATTGGTTGGACCAGTTGTGAGAGAACATGGTGGATATATTG
ACAAGTATTTGGGTGATGGTATTTTGGCATTGTTTTTGACTCCTGGTCAATCTGTTTTAGCAGCGATGGAAATA
CAAAGAAGATTATTAGAATTCAATAAGAGTAAGAAATATCCAACAGTTAGAGTTGGAATTGGAATTGCAAGA
GGTAAATGTGCAGTTGGATTGATTGGTGAAGATCAAAGAGTTGATCCAACCATTATTGGAGATACTGTCAATT
TGGCAGCTCGTTTGGAATCTTTGACTAAACATTACAGAGTTGACATTCTCGTTACGAAGGAAGTAATTGAAAC
ATCTCCACTTCTTCCAAAGAGGAATCAAAGAAAAATAGGCCGCTTAGCAGTTGTTGGAAGACAACAAGCAAGT

TGGGTATTTGAAATTCTCACAAGAACACCTTCAACAGTTTCGAATAACTCTCACGAATTGAAAGCCAAAAACAA
GACCAACTTTGAAGATGCTATTGAGATAATGTCTGGAAGTTACTCTCATGGTGAATGCGTTCCAGATAAGCTT
ACAATTGATGGACAGAAACACAATTTTGGGGTGGTGGATTCCATGAATATGAGCTCAACTATGAATAATCTTA
AAAGTGAAGATGTAGTTAAGGCGATTGAGTTATTTGGAAAGGTTGTGAGCAGAGATCCGACTGATTTCGTGG
CTAATATGCGATTGGAAAAACTCAGAGAAATGGTGGACGACGTTAGTATGCGAAGCTCATGG

>PAS1

CGCGTTGGGAGCTCTCCCATATGGTCGACCTGCAGGCGGCCGCGAATTCACTAGTGATTTTACTCGAGCTAGG
ACTCCCACATTGGCTTCTCCATTTCCTTTGGCTTGTGCTTTGAGATCGGCAACAGTCTTTTCCAGTAATTCTCTAT
CCTTCTTTTCGAACATTGTGAATACTTGAGCACCTACAATATCAGATTGTTTATAACCAAACATTCTTTGGGCTG
CAGGATTTATCAAGTCAATCAAACCAGATTCATTACACAAGATGGAACCATCTACAGAGGCATTAAGGATACT
TCTCACATTAGATGAGTCGCCACTATTTTGTTTCTTGTTCTTTCTTTGGAAGAGTTCAACCAATCCATTTGGTAC
AGAATTATACAAGATAAAGTTTCTCAAATGCTCATTACTATCAAGAATATTGAGAGGGATATAATTTAGCATTG
ATCTTAAAGATTGAACGTGGCTAAAGTGAGACACCATATGCACAATCGAATTCCCGCGGCCGCCATGGCGGCC
GGGAGCATGCGACGTCGGGCCCAATTCGCCCTATAGTGAGTCGTATTACAATTCACTGGCCGTCGTTTTACAA
CGTCGTGACTGGGAAAACCCTGGCGTTACCCAACTTAATCGCCTTGCAGCACATCCCCCTTTCGCCAGCTGGCG
TAATAGCGAAGAGGCCCGCACCGATCGCCCTTCCCAACAGTTGCGCAGCCTGAATGGCGAATGGACGCGCCC
TGTAGCGGCGCATTAAGCGCGGCGGGTGTGGTGGTTACGCGCAGCGTGACCGCTACACTTGCCAGCGCCCTA
GCGCCCGCTCCTTTCGCTTTCTTCCCTTCCTTTCTCGCCACGTTCGCCGGCTTTCCCCGTCAAGCTCTAAATCGG
GGGCTCCCTTTAGGGTTCCGATTTAGTGCTTTACGGCACCTCGACCCCAAAAAACTTGATTAGGGTGATGGTTC
ACGTAGTGGGCCATCGCCCTGATAGACGGTTTTTCGCCCTTTGACGTTGGAGTCCACGTTCTTTAATAGTGGAC
TCTTGTTCCAAACTG

>PP_PFK

GCTGGAGCTTGCAAGCTTCACGTGATATCCCAAGCTTGGCATATGAGCGTGGTGGTGCCGAAAGATGTGCCG
ACCCTGGGCATTCTGGTGGGCGGCGGCCCGGCGCCGGGCATTAACGGCGTGATTAGCAGCGTGACCATTGAA
GCGATTAACAACGGCTATCGCGTGCTGGGCTTTCTGGAAGGCTTTAACTATCTGATTGCGCAGGATGATAGCA
AAATTGTGGAACTGACCATTGATGCGGTGAGCCGCATTCATTTTGAAGGCGGCAGCATTCTGAAAACCAGCCG
CGCGAACCCGACCAAAAAAGCGGAAGATCTGACCAAATGCGTGAAACAGCTGCAGAAATTTAACGTGAGCCT
GCTGGTGACCATTGGCGGCGATGATACCGCGTTTAGCAGCATGAGCATTGCGAAAGCGGCGAACAACGAAAT
TCATGTGTGCCATGTGCCGAAAACCATTGATAACGATCTGCCGCTGCCGTATGGCATTCCGACCTTTGGCTATG
AAACCGCGCGCGAATTTGGCGCGAGCGTGGTGCGCAGCCTGATGAGCGATGCGCAGACCGCGAGCCGCTAT

TTTATTGTGGTGGCGATGGGCCGCCAGGCGGGCCATCTGGCGCTGGGCATTGGCAAAAGCGCGGGCGCGCA
TCTGACCCTGATTCCGGAAGAATTTACCAACGAAGCGGGCGAAATTCAGGTGACCTTTAAACGCATTTGCGAT
CTGATTGAAAGCAGCATTATTAAACGCCTGGCGCTGGGCAAAGATCATGGCGTGATTATTCTGGCGGAAGGC
CTGCTGGAATATATGAGCACCGAAGAACTGAAACAGGCGTTTGGCAACCAGCTGAAATATGATGCGCATGAT
CATATTATGCTGGCGGAACTGGATTTTGGCCGCCTGGTGCGCGATGAAATGCGCGATCGCGTGAGCAAACGC
GGCCTGAAATTTGCGTTTACCGAAAAAAACCTGGGCTATGAACTGCGCTGCGTGAGCCCGAACGCGTTTGATC
GCGAATATACCCGCGATCTGGGCAACGGCGCGGCGCGCTATCTGCTGAGCGGCGGCAACGGCGCGCTGATTA
GCGTGCAGGGCGATAAA

Copyright Statement

I confirm that, unless indicated otherwise, I undertook all of the work presented in this report. Any work performed by other parties is fully acknowledged.